Université d'Ottawa · University of Ottawa

Immunochemical study of human apolipoprotein E: Development of LDL-receptor mimetic monoclonal antibodies, using recombinant DNA approaches

written by
Robert L Raffaï

Thesis presented to the School of Graduate Studies
in view of obtaining the title of
Philosophiæ Doctor (Ph.D.)
in Biochemistry

Faculty of Medicine
Department of Biochemistry
University of Ottawa

August 1997

TABLE OF CONTENT

SECTION 2

SECTION 3

SECTION 4

SECTION 5

List of Figures

List of Tables

List of Abbreviations

BSA	bovine serum albumin
CDR	complementary determining region
CETP	cholesteryl ester-transfer-protein
DMPC	dimyrystoylphosphatidylcholine
DMEM	Dubelco's minimal essential medium
E. coli	Escherichia coli
Fab	antigen-binding fragment of an antibody
rFab	recombinant Fab
FH	familial hypercholesterolemia
FPLC	fast protein liquid chromatography
HAT	hypoxanthine + aminopterin + thymidine
HDL	high density lipoprotein
HL	hepatic lipase
HSPG	heparan sulfate proteoglycan
IDL	intermediate density lipoprotein
LCAT	lecithin-cholesterol-acyltransferase
LB	Luria's broth
LBA	Luria's broth ampicillin
LBAT	Luria's broth ampicillin tetracycline
LDL	low density lipoprotein
LDLr	low density lipoprotein receptor
LPL	lipoprotein lipase
LRP	low density lipoprotein receptor related protein
mAb	monoclonal antibody
PCR	polymerase chain reaction
PBS	phosphate buffered saline
Phab	phage-displayed antibody
SOE	splice overlap extension PCR

SPR	surface plasmon resonance
STE	sucrose 20% - tris 10mM-EDTA 5mM
TE	tris 10mM – EDTA 1mM
VLDL	very low density lipoprotein

Dedications

I dedicate my thesis to my entire family, especially to my parents and to Alex. Also, I dedicate my thesis to all of those who enjoy to dream and persevere.

Acknowledgements

There are many people whom I would like to personally acknowledge for having taken part of my graduate research education. However, I will limit myself to those who had the mŏst profound influence on me during that period of my life. Primarily, I acknowledge Dr. Marc Therrien, who as a graduate student, was my very first Mentor. Mark introduced me to the field of molecular biology in 1988, while I was a summer student in Dr. Jacques Drouin's laboratory. Mark helped influence my mode of thinking as a young "lab rat". I acknowledge Dr. Ross Milne for having accepted me as one of his graduate students, and for having provided me with a challenging project, which has allowed me to evolve as a scientist. To this day, I remember my first encounter with Ross, when on one rainy morning I barged into his small overburdened office, and startled him with my adamant desire of becoming a pupil under his tutelage. I hope that one day I will achieve the human height that Ross possesses, which caused me to dedicate myself under his supervision. I regret not one day spent with this instructor. I wish to acknowledge my co-supervisor, Dr. Eric Rassart, in whose laboratory I spent the most enjoyable three years of my entire life. Eric provided a laboratory atmosphere, which to this day I have never again encountered. The friends I made in Eric's laboratory, will never leave my heart. Specifically, I acknowledge Dr. Xingbo Wang who helped me get started as an independent graduate student. I will always remember my good friends Marc Desforges, Benoit Barbeau, Richard Bergeron, Sylvain Beausoleil, Stephane Vincent, Laurence Therisse, and all those which I cannot include here, but who remain well within me.

I would like to acknowledge Drs. Marcel, McPherson, Schultz, Sparks and Yao, of the University of Ottawa Lipoprotein Research Group, who allowed me to complete my graduate research in a well organized scientific environment. I convey special thanks to Dr. Ruth McPherson who provided invaluable human plasma specimens for my experiments, and to Dr. Zemin Yao who instilled within me the philosophy related to graduate studies. For this I will always remember Zemin. I acknowledge Dr. Roger MacKenzie form the National Research Council of Canada, for having introduced me to modern techniques of analytical immunochemistry. I acknowledge Mrs. Julie Normand, who was the best at solving academic problems, and who was a great friend. Finally, I would like to acknowledge some of the individuals of the Lipoprotein Research Group, with whom I developed special relationships. Firstly, I acknowledge my good friends Xingyu Wang, Philippe Frank and Errol (Pinecone) Chamlioglu, with whom I had many strange adventures, and with whom I hope to remain in constant contact for the rest of my life. I acknowledge all of the members of Ross Milne's Laboratory, to whom I sincerely wish the very best in life. I acknowledge Jelena Vukmirica, my enduring friend and lab partner, who was a great source of inspiration for my closing experiments at the University of Ottawa, and more importantly, for my current ones at the Gladstone Institute in California. Lastly, I acknowledge my current supervisor, Dr. Karl Weisgraber, who provided all of the apolipoprotein E samples needed for my studies, and who graciously allowed me to complete my thesis in his laboratory.

I wish to thank Dr. Ross Milne, the Heart and Stroke Foundation of Canada, and the Fonds pour la Formation de Chercheurs et l'Aide à la Recherche, for financial support of my graduate studies.

Abstract

Apolipoprotein (apo) E is a 299 amino acid polypeptide that plays an important role in plasma lipoprotein metabolism. A major physiological function of apoE resides in its ability to be specifically recognized by cellular low-density-lipoprotein receptors (LDLr). A common apoE isoform is defective in its binding to the LDLr and its inheritance can lead to hyperlipidemia. In addition to apoE genetic polymorphism, apoE interaction with the LDLr also depends on apoE conformation. While lipid-free apoE cannot interact with the LDLr, upon binding to lipid, apoE undergoes a conformational change that renders it receptor-competent. Within plasma lipoproteins, apoE is conformationally heterogeneous, with only a subpopulation of apoE molecules having the ability to mediate binding to the LDLr. The goal of my thesis was to investigate the structural modalities that determine the ability of LDL to bind to the LDLr. To this end, I have made use of novel recombinant antibody methodologies, in order to probe the structural basis of the apoE-LDLr interaction. I demonstrate that a monoclonal antibody that is specific for the LDLr binding site on apoE resembles the LDLr in terms of fine specificity and primary structure. Furthermore, by in vitro mutagenesis, I was able to generate a series of variants that differ from the parental antibody in both affinity and apoE isoform specificity. Of particular interest, one variant acquired the ability to recognize apolipoprotein B100, the other ligand of the LDLr. I argue that this variant is an antibody mimetic of the LDLr. This panel of anti-apoE recombinant antibodies will be useful reagents for determining the mechanisms involved in the interaction of the LDLr and its ligands. In more general terms, it offers a unique model for studying the molecular recognition processes that occur between protein macromolecules.

Prologue

Plan of the thesis

The human body is faced with the problem of providing cells with the cholesterol that they require while, at the same time, maintaining plasma cholesterol levels at concentrations below those that promote atherosclerosis. One mechanism by which this is accomplished is through cell surface receptors that specifically bind the plasma lipoproteins that are responsible for the transport of lipids in the circulation. A number of different receptors have been identified that are specific for the protein components of the lipoproteins, the apolipoproteins. Several of these receptors, including the well characterized low density lipoprotein (LDL) receptor, bind apolipoprotein (apo) E. As a consequence, apoE plays a key role in plasma lipoprotein metabolism. This role for apoE is underscored by the hyperlipidemia and atherosclerosis that is seen in humans and experimental animals who have genetic apoE deficiency. Inheritance of genes encoding apoE variants that show reduced affinity for cell surface receptors is also associated with abnormal lipoprotein profiles and premature atherosclerosis. The principal goal of my Ph.D research project was to better understand the structural basis for the interaction of apoE with cell surface receptors. I have taken an immunochemical approach to this problem. Specifically, I have attempted to prepare, characterize and define the binding mechanisms of anti-apoE monoclonal antibodies (mAbs) that recognize the same

confromational epitope on apoE as is recognized by the LDL receptor. I refer to mAbs that have this property as antibody mimetics of the LDL receptor.

As an introduction to my research, I present, in Chapter I, a summary of the current knowledge of the structure and biology of apoE and its specific receptors, their roles in lipoprotein metabolism and in the development of atherosclerosis. Furthermore, in light of the important role of antibodies in my research, I give an overview of the structure and biology of antibodies and of the most recent advances in technologies related to antibody production.

Our laboratory has previously characterized two murine anti-human apoE monoclonal antibodies (mAb), 1D7 and 2E8, that can block apoE-mediated binding to the LDL receptor. These mAbs have proven to be excellent probes for the study of apoE structure and function. My first objective was to define the respective fine specificities of these two antibodies by determining their patterns of reactivity with a series of apoE variants that are defective in binding to the LDL receptor. As described in Chapter II, I demonstrate that the epitopes of both antibodies coincide with the apoE LDL receptor-binding site. In particular, I show that the fine specificity of the 2E8 mAb is very similar to that of the LDL receptor. My second objective was, therefore, to determine if the similarity in the apoE specificity of 1D7, 2E8 and the LDL receptor, reflected homologies in primary structure. To this end, I have cloned and determined the sequence of cDNAs encoding the heavy and light chains of 1D7 and 2E8. Although they react with overlapping epitopes, I show that there is little sequence homology between the antigen-

binding sites of 1D7 and 2E8. In contrast, I demonstrate that there is a striking similarity between sequences in the 2E8 heavy chain that contribute to the antigen-binding site and sequences within the ligand-binding domain of the LDL receptor. This suggests that 2E8 and the LDL receptor may bind apoE by a similar mechanism and, as a consequence, I propose that 2E8 possesses characteristics that would be expected of an antibody mimetic of the LDL receptor.

A third objective was to modify the binding site of the 2E8 mAb by *in vitro* mutagenesis to further increase its resemblance to that of the LDL, in order to make it a true antibody mimetic. In Chapter IV, I detail experiments that I performed to optimize the expression of 2E8 Fab fragments in *E. coli*, and to develop a purification protocol for the recombinant antibody. I show that the immunoreactivity of the recombinant Fab fragments are identical to that of Fab fragments produced by papain digestion of 2E8 IgG. Chapter V, describes the production and characterization of 2E8 variants by site directed mutagenesis to identify the role of specific residues in the binding of apoE. I demonstrate the importance of certain acidic residues within the 2E8 heavy chain in determining the affinity and fine specificity of the mAb. Other variants were produced to alter the 2E8 sequence in order for it to more closely resemble the ligand-binding domain of the LDL receptor. One of these variants showed an increased affinity for apoE, whereas another variant acquired cross-reactivity with apoB, and showed a selective increase in affinity for lipid-associated apoE, properties also shared by the LDL receptor.

I have also cloned and expressed the cDNA encoding an antibody specific for human atrial natriuretic factor (ANF), a cardiac hormone that plays an important role in salt and water balance, and in maintaining blood pressure. The goal of this subproject was to have a recombinant antibody that could serve as a control in the expression experiments for the anti-apoE mAbs and to be eventually used as an immunochemical probe in structural studies of ANF. Chapter III is a description of the cloning and characterization of the cDNA of this anti-ANF mAb.

In Chapter VI, I discuss the results of my experiments in relation to the three-dimensional structure of the 2E8 mAb that has been recently determined through a collaboration with investigators at the Gladstone Institute for Cardiovascular Research of the University of California, San Francisco. As well, I present my views on the impact of my research and on possible future directions.

Chapter I

Overview of serum lipoprotein metabolism

I. The Need for Lipid Mobilization within the Body

As life on earth evolved from simple unicellular organisms, a vascular system became a necessity for those organisms which were differentiating into large, anatomically more complex, multi-organ individuals. An elaborate array of veins and arteries allowed for all tissues to have access to essential nutrients that include water-insoluble lipids. Our bodies, along with those of many other species, have the capability of absorbing lipids from our diets, and making use of them for the subsistence of cells. Once ingested, dietary lipids can serve as structural material, as a source of direct chemical energy or for potential energy storage. Because cellular existence relies on the use of water as a solvent in which all biochemical reactions occur, a process was needed for the solubilization of metabolic lipids. The system which arose in order to solve the problem of lipid transport within the blood, is commonly referred to as the "lipoprotein distribution system", with the lipoprotein being the unit component which renders lipids soluble within our blood (Davis, R., and Vance, J.E., 1996).

II. Serum Lipoproteins

As depicted in Figure I-1, lipoproteins are macromolecular assemblies composed of a neutral lipid core, surrounded by a monolayer of phospholipid, free cholesterol and certain specific proteins. Lipoproteins originate primarily from specialized cells in the liver and intestine. Intestinal mucosal cells and liver hepatocytes can assemble hydrophobic lipids into water soluble lipoproteins. The physical and chemical properties of any plasma lipoprotein, will differ depending on the origin of its synthesis, and to the extent to which it was metabolically modified. The protein component of the lipoprotein consists of various apolipoproteins, which collectively serve both structural and

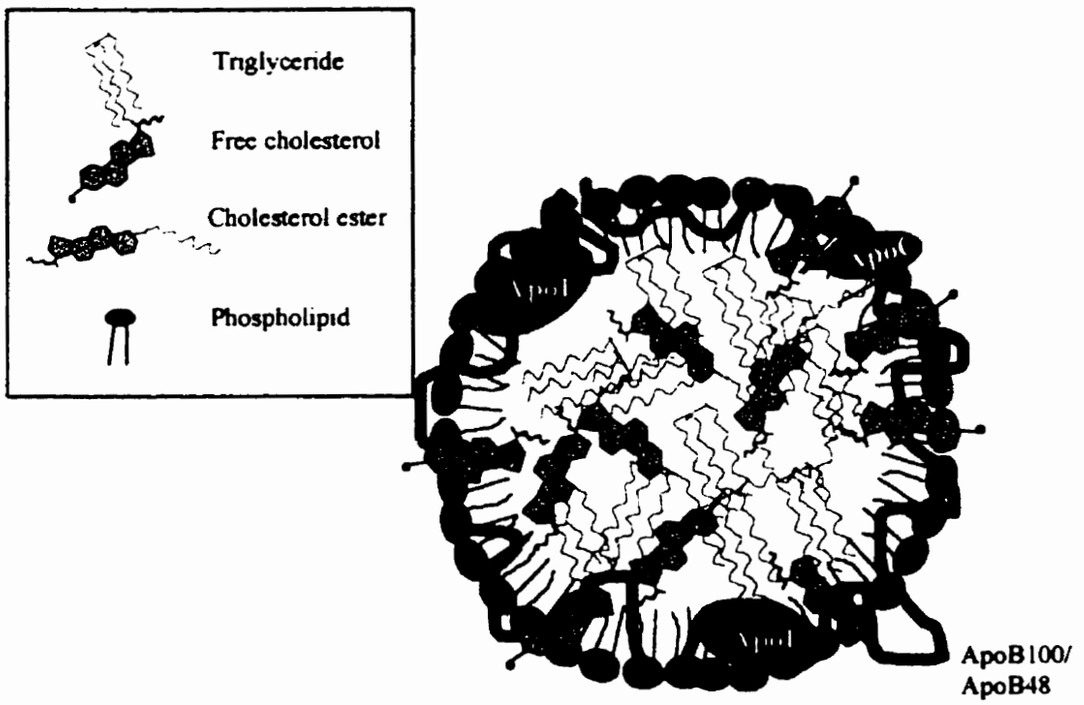

Figure I-1 Schematic diagram of a metabolic lipoprotein particle.

This figure depicts the chemical composition of a metabolic lipoprotein. Typically, lipoproteins are composed of a neutral lipid core consisting of cholesterol esters and triglycerides. The lipid core is surrounded by a single layer of phospholipid and certain apolipoproteins, which collectively allow the lipoprotein to be soluble in plasma, and direct its metabolic fate (adapted from Davis, R. and Vance, J.E., 1996).

functional roles (Methods in Enzymol. 128/129, 1989). Their primary purpose resides in their emulsification capability, which renders the lipoprotein water soluble. In addition, most apolipoproteins have acquired diverse physiological functions, which greatly enhance the process of vascular lipid distribution. The relevance of the metabolic events catalyzed by the apolipoproteins, are exemplified by the clinical observations of inborn errors of lipoprotein metabolism. Genetic anomalies of most of the apolipoproteins have been documented, and in many cases they lead to premature atherosclerosis.

Following their release into the circulation, lipoproteins undergo continuous vascular remodeling, a process catalyzed through the action of specific lipolytic enzymes and lipid transfer proteins. These enzymes, which will be described later, act in concert within the blood in the orchestrated transformation of lipoproteins, which are either depleted or supplemented with structural material. As heterogeneous suspensions of lipid and protein, lipoproteins have been classified into several subfractions according to their inherent physical properties. Among the criteria that are used for the classification of plasma lipoproteins are their site of origin, their hydrated density and size, their apolipoprotein content and their electrophoretic mobility in agarose.

III. The Major Plasma Lipoproteins.

As indicated above, plasma lipoproteins are heterogeneous in their hydrated densitites, ranging from 0.93 to 1.21 g / ml, a property that permits their fractionation by

equilibrium ultracentrifugation in salt gradients (Gofman, J.W., *et al.* 1949; Methods inEnzymol. 128/129, 1989).

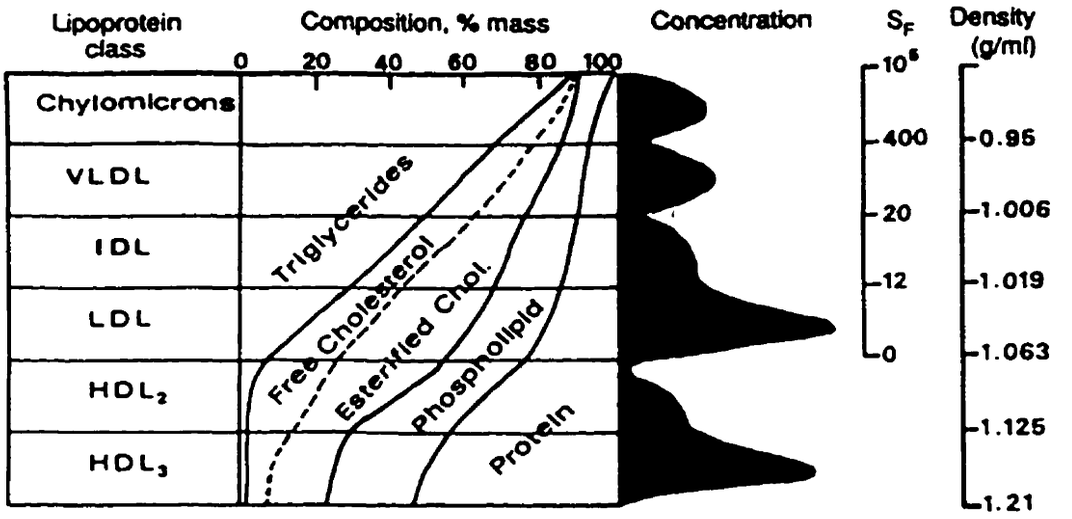

Figure I-2 **Classification and chemical composition of lipoproteins using equilibrium ultracentrifugation.**

This figure depicts the clasification of serum lipoproteins, following their separation through ultracentrifugation. As shown by the figure, the higher the lipid to protein ratio, the lower the density of the particle. Thus, lipid-rich chylomicrons display the lowest density, and are resolved before any of the other lipoproteins using this methodology. In fact, if left undisturbed, chylomicrons will float to the top of freshly collected blood, giving rise to a creamy layer (adapted from Davis,R., and Vance, J.E., 1996).

High density lipoproteins (HDL) are isolated in fractions of density ranging between 1.063 and 1.210 g / ml). The principal apolipoproteins of HDL are apoAI and apoAII, with smaller amounts of apoCI, apoCII, apoCIII, apoE and apoAIV. Unlike the other lipoprotein classes, HDL do not appear to originate from a unique cellular location. The majority of HDL particles are thought to arise in the plasma both in response to the catabolic shedding of surface phospholipids from TG-rich lipoproteins, and from cholesterol efflux from peripheral cells (Tall, A.R., and Small, D.M., 1978). ApoAI itself is synthesized by hepatocytes and intestinal enterocytes. HDL are well recognized as being involved in the delivery of cholesterol to steroidogenic tissues, a process that

appears to be, at least in part, receptor-mediated (Steinberg, D.A, 1996). In addition, HDL are believed to be instrumental in the recycling of cholesterol from extrahepatic tissues to the liver, a process refered to as "Reverse Cholesterol Transport" (Fielding, C.J., and Fielding, P.E., 1995). For this reason, elevated serum levels of HDL are generally regarded as being protective against atherogenesis (Breslow J.L., 1996).

A second class of serum lipoproteins, very low density lipoproteins (VLDL), which originate from the liver are enriched in neutral lipid and are isolated from plasma at a density range of 0.95 and 1.006 g / ml. VLDL contain a single molecule of apoB100 as well as apoE and a complement of apoCs. Upon their entry into the bloodstream, these large triglyceride rich (TG-rich) VLDL are immediately subjected to modification through lipolysis and lipid transfer. Owing to these processes, the lipoproteins shrink in size with a concomitant increase in their buoyant density and a gradual enrichment in cholesterol esters and depletion of triglycerides. The remodeling of VLDL by lipoprotein lipase and lipid transfer proteins, gives rise to a series of smaller, cholesterol-enriched lipoproteins including intermediate density lipoproteins (IDL) with a density ranging between 1.006 and 1.019 g / ml, and low density lipoproteins (LDL) which float in density ranges between 1.019 and 1.063 g / ml. During the conversion from VLDL to LDL, there is a loss of apolipoproteins such that the sole protein component of LDL is a single molecule of apoB100 (Havel, R.J., 1995).

The chylomicrons consititute a final lipoprotein class. Chylomicrons are large triglyceride-rich particles which are produced in the gut, and which can be isolated in

density ranges of less than 0,95 g / ml. They contain a single molecule of apoB48 (a species of apoB that is composed of the amino terminal 48% of apoB100 and that is generated by a tissue specific RNA editing process (Powell, L.M. *et al.* 1987), as well as apoE, apoCs, apoA-I, and apoA-IV. Like VLDL, chylomicrons undergo rapid modification within the plasma through the activity of lipases and lipid transfer proteins which generates a population of lipoproteins, called chylomicron remnants, that are heterogeneous in terms of size and density and are relatviely enriched in cholesterol. Chylomicron remnants are not converted to LDL, but are rapidly cleared from the circulation by the liver. Defects in the metabolism and clearance of TG-rich lipoproteins, can lead to hyperlipidemia and premature atherogenesis (Breslow, J.L., 1996; Mahley, R.H., and Rall, S.C. Jr., 1995).

Section 1

Specifics concerning lipoprotein metabolism

As the main goal of my Ph.D. research was to define mechanisms by which lipoproteins bind to the LDL receptor, I will describe only the metabolism of those lipoproteins which directly interact with the LDL receptor. Most of the information pertaining to the general metabolism of TG-rich lipoproteins has been obtained from the general references listed below. (Human physiology, 1992; Biochemistry of lipids

lipoproteins and membranes, 1996; Methods in Enzymology vols. 128 and 129, 1989; The Metabolic and Molecular Bases Of Inherited Disease, 1995).

1.1 Metabolic pathways for triglyceride-rich lipoproteins

With the exception of bacteria (Ingrahm, J.L. *et al.* 1983), most living organisms make use of lipids as a source of metabolic energy. The major lipids that are utilized by mammals are triglycerides, cholesterol and phospholipids. Triglycerides are used for both energy expenditure and storage. Phospholipids and cholesterol on the other hand, serve mainly as building blocks for cellular membranes and are important sources of raw material for intra and extracellular signalling molecules. These lipid molecules share the properties of being miscible and metabolically linked, thus readily interconverted through the action of the acetyl-CoA enzymatic processes within the cell. Much of our bodily lipid needs are derived from dietary sources, however, a substantial amount of lipid is synthesized from non-fatty material, mainly from carbohydrate within the liver.

Within the body, there exists two well defined pathways which participate in lipid distribution. The chylomicrons produced by the intestine and the VLDL produced by the liver serve as the initial vehicles in the conveyance of lipids to peripheral cells. The course travelled by the chylomicron is termed the exogenous pathway, since its lipid component is almost exclusively of dietary origin. The VLDL metabolic course on the other hand, is known as the endogenous pathway, which results in the redistribution of energy stores from within the liver. In both cases, the primary objective of these lipid pathways is to provide peripheral cells with a source of triglycerides. As only a few cell types, including liver hepatocytes and the adipocytes, have the ability to synthesize

triglyceride, it is imperative for all other cells of the body to have access to this metabolically essential molecule. A diagram depicting lipoprotein turnover and metabolism is shown in Figure I-3.

1.2 The Exogenous Lipoprotein Pathway

Chylomicrons are exclusively synthesized by intestinal enterocytes for the transport of dietary fat and fat-soluble vitamins (Hussain, M.M., *et al.*1996). Chylomicrons are very large lipoproteins with a diameter of 75-1200 nm, and are composed primarily of triglyceride. The nascent lipoprotein contains a single molecule of apoB48 which remains with the particle throughout its short metabolic existance, and is the only one which is strictly required for assembly. In addition to apoB48, nascent chylomicrons contain multiple copies of smaller apolipoproteins such as apoAI and apoAIV.

Following a lipid-rich meal, dietary fat is hydrolyzed within the lumen of the intestine via the action of acid pancreatic lipases. The products of fat digestion (free fatty acids, monoglycerides, lysolecitin, and free cholesterol) are then absorbed as mixed micelles by the apical face of the intestinal enterocytes. These cells then re-esterify these lipids in the smooth endoplasmic reticulm as triglycerides, phospholipids, cholesterol ester, and rapidly use them for the assembly of chylomicrons which are then secreted into the intestinal lymph, through their basolateral face. Chylomicrons enter the venous bloodstream following passage through the thoracic duct. Upon entering the circulation, chylomicrons acquire other apolipoproteins including apoE and the various apoC's, by

simple exchange with other lipoproteins, primarily HDL. As described later, the acquisition of apoE and apoC's from HDL is followed by a concommitant loss of apoAIV. As a source of apoC's and apoE, HDL participate in the controlled metabolism (apoCs) as well as receptor-mediated uptake (apoE) of the TG- rich lipoproteins.

1.3 The Endogenous Lipoprotein Pathway

This pathway, originating in the liver, serves in the distribution of pre-existing lipid as well as lipid derived from carbohydrate. It operates continuously, presumably in order to provide the body with a constant source of TG in the fasting as well as the postprandial state. VLDL, assembled by human hepatocytes, contain as a major structural protein component, a single molecule of apoB-100. Other apolipoproteins that are incorporated onto nacent VLDLs, include many apoC's and apoE molecules. Following passage through the secretory pathway of the cell, the nascent VLDL are released within the chyme that exists in the space of Disse. Nascent VLDL are smaller than chylomicrons, with an average diameter less than 80 nm. Once released within the plasma, they rapidly acquire additional apoCs and apoE from the HDL population. The production rate of VLDL is regulated by the liver and can be induced by the consumption of calories, alcohol and carbohydrates in sensitive individuals (Havel, R.J., and Kane, J.P., 1995)

1.4 Cellular Assembly of Triglyceride Rich Lipoproteins

Both the exogenous and endogenous pathways are similar in their modes of lipoprotein assembly and secretion into their respective splandic circulations. The TG-

rich lipoproteins are assembled within the endoplasmic reticulum (ER), where triglycerides synthesized from monoglycerides and free fatty acids serve as starting material. In a yet undefined way, a liquid droplet of triglyceride is fabricated on the inner leaflet of the plasma membrane, where a segment of a newly synthesized portion of an apoB protein permits an association between the hydrophobic protein structure and the liquid core of triglyceride (Schumaker, V., 1992; Hussain, M.M, *et al.* 1996).

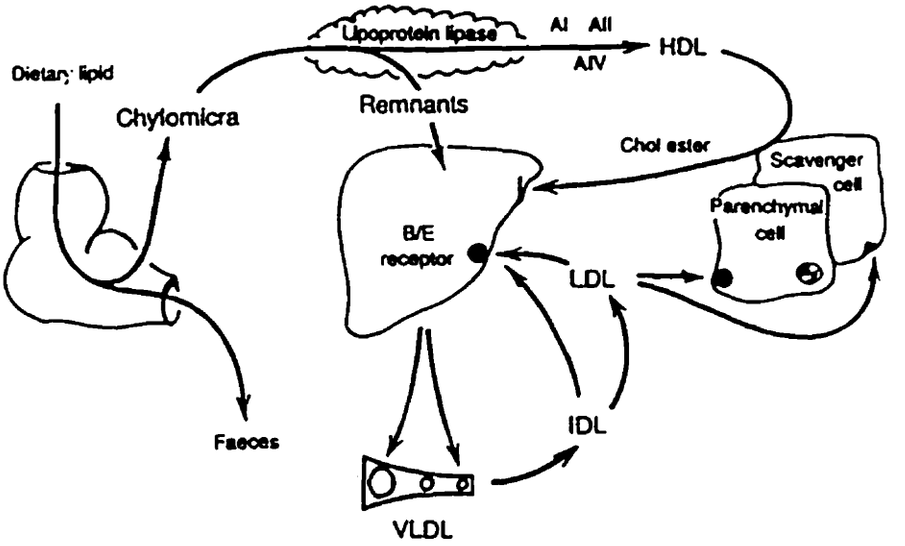

Figure I-3 Serum lipoprotein metabolism.

Figure depicting the vascular metabolism of serum lipoproteins. The sites of synthesis of all three classes of lipoproteins are shown, in addition to their site of final cellular uptake. In addition, the figure illustrates the enzyme mediated conversion of the lipoproteins, which occurs within the blood (adapted from Shumaker, V., 1992).

A recently characterized endoplasmic reticulum resident protein seems to serve in the lipidation of the nascent apoB polypeptide (Wetterau, J.R., *et al.* 1997). The microsomal transferase protein (MTP), has been shown to facilitate the assembly of TG-rich particles in cultured rat and human cells expressing recombinant forms of apoB (Gordon, D.R., *et al.* 1995). As shown in Figure I-4, MTP is thought to recruit triglycerides and assemble them onto apoB, in a co-translational lipidation process (Chuck, S.L., *et al.* 1993, Wang, S., *et al.* 1996). There is recent evidence that,

subsequent to the translocation of apoB, additional lipidation of nascent apoB may occur. This process of TG-enrichment of primordial apoB lipoproteins has been termed the "Second Step of VLDL Assembly", and relies on the MTP catalyzed enrichment of VLDL within the endoplasmic reticulum (Wang, Y., *et al.* 1997). Mature VLDL particles then transit through the Golgi apparatus where they acquire additional phospholipids (Yao, Z.M, and Vance, D.E., 1989) and are packaged in secretory vesicles, exported to the plasma membrane and released to the space of Disse, where they gain access to the venous mesentric circulation.

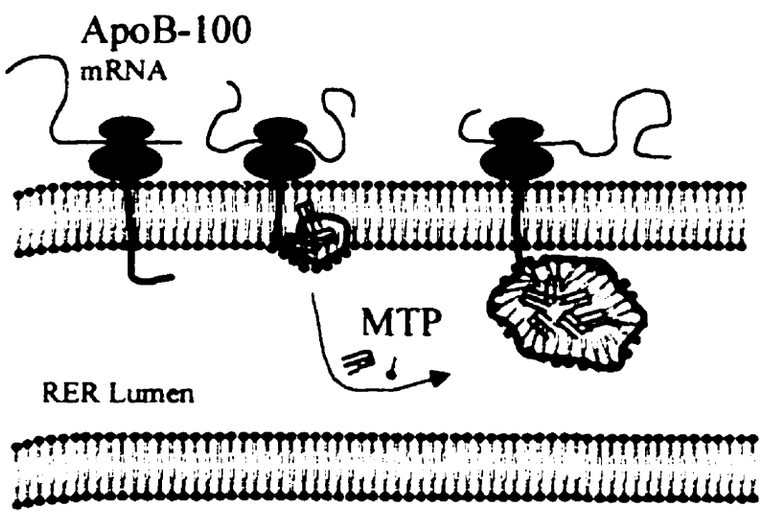

Figure I-4 The assembly of apoB-containing lipoproteins in the endoplasmic reticulum

This figure depicts the cellular asembly of TG-rich lipoproteins. As shown by the figure, a single molecule of apoB serves to initiate the assembly of the lipoprotein, which emerges from within the inner leaflet of the ER membrane. The enzyme MTP is believed to play a key role in the maturation of the lipoprotein, by causing an active addition of triglyceride and phospholipid, thus allowing it to grow in size (adapted from Davis, R., and Vance, J.E., 1996).

1.5 Serum Catabolism of Triglyceride Rich Lipoproteins

The metabolism of TG-rich lipoproteins within the circulation, occurs to a large extent through the lipolytic activity of plasma lipases. Following an injection of heparin, these activities increase in the plasma, owing to the release of the lipases from their

heparan proteoglycan anchored sites on the surface of the vascular endothelium. At least two distinct lipases are implicated, one of hepatic and one of extra-hepatic origin (Manzato, E., *et al.* 1986). As shown in Figure I-5, biologically active lipoprotein lipase (LPL), which is a serine esterase, exists as a dimer attached to the glycocalyx on endothelial cells lining the luminal surface of the capillaries, and is of extra-hepatic origin (Brunzel, J.D., 1995; Zambon, A., *et al.* 1996). LPL is synthesized in parenchymal cells, primarily adipose tissue and skeletal muscle, from where it is transported to the intimal surface of the vascular endothelium, to its sites of attachment (Pedersen, M.E., *et al.* 1983). This enzyme requires the presence of apoCII (LaRosa, J.C., *et al.* 1970), which serves as a co-factor, in order to hydrolyze TG-rich lipoproteins. In addition to its lipolytic activity, LPL bound to the surface of lipoproteins has been found to facilitate their uptake by binding to the remnant lipoprotein receptor (Beisiegel, U., *et al.* 1991). Hepatic lipase (HL) on the other hand, is found exclusively attached to the endothelium lining the liver and certain steroidogenic tissues. It is heparin releasable and is not dependent on a co-factor for activity. The role of hepatic lipase seems to be somewhat more elusive than that of lipoprotein lipase. In fact, hepatic lipase has been implicated in the hydrolysis of phospholipids as well as triacylglycerols, thereby being directly involved in the generation of LDL from VLDL remnants (Montalto, M.B., and Bensadoun, A., 1993). In addition, the activity of hepatic lipase has been demonstrated to greatly modulate the clearance of remnant lipoproteins from the circulation (Sultan, F., *et al.* 1990), presumably by causing lipoprotein-bound apoE to become more exposed, and more readily available for receptor-mediated interaction (Brasaemle, D.L., *et al.* 1993).

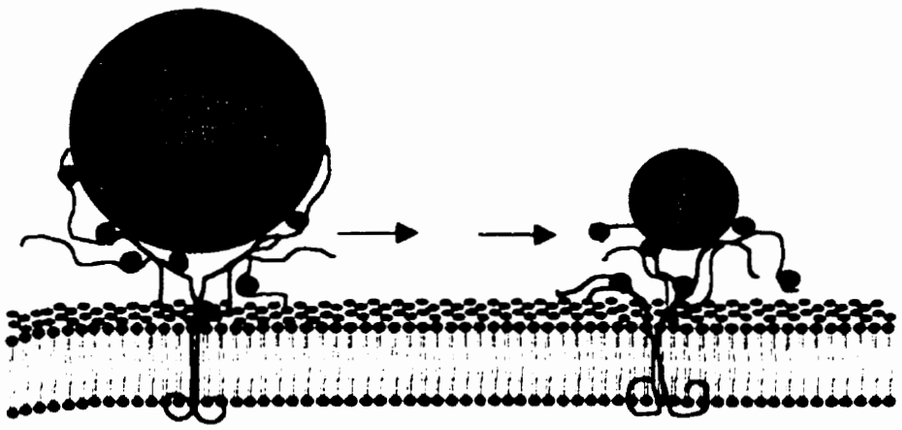

Figure I-5 Lipoprotein lipase in the remodeling of TG-rich serum lipoproteins.

This figure illustrates the enzyme LPL which exists as a dimer bound to heparan sulfate proteoglycans associated to the glycocalynx of the vascular endothelium. The activity of the lipase is dependant on the presence of its cofactor, apoCII on the surface of the lipoprotein. The activity of this enzyme causes the near complete hydrolysis of the TG within the lipoproteins. In addition, lipoprotein-bound LPL has been shown to facilitate the uptake of remnant lipoproteins, by interacting specifically with the LRP (adapted from Brunzel, J.D., 1995).

As chylomicrons and VLDL circulate in the blood, most of the TG and some of the surface phospholipids are hydrolyzed by LPL. This hydrolytic activity results in the generation of smaller particles called remnants. Concomitant with the lipolysis of the core triglycerides by LPL, the surrounding tissue absorbs most of the released fatty acids by a direct movement into the cell, whereas the remainder become bound to plasma albumin, and circulate in the plasma (Scow, R.O., *et al.* 1979) (Figure I-6). As mentioned above, the functional activity of LPL is made possible by the presence of its co-factor, apoCII, present on the surface of lipoproteins.

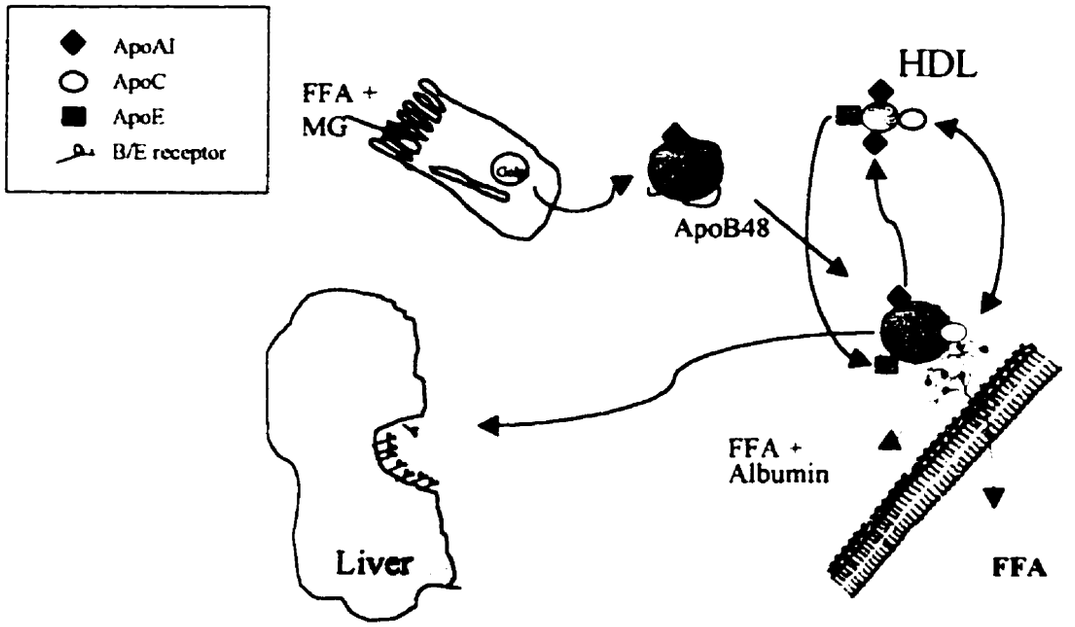

Figure I-6 **Plasma lipolytic conversion of TG-rich lipoproteins; cellular assimilation of the hydrolysed TG.**

This figure depicts the metabolic fate of a chylomicron within the circulation. Immediately following its entry into the blood, TG-rich lipoproteins are rapidly converted to remnants through the action of LPL. Liberated free fatty acids are then either directly assimilated by the underlying tissue, or become bound to plasma albumin. Concomittant with TG hydrolysis is the reduction of particle size, which induces a movement of apolipoproteins between the various particles. The remnants thus acquire apoE at the expense of the apoAs and Cs, which return to the HDL. With the acquisition of apoE, the remnants thus become competent for uptake by apoE-specific cell surface receptors present in the liver, which allow for their rapid clearance (adapted from Kane, J.P., Havel, R.J., 1995).

This exchangeable apolipoprotein is acquired by the triglyceride-rich lipoproteins from the HDL population. In addition to serving as a co-factor for LPL, apoCII, as well as apoCIII, inhibit receptor-mediated uptake of lipoproteins (Shelburne, F., *et al.* 1980; Windler, E., *et al.* 1980; deSilva, H.V., *et al.* 1996). They do so, both by excluding apoE from the surface of the lipoprotein, and by restricting its access to the LDL receptor through steric hindrance. As the TG-rich lipoprotein becomes progressively depleted in core material, both apoCII and apoCIII dissociate from its surface, allowing apoE to

readily associate with the particle and promote receptor-mediated endocytosis of the remnant.

In addition to lipolysis of core lipids, LPL also hydrolyzes surface phospholipids, although at a rate that is much less than that of core hydrolysis (Montalto, M.B., and Bensadoun, A., 1993). Chylomicron remnants are characterized by a considerably smaller spherical size, comprising some 4 % of the its original mass. Following the rapid depletion of the core triglycerides, a substantial surplus of surface material consisting of phospholipid, free cholesterol and protein are generated. In fact, these TG-depleted lipoproteins acquire strange dumbell shapes until the excess phospholipid and cholesterol is removed. In 1979, a mechanism was proposed whereby this excess material is somehow lost through a budding process, and becomes associated with the HDL population (Tall, A.R., and Small, D.M., 1979; Redgrave, T.G., and Small, D.M., 1979).

Remnants resulting from LPL hydrolysis retain their basic structural protein component; apoB-100 or B-48, indicative of their hepatic or intestinal origin, as well as some apoC and apoE which they can freely obtain from HDL (Figure I-6). Through an exchange process mediated by the plasma enzyme cholesteryl ester transfer protein (CETP), remnants become progressively enriched with cholesteryl esters (Figure I-7) (Tall, A.R., *et al.* 1997). In man, the majority of cholesteryl esters originates in the plasma, within the HDL population through the activity of the enzyme; lecithin cholesterol acyl transferase (LCAT), which converts free cholesterol and excess surface phospholipid present in HDL into cholesteryl esters (Glomset, J.A., 1968).

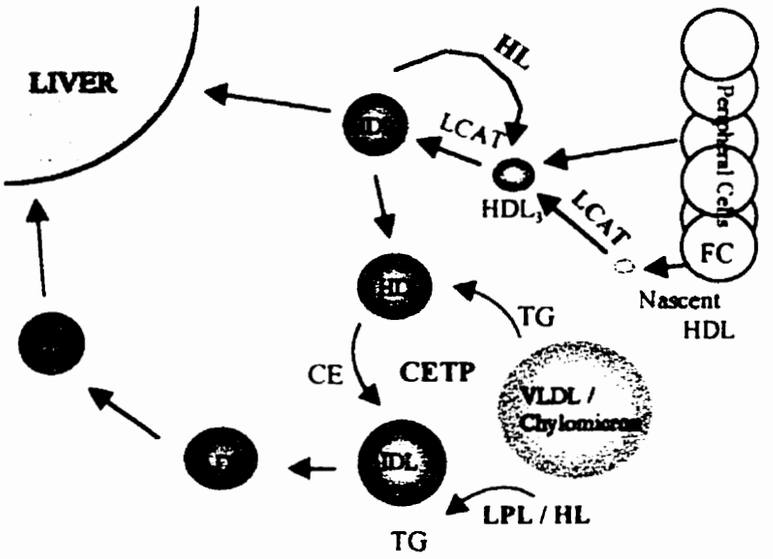

Figure I-7 Serum lipoprotein remodeling.

This figure depicts the metabolic consequences of plasma lipoprotein modifying enzymes. CETP causes the transfer of neutral lipids between the HDL and the TG-rich lipoproteins. LCAT is instrumental in the generation of HDL, and its activity is known to be dependant on the presence of its cofactor, apoAI. Finally, the activities of peripheral LPL, as well as that of liver restricted HL, cause the generation of remnant lipoproteins (adapted from Kane, J.P., Havel, R.J., 1995)

CETP can, in turn, mediate the transfer of cholesteryl esters from HDL to VLDL with the reciprocal transfer of triglyceride from VLDL to HDL. With the constant reduction in core triglyceride, and with the acquisition of cholesteryl-esters, these lipoproteins become IDL, and with additional loss of triglyceride as well as surface apolipoproteins, they become LDL (Tall, A.R., *et al.* 1997).

The removal of remnant lipoproteins from within the plasma, occurs mainly through high-affinity, receptor-mediated endocytosis by liver parenchymal cells (Figure I-6) (Mahley R.W., 1988; Havel, R.J., and Kane, J.P., *et al.* 1995). It is widely believed that, when present in elevated levels within the plasma, remnant lipoproteins are

atherogeneic (Havel, R.J., *et al.* 1995). On the other hand, nascent unmodified chylomicron particles, per se, do not appear to be atherogenic, since premature atherosclerosis does not occur in individuals suffering from familial deficiency of either lipoprotein lipase or apoCII, where chylomicrons and VLDL in very high concentration, circulate for prolonged periods of time. Thus, at least some hydrolysis of chylomicrons appears to be necessary in order to generate "toxic" atherogenic substances. A blockade, or slowing at any step in remnant clearance can lead to their accumulation in plasma (Brunzell, J.D., 1995). An accumulation of chylomicron and / or VLDL remnants leads to the appearance of a subpopulation of particles called, β-VLDL, indicative of their electrophoretic mobility characteristic (Uttermann, G., *et al.* 1977; Mahley, R.W., 1988)

1.6 The Space of Disse, a critical location for the final alteration and uptake of Remnant Lipoproteins

As shown in Figure I-8, circulating remnant lipoproteins eventually find their way to the space of Disse, by filtration through the fenestrations of the liver capillary endothelial bed, and perhaps also through transcytosis across the endothelium. Both nascent as well as remnant lipoproteins intermix within the space of Disse, and only their intrinsic physical properties will dictate as to their secretion into the venous mesentric circulation, or to their uptake by hepatocytes.

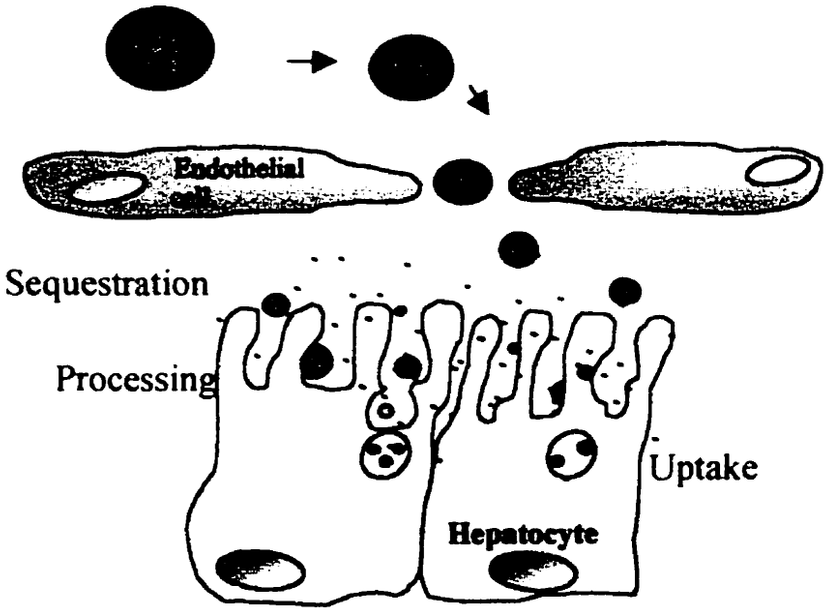

Figure I-8 Sequestration of remnant lipoproteins in the space of Disse

This figure depicts the anatomical location of the final alteration of the remnant lipoproteins, which will allow their rapid clearance from the circulation. Remnants gain access to the space of Disse in the liver lobules, due to the small fenestrations. Once within this location, the remnants become enriched in apoE (blue dots), and are rapidly sequestered by heparan sulfate proteoglycans (HSPG) associated with the endothelial lining. Subsequent to their sequestration, the remnants are then internalized by the HSPG, cell surface receptors, or both (adapted from Mahley, R.W., and Rall, S.C., 1995)

The sequestration of the remnant lipoproteins within the space of Disse may be the first step in the clearance of remnants as shown in Figure I-8 (Mahley, R.W., and Hussain, M.M., 1991). It has been proposed that the accumulation of remnants occurs through their interaction with cell surface heparan sulfate proteoglycans (HSPG). ApoE is known to bind avidly to heparin (Mahley, R.W., *et al.* 1979; Weisgraber, K.H., *et al.* 1986), and especially to heparan sulfate of hepatic origin (Ji, Z.S., *et al.* 1993). In fact, it is well established that heparan sulfate proteoglycans form a continuous layer on the surface of the microvilli of hepatocytes (Stow, J.L., *et al.* 1985; Sanan, D.A., *et al.* 1997).

The high local concentration of apoE within the Space of Disse (Hamilton, R.L., *et al.* 1990) causes the remnants to become enriched in apoE, which can mediate their binding to the hepatocyte cell surface, a mechanism known as "secretion recapture of apoE" (Ji, Z.S., *et al.* 1994). Liver derived hepatic lipase interacts with cell surface proteoglycans (Doolittle M.H., *et al.* 1987), and is known to be involved in the final processing of the remnants (Brunzell J.D., 1995). In fact, the treatment of chylomicrons with hepatic lipase, results in a more rapid clearance of the remnants by rat liver (Borensztajn, J., *et al.* 1988; Shafi, S., *et al.* 1994). Furthermore, it has been demonstrated that *in vivo* antibody-mediated inhibition of hepatic lipase retards chylomicron clearance (Sultan, F., *et al.* 1990).

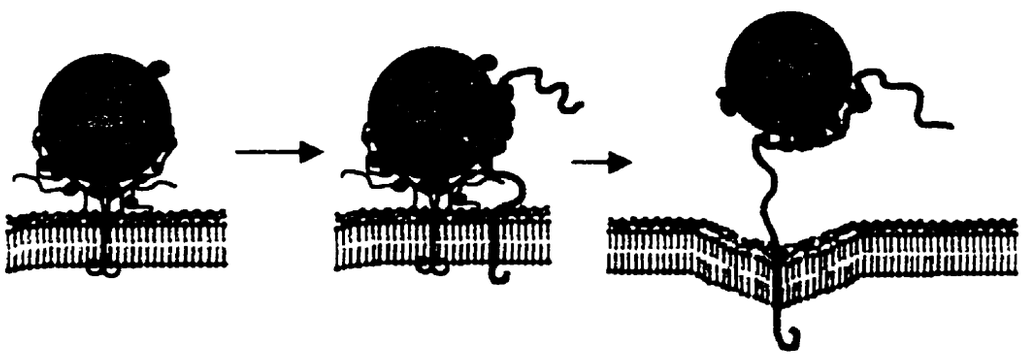

Figure I-9 The final events in remnant lipoprotein metabolism, including their apoE and LPL mediated internalization, through HSPG and the LRP.

This figure depicts the final event of TG-rich lipoprotein metabolism. ApoE-enriched remnant lipoproteins attach to HSPGs and are then directly internalized, or are passed onto the LRP for internalization. Which ever way is the predominant mode of remnant internalization, both molecules seem to actively participate in the clearance of the remnants (adapted from Mahley, R.W., and Rall, S.C., 1995)

The culminating step in this metabolic process, is the apoE-mediated uptake of the remnant lipoproteins by cell-surface receptors. The importance of apoE in remnant lipoprotein uptake is exemplified by the pathological accumulation of these lipoproteins

in the plasma of individuals who have inherited receptor-defective variant isoforms of apoE (Hui, D.Y., *et al.* 1984). Similarly, there is an accumulation of remants in mice that are deficient in apoE as a result of experimental gene targeting (Plump, A.S., *et al.* 1992; Zang, S.H., *et al.* 1992). The LDL receptor is capable of mediating the uptake of apoE-containing remnant particles. While the LDL receptor binds both apoB-100 and apoE, with affinities of 2.6×10^{-9} M (Pitas, R., *et al.* 1980), apoE enriched remnants bind with greater avidity, presumably due to multiple interactions between the remnant and several sites on the receptors (Innerarity, T.L., *et al.* 1978; Pitas, R. *et al.* 1979; Innerarity, T.L., *et al.* 1981). This higher avidity likely contributes to the much more rapid, apoE mediated, hepatic uptake of chylomicron remnants (minutes to hours) compared to the apoB-mediated uptake of LDL (2 to 3 days).

In addition to the LDL receptor, there is strong evidence for the existance of a second "hepatic remnant lipoprotein receptor" that would recognize apoE- but not apoB100-containing lipoproteins. Humans and animals who genetically lack functional LDL receptors, accumulate apoB100-containing lipoproteins, especially LDL in plasma, whereas chylomicron remnants are cleared normally. In fact, apoE-enriched remnants were shown to be cleared at an enhanced rate in Watanabe rabbits which do not express functional LDL receptors (Mahley, R.W., *et al.* 1988). In 1988, the low density lipoprotein receptor related protein or LRP was cloned, and proposed as a candidate for the putative remnant lipoprotein receptor (Herz, J., *et al.* 1988).

1.7 The Low-Density-Lipoprotein Receptor-Related Protein (LRP), a candidate for the Chylomicron Receptor

The LDL receptor-related protein or LRP, was first proposed to be a likely candidate for this receptor activity, on the basis of its striking structural similarity to the LDLr (Herz, J., *et al.* 1988). Indeed, the LRP was shown to be specific for apoE-enriched lipoproteins (Kowal, R.C., *et al.* 1989; Beisiegel, U., *et al.* 1989). The LRP is a member of the LDL receptor super gene family, which also includes the gp 330 receptor, and the VLDL receptor (Figure I-10).

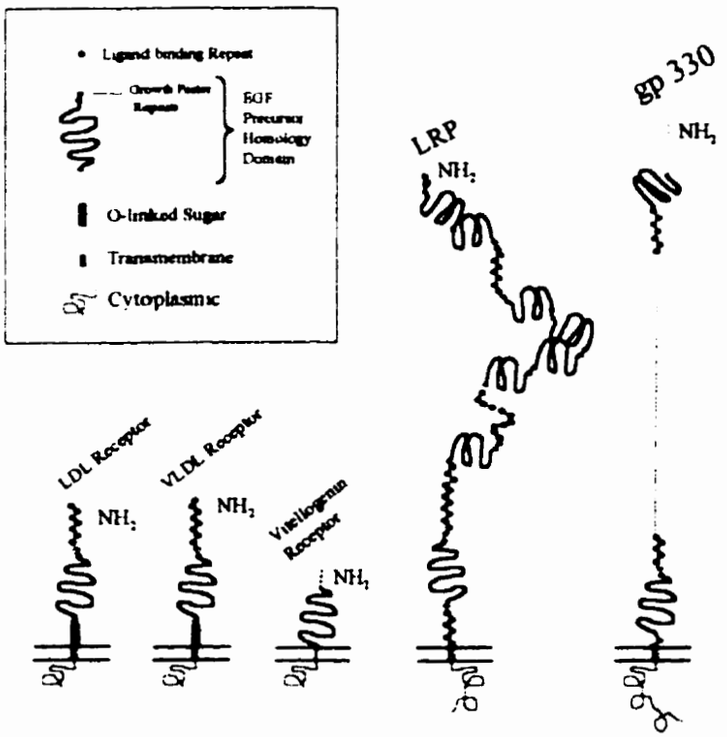

Figure I-10 The LDL Receptor super gene family.

This figure depicts some of the identified members of the LDL receptor super gene family. All were originally identified through their homology to some of the conserved domains of the LDLr. The VLDLr, LRP and gp 330 were cloned owing to their homology to the ligand binding domain of the LDL receptor (adapted from Goldstein, J.L., *et al.* 1995).

Under physiological conditions, both the LDLr as well as the LRP appear to be equally effective in mediating the uptake of chylomicron remnants within the liver. The LRP is an extremely large, multifunctional cell surface receptor. ApoE is but one of its many known ligands, which also include; lipoprotein lipase (Beisiegel, U., *et al.* 1991), the activated protease inhibitor α_2-macroglobulin (Kirstensen, T., *et al.* 1990), plasminogen activator inhibitor (Nykjaer, A., *et al.* 1992), and lactoferrin (Huettinger, M., *et al.* 1992). The LRP resembles the LDLr in being a chimeric protein whose gene appears to have been assembled by exon shuffling, and includes structural domains that are similar to those that constitute the LDLr including 31 imperfect cysteine rich repeats, that are highly homologous to the 7 cysteine-rich repeats that constitute the ligand-binding domain of the LDLr.

As shown in Figure I-9, the LRP is thought to work in concert with cell-surface HSPGs. ApoE-enriched remnants would first associate with HSPGs that would form a complex with the LRP, or transfer the remnant to the LRP for eventual internalization by the hepatocytes. It would appear that this collaboration between HSPGs and the LRP is essential, since the LRP alone is incapable of mediating cell surface binding (Ji, S.Z., *et al.*1993; Ji, S.Z., *et al.* 1994). However, it is believed that the HSPGs may by themselves be capable of promoting the effective plasma clearance of the chylomicrons (Mahley, R.W., unpublished opinions)

Section 2

The Low-Density-Lipoprotein Receptor

2.1 Historical Perspectives Relating to the Discovery of the LDL-Receptor

In their attempt to elucidate the molecular basis of the inheritable metabolic disorder which leads to pathologically elevated levels of plasma cholesterol, or familial hypercholesterolemia (FH), Drs. Brown and Goldstein discovered, in 1974, the major physiological mechanism which regulates plasma cholesterol homeostasis (Goldstein, J.L., and Brown, M.S., 1974). In 1953, Gould and collaborators had demonstrated the existence of a negative feedback mechanism in the hepatic cholesterol biosynthetic pathway, using experimental dogs fed with high levels of dietary cholesterol (Gould, R., *et al.* 1953). Brown and Goldstein showed that the addition of LDL, but not HDL to the culture medium, could down regulate endogenous cholesterol synthesis at the level of the rate-limiting enzyme, 3-hydroxyl methyl glutaryl Co-A reductase (HMG Co-A reductase), in cultured human skin fibroblasts of normal individuals. In contrast, the HMG Co-A reductase activity in fibroblasts from FH patients was insensitive to the presence of exogenous LDL. Following a series of elegant experiments, Brown and Goldstein showed that the defect in the FH fibroblasts resulted from an inability to extract

cholesterol from LDL due to the lack of a high affinity cell surface receptor for LDL. (Anderson, R.G.W., *et al.* 1976, 1977). It was shown that when LDL bound to the LDL-receptor (LDLr) on normal fibroblasts, it was quickly internalized and that within 60 minutes, the protein component was completely hydrolyzed.

2.2 The Role of the LDL- Receptor in Cholesterol Homeostasis

The LDLr is a transmembrane glycoprotein consisting of 839 amino acids. This receptor is expressed on the surface of all cells of the body, and has a high affinity for apoE-enriched VLDL remnants as well as for apoB-100 containing LDL (Brown, M.S., and Goldstein 1986; Mahley, R.W., 1988). The LDL-receptor pathway was first described by Brown and Goldstein, and it is the prototype of many ligands that are taken up by receptor-mediated endocytosis. (Pastan, I.H., and Willingham, M.C., 1981; Bretscher, M.S., and Pearse, B.M.F., 1984; Czekay, R.P., *et al.* 1997). The LDLr is translated as a pro-protein in the endoplasmic reticulum, where its secretory sequence is cleaved. This 120 kDa protein undergoes extensive glycosylation in the Golgi apparatus to yield a 160 kDa mature protein. As shown in Figure I-11, following their emergence on the cell surface, some 45 minutes after synthesis, the receptors quickly cluster in clathrin-coated pits (Anderson, R.G.W., *et al.* 1976), whether bound to lipoprotein ligands or not. Within three to five minutes of their formation, the coated pits are internalized within the cell as coated endocytic vesicles, thereby removing lipoprotein-bound cholesterol, and other lipids from the circulation.

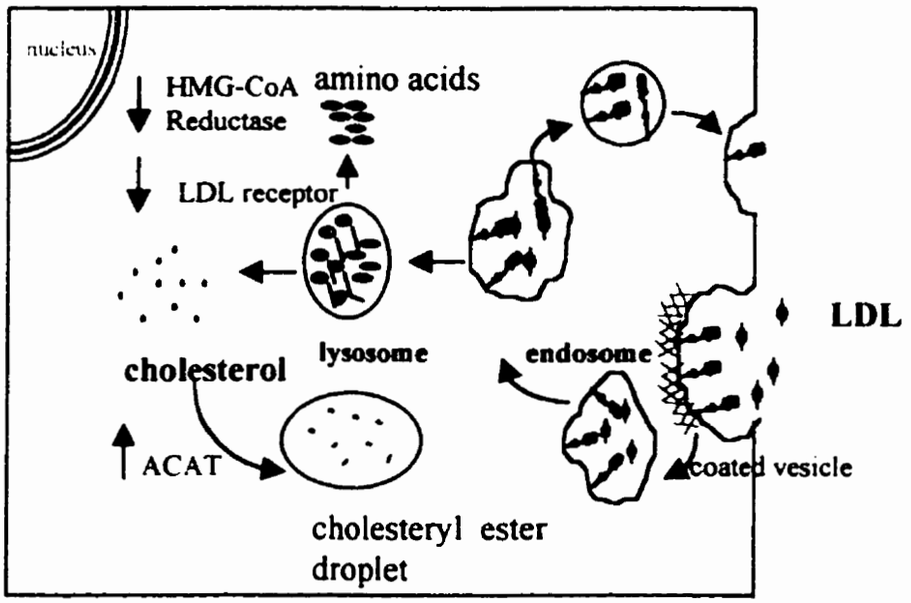

Figure I-11 The LDL-Receptor Pathway

This figure depicts the cellular events which characterize the LDL Receptor pathway. Following their emergence on the cell surface, LDLrs gather into clatrin coated pits whether bound to lipoproteins or not. The clustered complex is then quickly internalized into vesicles which become acidified through the action of proton pumps. A drop in pH causes the uncoupling of the receptor-ligand complex, with the concominant catabolism of the lipoprotein and the recycling of the receptors to the cell surface. The accumulation of intracellular cholesterol cause the modulation of certain enzyme activities (adapted from Goldstein, J.L., *et al.* 1995).

Once internalized within the cell, the vesicles rapidly lose their clathrin coat and fuse with many other such newly formed vesicles resulting in the formation of large irregularly shaped organelles called endosomes or "receptosomes". These organelles become acidified through the action of ATP-driven proton pumps, which reside within the plasma membrane (Helenius, A., *et al.* 1983). When the intravesicular pH falls to 6.5, the LDLr dissociates from its lipoprotein ligand. The liberated receptors then migrate, along with other receptors, to distal regions of the organelle, where they pinch off and return to the cell surface for further use, whereas the lipoproteins are hydrolyzed within lysozomes. The recycling time for an LDL receptor is about ten minutes, and the LDLr can be reused up to 150 times, during its 10-30 hour life-span.

The lipoprotein-derived cholesterol that is delivered to the cells is then esterified to free fatty acids, through the action of the intracellular enzyme acyl-coenzyme A : cholesterol acyltransferase (ACAT), and stored as lipid droplets. Such accumulation of cholesterol within the cell is sensed, and causes the down regulation of LDLr synthesis at the transcriptional level. As previously mentioned, the activity of the biosynthetic enzyme, HMG Co-A reductase is also down-regulated in the presence of excess cholesterol, through complex mechanisms that include modulation of transcription, mRNA stability and protein stability (Goldstein, J.L., *et al.* 1985). The importance of the LDLr in cholesterol uptake is exemplified in humans who lack functional LDLr and consequently suffer from the disorder FH, as well as in animal models of the human disorder.

2.3 Structure and Molecular Biology of the LDL Receptor

The LDLr gene is a mosaic of exons which share an evolutionary history with exons of several other genes, suggesting that the gene was assembled by exon shuffling (Goldstein, J.L., *et al.* 1985). The human gene is located on the distal short arm of chromosome 19. It spans 45 Kb and is divided into 18 exons and 17 introns. The protein is composed of five discrete functional domains, encoded by the combination of various exons, as depicted in Figure I-12. Exon 1 encodes a short 5' untranslated region as well as the signal sequence composed of 21 hydrophobic amino acids. Exons 2 to 6 encode the ligand binding region, which is composed of seven imperfect repeats of a 40 amino acid, cysteine-rich sequence.

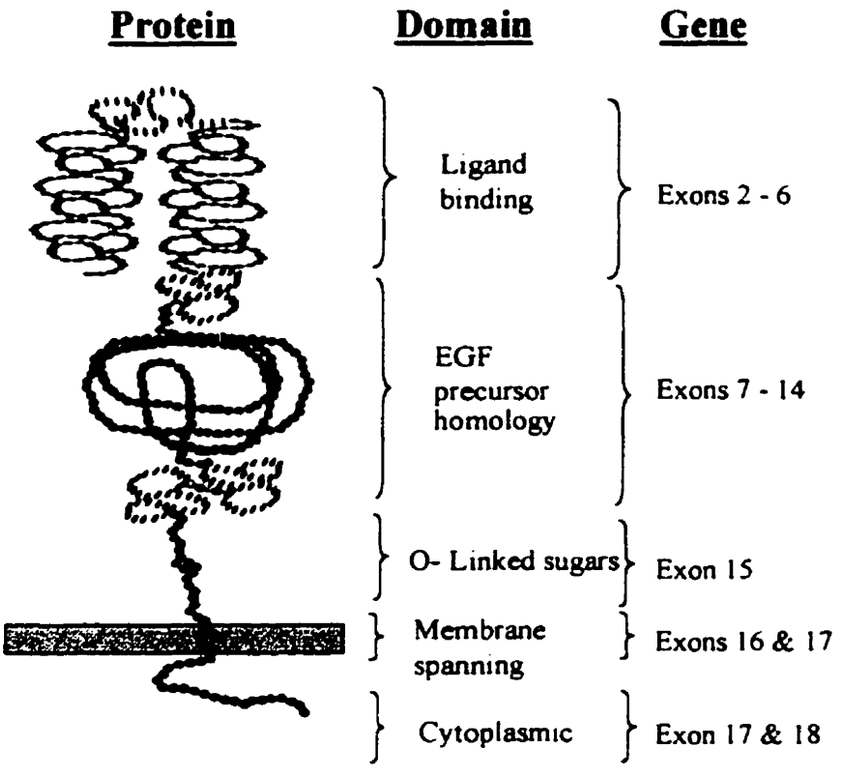

Figure I-12 The LDL Receptor.

This figure ilustrates the structural organization of the LDLr gene and protein. The protein is composed of structural domains, which are known to contribute to the various functions of the protein. The ligand binding domain, which is madeup of seven inperfect cysteine-rich sequences, is responsible for ligand binding. The EGF precursor homology domain is essential for receptor recycling and appears modulate ligand binding. The O-linked sugar domain as of yet has no clear function, but may serve in helping the receptor project off the surface of the cell. Finally, there is a membrane spanning domain and a cytoplasmic domain which allow for clustering, internalization and recycling respectively (adapted from Goldstein, J.L., *et al.* 1995).

These repeats show strong resemblance to sequences found in the blood complement factors: C7, C8a, C8b, and C9. All of the repeats contain six cysteines, that form three intra-repeat disulfide bonds. The three-dimensional structure of repeats 1 and 2 has recently been solved using NMR spectroscopy (Daly, *et al.* 1995, 1995). As well, the arrangements of the three disulfide bonds of one of these repeats, has also been determined (Bieri, S., *et al.* 1995). In aqueous solution, the three-dimensional structure contains a β-hairpin followed by a series of turns. Within the structure, the disulfide

links were determined to consist of residues Cys 6 bonded to Cys 18, Cys 13 to Cys 31, and Cys 25 to Cys 42. At the C-terminal end of each the seven repeats, a cluster of negatively charged amino acids, consisting in part of an "Asp-X-Ser-Asp-Glu" (DxSDE) motif is invariably present. It has been thought that these clusters of negatively charged residues interact with clusters of positively charged residues on apoB-100 and apoE (Goldstein, J.L., *et al.* 1985). As will be described later, the receptor binding site on apoE includes a positively charged cluster of amino acids, all residing on the same side of an alpha helix, exposed to solvent (Lalazar, A, *et al.* 1988; Wilson, C., *et al.* 1992). More recently, it has been proposed that the DXSDE motif may in fact be important in the formation of a calcium binding site, which appears to be essential for the proper folding of the repeat (Blacklow S.C., *et al.* 1996). In support of a role for calcium in maintaining the conformation of the LDLr ligand-binding domain, the interaction of the LDLr with apoB or apoE is known to be calcium-dependent and an anti-LDLr monoclonal antibody has been isolated that is specific for a calcium dependent conformational epitope within the first cysteine-rich repeat (Biesigel, U. *et al* 1981).

Each of the seven cysteine-rich repeats is encoded by a single exon, with the exception of repeats 3, 4 and 5, which are encoded by exon 4. Since the splice junctions for exons 2 to 7 are in frame, the deletion of any one exon does not disrupt the reading frame of the mRNA, and permits its translation into protein. It has been shown by deletion mutagenesis that not all of these repeats contribute equally to lipoprotein binding, but rather seem to contribute in an independent way. Repeat one was shown to contribute very little to either apoB or apoE binding. LDL binding is reduced up to 95%,

with the deletion of any one of the remaining six repeats, whereas β-VLDL binding, which is mediated almost exclusively through apoE, is reduced by 50% with the deletion of the fifth repeat, but is relatively insensitive to the loss of any of the other repeats. A naturally occurring variant of the LDLr, which involves the loss of both the first and second repeats, results in normal binding to β-VLDL, however, binding to LDL is reduced by 29% (Esser, V., *et al.* 1988; Russell, D.W., *et al.* 1989). The LDLr may, therefore, use a combination of repeats two to seven in order to bind LDL whereas, the use of repeat five is sufficient in order to bind apoE-containing lipoproteins. Other interpretations of the these mutagenesis studies are, however, possible. The more stringent requirement for LDL versus β-VLDL binding by the receptor, creates a situation where an FH individual with an exon deletion in the receptor-binding domain may have a selective inability to remove LDL but not VLDL (or IDL) from the circulation (Goldstein, J.L., *et al.* 1985).

Exons 7 to 14 of the LDLr encode the 400-amino acid epidermal growth factor (EGF) precursor homology domain, thus termed due to its 33 % resemblance to a portion of the EGF precursor. This region includes three growth factor repeats, which consist of 40-amino acid cysteine-rich sequences that differ from the cysteine-rich repeats found in the ligand binding domain. The two first growth factor repeats are contiguous and are separated from the third repeat by a stretch of 280-amino acids that contains five copies of a conserved Tyr-Trp- Thr- Asp (YWTD) motif, that is repeated once every 40 to 60 amino acids. The EGF precursor homology domain is required for acid-dependent dissociation of lipoproteins from the receptor in endosomes during receptor recycling.

Presumably, it also serves to position the ligand-binding domain so that it can bind to LDL on the cell surface. This domain is known to be calcium dependent for its proper folding, and physiological function (Downing, A., *et al.* 1996). Mutant forms of the receptor which lose the capacity to bind calcium in this domain, are incapable of interacting with LDL, and lead to an FH phenotype.

Exon 15 encodes a segment comprised of 58 amino acids rich in serines and threonines, many of which serve as sites of attachment for O-linked carbohydrate chains. While this domain of the LDLr is not essential for internalization of LDL by cultured fibroblasts, deletion of this exon in two families did lead to a heterozygous FH phenotype, indicating a possible role for this domain in the function of the receptor within the liver. It has been postulated that extensive glycosylation at this site may permit interactions with the cell surface heparin proteoglycans to keep the LDLr extended from the surface of the cell, and accessible to circulating plasma lipoproteins (Goldstein, J.L., *et al.* 1985)

Exons 16 and the 5' end of exon 17 encode the residues of the membrane-spanning domain which consists of 22 hydrophobic amino acids. The remainder of exon 17 as well as the 5' end of exon 18 code for the remaining 50 amino acids that correspond to the intracellular or cytoplasmic domain. This domain is divided into two functional halves; one of which directs the receptor to the clathrin coated pits and the second which targets the receptor to the sinusoidal surface of the polarized hepatocytes. The remainder of exon 18 encodes a 2.6 Kb 3' untranslated region.

2.4 Regulation of the numbers of LDL-r on cell surfaces

The active promoter of the LDLr is composed of a 200 bp segment located immediately upstream of the initiator methionine codon. This 5' flanking region contains most, if not all, of the necessary cis-acting DNA sequences responsible for the sterol-regulated expression of the gene in mammalian cells. Three imperfect direct repeats consisting of 16 bp each, two A / T-rich sequences and a cluster of mRNA initiation sites, all function in the regulated transcription of this gene. Two of the direct repeats, repeats 1 and 3, interact with the positive transcription factor Sp1. However these sequences by themselves are not sufficient to provide high level transcription. The second direct repeat, which contains the conditional-positive sterol regulator element one or "SRE-1", is needed in addition to the Sp1 sites in order to give rise to high levels of transcription (Sudhof, T.C, *et al.* 1987).

The SRE-1 element is a 10 bp sequence that is also found in the promoter of the enzyme HMG-CoA synthase which is known to be regulated by sterols, and in the promoters of many other biosynthetic enzymes responsible for the synthesis of cellular lipids. When cells are grown in the absence of sterols, the SRE-1 synergizes with the Sp1 site in promoting the transcription of the LDLr, an activity it loses upon the accumulation of sterols. In a yet undetermined way, a family of intracellular proteins, of which there exist two closely related forms in addition to some splice variants, termed the SREBP-1 and 2, or SRE binding proteins, act as intracellular sterol gauges. The SREBP-2 is by far the best characterized form of this group of transcription factors, and to date all other forms are believed to act with a certain amount of redundancy. One of the two splice

variants originating from SREBP-2, termed ADD-1, is produced by pre-adipocytes which are actively engaged in differentiating into mature adipocytes. Presumably, ADD-1 activates the transcription of certain genes involved in lipid metabolism within mature adipocytes (Goldstein, J.L, *et al.* 1995).

In situations of cellular cholesterol abundance, SREBP-2 is associated with the membrane of the nuclear envelope and endoplasmic reticulum, through two transmembrane domains, and exists as a looped structure directed to the cytoplasm. Upon cholesterol deprivation, both transmembrane domains become the substrate for proteolytic cleavage by two specific intracellular proteases. The proteases are known to act in an ordered sequence, with the hydrolytic activity of the one responsible for the initial cut being strictly regulated by the presence of cholesterol (Duncan, E.A., *et al.* 1997). The SREBPs are members of the basic-helix-loop-helix-leucine zipper (bHLH-ZIP) family of transcription factors. Members of this family are known to bind DNA either as homodimers or heterodimers. DNA binding is mediated by the basic region, and dimerization is mediated by the helix-loop-helix and leucine zipper structures.

The released NH2-terminal fragment of SREBP-2, which contains a nuclear localization signal, then transits across the nuclear membrane and associates with SRE-1 through its bHLH-ZIP domain, giving rise to greatly enhanced promoter activity. The SREBP-1 and SREBP-2 are unlike all other members of bHLH-ZIP family in two important ways. First they are much larger, consisting of 1147 and 1141 amino acids respectively, compared to the 160-536 amino acids for other members of the family.

Secondly they do not recognize palindromic sequences, but rather the SRE-1 sequence element which contains the direct repeat of CAC (5'-TCACCCCAC-3').

2.5 LDL-Receptor mutations causing Familial Hypercholesterolemia

Brown and Goldstein, have, over the years, assembled a collection of cultured fibroblasts of some 157 unrelated FH homozygous and 13 FH heterozygous patients in their laboratory, at the University of Texas South-Western Medical Center. These cell strains are designated the Dallas collection. Approximately 41 % of the FH homozygotes in this collection are true homozygotes as determined by haplotype mapping as well as by mutational analysis. The remaining FH homozygotes are compound heterozygotes, having inherited two different non-functional alleles. Since the same mutation has rarely been identified in unrelated individuals, the Dallas collection contains some 190 different mutant alleles of the LDLr. However in certain ethnic populations, a specific mutant allele of the LDLr has achieved a high frequency through a founder effect. Examples of this occurrence include the French Canadians, Afrikaners, Lithuanian Jews, Finnish, and Christian Lebanese.

Molecular analysis of 127 LDLr genes has been very informative with respect to the function of the various domains of the protein in relation to its structure. In fact, all of the known mutant alleles can today be subdivided into five classes that were determined by the functional behavior of the mutant receptors (Figure I-13). Class 1 alleles fail to produce an immunoprecipitable protein (null alleles). Class 2 alleles are

produced but are not transported to the cell surface. Presumably there is a problem with the intracellular folding of these alleles and they are simply retained within the cell and ultimately degraded. Class 3 mutants are expressed on the cell surface but are incapable of interacting with their apolipoprotein ligands. As stated previously, the binding properties of the receptor are conveyed by the collective co-operation of the cysteine-rich sequences that comprise the ligand-binding domain. Class 4 mutants fail to cluster within clathrin coated pits, and hence are unable to mediate the endocytosis of bound lipoproteins. Finally, class 5 mutant receptors function normally in their internalization of bound LDL, but fail to undergo pH-dependent dissociation from the ligand and, as a consequence, are not recycled.

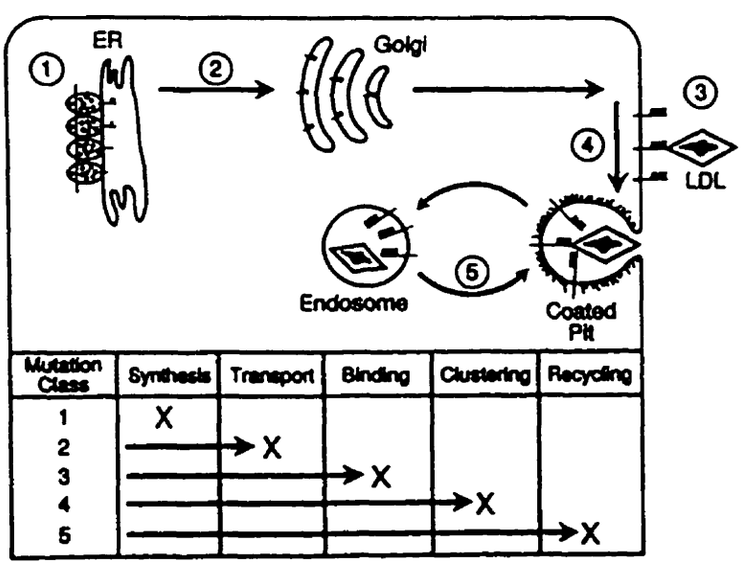

Figure I-13 Mutations causing defective LDL receptors.

This figure depicts the five classes of LDLr mutations that lead to HF. Class 1 mutants fail to be synthesized, whereas class two mutants fail to be transported to the cell surface. Class 3, 4 and 5 mutants are synthesized and transported to the surface, but each one fails in some way to function adequately in the receptor cycle. Class 3 mutants fail to bind LDL, whereas class 4 mutants bind LDL but do not cluster into coated pits and are not internalized. Finaly, class 5 mutants bind and internalize LDL, but fail to recycle (adapted from Goldstein, J.L, *et al.* 1995).

Section 3

Atherosclerosis

Much of this section has been written with the extensive use of the following volumes as a source of reference:

-Molecular Genetics of Coronary Artery Disease 1992.

-Atherosclerosis Reviews volume 25 1993.

-Atherosclerosis X (International Congress Series) 1994

3.1 The Etiology of Atherosclerosis

Atherosclerosis is a disease of the vascular system, which is known to arise due to multifactorial interactive events within this tissue, and whose pathobiology is, as yet, poorly defined. The disease culminates in the obstruction of blood flow, resulting in ensuing cellular anoxia and death. The pathology is recognized as the progressive growth of an "atherosclerotic plaque" which occurs in the area located between the endothelial cell layer and the internal elastic lamina, called the intimal space or "intima" . It has been well established that, within the vasculature, there are certain sites which are more inclined to plaque development, and such locations have been termed "sites of predilection" (Feldman D.L., *et al.* 1984; Stary, H.C., 1987) that include the coronary

arteries as well as the large arterial branches of the aorta. The consequences of premature atherosclerosis, in particular myocardial infarctions, collectively serve to place this disorder as the most important cause of mortality in industrialized nations.

3.2 The Evolution of an Atherosclerotic Plaque

The actual physical composition of an atherogenic plaque is not at all well definined in terms of ultrastructure. Morphologically, a plaque appears to result from the conversion of a fatty streak, made of dysfunctional macrophages, into a fibrous plaque composed of various cell types (Jonasson, L., *et al.* 1986), cellular debris which may originate from necrosis, and chemically inert deposits formed mostly of crystallized cholesterol. The elucidation of certain, well established physiological mechanisms which lead to the initiation and progression of an atherosclerotic plaque, have served to stimulate research related to the possible reversal of the disease and to the physiology of plaque regression.

3.3 The Fatty Streak

The incipient event now accepted as the origin of an atherosclerotic plaque, is the fatty streak which is composed of tiny aglomerations of lipid layden smooth muscle cells and leukocytes within the intima which have been called foam cells. Such macrocellular agglomerations develop spontaneously in healthy experimental animals which are fed cholesterol-rich diets, and in animal models of human disorders of lipid metabolism (Rosenfeld, L., *et al* 1989). In fact, autopsies performed on non-cardiovascular related

infant deaths reveal that, within the human population, the development of such lesions early in life is quite frequent and, by and large is considered normal (Stary, H.C., 1987).

3.4 The Endothelium

The entire inner surface of the mammalian vasculature is covered by a continuous, unicellular layer of endothelial cells. The variability in the cellular permeability of the endothelium, is a function of the inducible cell surface expression of integrin and selectin counterreceptors, which serve to anchor leukocytes to the endothelium, and allow their entry, which occurs through transendothelial cell migration (McEver, R.P., 1993). As will be presented below, the entry of phagocytic cells into intimal spaces of the vasculature, forms the basis of the modern concepts of lipoprotein-derived atherogenesis.

3.5 Response to Injury Model

For almost 150 years, investigators have known that physical or chemical injury to the endothelium can lead to the formation of vascular lesions. The "response to injury" model, which describes the genesis and evolution of atherosclerotic lesions within the vasculature, was first elaborated by Russell Ross and his colleagues at the University of Washington (Ross, R., 1986). The underlying initiator of an atherogenic event, as defined through this theory, is physical damage to the vascular endothelium. Cell culture experiments have demonstrated that high levels of plasma LDL, oxidized LDL, as well as certain inflamatory cytokines, can cause either direct toxicity (Steinberg,

D., 1997), stimulation of endothelial cells, or act as chemoattractants for circulating monocytes (Cushing, S.D., *et al.* 1990). In response, endothelial cells upregulate the expression of a certain class of cell adhesion molecules (McEver, R.P., 1993). that have an immunoglobulin-like structure, and serve as counter-receptors for leukocyte integrin and selectin molecules.

The vascular cell adhesion molecule-1 or VCAM-1, rapidly accumulates on endothelial cell surfaces upon stimulation with cytokines, and has been shown to be expressed on endothelial surfaces at sites of atheromas (Cybulsky, M.I., and Gimborne, M.A., 1991). The presence of this integrin receptor has been suggested to play a role in the pathologic recruitment of monocytes which, as will be described in section 3.3, are directly implicated in the oxidative modification of LDL, and which consequently lead to foam cell development.

3.6 Lipoprotein Derived Atherosclerosis

Of the various classes and types of plasma lipoproteins, LDL is the most atherogenic. Seemingly, the atherogenicity of lipoproteins stems directly from their uncontrolled cellular uptake, through a class of cell surface receptors termed "scavanger receptors" present on activated macrophages and smooth muscle cells (Kreiger,M., and Herz, J., 1994) whose normal physiological role is thought to be in non-adaptive immunity. These scavenger receptors can recognize chemically modified LDL but not native LDL (Goldstein, J.L, *et al.* 1995). While much of the LDL within the intima is

believed to be cleared nomally through LDL receptor-mediated uptake by resident macrophages and smooth muscle cells, in pathological situations, LDL can be chemically modified by oxidative processes within the intima and thus become a ligand for the scavenger receptor. Other cell surface receptors that can internalize lipoproteins in an uncontrolled way, including TG-rich lipoproteins, could also be implicated (Bradley, W.A., and Gianturco, S.H. (1994); Ramprasad, M.P., et al. 1995; Gyton, J.R., 1995).

In response to endothelial injury, which may in fact be due to excessive plasma cholesterol, circulating monocytes adhere to the wounded endothelial area and infiltrate the intima. Once within this anatomical location, the monocytes can differentiate into activated macrophages, which in turn are known to generate and release oxidative intermediates, such as superoxide ions. It is these oxidative intermediates which are then believed to chemically modify both the protein and lipid components of the LDL which transforms it from a ligand for the LDLr to one for the scavenger receptor. As described in section 3.2, the progressive accumulation of lipid-laiden macrophages and smooth muscle cells within the intima, lead to the formation of fatty streaks. Progression of fatty streaks to atherosclerotic lesions is a function of the individual's lipid profile, and particluarly, circulating LDL levels.

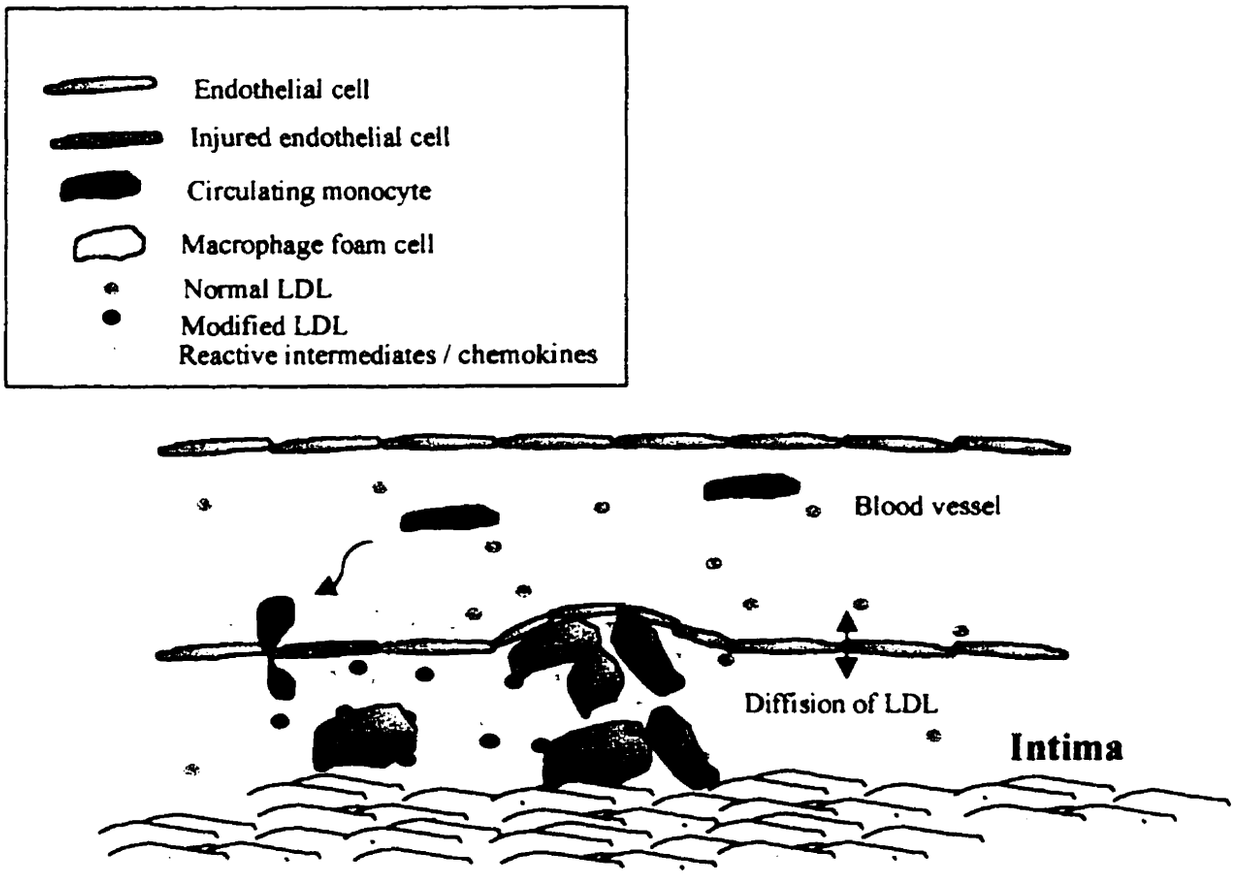

Figure I-14 Atherosclerosis development

As shown by the figure, many factors appear to contribute to the occlusion of an artery. Endothelial tissue damage, which may result from various causes, gives rise to reactive chemical substances which rapidly modify circulating LDL. The LDL, in turn, filter into the intimal space of the vasculature. The modified LDL act as chemoattractants to blood-borne circulating monocytes, which infiltrate the intima, and actively clear the modified LDL lipoproteins, through a non-regulated receptor-mediated process. The excessive uptake of such lipoproteins, eventually cause the macrophages to become dysfunctional "foam cells" which accumulate and collectively serve to generate a component of the occlusion. Other components of the atherosclerotic plaque include, crystalized cholesterol liberated from necrotic foam cells, and various forms of lymphocytes (adapted from Ross, R., 1986).

Section 4

Apolipoprotein E

The three general references cited below were used extensively to describe the structural and functional relationships of human apolipoprotein E.

-Weisgraber, K.H., 1994.

- Mahley, R.W.. 1988.

- Mahley, R.W. and Rall, S.C., 1995

4.1 Human Apolipoprotein E

Apo E, first discribed by Shore and Shore in 1973 (Shore, V.G., and Shore, B., 1973) as the arginine-rich plasma protein of VLDL, is the best understood apolipoprotein in terms of structure as well as function. The 3.7 kilobase apoE gene is located on human chromosome 19, and is composed of 4 exons separated by three introns (Das, H.K., *et al.* 1985; Paik, Y.K., *et al.* 1985). The apoE gene lies in close proximity to the genes encoding the C apolipoproteins. In fact, based on nucleotide homology and

similiarities in the intron-exon organization, the genes encoding apoE the apoCs and the A apolipoproteins appear to constitute a multigene family that has arisen from a common ancestral gene through gene duplicative events. Members of the apolipoprotein gene family have, in common, the amphipathic alpha-helix as part of their secondary structure, a property that is essential for their ability to reversably associate with lipoprotein particles (Segrest, J.P., *et al.* 1994).

The transcription of the apoE gene is driven by at least two enhancer elements, one of which is located intracistronically and seems to be active in all tissues expressing the protein, and by a second one which functions solely in liver parenchymal cell and is located some 13 kbs 3' of the gene, and which also controls the expression of apoC-I (Simonet, W.S., *et al.* 1993). The major site of apoE expression is in the liver, followed by the brain, where it is produced mostly by astrocytes (Pitas, R.E., *et al.* 1987). Since the blood-brain barrier prevents any infusion of plasma lipoproteins, apoE produced by astrocytes is postulated to take part in lipid distribution within the CNS (Mahley, R.W., 1988). Recently, it has been demonstrated that apoE directly participates in nerve regeneration, presumably through local lipid delivery to cells in need of cellular membrane reconstruction (Mahley, R.W., and Rall, S.C., 1995). In addition to liver cells, which secrete almost 90% of the total plasma apoE, macrophages are known to be capable of producing large quantities of apoE within the interstitial spaces of various organs. In fact, most of the apoE present within the remaining organs of the body is thought to originate from infiltrating macrophages (Basu, S.K., *et al.* 1981, 1982). The presence of apoE, both within the circulation as well as within interstitial spaces, allows

it to readily associate with triglyceride-rich remnant lipopoteins. As previously mentioned, lipoprotein-bound apoE facilitates their metabolic conversion to remnant lipoproteins, as well as their uptake via cell surface receptors, through the interaction with cell surface receptors and proteoglycans.

The mature messenger RNA encoding apoE is translated into a 317 amino acid secreted pro-protein which is post translationally cleaved at the amino terminus, releasing an 18 amino acid signal sequence. While apoE can be glycosylated on threonine 194, it is now believed that only a subset of cells actually secrete apoE as a glycoprotein. This glycosylation imparts size and electrophoretic heterogeneity that has no obvious physiological consequences. Human apoE is a 34 kDa protein that exists as three common isoforms within almost all ethnic populations. The isoforms are encoded by three separate and co-expressed alleles termed ε2, ε3 and ε4, which occur with an approximate frequency of 10, 70 and 20% frequency, respectively, within the general population.

The polymorphisms which occur at residues 112 and 158, that are resolvable by isoelectric focusing (Zannis, V.I., and Breslow, J.L., 1981; Menzel, H.L., and Uttermann, G., 1986), consist of cysteine and arginine interchanges (Weisgraber, K.H., *et al.* 1981). The most common isoform, apoE3, has a cysteine at position 112 and an arginine at position 158. As shown in figure IV-15, apoE3 migrates between the the two other forms on an isoelectricfocusing gel, with apoE2 (Cys^{112}, Arg^{158}) being closest to the anode, and apoE4 (Arg^{112}, Arg^{158}) migrating closest to the cathode.

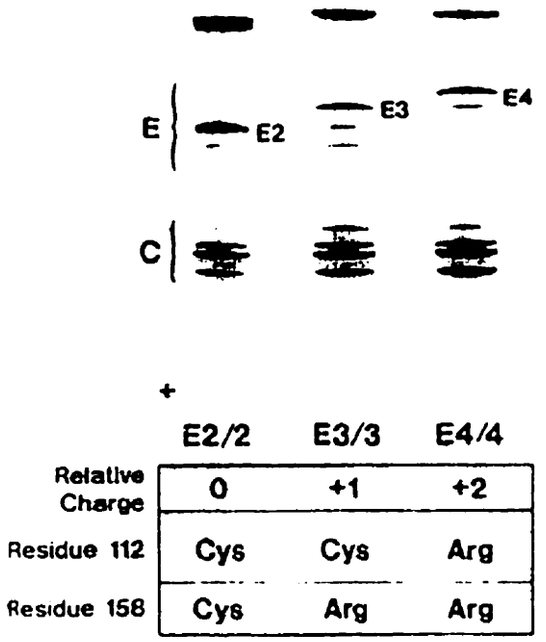

Figure L15 Isoelectric focussing of human apoE.

This figure presents the common forms of human apoE, as resolved through isoelectric focusing. ApoE2 containing two cysteines at the polymorphic sites, is the most acidic of the isoforms. ApoE4 which contains two arginines at the polymorphic sites is the most basic, and thus migrates closer to the cathode. ApoE3 which has a cysteine at position 158 and an arginine at position 112 has an isoelectric point intermediate between those of apoE2 and apoE4. All three major isoforms also show electrophoretic heterogeneity due to sialylated forms of the proteins (adapted from Weisgraber, K.H., 1994).

ApoE polymorphisms influence; apoE-mediated binding to cell surface receptors and proteoglycans, post prandial lipemia, apoE distribution in lipoprotein subfractions and plasma lipid levels. In addition to its established roles in lipoprotein metabolism, apoE is known to be implicated in other, apparently unrelated, physiological events. The inheritance of the ε4 allele has recently been shown to be highly associated with susceptibility to the development of the late onset form of Alzheimer's disease (Strittmatter, W.J., *et al.* 1993). The mechanism for this association has not been determined but could involve apoE isoform-specific differences in the interactions of apoE with either the β-amyloid pepide or with microtubule-associated proteins within neurons, in apoE-mediated modulation of neuronal outgrowth or in the ability of apoE to scavenge oxidative free radicals (Higgins,G.A., *et al.* 1997). A role for apoE has also been proposed within the immune-system. ApoE-containing lipoproteins, as well as

peptide fragments of apoE can modulate lymphocyte activation by inducing lymphocytes to be resistant to proliferation (Curtiss and Edington 1976, 1978; Hui *et al.* 1980a,b; Pepe and Curtiss 1986). The mode in which apoE acts as an immunoregulator is not fully known, but seems to involve a low *affinity* cell surface receptor distinct from the LDLr. Finally, apoE is being recognized as a protein with a specific role in the blood coagulation process, acting as an inhibitor of platelet aggregation through the L-arginine:nitric oxide pathway (Riddel, D.R., *et al.* 1997).

4.2 ApoE Structure

The biphasic denaturation curves recorded by circular dicroism in chemical denaturation experiments, have indicated that apoE is made up of two independantly folded domains. The first transition is typical of many of the plasma apolipoproteins which have quite low energies of stabilization, whereas the second transition more closely resembles that of stable globular proteins (Wetterau, J.R.. et al. 1988). Limited proteolytic digestion of apoE with the enzyme thrombin, which cleaves at residues 199 and 215 (Innerarity, T.L., *et al.* 1983), yields two fragments which respectively possess the same two free energies of stabilization that are seen for the entire protein (Wetterau, J.R. *et al.* 1988). The amino terminal 22 kDa has the thermodynamic stability of a globular protein, whereas the carboxy terminal 10 kDa fragment has that of a typical apolipoprotein. Finally, the two structural domains have been shown to also represent functional domains (Aggerbeck, L.P., *et al* 1988).

The 22kDa frangment exhibits low affinity for lipids but includes the residues responsible for interaction with the LDLr and with heparin. The C-terminal 10 kDa fragment, on the other hand, has high affinity for lipids but is unreactive with cell surface receptors. In solution, apoE self-associates as a tetramer, a property that is imparted by the C-terminal domain which is postulated to be composed of many small amphipathic α-helices, a structure that is also observed in many other exchangeble apolipoproteins. This multi-helix structure is most likely responsible for apoE's reversible association with lipoproteins (Segrest, J.P., *et al.* 1994).

Although these two domains appear to exist as separate moieties in solution, and have distinct functional roles in lipoprotein metabolism, there is increasing evidence for molecular co-operation between these two domains on the surface of lipoproteins (Innerarity, T.L., *et al.* 1984; Weisgraber, K.H., 1994). For example, while the carboxy-terminal domain is primarily responsible for interaction of apoE with lipoprotein surfaces, the substitution of Arg^{112} by Cys within the amino terminal domain in human apoE alters the lipoprotein class distribution of apoE (Weisgraber, K.H., 1990). In fact, a positively charged residue at position 112 has been shown to enhance apoE affinity for TG-rich lipoproteins. Structural analysis has shown that the presence of an arginine residue at position 112 of apoE4 causes a change in the orientation of the Arg^{61} side chain when compared to that in apoE3. This change of conformation of Arg^{61} prevents it from forming a natural salt-bridge with Glu^{255} in the carboxyl terminal domain, (Dong, L.M., *et al.* 1996 , Dong, L.M., and Weisgraber, K.H., 1996). The loss of this natural salt-bridge is responsible for the lipoprotein distribution preference between apoE3 and

apoE4 and, as a consequence, individuals homozygous for the E4 allele carry most of their apoE on VLDL and chylomicron remnants, whereas, the apoE in individuals who have not inherited an ε4 allele, preferentially distribute to HDL. While this finding clearly demonstrates the biological importance of domain interactions in apoE, there may also be clinical implications. The apoE enrichment of TG-rich remnants in apoE4 individuals may promote their hepatic uptake that could subsequently lead to down-regulation of the LDLr in hepatocytes. Inheritance of the ε4 allele has been associated with increased plasma cholesterol levels and, in some studies, increased risk of cardiovascular disease.

4.3 Three dimensional structure of the 22 kDa fragment

The structure of the 22 kDa amino terminal domain of all three common apoE isoforms, as well as a recombinant apoE2 receptor-competent form, have recently been solved at the atomic level (Wilson, C., *et al.* 1991; Dong, L.M., *et al.* 1997). X-ray crystallographic analysis of this domain has established the spatial arrangement of at least 80% of the residues. The data revealed that this domain indeed resembled a stable globular protein, in being made-up of five helices, four of which are packed as a tight bundle, as shown in figure IV-16. These four unusually long helices, consisting of 19, 28, 36, and 35 amino acids, were found to be arranged in an antiparallel fashion. This mode of helix packing allows for hydrophobic association amongst neighboring helices, through leucine zipper-type interactions and are, in part, responsible for the strong thermodynamic stability of this domain.

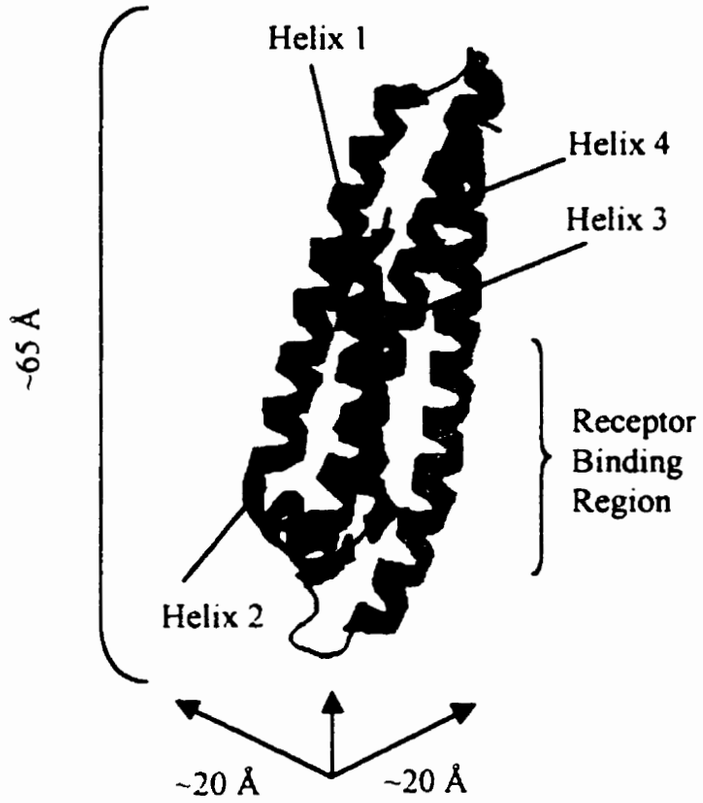

Figure I-16 The three dimensional structure of the 22 kDa fragment of apoE.

Ribbon model of the structure of the 22 kDa fragment of human apoE3. Four of the five helices (helices 1-4) are arranged in an antiparallel four helix bundle. The four-helix bundle can be viewed as a rectangle, with approximate dimensions of 20 x 20 x 65 Å. The receptor-binding region of apoE (~ residues 130-150) is indicated on helix 4 (adapted from Weisgraber, K.H., 1994).

Of the 199 amino acids which make up the 22 kDa fragment of apoE, more than one third consist of charged residues. The crystal structure includes atomic coordinates for 24 basic and 24 acidic residues. The side chains of these charged residues are solvent exposed and most participate in intramolecular salt bridges. Half of the intramolecular salt bridges are intra-helical whereas the remainder are formed between residues on neighboring helices. Together with the hydrophobic interactions discussed above, these

numerous strong electrostatic interactions between the helices of the bundle contribute to the high free energy of stabilization observed for this domain (Wetterau, J., *et al.* 1988).

The residues implicated in LDL receptor binding reside on the fourth helix and are exposed to solvent. The side chains of these amino acids, located between residues 136 and 150, are not implicated in any electrostatic interactions, and form a large area of positive potential on an electrostatic potential map, that extends some 15 angstroms off the surface of the protein. As mentioned earlier, the positively charged side chains of these arginine, lysine and histidine residues, may all take an active part in interacting with the negatively charged residues present in the consensus sequence repeats found in the ligand binding domain of the LDL receptor. Indeed, early selective chemical modification experiments made on apoE, demonstrated that lysyl and arginyl residues were important in the interaction of apoE with the LDL receptor (Mahley, R.L., *et al.* 1977; Weisgraber, K.H., *et al.* 1978). Many naturally occuring mutant forms of apoE, as well as variants generated by site-directed modifications in which basic residues within the receptor binding site have been replaced by neutral or acidic residues, are defective in binding to the LDL receptor. The fact that no single replacement results in complete loss of receptor-binding capability, implies that there may be co-operative interactions between these basic residues and the acidic residues within the cysteine rich repeats of the ligand binding domain of the LDL receptor (Mahley, R.L., *et al.*1988; Brown, M.S., and Goldstein, J.L., 1986).

4.4 Mechanisms of ApoE / LDL-Receptor interaction

ApoE3 and apoE4 are receptor competent only when associated with lipid (Innerarity, T.L., *et al* 1979). The modification of apoE tertiary structure, brought about by its association with lipid, is thought to expose an epitope that is absent in the lipid-free state (Weisgraber, K.H., 1992). In fact, it is believed that, even on the surface of circulating lipoproteins, there are actually two functional forms of apoE, receptor active/inactive. These two apoE conformational states differ in their respective susceptibility to thrombolytic digestion (Bradley, W.A., *et al.* 1984). It has been postulated that, as apoE is initially acquired by large TG-rich lipoproteins within the circulation, it exists as a receptor incompetent form and can mediate binding only after the particle undergoes intravascular remodeling. The loss of surface-bound apo CIII has been correlated with increased apoE-mediated binding to lipoprotein receptors, suggesting that apoCIII might act as a steric inhibitor of apoE in terms of receptor binding (Shelburne, F., *et al.* 1980; Windler, E., *et al.* 1980; Da Silva *et al.* 1996). In addition, the particle diameter and / or lipid composition may modulate apoE conformation and apoE may become receptor-competent only after the TG-rich lipoprotein has been subjected to the action of intravascular lipases and lipid transfer proteins (Weisgraber, K.H., 1994).

ApoE2 differs from wild-type apoE3 by having an arginine to cysteine substitution at position 158. This residue lies outside the receptor binding region, which has been determined to be made-up of residues 136-150 (Weisgraber, K.H., *et al.* 1994). Within the receptor binding site on the fourth helix of the four helix bundle, all of the

positively charged residues are found to have their side chains exposed to the solvent and thus free to interact with the ligand-binding domain of the LDL receptor. Since Arg^{158} lies outside of the receptor binding site, its contribution to the receptor interaction has been thought to be indirect (Innerarity, T.L. *et al.* 1984, Wilson, C., *et al.* 1994).

Recently it has been shown that the replacement of Arg^{158} by cysteine, as occurs in apoE2, disrupts salt bridges which normally exist between Arg^{158}, Asp^{154} and Gln^{96}. As a consequence, in apoE2, Asp^{154} finds a new salt bridge partner in Arg^{150}, which causes the side chain of Arg^{150} to shift out of the receptor binding region, which gives rise to a molecule with low affinity for the LDLr (Wilson, C., *et al.* 1994, Dong, L.M., *et al.* 1997).

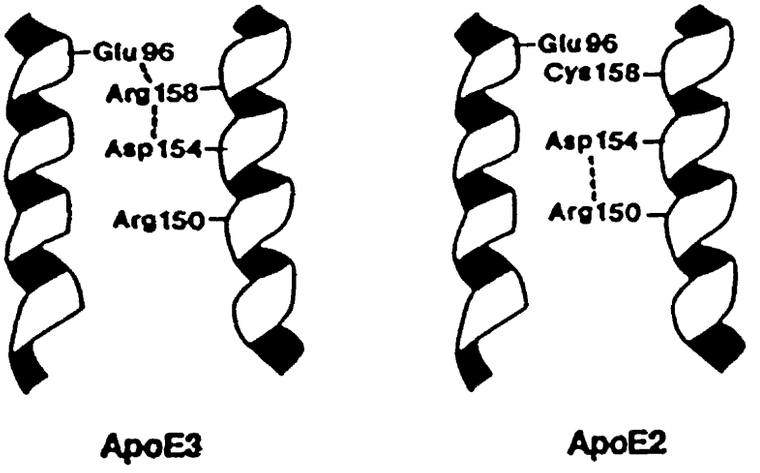

Figure I -17 Comparison between the apoE2 and E3 structures.

Salt bridges in the 22-kDa fragment of apolipoprotein E3 and E2. In apoE3, Arg158 forms a salt bridge (---) with Glu96 and Asp154. In apoE2 the loss of Arg158 results in the formation of a salt bridge between Asp154 and Arg150. Arg150 swings out of the basic cluster of side chains in the receptor domain to form thei bond (adapted from Weisgraber, K.H., 1994).

To test the hypothesis that the Asp^{154}-Arg^{150} salt bridge is responsible for receptor incompetence of apoE2, this salt bridge was disrupted in apoE2 by mutating Asp^{154} to an

alanine. This replacement increased the receptor binding activity of apoE2 to 80% of normal binding activity which suggested that the disruption of the Arg^{150}-Asp^{154} salt bridge allowed the arg^{150} side chain to return to the receptor binding region. The crystal structure of the apoE $Ala^{154}Cys^{158}$ variant confirmed that both the backbone structure and the orientation of the Arg^{150} side chain were essentially identical to those of apoE3 (Figure I-17). In both proteins, the Arg^{150} side chain points in a similar direction, away from the site of residue 154. While there are examples in the literature that exemplify the functional importance of salt bridges within proteins, the case of apoE2 is unique in that the loss of one salt bridge promotes the formation of a new salt bridge which, in turn, is responsible for the defective behavior of the isoform.

The ability of apoE2 to bind to cell surface receptors can be highly variable. ApoE2 incorporated into discoidal DMPC vesicles is invariably defective, while the binding capabilities of apoE2 on spherical lipoproteins can vary from defective to near normal, depending on the lipid composition of the lipoprotein (Innerarity, T.L., *et al.* 1979 and 1986). This variability in binding activities has been suggested to account for the fact that, although apoE2 is associated with type III dyslipoproteinemia, homozygosity as well as additional genetic and environmental factors are needed in order for an individual to express the full blown disorder. Factors that predispose homozygous apoE2 individuals to type III dyslipoproteinemia, such as high-fat diets and obesity, may alter the lipid composition of lipoproteins and thereby affect the conformation of apoE, and its susceptibility to form an Arg^{150}-Asp^{154} salt bridge (Innerarity, T.L., *et al.* 1986).

Section 5

The Antibody

Much of the material covered in this section has been referenced from the following texbooks of immunology:

-Fundamental Immunology, 1988.

-Immunoglobulin Genes, 1995.

5.1 Introduction

The antibody was discovered in 1890 by Von Behring and Kitasato when they showed that the serum of animals immunized with bacterial toxins could passively protect a second naive animal from a lethal dose of the same pathogen (Von Behring, E.A., and Kitasato, S., 1890). Bordet subsequently demonstrated that an immune response could not only be mounted against infectious organisms, but specific antibodies could also be elicited by injection of non-pathogenic material and, as was later shown, even synthetic molecules not found in nature. The analytical study of the antibody molecule was begun as early as 1907, when Arrhenius coined the term

"immunochemistry" and published a series of lectures entitled, Immunochemistry: The application of the principles of Physical Chemistry to the Study of the Biological Antibodies (Arrhenius, S., 1907). This publication marked the initiation of the mathematical study of antibody-antigen complex formation. The investigation of antibody recognition however, truly began in the late 1930's, largely through the efforts of Dr. Karl Landsteiner who elucidated many of the fundamental principles of immunochemistry using molecular approaches (Landsteiner, K., 1945). He demonstrated the exquisite sensitivity of the antibody-antigen interaction and predicted that this specificity reflected shape and chemical complementarity between antigen and antibody. This prediction was confirmed some fifty years later with the first determinations of the tertiary structure of antigen-antibody complexes.

The myriad of foreign molecular structures that can elicit a humoral immune response and be specifically recognized by antibodies makes the immunoglobulins the most diversified family of proteins in the organism. To generate this extreme diversity, a sophisticated mechanism of gene assembly and somatic mutation has evolved. Although such a process capable of creating molecules with a wide spectrum of binding specificities may provide effective protection against infectuous agents, it also introduces the risk of generating antibodies capable of reacting with self molecules leading to automimmune disease. As a consequence, immunological tolerance, a product that co-evolved with adaptive immunity, normally ensures that immune responses are limited to foreign antigens.

5.2 Antibody Structure (IgG)

An antibody consists of two or more cysteine-linked identical heterodimers. Each individual heterodimer is composed of a light chain composed of 210-220 amino acids, and a heavy chain composed of 440-450 amino acids. They are assembled and generated within a single cell type, the B lymphocyte. Both the light and the heavy chains are composed of independently folded domains of approximately 110 amino acids. These domains are encoded separately, within the immunoglobulin gene locus.

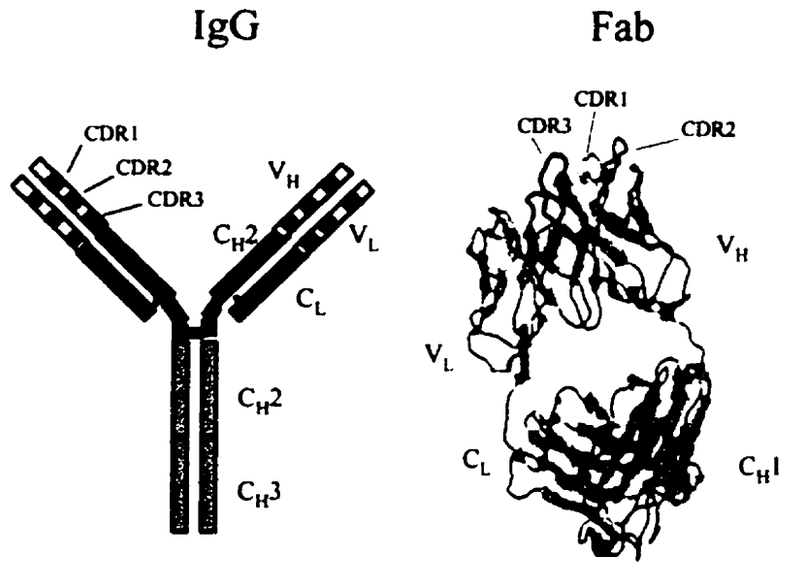

Figure I-18 Antibody structure (IgG).

This figure illustrates the structure of an antibody. An IgG is composed of two identical heavy chains and two light chains. The heavy chains are composed of one variable and three constant domains. The light chains are composed of one variable and one constant domain. The variable domains are composed three hypervariable regions or CDRs, which when observed in the three dimensional structure of an Fab molecule, join on the surface of the molecule. The collective surface generated by the joining of the six CDRs forms the antigen binding site or the antibody paratope (adapted from Fundamental Immunology, 1988).

The tertiary structure of the domains is the so-called immunoglobulin fold (Figure I-18), a common structural motif that is shared by many other proteins and is often associated with recognition processes.

The immunoglobulin fold is best described as two antiparallel β-sheets packed tightly against each other forming a compressed β-barrel. Both the variable as well as the constant regions adopt this folding pattern, albeit with varying numbers of β-strands within the sheets. A constant domain forms a β-barrel using two antiparallel β-sheets containing 3 and 4 β-strands, respectively, whereas variable domains of both light and heavy chains, fold into a β-barrel using two antiparallel β-sheets containing 5 and 4 β-strands, respectively. The pattern of folding adopted by the immunoglobulin molecule, allows for this class of proteins to expose a high number of amphipathic as well as hydrophobic residues to the aqueous solvent, which would otherwise tend to bury themselves within the protein interior (Padlan, E., 1994).

Within the primary sequence of both light and heavy chain variable domains, there are three short sequences, originally called hypervariable regions, now called complementarity-determining regions (CDRs), that differ greatly from one antibody to another. The intervening sequences between CDRs, that show much less variablity between antibodies, have been called the framework regions. As early as 1968, the CDRs of the heavy and light chains were proposed to mediate antigen binding and confer specificity to the antibody (Kabat, A., 1968). The first atomic structures corresponding to

antibody Fab segments, solved through x-ray crystallography, confirmed this early hypothesis. The framework regions of the variable domain form the β-strands of the immunoglobulin fold with the CDRs forming distal loops that join sequential strands. The six CDRs loop off the scaffold composed of the framework regions to form a continuous surface that is responsible for binding to antigen.

The immunoglobulin light and heavy chains are composed of a single variable and one or more constant regions. The light chain contains only one constant region, of which there exist two forms or isotypes; kappa (k) and lambda (λ). The heavy chain is composed of three to four constant domains depending on the heavy chain isotype of which there are nine in humans; μ, γ1, γ2, γ3, γ4, α1, α2, δ and ε which in turn define the immunoglobulin classes and subclasses of the human humoral immune system, IgM, IgG1, IgG2, IgG3, IgG4, IgA1, IgA2, IgD and IgE, respectively. The most prevalent immunoglobulin class in human serum is IgG, followed by IgM. Although the isotypic difference of the light chain seems to serve no purpose, the heavy chain isotypes are responsible for the various effector functions of the antibody. In addition, the isotype of the heavy chain dictates the quaternary structure of IgM and IgA antibodies. In view of the high sequence homology among the isotypes of all antibody constant regions (30-40%), it is believed that they probably evolved from a common progenitor, through gene duplication mechanisms.

B lymphocytes originate from multipotential stem cells, which reside, for the most part, within the marrow of large bones in adult mammels. As a B cell matures, it expresses a unique antibody molecule on its cell surface. The surface immunoglobulin is the recognition unit in the process of antigen-driven selection, first described by Burnet in 1959 (Burnet, F.M., 1959). A complex mechanism of genetic reorganization has evolved within the B cell, which permits the generation of an antibody repertoire which can complement the universe of foreign antigens.

5.3 Generation of Diversity in an Antibody Response

Since the antigen binding domain is of interest to my thesis, I will refrain from discussing the assembly and the various effector functions of the immunoglobulin which pertain to the constant regions. I will concentrate on the mechanisms of antibody diversity generation, and the techniques of modern biology that can be used to emulate this process, for the creation of tailor-made antibodies.

The mechanisms which allow the creation of diversity from a single locus on a chromosome, were elucidated in the mid-1970's through the early 1980's, largely through the efforts of Drs. Tonegawa, Milstein, Kabat, Leder, Hood, Baltimore, Alt as well as many others. Collectively, these investigators demonstrated that only a part of the diversity of the humoral immune response is encoded in the germline and that much of the diversity is generated by other mechanisms that include genetic rearrangement, non-templated nucleotide addition and somatic mutation.

5.4 The V-D-J Recombination System

Much of the diversity within the antibody repertoire, is generated by the random assembly of its complement of variable regions and, following antigen-driven selection, by hypermutation or "affinity maturation" (Milstein, C., 1990). The variable region genes are organized in a discontinuous manner within the germline. The processes which lead to the assembly of a functional variable region, begin with the selection of one of many V region genes from within a family of some three hundred, in the human. In the case of the kappa light chain locus, one member of the variable region recombines, through a random selection process, with one member of a second group of smaller variable segments, termed the J or joining region mini-genes, of which there are a few hundred in the human (Figure I-19). As a result of the rearrangement, the intervening material is lost from the chromosome, and can be isolated as small circular DNA fragments. This V-J segment represents a complete variable light chain which is transcribed and spliced to the constant region at the mRNA level. The heavy chain variable region, on the other hand, contains an additional element that further adds to its diversity. This segment is termed the D or diversity region, which encodes primarily the third hypervariable reagion. There are 10 D mini-genes within the heavy chain locus, which can be subdivided into 3 families (Tonegawa, S., 1983). The joining of the D and J segments corresponds to the earliest event of the heavy chain rearangement, followed by the recombination of a variable segment with the D-J product. The random selection of the various segments that comprise a variable domain together with the additional

diversity contributed by the association of heavy and light chains can potentially give rise to an estimated 10^8 different molecules in the human. An additional process which functions within B lymphocytes in order to generate antibody diversity is known to operate at the DNA level. (Alt, F.W., and Baltimore, D., 1982)

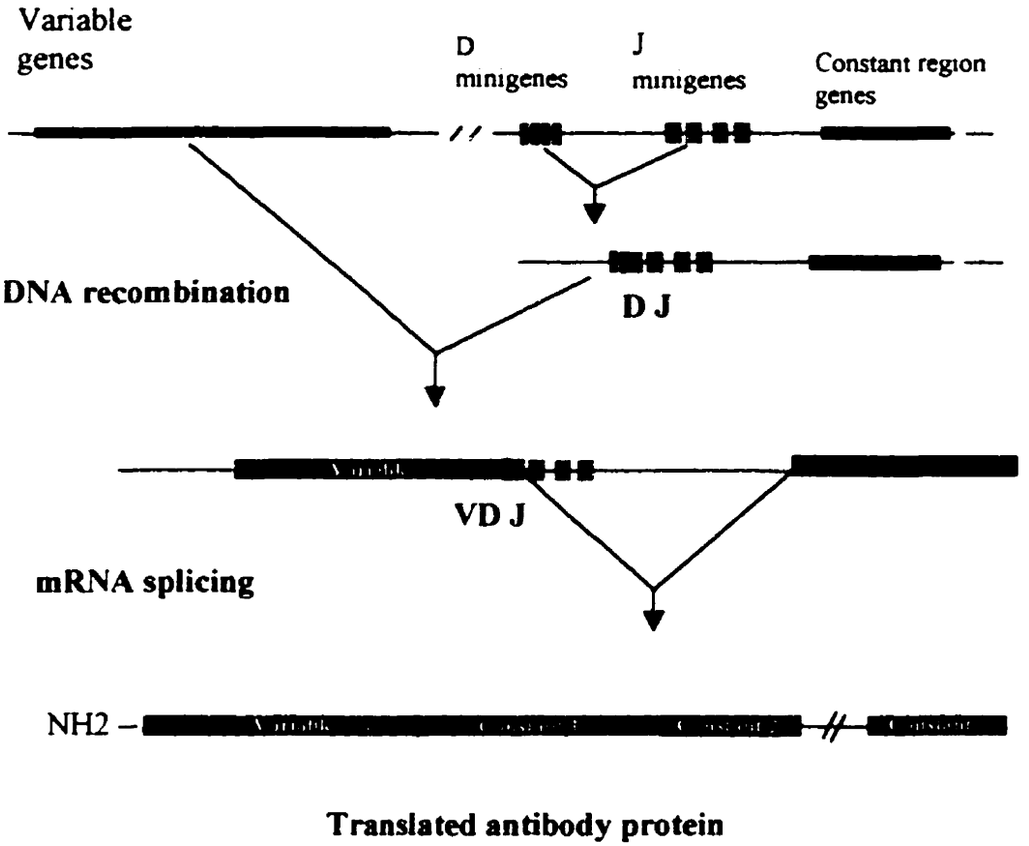

Figure I-19 The V-D-J recombinantion system

This figure illustrates the process of immunoglobulin gene rearrangement, which joins segments of the variable domain at the DNA level and, through splicing of the mRNA, assembles both the variable and constant regions. Thus a single member of the variable region family of genes is chosen to be joined with one of four J minigenes, to form an entire light chain variable region. A complete heavy chain variable region is first assembled by joining one of four D minigenes with one of four J minigenes. The joininig process leading to the formation of the DJ product is accompanied by the addition of a small number of nucleotides in the junction called N-terminal addition. The consequence of this process is the further enhancement in the diversity of the antibody combining site, as this segment of the molecule corresponds to the CDR3. The D-J product is then rearranged with a unique member from within the variable region family of genes, leading to the creation of the entire heavy chain variable region. Upon their transcription, the mRNA matures into complete light and heavy chains by the splicing of the domains (adapted from Fundamental Immunology, 1988).

The enzyme terminal nucleotidyl transferase was shown to catalyze the addition of non-germline encoded nucleotides into the sites of recombination in the light and heavy chains. This non-templated addition of nucleotides at the V/J, and D/J junctions further increases the potential diversity of antibodies by an order of 10^{10}. The cumulative result of the mechanisms described above, is the generation of a large set of B lymphocytes, each of which expresses one antibody out of a large repertoire of antibody specificities. The generation of this diversity is independent of the exposure to antigen. When the organism is exposed to a foreign antigen, those B lymphocytes which express the cognate immunoglobulin receptor on their cell surface bind the antigen and are induced to proliferate and to differentate into antibody-secreting plasma cells or to memory B cells. The antibodies that are secreted by plasma cells following a primary exposure to antigen are usually of moderate affinity, typically in the micromolar range, whereas, those antibodies analyzed following subsequent exposure of the animal to the same antigen, are generally of much higher affinity, in the order of 10^{-8} to 10^{-9}M. This phenomenon has been called affinity maturation. A biological mechanism, operating within the B cell, but outside of the genetically assembled antibody information, must be accountable for the increased affinities of the antibodies of a secondary immune response.

5.5 Affinity Maturation of the Antibody

The process of antibody affinity maturation, which was discovered by Milstein and others (Bereck, C., and Milstein, C., 1987), has been shown to result from the

somatic hypermutation of the variable region sequences of both the light and heavy chains. This process occurs solely in B cells selected for active antibody production during an immune response. Plasma cells have a short life span, and most die within 10 days. However, a small subset of the B cells which were active in antibody generation, migrate to specialized locations within secondary lymphoid organs termed germinal centers (Kelsoe, G., 1996). Within this specialized environment, B cells are stimulated to undergo limited rounds of proliferative division, with the concomitant hypermutation of the variable regions. Although alterations occur throughout the entire varible region, the CDRs are especially susceptible to modification. While in part, this localization of mutations within the CDRs reflects the effects of antigen selection, the nucleotides encoding the CDRs also appear to represent "mutation hotspots".

A mechanism of error-prone replication causing point mutations within the DNA encoding the immunoglobulin variable region, results in the generation of new subclones of B cells that express cell surface immunoglobulin with slightly altered antigen-binding sites. These amino acid substitutions can either increase or decrease affinity to antigen. Following this event, the B cells then egress from the germinal centers, and reenter the circulation. Upon re-exposure to the original antigen, the subpopulation of B cells that express immunoglobulin receptors with increased affinity for antigen will rapidly expand, and differentiate into plasma cells that secrete the high affinity antibodies that characterize the secondary immune response. While somatic mutations that increase the affinity of the antibody for the antigen are responsible for affinity maturation, even

mutations that cause a decrease in affinity can potentially contribute to the functional diversity of the immune system.

5.6 Antibody-Antigen Interaction

In the early to mid 1980s the first structures of co-crystals of antigen and Fab fragments were solved by X-ray diffraction. The crystal structures of many different antibody-antigen complexes have now been determined including those formed with antigens as varied as large proteins, peptides, carbohydrates and small hydrophobic molecules.

Amit and collaborators in 1985 (Amit, A.G., et al. 1986), described the first structure of an Fab / protein (hen egg white lysozyme (HEL)) immune complex at the atomic level. The binding face formed by all six CDRs of the anti-HEL Fab fragment was relatively flat, with a surface area of about 750 A^2 in contact with the antigen. More precisely, the CDR3 of both the light and heavy chains were located in the middle of the binding surface surrounded by the remaining four CDRs. Davies subsequently demonstrated that the specific mechanisms used by three other anti-HEL antibodies to bind to HEL were similar, even though the antigenic determinants on the HEL were different. In all cases there was good general physical complementarity between the interacting surfaces (Davies,D., 1990).

Although most contact residues contributed by the antibody to the complex are located in the CDRs, it is now known that certain framework residues in close proximity to the CDRs, are almost invariantly present in all antibody light and heavy chains and

contribute to the formation of an immune complex (Mian, I.S., *et al.* 1991). In 1989, a group headed by Cyrus Chothia proposed that several key residues in either the CDRs or the adjacent framework regions largely determine the backbone conformations of the CDR loops. They suggested, moreover, that there are only a limited number of CDR backbone structures which they called canonical loops (Chothia, C. *et al.* 1989). These key residues dictate which class of canonical loop structure that an individual CDR adopts through their packing and ability to participate in hydrogen bonds. Four canonical structures have been proposed for light chain CDR1, one for light chain CDR2, three for light chain CDR3, one for heavy chain CDR1 and four for heavy chain CDR2. Because of the variability in sequence and length, no canonical structures have been defined for heavy chain CDR3. Almost all CDRs whose crystal structures have been determined to date, conform to one of the canonical structures.

In addition to conserved residues that determine the canonical structures of CDR loops, tryptophane and tyrosine have been found to be over-represented in antibody CDRs and to be present, almost invariably, at certain key contact sites in antibody-antigen interactions (Mian, I.S., *et al.* 1991). The inherent chemical nature of these two residues endows them with the capability of participating in many types of chemical bonding with amino acids of the antigen, which may contribute to the plasticity of the interactions in an immune complex. Their amphipathic nature allows them, on the one hand, to form hydrophobic interactions and, on the other, to stabilize polar and electrostatic counter charges with the π electron system associated with their aromatic rings. It has been suggested that these two particular residues confer the strong

hydrophobic energy needed for the high affinity of the antibody, and that additional residues interspaced throughout the CDRs confer the fine tuning of the interaction, through ionic, van der Walls and hydrogen bond formation.

The physico-chemical nature of the interactions which occur in antigen-antibody complexes, are similar to those which form the basis of protein-protein recognition in general (Webster, M.D., *et al.* 1994; Davies, D., 1997). All of the non-covalent chemical interactions are used in antibody-antigen recognition, including hydrophobic, hydrogen, van der Waals, and ionic interactions. The sum of all the interactions that contribute to the immune complex determine the affinity of the antibody for a particular antigen. The affinity is a measure of the tendency of complex formation, and is constant for a given system, imparting the high specificity observed in the recognition process of these molecules. Antibody affinity can be measured analytically using several different approaches (Neri, D., *et al.* 1996).

The complementary nature of antibody binding has been confirmed (Lawrence, M.C., and Colman, P.M., 1993) and, in all cases, extensive use of intermolecular attractive forces are employed (Braden, B.C., and Poljak, R.J., 1995). In the complex formed between the hapten, phosphocholine, and the antibody McPC603, several well-placed amino acid residues hold phosphocholine in place in the antibody binding pocket. The negatively charged carboxylate group of an aspartatic acid residue forms a salt bridge with the quaternized amine of the choline. In addition, the guanidinium group of an arginine uses both H-bonding and charge-charge interactions with the negatively-

charged phosphate group present at the other end of the phosphocholine molecule (Padlan, E.A. *et al.* 1985)

The participation of charged residues is not always a prerequisite for a successful interaction. The Fab 26-10 - digoxin complex illustrates the importance of hydrophobic interactions. The digoxin molecule is composed of both a hydrophilic sugar moiety and a hydrophobic steroid ring. The antibody recognizes only the steroid ring while the hydrophilic sugar extends out of the antibody binding pocket and into solution. Hence the affinity expressed by Fab 26-10 stems from extensive contacts between the steroid ring of digoxin and hydrophobic aliphatic/aromatic amino acid side chains located inside a highly shape-selective binding pocket. Van der Waals contacts are used extensively by antibodies to conform to the shape of an antigen. For instance, in the crystal structure between the Fab 1F7 and a chorismate mutase transition state analogue, some 90% of the surface area (180 $Å^2$) of the hapten is in tight contact with amino acid residues present in the antibody binding site (Haynes, M.R., *et al.* 1994).

In antibody-protein complexes, interfacial contacts have been shown to vary between 680 and 880 $Å^2$ (Davies, D., *et al.* 1990; Padlan E.A., 1994). In many of these structures, all or almost all, water molecules have been excluded from the contact interface. This exclusion of interfacial water seems to be a common feature of antibody binding, and its physical consequence is the generation of the hydrophobic effect of the reaction. In other cases, however, water molecules have been found to remain at the complex interface, and to form a network which actively participates in complex formation. The small size of the water molecule allows it to fill gaps of unmatched

surfaces as depicted in many structures (Davies, D., *et al.* 1996). Moreover, being capable of acting as both a donor and an acceptor of hydrogen bonds, water molecules can participate in the energetics of complex formation, by physically bridging the two surfaces. In the complex formed by the Fab Se155-4 and the O-antigen from pathogenic Samonella of subgroup B, a water molecule has been shown to bridge antigen and antibody by direct H-bonds (Cygler, M., *et al.* 1994). Evidence for the importance of the binding energy contributed by interfacial water, was exemplified by reducing the water concentration, and measuring the calorimetric value of antibody binding (Goldbaum, F.A., *et al.* 1996). Finally, interfacial solvent water molecules have been shown to help an antibody adapt to its antigen, without having to alter the conformation of certain of its CDR residues (Fields, B.A., *et al.* 1996; Padlan E.A., 1994).

The careful analysis of immune complexes which occur between Fabs and their corresponding antigen, has revealed an often unequal usage of CDRs in the recognition process. For instance, it is known that antibodies commonly use both the light as well as the heavy chain in order to recognize a protein antigen. The immune complex often occurs through the participation of residues found in all six hypervariable regions. However, in many instances, CDR3 of the heavy chain has been observed to play a more important role in the molecular interaction due, at least in part, to its position in the centre of the immune complex, flanked by the other CDRs. Moreover, the length of HC CDR3 has been shown to be instrumental in the design of the paratope topography. In two instances, a short HC CDR3 has been found to generate a groove which serves to favorably bury a bulky side chain of the corresponding antigen (Padlan, E.A., 1994). The

pivital role played by HC CDR3 does not, however, apply to all studied cases. In one solved complex between an Fab fragment and the reovirus, CDR2 of the light chain was found to contribute the largest binding energy of the complex (Bruck, C., *et al.* 1986).

While between 15 to 20 residues of the antibody may be in contact with antigen in an immune complex, there exists, what has been called an "energetic", "critical" or "core" paratope that makes the major contribution to the binding energy. These core residues within the antibody paratope, are usually clustered within the center of the complex, whereas those residues that contribute less to the binding energy tend to be situated at the periphery of the interface (Hawkins, R.E., *et al.* 1993). Observable consequences from such antibody paratopes, is appreciated through an antibody's ability to recognize and react with only a portion of its epitope, the so-called functional epitope (Van Regenmortel, M.H.V., 1992). This is, in fact, the case for many antibodies which can recognize denatured proteins in Western blotted polyacrylamide gels, as well as short linear peptides corresponding to a segment of the parent polypeptide antigen. The ability of an antibody to recognize such a small and perhaps distorted portion of the original epitope with high affinity, attests to that portion of the antigen being part of the antibody's critical or energetic epitope.

Although most antibody-antigen complexes occur owing to solvent exclusion at the interface, and to subsequent complementary association and residue burial between the macromolecules, the existence of induced fit mechanisms employed by certain antibodies, have been documented (Rini, J.M., *et al.* 1992; Padlan E.A., 1994). The side

chains of individual residues within CDRs can be reoriented, there can be movement of complete CDRs or displacement of the heavy chain variable region relative to that of the light chain in order to accomodate antigen binding (Wilson, I.A., Stanfield, R.L., 1994). Likewise, there can be changes in the conformation of the antigen to facilitate the interaction with antibody (Davies, D., 1996). The required energetic input allowing such changes in conformation have been documented not to impede complex formation. Lastly, through the careful study of the limited number of solved immune-complexes, it would appear as though the heavy chain CDR3 is the one which is the most, if not the only one, involved in major structural rearrangements. This unique feature of structural mobility displayed by this CDR, may well explain why no canonical structure has to this day been identified (Bath, T.N., *et al.* 1994; Padlan, E. 1994; Verdaguer, N., *et al.* 1996).

The high specificity and discriminatory power of antibodies does not necessarily prevent them from recognizing closely related structures. Cross-reactive mAb binding is often taken as proof of structural similarities between macromolecules, and can even be interpreted to mean that proteins have similar functions (Gershoni *et al.* 1997). In addition to cross-reactivity between structurally related molecule, occasionally, different molecules that are of very different origin and that share no obvious structural homology can be recognized by a single antibody molecule. Many examples of this phenomenon have been described, some of which are responsible for auto-immune disorders. As an example, antibodies elicited to certain bacterial polysaccharides can cross-react with red cell glycoproteins and eventually provoke chronic anemia. The display of an identical three-dimensional surface on two different antigens generally forms the basis of such

molecular mimicry. There are numerous examples of molecular mimicry both in nature and in scientifically devised systems. Most interestingly, is the mimicry of protein hormone ligands by small peptides that correctly interact with the hormone receptor (Livnah, O. *et al.* 1996). In addition, there are examples of the primary structure of a ligand sequence known to interact with a specific receptor being incorporated into the CDRs of an antibody. The antibody thus serves as a scaffold for presenting the specific binding sequence to the receptor (Smith, J.W., *et al.* 1994).

5.7 Monoclonal Antibody Technology

In 1975, Kohler and Milstein devised a methodology to immortalize specific B lymphocytes (Koeler, G., and Milstein, C., 1975). The immortalized cells, called hybridomas, could be cloned and, when either maintained in culture or injected into syngeneic mice, they would secrete large amounts of homogeneous antibody. To generate hybridomas, spleen cells from immunized mice are fused with cells of an established murine plasmacytoma cell line. The resultant hybrid cells inherit the potential to secrete specific antibody from the splenic B cell parent and the growth characteristics of the tumor cell parent. Once cloned, an individual hybridoma line secretes a single species of antibody. Monoclonal antibodies are now widely used for both research and, in a clinical setting, as diagnostic and therapeutic reagents.

Hybridoma technology does have some limitations. As monoclonal antibodies are generally of murine origin, they are recognized as foreign antigens by the human

immune system, a property that restricts their use as therapeutic agents. This problem may be overcome in the near future through the use of mice in which the endogenous immunoglobulin loci have been replaced with those of the human for the generation of hybridomas. A second problem is the diversity of specificities of antibodies that one can obtain using B lymphocytes from immunized mice for making hybridomas. As immunological tolerance will prevent the generation of antibodies which cross-react with self-proteins, the diversity of antibodies that one can obtain is limited. Newer methodologies that bypass immunization are being developed that should permit the production of antibodies having specificities that would not be obtained using classic hybridoma technology.

5.8 Bacterial Phage Display Libraries as a new source of mAbs

---

Much of the material described in the following sections, has been heavily referenced in the following general references:

- Human Antibodies from Combinatorial Libraries (Burton and Barbas 1994)
- Making Antibodies using Phage Display (Winter, G., *et al.* 1994)

With the advent of molecular biology cloning techniques, plasmid vectors were designed for the expression of recombinant antibodies, both in cultured animal cells and

within bacterial systems. These methods allowed for the generation of true man-made antibodies (Winter, G., and Milstein, C., 1991). Functional recognition units of an antibody could be produced within bacteria, without any of the restrictions imposed by the animal's immune system. Heterodimeric Fab molecules as well as single chain Fv fragments consisting of linked variable regions, could be assembled within a plasmid vector, expressed and recovered with binding capabilities identical to the parental immunoglobulin. Recombinant Fabs could be humanized, by grafting the antigen recognizing CDRs onto human framework regions, thereby reducing the immunogenicity of the antibody while still maintaining the binding capability. By mutagenesis techniques, the affinity and specificity characteristics of the antibody could be modulated and new effector functions could be introduced.

A major advancement in antibody science was the development of phage-display technology. In 1985, George Smith developed the technique of peptide phage-display libraries (Smith, G.P., 1985). This procedure consisted of generating a physical link between a functional peptide and the genetic information that encodes it, just as it is occurs within the B lymphocyte with respect to antibody production. In 1988, these investigators demonstrated the usefulness of this methodology for the selection of functional antibody molecules (Parmley, S.F., and Smith, G.P., 1988). In 1990 and 1991, two independent groups, headed by Greg Winter and Richard Lerner, modified this methodology for the display of functional antibodies on the phage surface and predicted that this approach would eventually replace classic immunization protocols for antibody production (McCafferty, J., et al. 1991; Barbas, C., et al. 1991).

Antibody display on the surface of filamentous phage can be achieved by fusing one of the antibody fragments to one of several phage-coat proteins. Owing to the presence of a bacterial leader sequence, expressed recombinant antibody heavy and light chains get secreted into the periplasm, where they can assemble. Progeny phage extrusion across the plasma membrane, following bacterial infection with M-13 helper phage, allows the fused antibody heavy chain to be assembled onto the surface of the phage, in company with the light chain. Subsequent to the cultivation of such a phage infected bacterial culture, recombinant phage particles displaying antibodies on their surface can be isolated from the media. The use of immunopanning protocols, where a desired antigen is fixed to plastic microtiter wells, permits the functional isolation of individual phage displaying antibodies with desired binding characteristics. The availability of antibody phage-display libraries, today represents an alternate method to generate monoclonal antibodies. Conceptually, isolation of monoclonal antibodies from a phage display library by immunopanning is similar to an *in vivo* immune response. Both the isolated phage and the B cell are selected through interaction of antigen with a specific antibody displayed on the cell surface and both the phage and the B cell contain the genetic material coding for that antibody.

5.9 Anti-Idiotypic Antibodies

Owing to the nature of the immune system, antibody molecules produced naturally in response to the stimulation of the humoral immune system, will contain

chemical structures which in themselves will potentially be recognized as foreign by the very system which created them. As antibody CDRs are progressively altered during affinity maturation, the antibody paratope drifts further away from its original germline encoded sequence, thus making the resulting antibody protein a target for antibody recognition. Neils Jerne was the first to propose the concept of antibodies specific to self-antibodies, through an interaction of the first antibodies private antigenic determinants, or idiotopes. He named this cascading generation of antibody driven antibody production, the idiotypic netwok (Jerne, N.K., 1974). Many have since agrued that the idiotypic network operated to keep the humoral immune system under a certain control, as natural anti-idiotypic antibodies would prevent the idiotypic antibody from interacting with its antigen (Avrameas, S., 1995). Notwithstanding the utility, or even the existance of such a regulatory mechanism of the humoral immune system, is the reality of anti-idiotypic antibody generation by vertabrates. Anti-idiotypic antibodies have long been thought of as being capable of transfering the structural information relating to the original antigen, to a second anti-idiotypic antibody. Experimentally, it was found that an antibody specific to a viral antigen was capable of transfering the internal immage of the viral protein to an anti-idiotypic antibody (Bruck, C., *et al.* 1986). In this case, it was demonstrated that the primary structure of the anti-idiotypic antibody's light chain CDR2 was similar to the primary stucture of the primary antigen. Many other cases of structural information transfer between antibody - anti-idiotypic antibody have since been demonstrated (Garcia, K.C., *et al.* 1992)

Chapter II

Molecular characterization of two monoclonal antibodies specific for human apolipoprotein E

Summary

In this chapter, I describe the fine specificities of the two mAbs, 1D7 and 2E8 which have both been previously found to recognize the LDL receptor-binding site of human apolipoprotein E (apoE) (Milne *et al.* 1981; Weisgraber *et al.* 1983). Using various mutant forms of apoE which have amino acid substitutions within the LDL receptor-binding site (Lalazar *et al.* 1988), I show that both antibodies share a very similar epitope. Most apoE variants that have reduced reactivity with the LDLr also have reduced reactivity with the mAbs. Interestingly, I have demonstrated that mAb 2E8 but not 1D7, is capable of distinguishing between receptor-active apoE isoforms and the common receptor-defective apoE2(Arg^{158}→Cys) isoform. I have exploited this property to demonstrate the potential utility of 2E8 as a reagent for determination of apoE phenotype.

In the second portion of this chapter, I describe the molecular cloning and characterization of the cDNAs that encode the light and heavy chains of the two anti-

apoE mAbs. Comparison of the deduced amino acid sequences of the respective light and heavy chains of the 1D7 and 2E8 showed that, although the two mAbs react with overlapping epitopes on apoE, their respective complementarity determining regions (CDRs), and especially those of the heavy chains, share little homology. The two mAbs, therefore, likely recognize different epitopes or topologies within a limited surface of the apoE molecule. There are seven acidic residues within the 2E8 heavy chain CDRs. Four of these negatively charged residues are located in the CDR2 and these can be approximately aligned with acidic amino acids in the fifth cysteine-rich repeat of the ligand-binding domain of the LDLr. Based on the fine specificity and primary sequence of the 2E8 heavy chain, I propose that 2E8 and the LDLr may use a common mode of interaction with apoE and that it may represent a potential antibody mimetic of the LDLr.

Objective

The first objective of this chapter was to determine the fine specificities of two mAbs which share as a common epitope, the LDL receptor-binding site of human apoE. The second objective was to elucidate the primary structures of both the light and heavy chains of these two antibodies, the result of which would serve as a starting point for the analysis of the underlying molecular basis of their cross-reactivity and their specificity for the apoE LDLr-binding site.

Introduction

A part of the results presented in this chapter has been previously published (Raffaï *et al.* 1995). As described in Chapter I, human apolipoprotein E (apoE) is a 34-kDa protein consisting of 299 amino acids which is a functionally important constituent of chylomicrons and very low, intermediate and high density lipoproteins (VLDL, IDL, HDL) (Mahley 1988). Serving as a ligand for members of the low density lipoprotein receptor (LDLr) family of cell surface lipoprotein receptors, apoE is a major modulator of lipoprotein metabolism. The most common apoE isoforms, apoE2, apoE3 and apoE4, which are distinguishable by isoelectric focusing, are encoded by 3 codominantly expressed alleles. ApoE3, the most common of the three, is considered to be the wild type, whereas apoE2, apoE4 and the even rarer isoforms, to be variants. The most frequently observed form of apoE2 differs from apoE3 by the substitution of a cysteine for an arginine at residue 158, whereas apo E4 differs from apoE3 by the replacement of a cysteine by an arginine at residue 112. Variant forms of apoE, such as apoE2($Arg^{158}\rightarrow Cys$), that show defective binding to the LDLr are, in part, responsible for the expression of type III hyperlipoproteinemia (Utermann 1977; Zanis and Berslow 1980). In addition, apoE polymorphism can influence plasma lipid levels (Davignon *et al.* 1988), postprandial lipemia (Brenninkmeijer *et al.* 1987; Weintraub *et al.* 1987; Brown and Roberts 1991), apoB metabolism (Demant et al. 1991), the lipoprotein subclass distribution of apoE (Gregg *et al.* 1986; Steinmetz *et al.* 1989; Weisgraber 1990) and susceptibility to Alzheimer's disease (Strittmatter *et al* 1993, Weisgraber and Mahley, 1996).

The limited proteolytic digestion of apoE with the enzyme thrombin, has shown that the molecule is composed of two structural domains (Wetterau *et al.* 1988, Aggerbeck *et al.* 1988), a 22-kDa amino-terminal domain that has relatively low affinity for lipid and includes the residues responsible for binding to the LDLr and a 10-kDa carboxyl-terminal domain that binds lipid with high affinity (Weisgraber 1990). Several lines of evidence (Mahley 1988; Mahley *et al.* 1977; Weisgraber *et al.*1978; Innerarity *et al.* 1983; Dyer and Curtiss 1991; Weisgraber *et al.* 1983; Lalazar *et al.* 1988) indicate that positively charged amino acids within the region of residues 136-150 directly participate in the interaction of apoE with the LDLr. The three-dimensional crystal structure of the amino-terminal 22-kDa thrombolytic fragment of human apoE has been solved (Wilson *et al.* 1991). The fragment is folded into an elongated four-helix bundle with the positively charged amino acids implicated in receptor-binding situated on the fourth helix and exposed to solvent, forming a discrete patch of positive potential, which extends some 15 Å off the surface of the protein.

The mAb 1D7 is one of a group of anti-human apoE mAbs that were first reported in 1981 (Milne *et al.* 1981). From a group of six mAbs, only 1D7 is capable of blocking apoE-mediated binding to the LDLr (Weisgraber *et al.* 1983). Antibody 1D7 has subsequently been used as an immunochemical tool, in order to distinguish between apoE- and apoB-mediated lipoprotein binding to cell surface receptors (Hui *et al.* 1984; Marcel *et al.* 1988; Sehayek *et al.* 1991) in addition to serving as a probe for the identification of the receptor-binding (Weisgraber *et al.* 1983) and heparin-binding sites of apoE (Weisgraber *et al.* 1986). In order to define the fine specificity of 1D7, I have

determined its reactivity with a series of apoE variants which differ in their affinities for the LDLr. In parallel with 1D7, I have similarly analyzed the reactivity of a second anti-apoE mAb, 2E8, which also blocks binding of apoE to the LDLr (Innerarity *et al.* unpublished observations). In both cases, the respective epitopes of 1D7 and 2E8 appear to coincide with the LDLr-binding site on apoE.

In triglyceride-rich lipoproteins, apoE appears to be heterogeneous with respect to its conformation or accessibility, with only a subpopulation of molecules being capable of mediating binding to the LDLr (Bradley *et al.* 1984). It has been reported that expression of the 1D7 epitope on very low density lipoproteins (VLDL) may correlate with the ability of the particle to bind to the LDLr (Sacks and Krukonis 1987). Thus, 1D7 may be specific for a conformational state of apoE that permits interaction of apoE with the LDLr or may react with a subpopulation of molecules whose receptor-binding site is exposed. My longterm goal was to identify or produce mAbs that would recognize the same functional epitope on apoE that is recognized by the LDLr. These antibodies would then be used as conformational probes in order to study the physical and chemical parameters that modulate expression of the LDL receptor-binding site of apoE. Attempts at achieving these goals are described in Chapter V of my thesis, where I describe the alteration of the primary structure, and consequently the binding specificity of mAb 2E8.

Methods

General techniques of molecular biology.- For most of the general techniques of molecular biology, I followed protocols described in the laboratory textbook "Molecular Cloning" (Sambrook *et al.* second edition). Other techniques that were used and either differed from, or were not described in Sambrook *et al.*, have been appropriately referenced.

2.1 Isolation of hybridoma RNA.- Total RNA was isolated from all hybridoma cell lines according to the methodology developed by Chomczmski (Chomczmski and Sacchi 1987). Hybridoma cells were grown in 10 cm Falcon culture dishes in Eagles modified DMEM media supplemented with 5% fetal bovine serum, in a humid incubator set at 37 ^{0}C with 5% CO_2. Ten such dishes were grown to confluency, generating on average some 10 x 10^8 hybridoma cells. The cells were collected from the dishes and placed into 50 ml conical tube, where they were pelleted at 1000 x g for 10 minutes. A single cellular pellet was formed in a conical tube which was inverted to remove all media. The pellet was then gently resuspended in 4 ml of solution D (4 M guanidine thiocyanate), then 1/10 of a volume of 2M sodium acetate, followed by an equal volume of phenol. The tube was then mixed vigorously using a vortex for 1 minute, and spun at 10 000 x g in a sorval RB-C5 centrifuge for 20 minutes. The supernantant was carefully removed in order to not disturb the buffy interface. To the supernatant was added an equal volume of a 50 % phenol / chloroform solution containing 1 % isoamylic alcohol, and was again mixed vigorously and spun as previously described. Once again the supernatant was

removed and to it was added an equal volume of isopropanol. The tube was then vortexed and chilled at -20 ^{0}C overnight. The following morning, the tube was spun at 15 000 x g, and inverted to remove all traces of supernatant. The pellet was resuspended in 400 µl of solution D, and transfered to a microcentrifuge tube. 40 µl of 2M sodium acetate were then added followed by 400 µl of ice cold isopropanol. The tube was incubated at -20 ^{0}C for an hour to allow the RNA to precipitate. The tube was the spun at 14 000 rpm in a microcentrifuge to pellet the RNA. The supernatant was poured off, and the pellet was washed with 1 ml of 70 % ethanol, and re-spun to fix the pellet. All traces of alcohol were removed and the tube was left to dry for 20 minutes at room temperature, after which the RNA pellet was disolved in 500 µl of DEPC treated TE pH 7.4. The concentration of RNA was evaluated using spectrophotometric analysis. The integrity of the RNA preparation was accessed by running a small amount of it on a 1 % agarose gel, and visualizing intact ethidium bromide stained bands, corresponding to the cellular ribosomal RNA molecules. In addition, to insure the presence of immunoglobulin mRNA, this type of gel could was analyzed using Northern blot analysis.

2.2 Purification of hybridoma poly (A^+) mRNA.- 300 µg of hybridoma total RNA was heat denatured at 95 ^{0}C, and immediately quenched on ice. It was then applied to an oligo-dT column (Sigma). The poly (A^+) mRNA was retained by the column in a high-salt buffer, and eluted in low-salt, according to the manufacturer's instructions. The integrity and concentration of the mRNA was determined using Northern blot analysis and UV absorbance.

2.3 Production of hybridoma cDNA.- The production of complementary DNA (cDNA) from the isolated hybridoma poly (A^+) mRNA, was accomplished through the use of a cDNA synthesis kit (Amersham). Briefly, 5 μg of poly (A^+) mRNA was used as a template in the synthesis of a first strand of DNA. The mRNA was mixed with oligo-dT primers (Pharmacia) at a concentration of 0.2 μM in a first-strand synthesis buffer, heated to 95 ^{0}C for 5 minutes and immediately quenched on ice. To the annealed product was added 1 U of Moloney Leukemia virus reverse transcriptase (Pharmacia), which was then transferred to a 37 ^{0}C incubator for 2 hours. The RNA / DNA hybrid was precipitated with alcohol and resuspended in 30 μl TE pH 8.0. The sample was then suplemented with 0.1 U of Rnase H (Pharmacia), and incubated at 17 ^{0}C for 1 hour. Immediately following this incubation, 3 U of *E.coli* DNA polymerase (Pharmacia) were added in addition to some second strand synthesis buffer containing the appropriate deoxy-nucleotides, and the sample was incubated at 37 ^{0}C for 1 hour. The double stranded cDNA was precipitated with ethanol, and resuspended in 30 μl of TE pH 8.0. Cloning adaptors, consisting of short double stranded DNA containing an EcoR1 site, were first ligated blunt-end to the extremities of the cDNA (Pharmacia), and then digested with EcoR1. The cDNA was then ethanol precipitated, dissolved in 30 μl of TE pH 8.0, and evaluated for DNA concentration, using UV absorbance.

2.4 Creation of a hybridoma cDNA library.- A cDNA library was created by inserting EcoR1-digested cDNA fragments, into an EcoR1 digested and dephosphorylated pUC18 vector (Stratagene). A total of 50 ng of cDNA, was on average mixed with 200 ng of pUC18, in a volume of 50 μl containing 2 U of T4 ligase. The

mixture was left at 16 ^{0}C overnight, and transformed into competent *E.coli* DH5α bacteria. The transformants were spread onto 4 large petri plates containg LBAT (LB-agar and ampicillin (100 μg / ml)), and grown at 37 ^{0}C overnight.

2.5 Preparation of ^{32}P radiolabelled cDNA probes.- Radiolabelled cDNA probes were routinely used in order to detect the presence of recombinant genes crosslinked to nylon membranes. The use of mouse kappa light chain and gamma (γ)-1 heavy chain, were used to identify the presence of the cloned hybridoma cDNA in various settings. The cDNA fragment to be used as the probe was cut out of the plasmid vector with the appropriate restriction endonucleases and purified by gel electrophoresis. Twenty ng of the purified fragment in a total volume of 10 μl heat-denatured and then immediately quenched on ice. Immediately following denaturation, 100 μl of a pool-oligo mixture, which contained a random set of hexamers in an appropriate DNA polymerase buffer (Pharmacia) was added to the denatured probe. Five μl of an α-dATP phosphorous-32 radionucleotide solution (Amersham), and 0.5 U of the Klenow fragment of *E.coli* DNA polymerase was then added to the reaction mixture. The tube was incubated for 2 hours at room temperature, and unincorporated radionucleotides were removed through the use of Sephadex G-25 spun column chromatography (Pharmacia).

2.6 Screening of a hybridoma cDNA library.- The cDNA library was screened for immunoglobulin light and heavy chains, using the GW-22 mouse kappa light chain constant region probe (Max *et al.* 1981), and the Pγ–1 mouse heavy gamma 1 heavy chain probe (Honjo *et al.* 1979) which were provided by Dr. Raffik Sekaly. Colony lift,

followed by hybridization with the appropriate radiolabelled probe was used in order to isolate positive bacterial clones. A nylon filter (Nytran, Amersham) was gently applied to the agar plates and pierced with a syringe containing India ink to allow subsequent orientation of the plates. The membrane was gently lifted off the agar and then incubated upside-down on a Whatman™ filter paper, previously soaked with a DNA denaturation solution (0.2 N NaOH, 2% SDS) for 10 minutes. The agar plate was put back into a 37 ^{0}C incubator for 8 hours to allow regrowth of the bacterial colonies. The filter was then transferred to a second Whatman™ filter soaked with neutralizing solution (3 M NaCl, 0.5 Tris pH6.8), incubated for 10 minutes and dried on paper towels. The membranes were then exposed to U.V. irradiation for 5 minutes, and finally rinsed in water to remove bacterial debris and salt residues. The detection of bacterial colonies positive for a plasmid coding for immunoglobulin light or heavy chains, were determined by incubating the membrane in a hybridization solution (6 x SSC) containing 5 ng of radiolabled constant region probe, overnight at 65 ^{0}C. The following day, the membrane was incubated for 20 to 40 minutes in washing solution (2 x SSC) at 42 ^{0}C, which removed non-specifically bound radiolabled probe. The membrane was then dried on paper towels, and exposed to X-ray film. The following day, the film was developed and the positive clones appeared as black dots on the film.

2.7 Isolation of positive clones from a cDNA library.- Positive clones were identified by superimposing the X-ray film on the agarose plate using the ink marks for orientation. At that point, a sterile pasteur pipette was inverted and stabbed into the agar which rested directly above the black spot. The agar plug was then transfered to LB

growth media, grown for 1 hour in a shaking incubator, and re-plated at low density for a secondary screening. Subsequent screenings were performed until an individual clone was properly isolated and identified.

2.8 Amplification of immunoglobulin genes using anchored PCR.- This technique allowed the amplification of genes using only one specific oligonucleotide primer (Loh *et al.* 1989). Typically, 10 μg of total hybridoma RNA was used as template in a reverse transcription experiment containing an immunoglobulin 3' constant region specific primer complementary to codons 224-232 located in the hinge region (5' - AGG CTT **ACT AGT** ACA ATC CCT GGG CAC A - 3') and which contains an Spe1 restriction site indicated in bold. Following the synthesis of the first strand of cDNA, the enzyme terminal deoxy-nucleotidyl transferase (Pharmacia) was used in order to add a 5' overhang consisting of guanosine nucleotides. A first round of amplification using an oligo-dC and the 3' hinge region primer, was carried out and the products were separated on a low melting point agarose gel (FMC Bioproducts, ME). The gel containing fragments with molecular weights ranging from 300 to 800 base pairs was excised and the products were used directly as template for a second round of PCR using the oligo-dC and an internal 3' constant region primer (5'-GGC AGC AGA TCC AGG GGC-3') corresponding to codons 125-130. This second amplification gave a specific 500 base pair product which was isolated and sub-cloned into p-Bluescript (Stratagene).

2.9 Characterization of cDNA clones by Southern blot detection.- Isolated bacterial clones which hybridized to the constant region probes were first analyzed by Southern blotting techniques in order to confirm the presence of an immunoglobulin cDNA inserted in the pUC18 vector (Stratagene). Recombinant plasmid DNA was prepared and digested with the endonuclease EcoR1, and run on a 1% agarose gel. Following the visualization of the released cloned fragments on a U.V. transilluminator, the gel was soaked for one hour in denaturation buffer (0.2 N NaOH, 2 % SDS) and for one hour in a neutralization buffer (3 M NaCl, 0.5 Tris pH 6.8), and the DNA was then transferred overnight, through capillary action, onto a nylon membrane. The following morning, the membrane was exposed to U.V. light for 5 minutes, and rinsed in water. The membrane was then treated as described above for the radio-detection of immunoglobulin constant regions.

2.10 Characterization of cDNA clones through DNA sequence analysis.- Following the identification of clones which seemed to be of large enough size to be full length, plasmid DNA was prepared and subjected to double strand DNA sequencing using the dideoxy chain termination method (Sanger *et al.* 1977). The Universal and Reverse oligonucleotide primers specific to the vector cloning site of the pBluescript plasmid (Pharmacia), were used to sequence the variable and constant regions of both the light and heavy chains. In addition, internal primers specific for the 5' region of the constant regions were used to sequence the variable regions.

2.11 Monoclonal antibodies - The production and characterization of mAbs 1D7, 3H1 and 6C5 have been described previously (Weisgraber *et al.* 1983; Milne *et al.* 1981; Weisgraber *et al.* 1986). Hybridoma 2E8 was the product of a fusion between spleen cells of a mouse immunized with purified human apoE3 and the non-secreting plasmacytoma cell line SP2-O. The mAb 2E8 was characterized according to the same criteria that were used for the other anti-apoE mAbs (Weigraber *et al.* 1983). Hybridoma 2H2 was originally produced in 1987, and is specific for the rat cardiac homone ANF or atrial natriuretic factor (Milne *et al.* 1987). The IgG fraction containing the mAbs were purified from the ascitic fluids of hybridoma-bearing mice, using affinity chromatography on Protein-G Sepharose (Pharmacia) as described below.

2.12 Purification of mAbs using protein-G chromatography.- mAbs were purified using Protein-G Sepharose (Pharmacia) chromatography according to the manufacturers recommendations. Briefly, a column filled with 3 ml of recombinant Protein-G Sepharose was used to retain hybridoma IgG present within the ascitic fluids of a mouse bearing the hybridoma tumour. The ascitic fluid was passed on the column at a flow rate of 0.5 ml / min. The column was then washed with PBS pH 7.8 until an $O.D._{280}$ nm reading of less than 0.01. The specifically bound IgG were then eluted from the column by using an acidic buffer (0.1 M glycine pH 3.0). Eluted IgGs were collected as 0.5 ml fractions, which were read at $O.D._{280}$ nm. Those fractions which gave an $O.D._{280}$ nm reading above 0.2 were pooled and dialyzed against PBS pH 8.0 overnight. The protein concentration of the resulting dialyzed mAb preparation was subsequently determined, and frozen in 100 µl aliquotes at -20 ^{0}C.

2.13 Radiolabelling of mAbs.- The radiolabeling of all mAbs was performed using the chloramine T method (Milne et al. 1983), using ^{125}I sodium iodine (Amersham). Briefly, 50 µg of the mAb was prepared in a volume of 170 µl of a phosphate buffer (0.3 M phosphate pH 7.2), and chilled on ice. Under a ventilated fume hood, the reaction was initiated by adding 20 µl of a freshly prepared, ice-cold chloramine T solution (90 µg /ml) to the mAb, quickly followed by the addition of 1 µCi of sodium iodine. The reaction was kept on ice for 30 minutes, and was stopped by the sequential addition of 20 µl of 1 M KI and 100 µl of 0.1% BSA. Free iodine was removed by passage of the reaction mixture on a 1.5 ml Dowex AG1-X8 ion-exchage chromatography column (BioRad), and the labeled IgG was collected in an 8 ml solution of 0.1 % BSA in PBS. Specific activities ranged from 1-2 x 10^4 cpm / ng protein.

2.14 Amino acid sequence sequence analysis and cleavage with CNBr at methionine residues.- Protein and peptide samples for sequencing were purified by SDS-PAGE and electroblotted onto sequencer stable PVDF membrane as described previously (Laycock *et al.* 1989). Automated gas-phase sequencing was performed on an Applied Biosystems 475A protein sequencing system (Foster City, CA.) incorporating a model 470A gas phase sequencer equipped with an on-line model 120A PTH analysis module. Cleavage of peptide bonds adjacent to methionine residues was effected by using CNBr. Freeze dried protein was dissolved in 500 µl of 88% (v/v) formic acid followed by the addition of solid CNBr. The reaction vial was flushed with argon, sealed and incubated in the dark at room temperature for 24 hours. The reagent and solvent

were removed under a stream of argon and the remaining material was suspended in Milli-Q water and freeze dried.

2.15 Preparation of apoE and production of apoE variants.- ApoE3, apoE2(Arg^{158}→Cys) and apoE2(Arg^{145}→Cys) were purified from plasma as reported by Weisgraber *et al.* (Weisgraber *et al.* 1981). The generation of the apoE variants apoE(Arg^{136}→Ser), apoE(His^{140}→Ala), apoE(Lys^{143}→Ala), apoE(Leu^{144}→Pro), ApoE(Arg^{150}→Ala) and apoE(Ala^{152}→Pro), their expression in *E.coli* and their purification have also been described (Lalazar *et al.* 1988). For comparison of purified plasma apoE and apoE produced by *E.coli*, purified, bacterially expressed apoE3 was included in some experiments (Vogel *et al.* 1985). For certain experiments, the isolated apoE was incorporated into dimyristoylphosphatidylcholine (DMPC) vesicles (Innerarity *et al.* 1984).

2.16 Sandwich apoE radioimmunometric assay. - Polystyrene wells (Removawells, Dynatech Laboratories, Alexandria VA.) were coated by an overnight incubation at room temperature with 100 µl of the capture mAb 6C5 at a concentration of 10 µg / ml in 5 mM glycine, pH 9.2. After washing with 0.15 M NaCl containing 0.025 % Tween 20 (NaCl-Tween), the wells were saturated by a 30 minutes incubation with a 1 % (w/v) solution of bovine serum albumin in phosphate-buffered saline (PBS-BSA). The wells were emptied and 100 µl of dilutions of apoE or apoE-DMPC complexes in PBS-BSA were added and allowed to incubate overnight at room temperature. After washing with NaCl-Tween the wells were filled with 100 µl of ^{125}I-1D7 , ^{125}I-2E8 or ^{125}I-3H1 diluted to

100 ng/ml in PBS-BSA. After an overnight incubation, the wells were washed and bound radioactivity was determined. The calculation of IgG mass bound was based on the specific activity of the ^{125}I-IgG.

2.17 Surface Plasmon Resonance. - The kinetics of 3H1, 1D7 and 2E8 binding to apoE and apoE variants were determined by surface plasmon resonance (SPR) using a BIAcore biosensor system (Pharmacia Biosensor). The SPR technology uses the optical phenomenom of surface plasmon resonance which detects changes in optical properties at the surface of a thin gold film on a glass support (sensor chip). The sensor chip carries a dextran matrix onto which one of the two reactants is covalently linked, while the other one is introduced in a flow passing over the surface. The resonance angle is a function of the refractive index in the vicinity of the surface which changes as the concentration of molecules on the surface is modified, and is expressed in resonance units (RU). A signal of 1000 RU corresponds approximately to a surface change of 1 ng / mm^2. SRP allows for interactions to be continuously monitored in real time and generates binding profiles, or sensorgrams, from which rate constants can be derived (Jonsson and Lofas 1990), thus association and dissociation rate constants can be mesured, and not only the equilibrium affinity constant. Primary amine groups of apoE3 and five variants apoE(Arg^{136}→Ser), apoE(His^{140}→Ala), apoE(Lys^{143}→Ala), apoE(Arg^{150}→Ala) and apoE(Arg^{158}→Cys) were covalently coupled to research grade CM5 sensor chips (Pharmacia Biosensor) using the amine coupling kit supplied by the manufacturer. The proteins were diluted to 20 µg / ml in 10 mM sodium acetate, pH 4.5, and 40 µl aliquots were injected over the activated chip surface. Unreacted moieties were blocked with ethanolamine. All measurements

were carried out in HEPES buffered saline (HBS) which contained: 10 mM HEPES pH 7.4, 150 mM NaCl, 3.4 mM EDTA, 0.005% Surfactant P-20 (Pharmacia). Analyses were performed at 25 ^{0}C and the binding of each antibody was tested at seven concentrations. Immobilizations and binding assays were carried out at a flow rate of 3 ml / min. Sensor chip surfaces were regenerated with 100 mM HCl and surface integrity was periodically checked with control antibody.

Association and dissociation rate constants were calculated by non-linear fitting of the sensorgram data (O'Shannesy *et al.* 1993) using the BIAevaluation 2.0 software (Pharmacia Biosensor). The dissociation rate constant is derived using the equation:

$$R_t = R_{to}\, e^{-k_{off}(t-t_o)}$$

where R_t is the response at time t, R_{to} is the amplitude of the response and k_{off} is the dissociation rate constant. The association rate constant can be derived using the equation:

$$R_t = \frac{k_{on}\, C\, R_{max}\, (1-e^{-(k_{on}C+k_{off})\, t})}{k_{on}C+k_{off}}$$

where R_t is the response at time *t*, R_{max} is the maximum response, C is the concentration of ligate in solution. k_{on} is the association rate constant and k_{off} is the dissociation rate constant.

2.18 Phenotypic determination of human apoE2(Arg^{158}→Cys) in human plasma.- mAb 2E8 was used in a sandwich radioimmunometric assay, in order to detect the presence of the apoE2(Arg^{158}→Cys) isoform in human plasma. The plasma of individuals of known apoE genotype were used to develop the methodology (kindly provided by Dr. Ruth McPherson, Ottawa Heart Institute Lipid Clinic). ApoE was quantified in fresh plasma from individuals of known apoE phenotype (E3 / E3, E3 / E2 and E2 / E2) using the solid phase sandwich immunometric assay described above with 6C5 and ^{125}I-3H1 as the capture and detection antibodies, respectively. Based on this result, the plasmas were diluted to equivalent apoE concentrations and a second, modified sandwich radioimmunometric assay was then performed using ^{125}I-2E8 mAb, as the detection antibody in order to determine the presence of the apoE2 isoform. Appropriately diluted plasma was added in serial dilutions to mAb 6C5 coated wells, incubated for 1 hour and washed using NaCl-Tween. ^{125}I-2E8 mAb was then added to the plates in a buffer containing 1% BSA, 0.01% Tween. Following an incubation of 1 hour, the plates were washed using NaCl-Tween, and counted on a gamma counter as previously described.

Results

1. **Fine specificity of mAb 1D7** - It has previously been shown that mAb 1D7 reacts with a cyanogen bromide fragment of apoE composed of residues 126-218 (Figure II-1) and with a synthetic peptide that includes apoE residues 139-169 (Weisgraber *et al.* 1983). To more precisely map the 1D7 epitope, I have taken advantage of a panel of recombinant apoE variants which were produced by site-directed mutagenesis and synthesized in a bacterial expression system (Lalazar *et al.* 1988) and which were kindly provided by Dr. Karl Weisgraber. For these studies, a solid phase apoE sandwich immunometric assay was developed as shown in Figure II-1. The mAb 6C5 was used as the anchor and bound apoE was detected with either ^{125}I-1D7 or ^{125}I-3H1. Elsewhere, evidence has been presented that the epitopes for anti-apoE mAbs 6C5 and 3H1 are entirely or partially situated between residues 1-13 and 243-272, respectively (Figure II-1) (Weisgraber *et al.* 1983, 1986). Antibodies 6C5 and 3H1 do not compete with each other for binding to immobilized apoE nor do they compete with 2E8 and 1D7 (Milne and Raffaï unpublished results). As the mutagenesis was confined to the receptor-binding region of apoE, the introduced amino acid substitutions should not influence binding of the variants to either 6C5 or to ^{125}I-3H1. Recombinant apoE3 was somewhat less immunoreactive with both 1D7 and with 3H1 than was purified plasma apoE3 (Figure II-2). This could be attributable to some protein denaturation or a decreased binding of recombinant apoE to 6C5 due to the presence of an amino-terminal methionine that is not present in mature plasma apoE. The differences in immunoreactivity observed between native and recombinant apoE3 are, however, minor

in comparison with the decreases in 1D7 immunoreactivity that resulted from amino acid substitutions in apoE. Amino acid substitutions at residues 143, 144, 150 or 152 almost totally eliminated binding of 1D7 and, as reported previously, the natural apoE variant apoE(Arg^{145}→Cys) showed reduced 1D7 immunoreactivity. In contrast, normal 1D7 reactivity was seen with apoE(Arg^{136}→Ser) and apoE(Arg^{158}→Cys) variants. ApoE(His^{140}→Ala) showed a large decrease in 1D7 binding compared to apoE3 (Figure II-2), however, when normalized for 3H1 binding (Figure II-3), this difference was lost. While it is possible that a substitution at residue 140 could modulate both the 1D7 and 3H1 epitopes, it is more probable that there is reduced binding to the anchor mAb, 6C5, perhaps as a result of denaturation or amino terminal proteolyis of the molecule. While lipid-free apoE is not a ligand for the LDLr, binding activity is restored if the apoE is incorporated into lipid vesicles (Innerarity *et al.* 1979). As it has been suggested that binding to lipid may induce a conformational change in apoE (Weisgraber *et al.* 1992), we have compared the 1D7 immunoreactivity of the apoE variants in a lipid-free and a lipid-bound form. However, as shown in Figure II-3, incorporation of the apoE into DMPC vesicles did not significantly change the observed fine specificity of 1D7.

2. **Fine specificity of mAb 2E8** - A second anti-human apoE mAb, 2E8, has been identified that blocks binding of apoE to the LDLr (Innerarity and Weisgraber, unpublished results). While the affinity of 2E8 for apoE is lower than that of 1D7, it can compete with 1D7 for binding to immobilized apoE and shows a pattern of reactivity similar to that of 1D7 with apoE proteolytic fragments (unpublished results). We have used the apoE variants to determine the fine specificity of 2E8 as was done for 1D7. The

results in Figure II-4 confirm the lower affinity of 2E8 for apoE compared to 1D7 but also demonstrate that, in general, the two antibodies have similar specificity with respect to the apoE variants. One notable difference, however, is that 2E8, unlike 1D7, shows decreased reactivity with apoE2(Arg^{158}→Cys). Antibody 2E8 does not discriminate between lipid-bound and free apoE nor does incorporation of apoE into lipid vesicles change its relative reactivities with apoE3 and apoE2(Arg^{158}→Cys) as shown in Figure II-5.

3. **Surface plasmon resonance** - In order to confirm the binding specificities of 1D7 and 2E8 which were determined by sandwich RIA, and to establish association and dissociation rate constants for the antibodies with the different mutants, we have studied their interactions using surface plasmon resonance (SPR). ApoE3 and the five variants, apoE(Arg^{136}→Ser), apoE(His^{140}→Ala), apoE(Lys^{143}→Ala), apoE(Arg^{150}→Ala) and apoE(Arg^{158}→Cys) were immobilized and were subjected to a pulse of antibody. Sensorgrams depicting the binding of the antibodies to the apoE variants as a function of time are shown in Figure II-6. The control antibody 3H1 reacted well with all of the variants including ApoE(His^{140}→Ala), indicating that the reduced reactivity observed by RIA may well have been due to a reduced capture of this mutant by the anchor antibody 6C5. The binding of 1D7 to the variants revealed the same fine specificity as that determined using the sandwich RIA. Again 1D7 had reduced reactivity with ApoE(Lys^{143}→Ala) and apoE(Arg^{150}→Ala). In the case of 2E8, the results obtained using SPR were also consistant with those obained using the sandwich RIA. Notably, the

reduced reactivity of 2E8 with ApoE(Lys^{143}→Ala), apoE(Arg^{150}→Ala), and apoE(Arg^{158}→Cys) have been confirmed.

This methodology has also allowed us to determine the association and dissociation rate constants, as well as the affinity of the antibodies for the individual ApoE variants (Table II-1). From Table II-1, it is apparent that the lower affinity of 2E8 compared to 1D7 and 3H1 for apoE3 is the result of a high dissociation rate constant. Moreover, the reduction of affinity of 1D7 and 2E8 for individual apoE variants can reflect changes in the association and / or the dissociation rate constants. For example, the reduced affinities of 1D7 for apoE(Lys^{143}→Ala) and apoE(Arg^{150}→Ala), compared to that for apoE3, is largely due to an increased dissociation rate constant, whereas the reduced affinity of 2E8 for apoE(Lys^{143}→Ala) reflects a reduced k_{on}. Reactivity of 2E8 with certain of the variants was too low to allow calculation of rate constants and affinities. As expected, the binding kinetics of 3H1 were similar with all of the apoE variants.

4. mAb 2E8 as an apoE phenotyping reagent.- As 2E8 showed little reactivity with the common apoE2(Arg^{158}→Cys) isoform, I have evaluated this mAb as a potential reagent to determine apoE phenotype. Human plasma was prepared from two apoE3 homozygotes, from two apoE2 / E3 heterozygotes and from six apoE2 homozygous individuals who attended the University of Ottawa Heart Institute Lipid Clinic. The apoE plasma content was then evaluated for every sample using a sandwhich radio-immunometric assay shown schematically in Figure II-7, and based on this result, the

samples were diluted to the same total apoE concentration (Figure II-8). The apoE2 phenotyping was then performed using a second sandwich radioimmunometric assay with 6C5 and ^{125}I-3H1 as the capture and detection antibodies, respectively. As shown in Figure II-9, the radiolabeled 2E8 mAb could clearly discriminate amongst individuals who were homozygous, heterozygous or lacked the apoE2 allele. The ^{125}I-2E8 binding curves that were obtained with plasma from apoE2 heterozygotes fell between those obtained with plasma from the apoE2 homozygotes and individuals who did not inherit an apoE2 allele.

5. Molecular cloning of 1D7, 2E8 heavy and light chain cDNAs - Total RNA from 1D7, 2E8 and 2H2 hybridoma cells was extracted according to the acid-guanidinium thiocyanate phenol chloroform method, and the integrity of freshly isolated nucleic acid was accessed by subjecting a small quantity to agarose gel electrophoresis. Figure II-10 illustrates an ethidium-bromide stained gel, showing intact 28S, 18S and 5S ribosomal RNA molecules. Poly(A+) mRNA was purified from total RNA preparations by oligo-dT affinity chromatography. Northern blot analysis was performed to insure the presence of light and heavy chain immunoglobulins transcripts. The constant region of a mouse kappa light chain (Max *et al.* 1981) and the first constant region of an IgG1a heavy chain (Honjo *et al.* 1979) were used as molecular probes for hybridization. Figure II-11 represents an autoradiogram depicting a Northern blot of a poly(A+) mRNA preparation probed for light and heavy chain presence. A unique signal was generated for both the light as well as the heavy chain, with the heavy chain being correspondingly

larger in size. This autoradiogram represents mRNA isolated from hybridoma 2H2, but similar results were obtained with all hybridoma preparations.

6. **The cloning of the light and heavy chains of mAb 1D7.-** In order to clone the entire light and heavy chains of mAb 1D7, a cDNA library was created by using 5 μg of poly(A+) 1D7 mRNA as template for reverse transcription with an oligo(dT) primer. Following the synthesis of the second strand, Not1 / EcoR1 adaptors (Pharmacia) were ligated to the cDNA. The cDNA was then digested with the endonuclease EcoRI, and the products were cloned into the bacterial pUC18 plasmid. Recombinant plasmids were transformed into DH5α competent *E.coli* bacteria by heat shock treatment, which on average generated some 50 000 bacterial colonies resistant to ampicillin, for every 200 ng of ligated plasmid. Colonies were screened by colony lift hybridization using the same radiolabeled IgG1a heavy chain and kappa light chain constant region probes that were used for northern analysis. Figure II-12 is an autoradiogram that illustrates the identification of immunoglobulin light chain positive clones by colony lift hybridization. Through this screening methodology, a number of positive clones were identified for both the light as well as the heavy chain. Plasmid DNA was prepared from 1.5 ml bacterial cultures and the length of the corresponding cDNA accessed by EcoR1 digestion followed by electrophoresis on a 1% agarose gel. The identity of the cDNA inserts were confirmed by Southern blotting followed by hybridization of the replicas with appropriate radio-labeled probes. In total, six heavy chain as well as 10 light chain clones, which appeared larger than 2.2 kb and 1 kb respectively, and which reacted with the constant region probes in southern blot experiments, were chosen for further

characterization. All clones were subjected to double stranded DNA sequencing. A unique, in-frame sequence was obtained for the heavy chain, whereas a bonafide light chain clone was identified in addition to two clones that represent the product of non-productive rearrangements at the kappa chain locus. The two non-functional light chain clones were determined to have originated from the B cell and the non-secreting myeloma fusion partner, respectively. The latter non-functional kappa gene has been previously described (Walfield *et al.* 1981). Both had deleterious frame shifts within the nucleotides encoding the variable region, occurring at the junction of the rearranged V and J segments. The nucleotide as well as the deduced amino acid sequences of the genuine immunoglobulin clones are presented in Figures II-13, II-14 and II-15, II-16 respectively.

7. **Cloning of the light and heavy chains of mAb 2E8**.- The cDNA encoding the 2E8 light chain was amplified by the polymerase chain reaction (PCR) (Mullis and Falcona, 1987), after reverse transcription of hybridoma mRNA, using one primer complementary to the 3' end of the kappa translated sequence (5'-GCG CCG **TCT AGA** ATT AAC ACT CAT TCC TGT TGA A-3'), and the other corresponding to the nucleotides encoding the amino terminal residues of the mature light chain (5'-CCA GGT CCG **AGC TC**G TGA TGA CCC AGT CTC CA-3'). Both the 5' and 3' region primers were based on previously compiled sequences (Huse *et al.* 1989) and contain, respectively, SacI and XbaI restriction sites indicated in bold, which facilitated the subsequent cloning of the PCR amplified products, for eventual expression. Following amplification, the 700 base-pair fragments corresponding to two immunoglobulin

domains were gel purified (Figure II-17) and subcloned, following Klenow and kinase treatment, into p-Bluescript(KS+) (Stratagene, CA) digested with SmaI (Sambrook *et al* 1989). The 2E8 heavy chain was cloned using anchored-PCR as described in the methodology section. However, for added clarity, a diagram depicting the procedure is presented in Figure II-18. All the cloned cDNAs were sequenced using the dideoxy chain termination method. Single unique in-frame sequences were obtained for the light and heavy chains, respectively (Figures I-13 and I-14).

8. Amino acid sequence analysis of the light and heavy chains of mAbs 1D7, 2E8 and 2H2 - To confirm that the cloned cDNAs do encode the respective heavy and light chains of the 1D7 and 2E8 Fabs, we have subjected the separated heavy and light chains of purified 1D7 and 2E8 IgG to amino terminal sequencing. As shown in Figure II-19, amino-terminal sequence was obtained for each immunoglobulin chain with the exception of the 1D7 heavy chain. Presumably, our lack of success at sequencing the amino terminal end the 1D7 heavy chain was a consequence of post-translational amino terminal modification that is frequently observed with immunoglobulin chains. We did, however, succeed in obtaining amino terminal sequence from a CNBr fragment of the 1D7 heavy chain that was generated by a cleavage following Met^{84} (Figure II-19). In all cases the amino acid sequences determined by direct peptide sequencing corresponded to those deduced from the nucleotide sequences of the respective cDNA clones.

9. Identification of the variable region gene families used in mAbs 1D7, 2E8.- Comparison of the variable region sequences of the three mAbs with those in the database of Kabat et al. (Kabat *et al.* 1991; Kabatman database internet server: http://immuno.bme.nwu.edu/scripts/subgroup.tc) indicated that the rearranged 1D7 heavy chain is a member of the mouse heavy chain variable region subgroup I(B) and possibly arose from within family IV as shown in Table II-2. Codons 103-117 were determined to have been derived from the mouse heavy chain J-minigene, MUSJH2 (Kurosawa and Tonegawa 1982). Its D-minigene however could not be identified owing either to the incomplete tabulation of members of this family of genes, or due to mutations that were introduced during affinity maturation of the antibody, and that rendered the segment unclassifiable. The 2E8 heavy chain gene is a member of the mouse heavy chain variable region subgroup II(C), which possibly originated from family IX (Table II-2), and includes sequences derived from the DSP2.2R+2 D-minigene (codons 99 to 103) (Kurosawa and Tonegawa 1982) and from the MUSJH3 J-minigene (codons 106-120) (Kabat et al.1991). Sequencing of the nucleotides encoding the C_{H1} showed that both heavy chains were of the γ1 subclass, thus confirming serological identification. The 1D7 and 2E8 light chains are both members of the mouse kappa variable subgroup V, and both contain sequences derived from the MUSJK5 kappa J-minigene (Kurosowa and Tonegawa 1982). While the 1D7 light chain could not be ascribed to any family within subgroup 5, that of 2E8 was found to have possibly arisen from family XX.

Both antibody light and heavy chains were found to conform to previously characterized murine antibody primary structures, in terms of the invariant presence of certain key residues. For example, both 1D7 and 2E8 have cysteine residues at positions 23 and 88 and at positions 22 and 92 of the light and heavy chains, respectively, which form intra-domain disulfide linkages that help to maintain the conformation of the respective variable domains. In addition, the well characterized light chain Glu^{38} and heavy chain Glu^{39}, known to be implicated in an interdomain hydrogen bonds, are also present in the two immunoglobulins. Other residues, which were often found to contact antigen in previously solved X-ray crystal structures of immune complexes, have been reported to be present in all variable regions. These residues are in general large aromatic amino acids such as tryptophan, phenylalanine and tyrosine. The side chains of these residues are known to possess a certain mobility, and can therefore orient themselves in order to accomodate the formation of a molecular complex with opposing residues originating from an antigen molecule (Mian *et al.* 1991). Indeed variable domains of 1D7 and 2E8 contain most of these conserved residues that are thought to facilitate the interaction with antigen, and provide plasticity to the paratope. These residues correspond in the light chain to: Trp 35, Tyr 36 in the light chain FR2, and in the heavy chains; Trp 36 and 46 in FR2, Tyr 57 in CDR2, Tyr 103 in CDR3 and Trp 104 in FR4.

10. Analysis of the complementary determining regions (CDR).- As the two anti-apoE mAbs, 1D7 and 2E8, were found to have similar fine specificities, it may be expected that they share homology in the 6 hypervariable or complementarity

determining regions (CDRs). As stated in the introduction, it has been determined that the amino acids which comprise the 3 CDRs of the light chain and the 3 CDRs of the heavy chain, interact directly with the corresponding epitope and are therefore largely responsible for antibody specificity. Comparison of the primary structure of the light chains of 1D7 and 2E8 shows considerable homology for the CDR1 and CDR2, which display 81% and 86% amino acid sequence homology. However, both light chains share almost no sequence identity for their CDR3. The 1D7 light chain contains two negatively charged residues which are found in CDR1 and CDR2 respectively, whereas the 2E8 light chain has no negatively-charged residues within its CDRs. There is little homology between the heavy chain CDRs of these two anti-apoE mAbs, and moreover CDR2 and CDR3 of 2E8 contain one and two additional amino acids respectively, as compared to the corresponding CDRs of 1D7. The heavy chain CDRs of 1D7 include 4 acidic amino acids whereas those of the 2E8 heavy chain contain 7 acidic residues. Lastly, as shown in Table II-3, all of the antibody CDRs, with the exception of both heavy chain CDR 3, could be assigned a canonical structure. This assignment was made using the "Chothia SDR template" program, available on the world wide web. ("http:www.biochem.ucl.ac.uk/cgi-bin/AndrewMartin/cothi.per"). The defined canonical structures are shown in Figure II-20 (taken from Edwards *et al.* 1992).

Discussion

In this chapter I have presented evidence that the epitopes of mAbs 1D7 and 2E8 coincide with the LDLr-binding site on apoE, that is situated between residues 136 and 150. It cannot be formally excluded, however, that the epitopes of 1D7 and 2E8 are located elsewhere on the molecule and may be disrupted by changes in conformation due to the amino acid substitutions that characterize the different apoE variants that I have tested. Nevertheless, it should be noted that a recent study which evaluated site-directed mutagenesis as a method for epitope mapping, revealed that mutations which caused a greater than 10-fold change in apparent antibody binding affinity (using methods analagous to those presented in Figure II-2) were correctly assigned to the epitope when confirmed by X-ray crystallography (Prasad *et al.* 1993). From results presented here and elsewhere (Weisgraber *et al.* 1983; Horie *et al.* 1992), it is very likely that Arg^{142}, Lys^{143}, Arg^{145}, Lys^{146} and Arg^{150} form part of the 1D7 and 2E8 epitopes. Furthermore, the lack of reactivity of apoE(Leu^{144}→Pro) and apoE(Ala^{152}→Pro) may indicate that either Leu^{144} and Ala^{152} are also directly implicated in the epitopes or, that a local conformational change induced by the introduction of a proline at these positions eliminates mAb binding. The relatively moderate decrease in reactivity of the apoE(Arg^{145}→Cys) variant would be consistent with the Arg^{145} side chain making only a minor contribution to the binding energy of the mAb-apoE complex in the case of both mAbs. In fact it has been shown, from the analysis of the x-ray crystal structure of apoE, that the side chain of Arg^{145} points

in a different direction compared to the positively charged cluster of residues within the ligand binding domain (Wilson *et al.* 1991). While the fine specificity of 2E8 is similar to that of 1D7, it is nevertheless notable that 2E8 and 1D7 differ in their relative affinities for apoE2(Arg^{158}→Cys) and apoE3, with 2E8 having little affinity for apoE2(Arg^{158}→Cys) (Figures II-2, II-3, II-4, II-6 and Table II-1). My results therefore indicate that the epitopes for mAbs 1D7 and 2E8 overlap with each other and with the LDLr binding site on apoE.

The ability of 2E8 to differentiate betweeen apoE3 and the receptor-defective, and clinically important isoform, apoE2 (apoE2(Arg^{158}→Cys)) could be potentially exploited in an antibody based test for the determination of apoE phenotype (Raffaï *et al.* manuscript in preparation). As shown in Figure II-9, when plasma is normalized for total apoE content, 2E8 can clearly discriminate between subjects who are homozygous, heterozygous or who have not inherited an allele encoding apoE2. Identification of an antibody that can differentiate between apoE2 and apoE3 should provide an impetus to generate other apoE isoform-specific antibodies. An antibody-based test for direct apoE isoform determination on plasma samples could offer advantages in terms of both time and expense when compared to the presently used methodologies based on isoelectrophoresis of isolated VLDL (Menzel and Uttermann, 1986) or PCR amplification of genomic DNA followed by endonuclease digestion (Hixson and Vernier, 1990). Given the associations that have been established between apoE genotype and both cardiovascular and neurological disease, it is probable that determination of apoE phenotype or genotype will become a standard clinical test.

The LDLr binds apoE only when the latter is associated with lipid emulsions (Innerarity *et al.* 1979). However, I observed that the incorporation of apoE into lipid particles does not change its immunoreactivity with either of the mAbs. It has been proposed that, in the presence of lipid, the four helix bundle of the amino terminal domain of apoE opens up to generate the receptor-active conformation (Weisgraber, 1992). While this lipid-driven unfolding would represent a major alteration in apoE tertiary structure, the changes in the secondary structure of the individual α-helices may only be minor. Consequently, the association of the protein with lipid would neither radically change the conformation nor mask the 1D7 and 2E8 epitopes. The reactivity of 1D7 with apoE synthetic peptides as short as 30 amino acids (Weisgraber *et al.* 1983) would indicate that its epitope does not require elaborate tertiary structure and is not composed of disparate regions of apoE primary structure. In the case of 1D7, the epitope may thus be continous or, as has been suggested earlier (Weisgraber *et al.* 1983), composed of one face of the α-helix that constitutes the secondary structure of this region. Nevertheless, it should be kept in mind that, while residues from within this helix may constitute the "critical epitope" that is recognized by the antibody, the antigenic surface in contact with antibody may be larger and include residues from elsewhere in the apoE molecule. While the critical epitope, itself, has been shown to be sufficient for high affinity binding to antibody (Hawkins *et al.* 1993), it has been predicted, based on size considerations alone, that antibodies will invariably contact more than one polypeptide segment in a folded globular protein (Barlow *et al.* 1986).

As described in Chapter I, it has been determined that the ligand-binding domain of the LDLr is situated at the amino-terminus and is made-up of seven imperfect repeats of a 40-amino acid cysteine-rich sequence that is characterized by a conserved cluster of acidic amino acids in the carboxy-terminal portion of the repeat (Goldstein *et al.* 1985). Repeats 3 through 7 appear to contribute to apoB-mediated binding of LDL, whereas, only repeat 5 appears to be critical for apoE-mediated binding of β-VLDL (Esser *et al.* 1988). It is long been thought that the binding of apoE and apoB100 to the LDLr may involve ionic interactions between basic amino acids of the apolipoproteins and acidic residues of the receptor (Brown *et al.* 1978; Basu *et al.* 1977). Chemical modifications of arginine and lysine residues in apoB100 and apoE (Mahley *et al.* 1977; Basu *et al.* 1977) and substitution of neutral amino acids for basic residues in the putative receptor-binding region of apoE reduce affinity of the apolipoproteins for the LDLr. Reductive methylation of lysine residues in apoE and apoB, which maintains the positive charge of the modified residues, also eliminates binding to the LDLr. This would suggest that, not only the positive charge, but also the structure of the basic residues contribute to the recognition of the ligands by the receptor. This is further supported by the observation that cysteamine treatment of apoE(Arg^{142}→Cys^{142}) restores a positive charge at residue 142 without rendering the molecule capable of binding to the LDLr (Horie *et al.* 1992). Moreover, the acid-mediated dissociation between the receptor and β-VLDL is not dependent on a simple titration of charged residues within the ligand binding domain (Davis *et al* 1987).

While basic residues located within the LDLr binding site of apoE contribute to the epitopes of both mAbs 1D7 and 2E8, the lack of similarity between the primary structures of the respective CDRs of the two mAbs, indicates that they recognize a similar region on apoE differently. Although the physical structure of the individual functional groups found within the two antibody CDRs are different, if considered in the context of a fully folded antibody combining site, they nonetheless may form a complex with apoE at an almost identical location. This could occur, if the antibodies use, for example, different relative planar angles of recognition. While it has been observed that oriented dipoles rather than counter charges are preferentially used in stabilizing charged residues in the formation of antigen-antibody complexes (Mian *et al.* 1991), both mAbs do, in fact, contain acidic residues within their respective CDRs that could potentially contribute to the binding energy of the antibody-antigen complex through the formation of salt bridges with basic residues of apoE in a manner similar to that which has been proposed for the interaction between apoE and the LDLr. In this case, the two anti-apoE mAbs differ in the distribution of their negatively charged amino acids amongst their respective CDRs. In the case of 1D7, the 6 acidic residues are distributed in the CDRs of both the heavy and light chains whereas, in 2E8, the 7 acidic residues are restricted to the heavy chain CDRs. Assuming that aspartic and glutamic residues of the two antibodies do make a major contribution to the binding energy of their respective immune complexes, this could indicate that 1D7 makes use of both chains for binding apoE, whereas, in 2E8, it is primarily the heavy chain that is responsible for antigen binding. It should, however, be emphasized that the surface of contact between antigen and antibody is large, and hydrogen bonds, van der Waals forces as well as electrostatic interactions

likely contribute to the binding energy. In Chapter V, I describe experiments in which I have used site directed mutagenesis to test the role of the acidic amino acids in CDRs of 2E8 in binding to apoE.

In addition to electrostatic counter charges, both antibodies possess similar residues at locations belived to be key for the association between an antibody and an antigen. The many tyrosines, tryptophans and phenylalanines which have been recorded to be present at putatively conserved "antigen contact sites" (Mian *et al.* 1991), indicate that the antibodies follow a general mode of association observed by other documented immunoglobulins. Supposedly, in the immune complex, much of the binding energy would be provided by these bulky aromatic residues which are known to be capable of rotating about their main chain axis, in order to allow the proper fit of an antigen. The fine tuning of the complex would presumably be provided by other residues of the six CDRs. Moreover, it is thought that that ionic and hydrogen bonds bring nearby antigen and antibody molecules together so that van der Waals and hydrophobic interactions can occur. This model of association has been proven in the protein-protein interaction between the enzyme Barnase and its natural inhibitor Barnstar, two well characterized proteins which display oppositely charged interacting surfaces. A good portion of the high affinity of the associated complex, has been ascribed to the strong electrostatic component. In fact, when this component was negated, by measuring the rate of association of the two proteins in 1 M NaCl, the affinity of the complex dropped by four orders of magnitude (Schreiber and Fresht, 1996).

ApoB, the major protein component of LDL, can compete with apoE for binding to the LDLr. Comparison of the primary structures of apoE and apoB has revealed a short sequence of apoB composed of residues 3359 and 3367 that resembles residues 140-150 of apoE with respect to the relative positions of basic amino acids (Knott 1985). It has been proposed that this characteristic distribution of basic residues could indicate that both apoproteins may be forming similar ionic interactions in their association with the ligand binding site of the LDLr. I have made an analogous comparison of the primary structures of the ligand-binding repeats of the LDLr and the CDRs of mAbs 1D7 and 2E8. Of the 7 acidic residues in the heavy chain CDRs of 2E8, 4 are clustered in CDR2. The spacing of the 4 aspartic and glutamic residues within CDR2 of the 2E8 heavy chain bears some resemblance to that of the acidic residues in the ligand-binding repeats of the LDLr (Figure II-19). Therefore, the CDR2 of the 2E8 heavy chain may mimic the postulated ionic interaction between the consensus sequence repeats of the LDLr and apoE. While the overall architecture of an antibody and that of the LDL receptor are clearly different, it is interesting to note that an anti-idotypic mAb prepared against a neutralizing anti-reovirus hemagglutinin mAb recognized the mammalian cell surface reovirus receptor and, in this case, the molecular mimicry resulted from homology in primary structure between the light chain CDR2 of the anti-idiotypic mAb and the viral hemagglutinin (Bruck *et al* 1986). In addition, it has been shown that certain anti-integrin antibodies which bind to the ligand binding site of platelet integrin $\alpha_{II}\beta_3$ contain the "Arg-Gly-Asp" integrin recognition motif in their antigen binding sites (Smith *et al.* 1994). Moreover, the activity of one such inhibitory antibodies could be emulated by synthetic peptides whose synthesis were based on the primary structure of these mAb

CDRs, including one which alone acts as a miniantibody by neutralizing human immunodeficiency virus type 1 in vitro (Smith *et al.* 1994; Williams *et al.* 1989; Levi *et al.* 1993) . Thus, the three dimensional structure created by an antibody CDR, may on some occasions provide a molecular replicate of a structure found on an unrelated, cross-reacting protein. As both the antibody CDRs and the cysteine-rich repeats of the LDLr are composed of looped protein segments, it is possible that their identity in primary structure, may confer them with the ability to function similarily in binding to apoE. The concept of mimicry between the 2E8 mAb and the LDLr will be expanded in Chapter V.

It is interesting to compare the structural requirements for apoE-mediated binding to the LDLr with those for 1D7 and 2E8 immunoreactivity (Figure II-21). Substitutions that result in the loss of a positive charge at residues 142, 143, 145, 146 or 150 produce a decrease in the ability of the variant to bind to both antibodies and to the receptor (Weisgraber *et al.* 1983; Lalazar *et al.* 1988; Horrie *et al.* 1992; Rall *et al.* 1982; Rall *et al.* 1982). Similarly, the introduction of proline residues at positions 144 and 152 decreases both antibody and receptor binding by either the replacement of a critical residue for binding or by disruption of apoE secondary or tertiary structure (Lalazar *et al* 1988). In contrast, several of the variants (eg. apoE(Arg^{136}→Ser) and apoE(Arg^{158}→Cys)) are defective with respect to LDLr binding but bind to 1D7 with high affinity (Lalazar *et al.* 1988; Rall *et al.* 1982). The binding of antibody 2E8 to apoE(Arg^{158}→Cys), on the other hand, is severely impaired (Figure II-6, Table II-1). It is thought that Arg^{158} is not directly implicated in binding to the LDLr but its replacement by a Cys in apoE(Arg^{158}→Cys) induces a conformational change in the receptor binding domain,

probably situated between residues 136 and 150 (Innerarity *et al.* 1984). In the crystal structure of the amino terminal domain of apoE3, Arg^{158} forms salt bridges with Glu^{96} and Asp^{154} and may help to stabilize the pairing of helices 3 and 4 (Wilson *et al.* 1991). In apoE(Arg^{158}→Cys), Arg^{150} forms a salt bridge with Asp^{154} (Wilson *et al.* 1994). The putative conformational change responsible for the decrease in binding affinity of apoE(Asp^{158}→Cys) for the LDLr may result from these reorganized salt bridges. As was described in Chapter I, the determination of the crystal structure of the apoE variant, apoE2(Asp^{154}→Ala, Arg^{158}→Cys), and the demonstration that it possessed near normal ability to bind to the LDLr provide strong evidence in support of this hypothesis (Dong *et al* 1997).

LDLr-binding and 1D7 immunoreactivity can also be distinguished by other criteria. Rat and mouse apoE, bind with high affinity to the human LDLr but have little 1D7 immunoreactivity (Weisgraber *et al.* 1983; Maurice *et al.* 1987). Finally, as discussed above, only lipid-bound apoE is recognized by the LDLr (Innerarity *et al* 1979) whereas neither mAb differentiates between free and lipid-bound apoE. Thus, while the apoE LDLr-binding domain and the 1D7 and 2E8 epitopes may coincide or overlap, the respective conformational elements that are recognized by the antibodies and the receptor are not identical. This situation, where two mAbs share a protein epitope, may be analogous to that which occurs between mAbs NC10 and NC41, both of which bind to an ovrlapping epitope on influenza virus neuraminidase. In this situation, it was found that both antibodies recognized the same protein epitope, through different CDR usage (Malby *et al.* 1994). More importantly, it was recently shown that it is possible for two

mAbs to recognize the electrostatic surface of a protein in dissimilar ways (McCoy *et al.* 1997).

It appears that apoE can be present in two forms in triglyceride-rich lipoproteins, one of which is resistant to cleavage by proteases and is not recognized by the LDLr and a second that is protease-sensitive and capable of binding to the LDLr (Bradley *et al.* 1984). ApoE may be converted from the first to the second form by either a change in conformation or in accessiblity that is induced by lipolysis of the particle or by both (Sehayek *et al.* 1991). As it has been proposed that 1D7 may distinguish between these two forms (Sacks *et al.* 1987), it may be a useful probe of the LDLr-binding site of apoE. Here I have identified a number of apoE residues that are critical for binding of the 1D7 and 2E8 mAbs and have demonstrated that the epitopes for both mAbs overlap with the LDLr-binding site on apoE. Moreover, based on both the criteria of specificity and on primary structure, I have presented evidence that one of the mAbs, 2E8, has some of the attributes of an antibody mimetic of the LDLr.

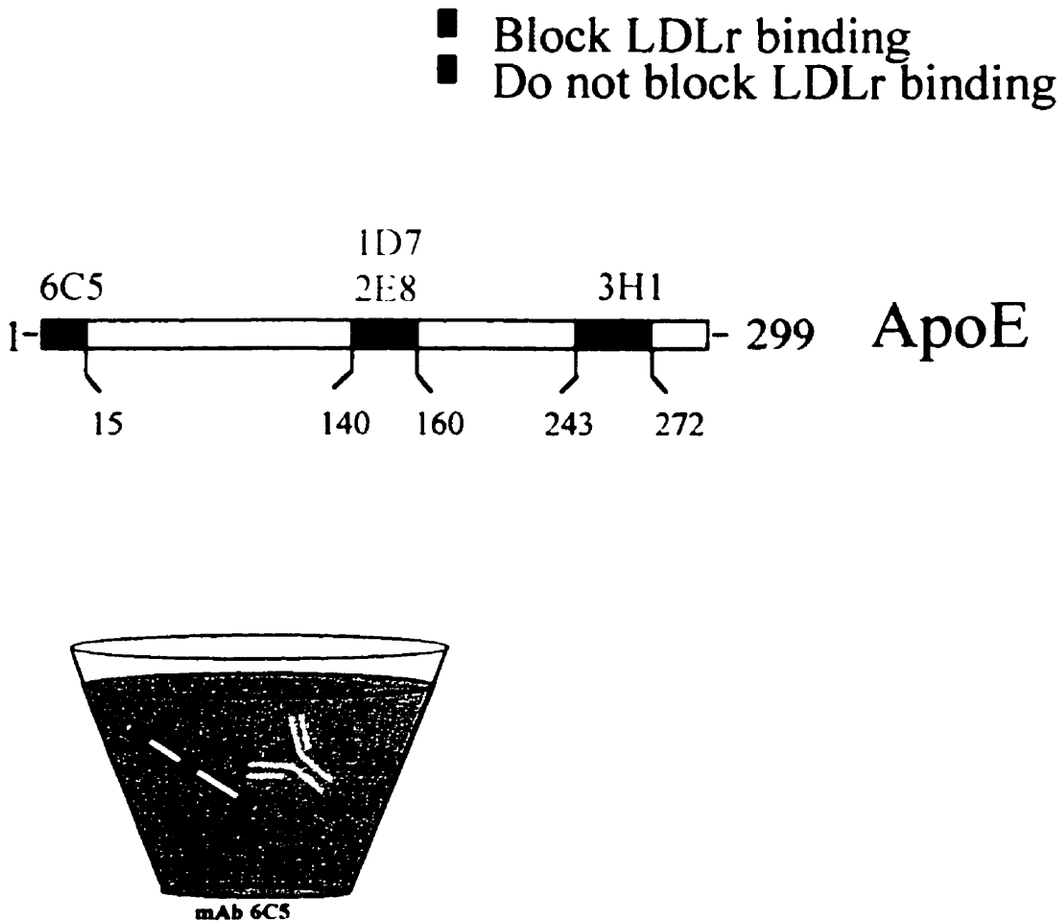

Figure II-1 Epitope map of human apoE and apoE sandwich radio-immunoassay.- This figure depicts an epitope map of human apoE. The epitope of mAb 6C5 has previously been shown to reside in the amino-terminal portion of the apoE, whereas that mAb 3H1 is situated in the carboxyl-terminal portion of the protein. Finally, the epitopes for both mAbs 1D7 and 2E8 have been shown to overlap with the LDLr-binding site of apoE. These mAbs were used to establish solid phase sandwich radioimmunometric assays to determine relative immunoreactivities of mAbs 1D7 and 2E8 with various LDLr-defective variant forms of apoE. As shown in the figure, mAb 6C5 was used to anchor apoE in microwells as its epitope is not influenced by the substitutions which characterize the variant forms of apoE. The relative affinities of mAbs 1D7 and 2E8 could then be assayed against a panel of apoE variants, by radio-iodinating the respective mAb. In all case, mAb 3H1 was used as a control antibody, as its epitope was not influenced by the amino acid substitutions which characterized the apoE variants.

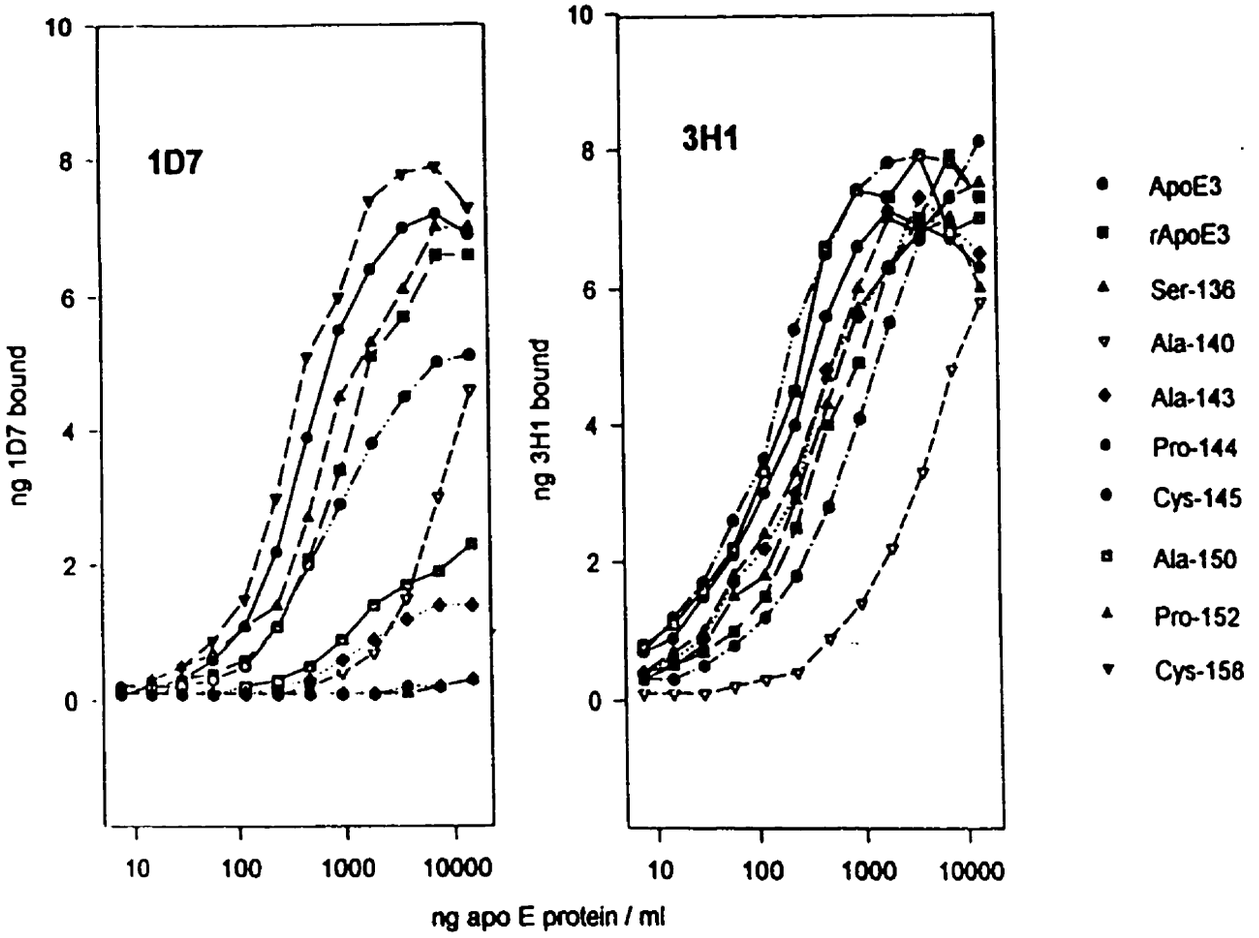

Figure II-2 Immunoreactivity of apoE variants with anti-apoE mAbs 1D7 and 3H1.- Serial dilutions of apoE variants were incubated in polystyrene microwells to which anti-apoE mAb 6C5 had been adsorbed. The wells were then washed and exposed to either ^{125}I-1D7 (left) or ^{125}I-3H1 (right) and, after washing, the bound radioactivity was determined. The bound ^{125}I-mAb mass was calculated from the specific activity of the labelled antibodies. Results from one experiment are shown with essentially identical results having been obtained in two other experiments.

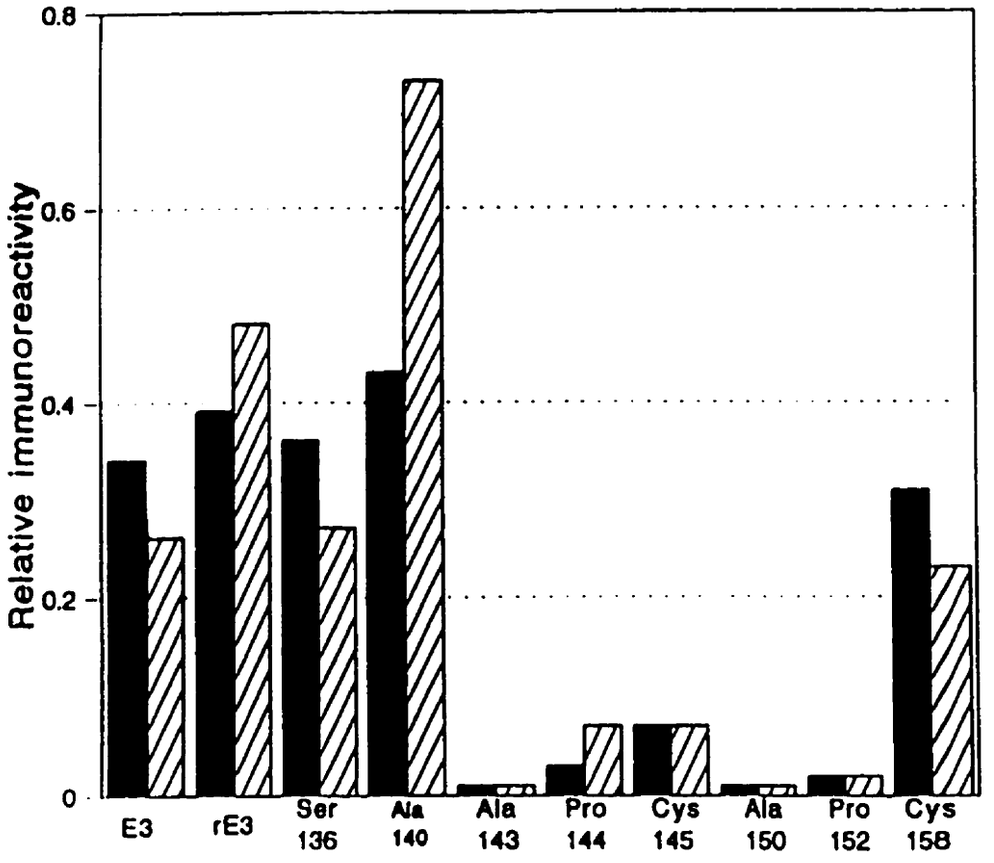

Figure II-3 Relative reactivity of mAb 1D7 with apoE variants. The relative immunoreactivity of apoE variants (closed bars) with mAb 1D7 was calculated from the results presented in Figure II.2 according to the formula: ng apoE necessary to have 3 ng of ^{125}I-3H1 bound / ng apoE necessary to have 3 ng of ^{125}I-1D7 bound. Results are also presented from the same experiment for apoE variants that had been incorporated into DMPC vesicles (cross-hatched bars).

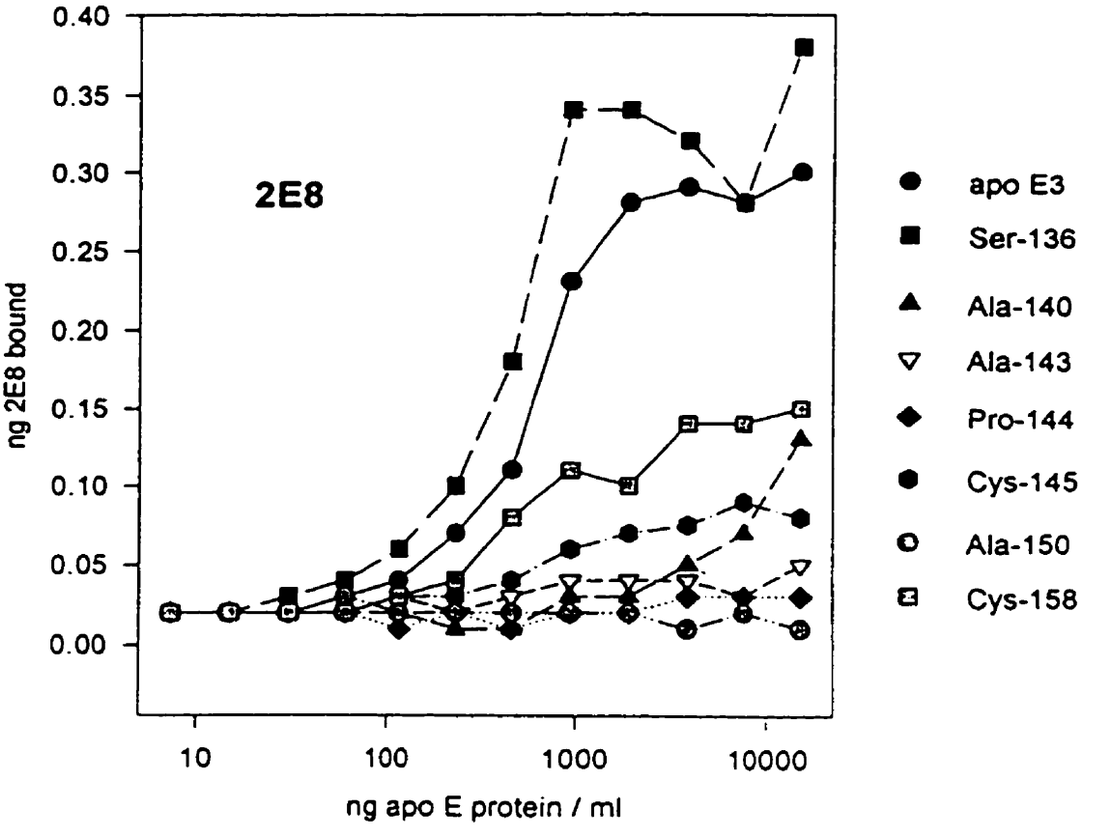

Figure II-4 Immunoreactivity of apoE variants with anti-apoE mAbs 2E8. Serial dilutions of apoE variants were incubated in polystyrene microwells to which anti-apoE mAb 6C5 had been adsorbed. The wells were then washed and exposed to ^{125}I-2E8 and, after washing, the bound radioactivity was determined. The bound ^{125}I-mAb mass was calculated from the specific activity of the labelled mAb.

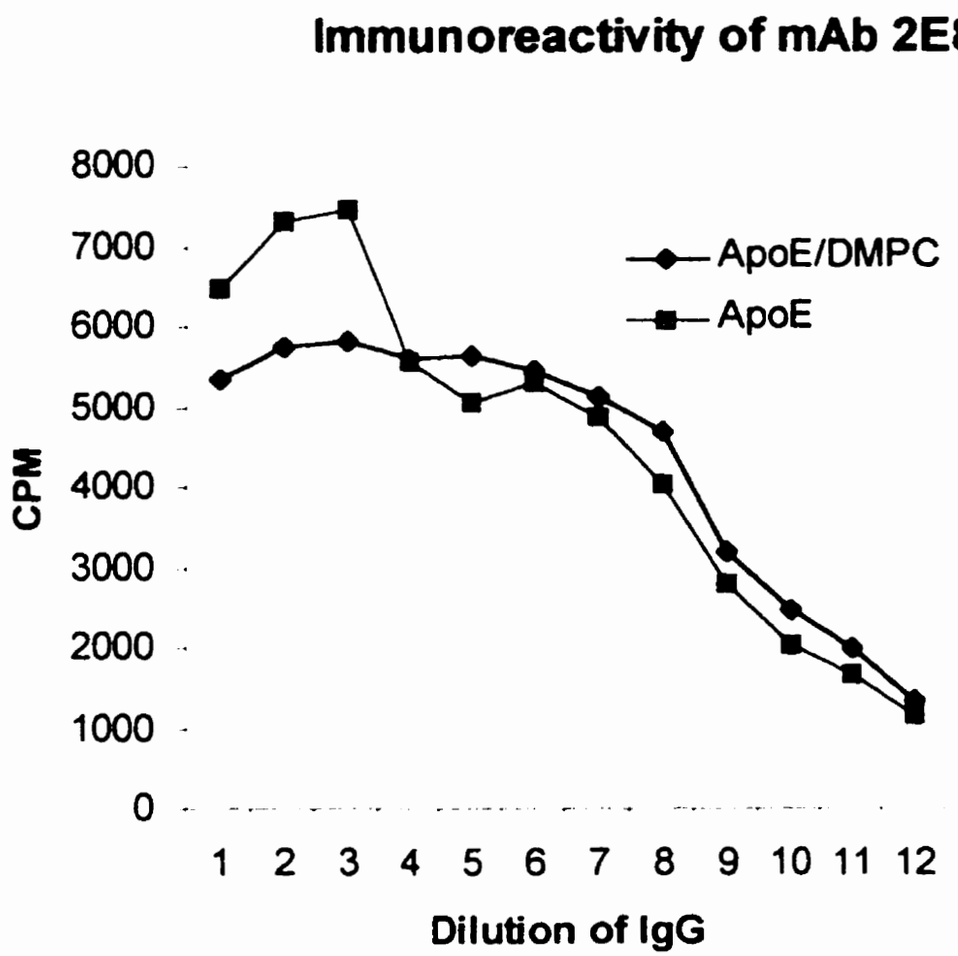

Figure II-5 Relative immunoreactivity of mAb 2E8 against lipid free versus lipid bound apoE.- Purified apoE was incorporated into DMPC vesicles as described in the Methods section. The 2E8 immunoreactivity of the lipid-bound or lipid free apoE was determined by a solid phase immunometric sandwich assay.

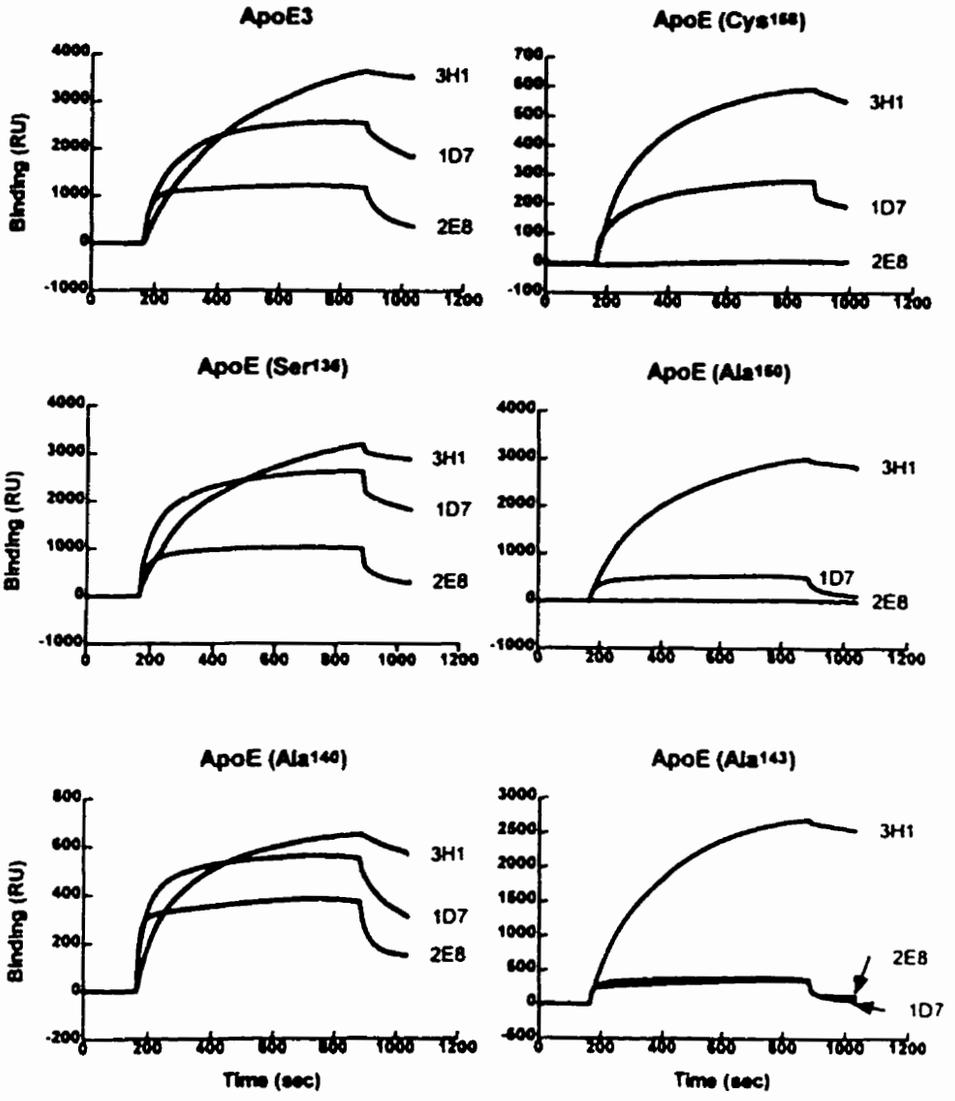

Figure II-6. Sensorgrams of ApoE variants with 1D7, 2E8 and 3H1 using SPR. These sensorgrams depict the kinetics of 1D7, 2E8 and 3H1 binding to apoE3, apoE(Arg^{136}→Ser), apoE(His^{140}→Ala), apoE(Lys^{143}→Ala), apoE(Arg^{150}→Ala) and apoE(Arg^{158}→Cys). The association phase of each sensogram begins at approximately 180 seconds and the dissociation phase at 850 seconds. The results that are illustrated were obtained with concentrations of 150 nM, 150 nM and 50 nM for 1D7, 2E8 and 3H1, respectfully.

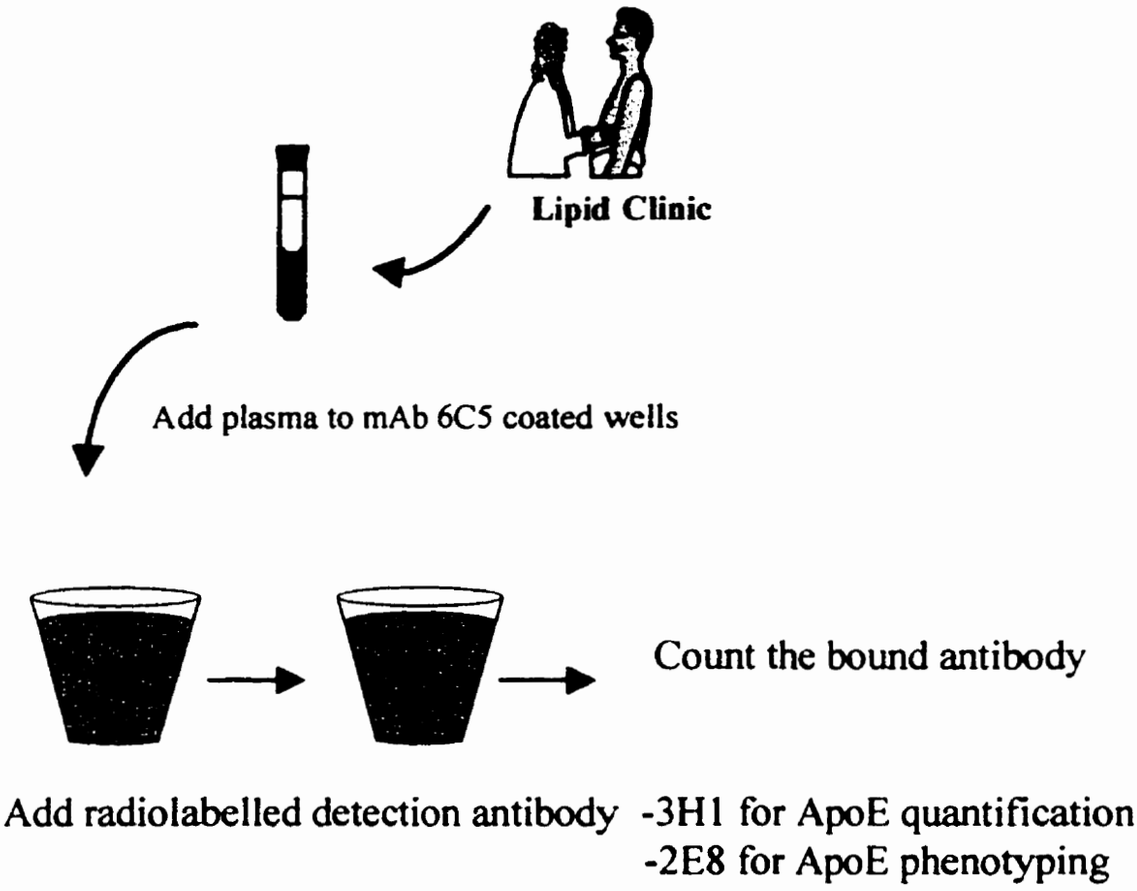

Figure II-7 Immunoassay format used for the evaluation of 2E8 as a reagent to determine the presence of the apoE2 isoform in plasma. The two mAbs; 3H1 and 2E8 were used in an immunometric assay in order to detect the presence of apoE2. Freshly isolated plasma was incubated as serial dilutions, in microtiter wells coated with mAb 6C5. The captured plasma lipoproteins were then subjected to immunodetection by the addition of ^{125}I labelled mAb 3H1 or 2E8. As shown in the two following Figures, mAb 3H1 served as an indicator of total plasma apoE regardless of the isoform, whereas mAb 2E8 served as an indicator of apoE2 presence.

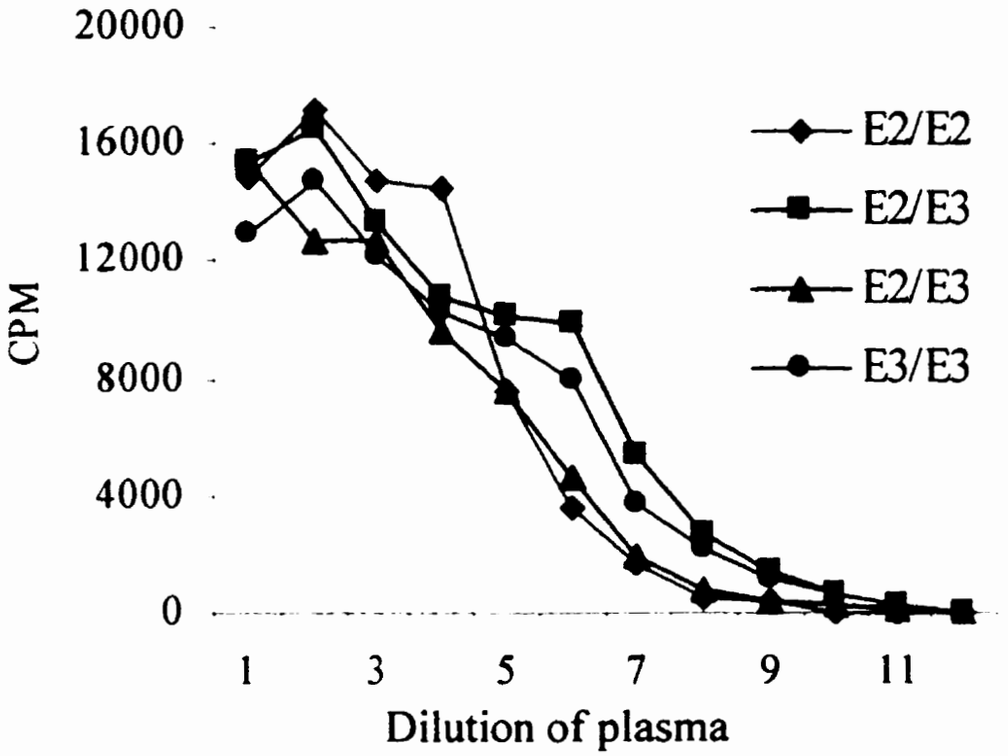

Figure II-8 Immunodetection of human apoE using mAb 3H1.- This Figure illustrates the standardization of plasma from individuals of known apoE phenotype with respect to apoE concentration. In the solid phase sandwich assay, apoE-containing lipoproteins were captured with mAb 6C5 and detected with ^{125}I-3H1. Neither 6C5 nor 3H1 discriminate between the common apoE isoforms.

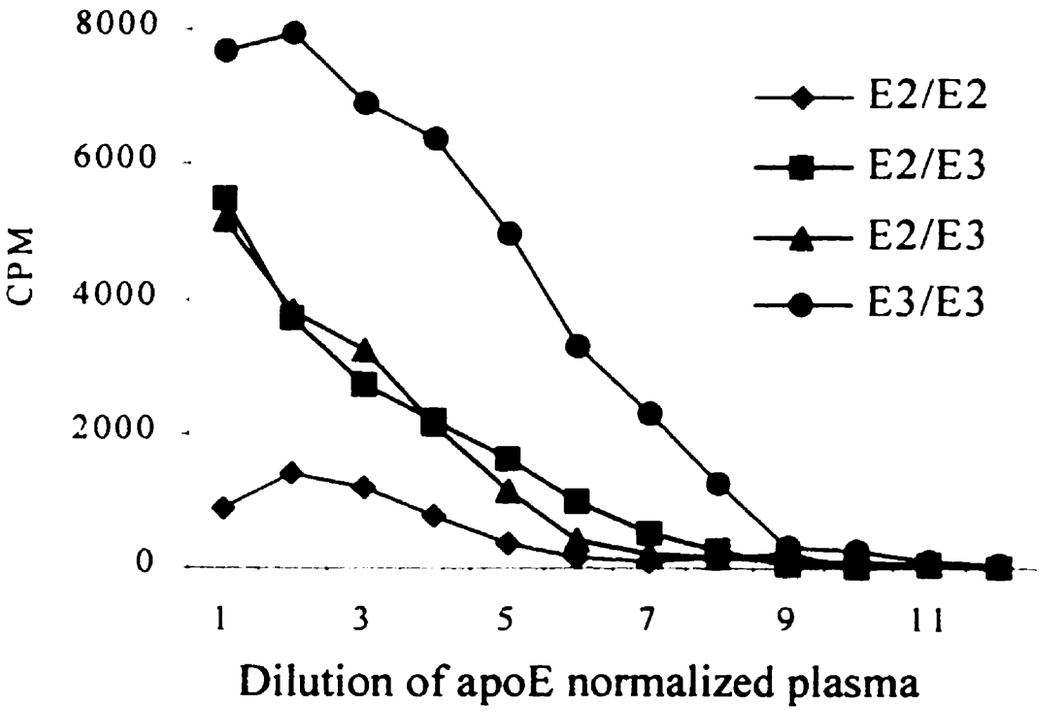

Figure II-9 Determination of apoE phenotype from human plasma.- Plasma of known apoE phenotype that had been adjusted for total apoE content was tested in a solid phase sandwich immunometric assay. ApoE-containing lipoproteins were captured using immobilized 6C5 and detected with ^{125}I-2E8. Using this format the assay can discriminate between individuals who are homozygous, heterozygous or do not carry the ε2 allele.

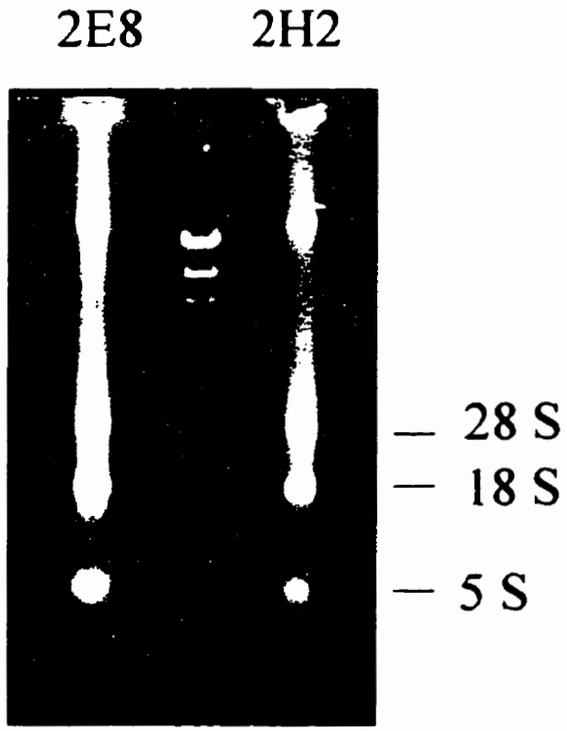

Figure II-10 Assessment of the integrity of freshly isolated hybridoma total RNA.- This Figure consists of a photographed agarose gel on which a small portion of freshly isolated total hybridoma RNA was separated, and stained with ethidium bromide. The presence of three well defined and undegraded bands, corresponding to the 28 S, 18 S and 5 S ribosomal RNA molecules, offered an indication as to the integrity of the isolated immunoglobulin mRNA.

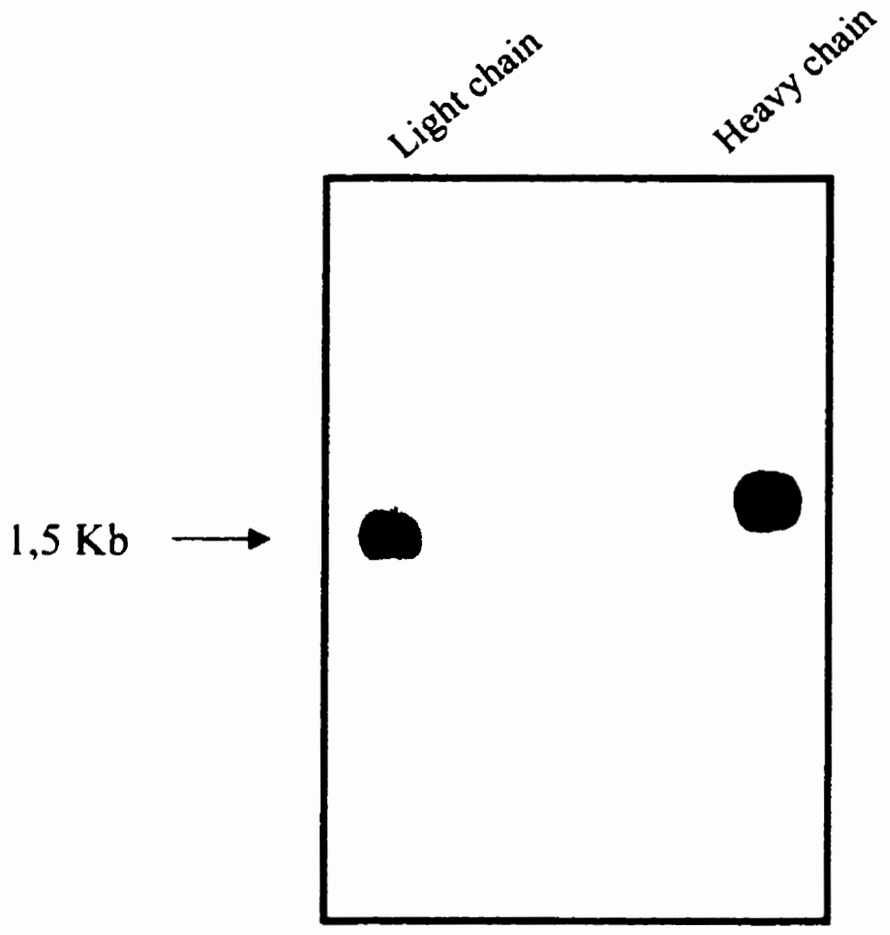

Figure II-11 Detection of the mRNA encoding the 2H2 mAb light and heavy chains.- This Figure represents a Northern blot transfer of poly(A^+) 2H2 hybridoma mRNA. A small amount of poly(A^+) RNA was separated on a 1 % agarose gel, and subsequently was transfered onto a nylon membrane. The membrane was then cut in half, and both portions were incubated either with a light chain or a heavy chain radiolabled constant region probe. Following appropriate washing, the two membranes were exposed to X-ray sensitive film. The appearance of two well defined bands corresponding to about 2.5 Kb and 1.5 Kb respectively, attest to the presence and to the integrity of the heavy and light immunoglobulin chains.

Figure II-12 Colony lift hybridization detection of cloned immunoglobulin chains.- This Figure illustrates a photographed autoradiogram corresponding to a primary screening of bacteria transformed with the 1D7 cDNA library. The membrane which served to lift off the bacterial clones was, in this case, incubated with a radiolablled light chain constant region probe.

Codon #1.

```
      AAT TGC GTG ATG ACC CAG ACT CCC AAA TTC CTG CTT GTA TCA GCA GGA
       *** *** *** *** *** *** *** **A --- --- A-- TCC AC- --- -T- ---
      *** *** *** *** *** *** *** **A CTC ACT T-- TCG -TT A-C ATT ---
```

CDR1

```
(17)  GAC AGG GTT ACC ATA ACC TGC AAG GCC AGT CAG
      --- --- --- -G- --C --- --- --- --- ---
      C-A CCA -CC T-- --T T-T --- --- T-A --- --- AGC CTC TTA GAT AGT

(28)  AGT GTC AGT AAT GAT GTA GCT TGG TAC CAA CAG AAA CCA GGG CAG GCT
      -A- --G G-- -C- -C- --- --C --- --T --- --- --- --- --A --A T--
      GA- -GA -AG -CA T-- T-G AA- --- CTG TT- --- -GG --- --C --- T--
```

CDR2

```
(44)  CCT AAA CTG CTG ATA TAC TAT GCA TCC AAT CGC TAC ACT GGA GTC CCT
      --- --- --A A-- --T --- -CG --- --- --- --G --- --- --- --- ---
      --A --G -GC --A --C --T CTG -TG --T --A -TG G-- T-- --- --- ---

(60)   GAT CGC TTC ACT GGC AGT GGA TAT GGG ACG GAT TTC TCT TTC ACC ATC
       --- --- --- --A --- --- --- -C- --- --A --- --- A-- C-- --- ---
       --C A-G --- --- --- --- --- -CA --- --A --- --- A-- C-G -AA ---
```

CDR3

```
(76)   AGC ACT GTG CAG GCT GAA GAC CTG GCA GTT TAT TTC TGT CAG CAG GAT
       --T -A- A-- --- T-- --- --- --- --- -A- --- --- --C --- ACA T--
       --- -GA --- G-- --- --G --T T-- -G- -G- --- -AT --C TG- --A -G-

(92)
       TAT CGC TCT CCT CCT ACG TTC GGT GCT GGG ACC AAG CTG GAG CTG AAA
       AGC A-- -A- --- -TC --- --- --- --- --- --- --- T-- --- --- ---
       ACA -AT -T- --- -AG --- --- --- -GA --C --- --A --- --A A-C ---
```

Figure II-13 Nucleotide sequences of 1D7, 2E8 and 2H2 light chains.- The nucleotide sequences of the variable domains of 1D7 (upper) and 2E8 (middle) and 2H2 (bottom) light chains are presented. CDRs are indicated in bold print and negatively charged residues within the CDRs are underlined. The asterisks indicate the nucleotides within the degenerate PCR primer that were used for cloning the 2E8 light chain cDNA. Codons are numbered and CDRs are identified according to Kabat *et al.* (Kabat *et al.* 1991).

Codon #1.

```
        CAG GTG CAC CTG AAG GAG TCA GGA CCT GGC CTG GTG GCG CCC TCA CAG
        G-- --T --G --- C-- C-- --T --G G-A -AG G-T --- AG- T-A GGG GCC
        G-- --- --G --- C-- C-- --A GG- --A -AG CTG GTG CG- --- GCG GCC

(17)    AGC CTG TCC ATC ACA TGC ACC GTC TCA GGG TTC TCA TTA ACC GGC TAT
        TCA G-C AAG T-G T-C --- --A -CT --T --C --- AAC A-T -AA -A- --C
        TCA --T AAG --- T-C --- -AG ACT --T --T -AC --- --C --T --- --C

                CDR 1
(33)    GGT GTA AAC TGG GTT CGC CAG CCT CCA GGA ACG GGT CTG GAG TGG CTG
        TA- A-C C-- --- --G AAG --- AGG --T -A- -A- --C --- --- --- A-T
        ACC A-G --- --- --G AAG --- AGC -AT --G -A- AAC --T --- --- A-T

(49)                                    CDR 2
        GGA TTG ATA TGG     GCT GAT GGA AGA ACA GAC TAT AAT TCA GCT CTC
        --- -G- --T GAT CCT -AA ATT --T GAT --T --A --- GTC C-G AAG T--
        --- C-T --T AAT CCT TAC A-- --T G-T --T AC- --C --C CAT AAG T-G

(64)
        AAA TCC AGA CTG AGC ATC AGC AAG GAC AAC TCC AAG AGC CAA GTT TTC
        C-G GG- -AG GCC -CT -TG -CT GCA --- -CA --- TCC -A- AC- -CC -A-
        --G GG- -AG G-C -CA T-T -CT GTA --- --G --A TCC --T AC- -CC -AC

(80)    TTA AAA ATG AAC AGT CTG CAA ACT GAT GAC ACA GCC AGG TAC TAC TGT
        C-G C-- C-C -G- --C --- AC- TC- --G --- --T --- GTC --T --- ---
        A-G G-C C-C CT- --- --- AC- T-- --G --- T-T --A G-C --T --- ---

(93)                                    CDR 3
        GCC AGA GAG GGG GTT GGT TAT CCC         TTT GAC TAC TGG GGC CAA
        AAT GC- -G- CAT -A- TAC G-C AGG GGA CGG --C CCT --- --- --- ---
        --A AAC TG- GAC TGG GA- G-G GA-         --- --- --- --- --G ---

(106)
        GGC AAC ACT CTC ACA GTC TCC TCA
        --G -CT CTG G-- --T --- --T G--
        --- --- G-- --- --- --- --- ---
```

Figure II-14 Nucleotide sequences of 1D7, 2E8 and 2H2 heavy chains. The nucleotide sequences of the variable domains of 1D7 (upper), 2E8 (middle) and 2H2 (bottom) heavy chains are presented. CDRs are indicated in bold print and negatively charged residues within the CDRs are underlined. Codons are numbered and CDRs are identified according to Kabat *et al.* (Kabat et al. 1991).

(1) *Asn Cys Val Met Thr Gln Thr Pro Lys Phe Leu Leu Val Ser Ala Gly*
Asp Ile --- --- --- --- Ser Gln --- --- Met Ser Thr --- Val ---
Asp Val --- --- --- --- --- --- Leu Thr --- Ser --- Thr Ile ---

CDR1

(17) *Asp Arg Val Thr Ile Thr Cys* ***Lys Ala Ser Gln***
Asp Arg Val Thr --- --- --- --- --- --- ---
Gln Pro Ala Ser --- Ser --- **Leu Ser** --- --- **Ser Leu leu Asp Ser**

(28) **Ser Val Ser Asn Asp Val Ala** Trp Tyr Gln Gln Lys Pro Gly Gln Ala
Asn --- --- --- **Ala** --- --- --- --- --- --- --- --- --- --- Ser
Asp Gly Lys Thr Tyr Leu Asn --- Leu Leu --- Arg --- --- --- Ser

CDR2

(44) Pro Lys Leu Leu Ile Tyr **Tyr Ala Ser Asn Arg Tyr Thr** Gly Val Pro
--- --- --- Met --- --- **Ser** --- --- --- --- --- --- --- --- ---
--- --- Arg --- --- --- **Leu Val** --- **Lys Leu Asp Ser** --- --- Pro

(60) Asp Arg Phe Thr Gly Ser Gly Tyr Gly Thr Asp Phe Ser Phe Thr Ile
--- --- --- --- --- --- --- Ser --- --- --- --- Thr Leu --- ---
--- --- --- --- --- --- --- Ser --- --- --- --- Thr Leu --- ---

(76) Ser Thr Val Gln Ala Glu Asp Leu Ala Val Tyr Phe Cys **Gln Gln Asp**
--- Asn Met --- Ser --- --- --- --- Asp --- --- --- --- --- **Tyr**
--- Arg --- Glu --- --- --- --- Gly Gly --- Tyr --- **Trp Gln Gly**

CDR3

(92) **Tyr Arg Ser Pro Pro Thr** Phe Gly Ala Gly Thr Lys Leu Glu Leu Lys
Ser Ser Tyr --- Leu --- --- --- --- --- --- --- --- --- --- ---
Thr His Phe --- Gln --- --- --- Gly --- --- --- --- --- Ile ---

Figure II-15 Deduced protein sequences of 1D7, 2E8 and 2H2 light chains.- The deduced protein sequences of the variable domains of 1D7 (upper) and 2E8 (middle) and 2H2 (bottom) light chains are presented. As done with the tabulated nucleotide sequences, CDRs are indicated in bold print and negatively charged residues within the CDRs are underlined. Amino acid residues represented in italics were confirmed by protein sequence determination. Codons are numbered and CDRs are identified according to Kabat *et al.* (Kabat *et al.* 1991).

(1) Gln Val His Leu Lys Glu Ser Gly Pro Gly Leu Val Ala Pro Ser Gln
Glu --- Gln --- Gln Gln --- --- Ala Glu Val --- Arg Ser Gly Ala
Glu --- Gln --- Gln Gln --- --- --- Glu --- --- Lys --- Gly Ala

(17) Ser Leu Ser Ile Thr Cys Thr Val Ser Gly Phe Ser Leu Thr **Gly Tyr**
--- Val Lys Leu Ser --- --- Ala --- --- --- Asn Ile Lys **Asp** ---
--- Met Lys --- Ser --- Lys Thr --- --- Tyr --- Phe --- --- **Tyr**

CDR1

(33) **Gly Val Asn** Trp Val Arg Gln Pro Pro Gly Thr Gly Leu Glu Trp leu
Tyr Ile His --- --- Lys --- Arg --- Glu Lys --- --- --- --- Ile
Thr Met --- --- --- Lys --- Ser His --- Lys Asn --- --- --- Ile

CDR2

(49) Gly **Leu Ile Trp Ala Asp Gly Arg Thr Asp Tyr Asn Ser Ala Leu**
--- **Trp** --- **Asp Pro Glu Ile** --- **Asp** --- **Glu** --- **Val Pro Lys Phe**
--- --- --- **Asn Pro Asn Gly** --- **Gly** --- **Thr** --- --- **His Lys** ---

(64) **Lys Ser** Arg Leu Ser Ile Ser Lys Asp Asn Ser Lys Ser Gln Val Phe
Gln Gly Lys Ala Thr Met Thr Ala --- Thr --- Ser Asn Thr Ala Tyr
--- **Gly** Lys Val Thr Phe Thr Val --- Lys --- Ser --- Thr Ala Tyr

(80) Leu Lys Met Asn Ser Leu Gln Thr Asp Asp Thr Ala Arg Tyr Tyr Cys
--- Gln Leu Ser --- --- Thr Ser Glu --- --- --- Val --- --- ---
Met Asp Leu Leu --- --- Thr Ser Glu --- Ser --- Gly --- --- ---

CDR3

(93) Ala Arg **Glu Gly Val Gly Tyr Pro Phe Asp Tyr** Trp Gly Gln
Asn Ala **Gly His Asp Tyr Asp Arg Gly Arg** --- **Pro** --- --- --- ---
--- Asn **Trp Asp Trp Asp Glu Asp** --- --- --- --- --- ---

(106) Gly Thr Thr Leu Thr Val Ser Ser
--- --- Leu Val --- --- --- Ala
--- --- Ala --- --- --- --- ---

Figure II-16 Deduced protein sequences of 1D7, 2E8 and 2H2 heavy chains.- The deduced protein sequences of the variable domains of 1D7 (upper) and 2E8 (middle) and 2H2 (bottom) light chains are presented. As done with the tabulated nucleotide sequences, CDRs are indicated in bold print and negatively charged residues within the CDRs are underlined. Amino acid residues represented in italics were confirmed by protein sequence determination. Codons are numbered and CDRs are identified according to Kabat et al. (Kabat et al. 1991).

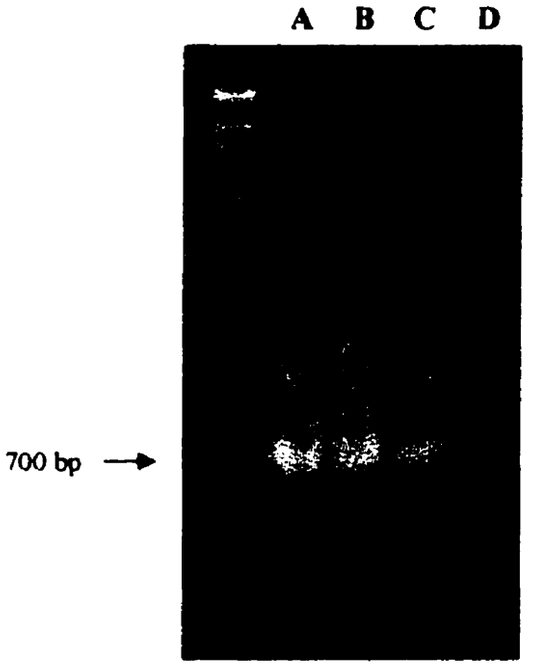

Figure II-17 Amplification of immnoglobulin light and heavy chains.- This figure illustrates PCR amplified light and heavy chain immunoglobulin sequences. All chains were amplified with their appropriate sense and anti-sense oligonucleotide primers. They were then resolved on a 1 % agarose gel and stained with ethidium bromide. The fragments could then be isolated from the gel and sub-cloned into a plasmid vector.

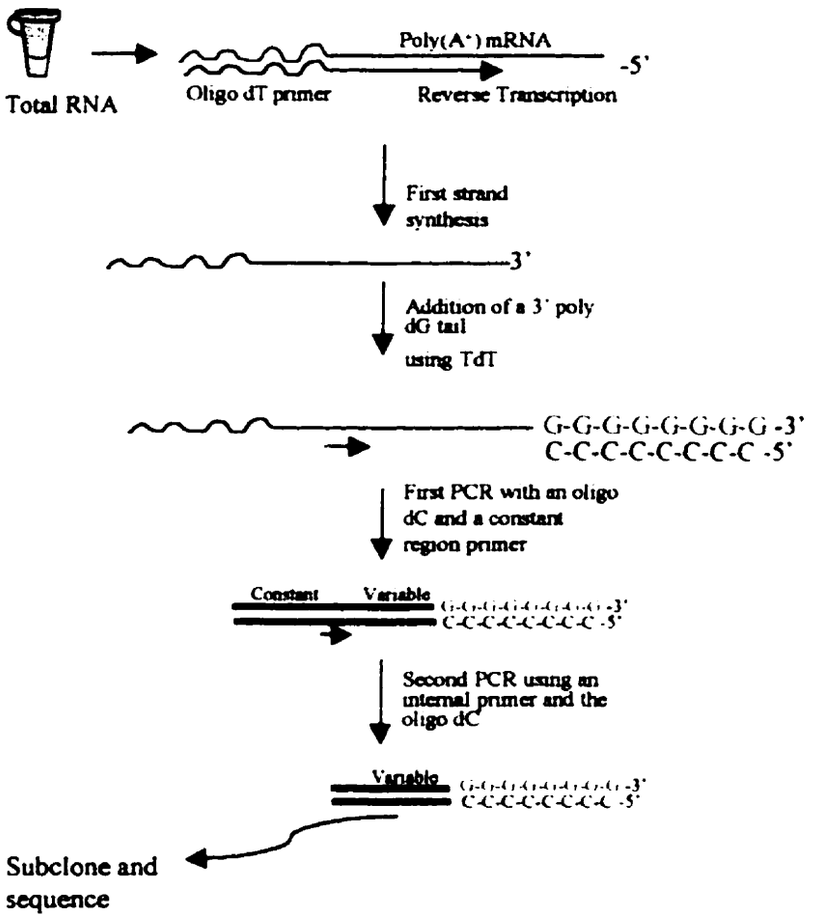

Figure II-18 Amplification of an immunoglobulin fragment using anchored PCR.-

The technique of anchored PCR was applied in order to amplify immunoglobulin fragments using a single homologous oligonucleotide primer. The Figure illustrates the steps leading to the generation of the amplified material. Initially, either poly(A+) of total RNA was subjected to reverse transcription, using an oligo dT primer. Following the synthesis of this first strand of cDNA, the enzyme Terminal-deoxy-transferase (TdT) was used to add a 3' overhang of poly-guanosines. This first strand of cDNA, complemented with a 3' poly dG tail, was then used as a template for a first round of PCR, using a oligo-dC primer and a 3' immunoglobulin constant region specific primer. The product of this PCR reaction resulted in a smear of DNA which could be resolved on a low melting point agarose gel. A section of this smear, corresponding to a range of molecular weights between 1 Kb and 500 bp, was cut out of the gel and used directly as a template for a second round of amplification. This time, the oligo-dC was used in conjunction with a immunoglobulin primer specific for the 3' end of the first constant region. This second PCR resulted in the amplification of a specific DNA species, corresponding to an immunoglobulin variable region. The subsequent sub-cloning of this amplified product, allowed for the identification of the primary structure of the immunoglobulin chain, which when determined, could serve to generate an appropriate PCR primer, which would allow the amplification of the the entire variable and first constant region of the gene.

Light chains (1D7 vs 2E8 vs 2H2)

Residue # 1.

```
Asn --- Val Met Thr Gln Thr Pro Lys Phe Leu Leu Val Ser Ala
Asp Ile Val Met Thr Gln Ser Gln Lys Phe Met Ser Thr Ser Val
Asp Val Val Met Thr Gln Thr Pro Leu Thr Leu Ser Val Thr Ile

Gly Asp Arg Val Thr Ile Thr --- Lys Ala
Gly Asp --- Val Thr
Gly Gln Pro Ala
```

Heavy chains (2E8 vs 2H2)

Residue # 1.

```
Glu Val Gln Leu Gln Gln Ser Gly Ala Glu Val Val Arg Ser Gly
Glu Val Gln Leu Gln Gln Ser Gly Pro Glu Leu Val Lys Pro Gly

Ala Ser Val Lys Leu
Ala Ser Met Lys Phe
```

1D7 heavy chain CNBr fragment

Residue # 83.

```
Asn Ser Leu Gln Thr Asp Asp Thr Ala Arg Tyr
```

Figure II-19 Partial protein sequence determination for mAbs 1D7, 2E8 and 2H2.- The amino-terminal protein sequences as determined for mAbs 1D7, 2E8 and 2H2 heavy and light chains are presented. The heavy chain sequence for the 1D7 heavy chain corresponds to a CNBr-generated fragment comprised of residues 83 to 90. Spaces filled with ---, indicate that the residue could not be accurately identified.

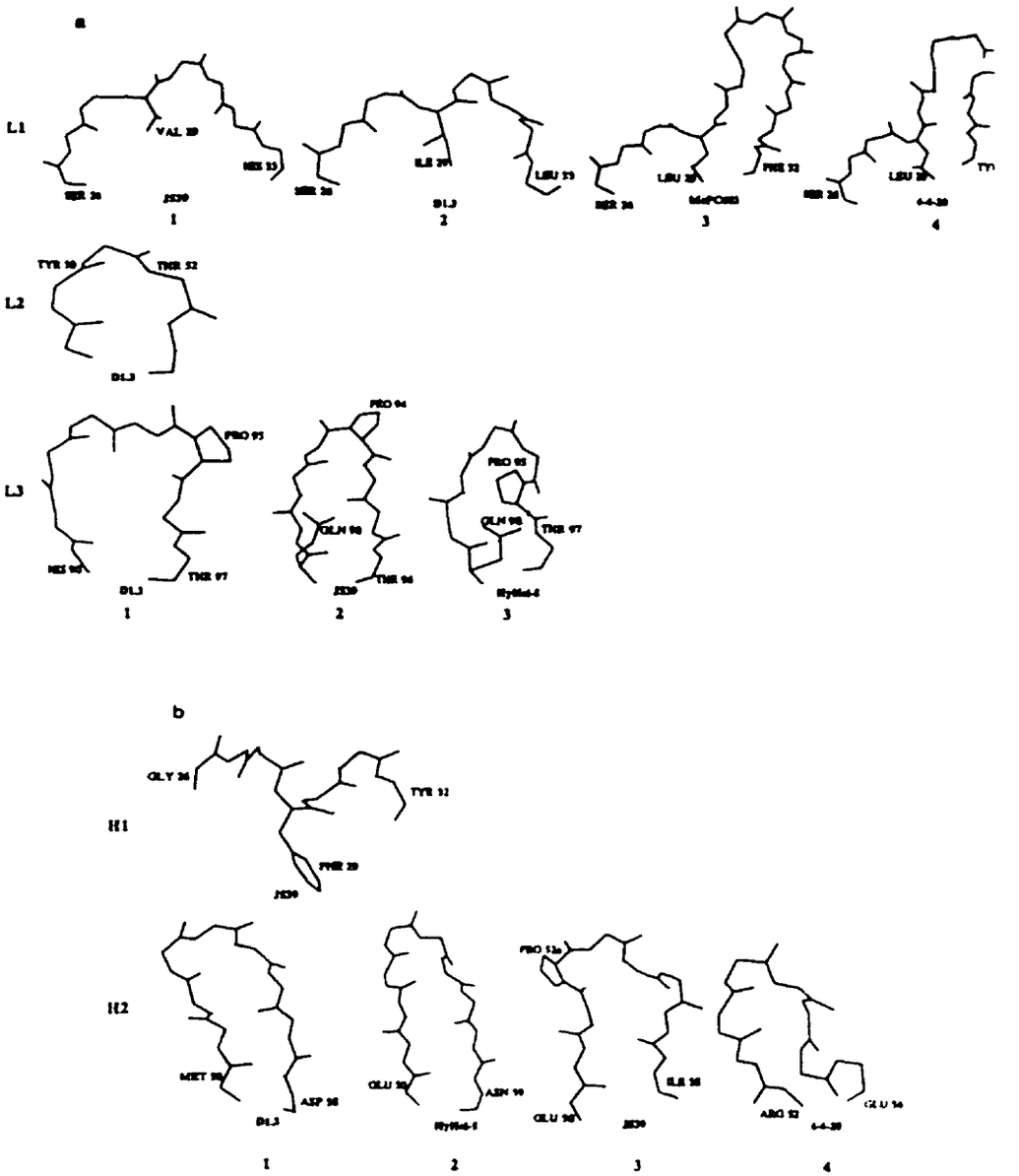

Figure II-20 Backbone conformations of the canonical structures for each antibody hypervariable loop.- This figure illustrates the conformations adopted by five of the six antibody hypervariable loops. These structures were compiled from the analysis of all known antibody X-ray crystal structures. The loops are viewed such that the solvent-accessible surface is at the top. Side chains important in determining the conformation of the loop are included, and hydrogen bonding is indicated as dashed lines (Edwards *et al.* 1992).

LDL receptor ligand binding repeat 5

195 210

Cys Asp Gly Gly Pro Asp Cys Lys Asp Lys Ser Asp Glu Glu Asn Cys

Trp Ile Asp Pro Glu Ile Gly Asp Thr Glu Tyr Val

50 60

2E8 heavy chain CDR2

Figure II-21 Comparison of the putative ligand binding site of the LDLr and the heavy chain CDR2 of 2E8.- Residue numbers 195 to 210 (cysteine-rich repeat number 5) of the human LDLr (upper) are compared to those present in the heavy chain CDR2 of mAb 2E8. Negatively charged residues are shown in red.

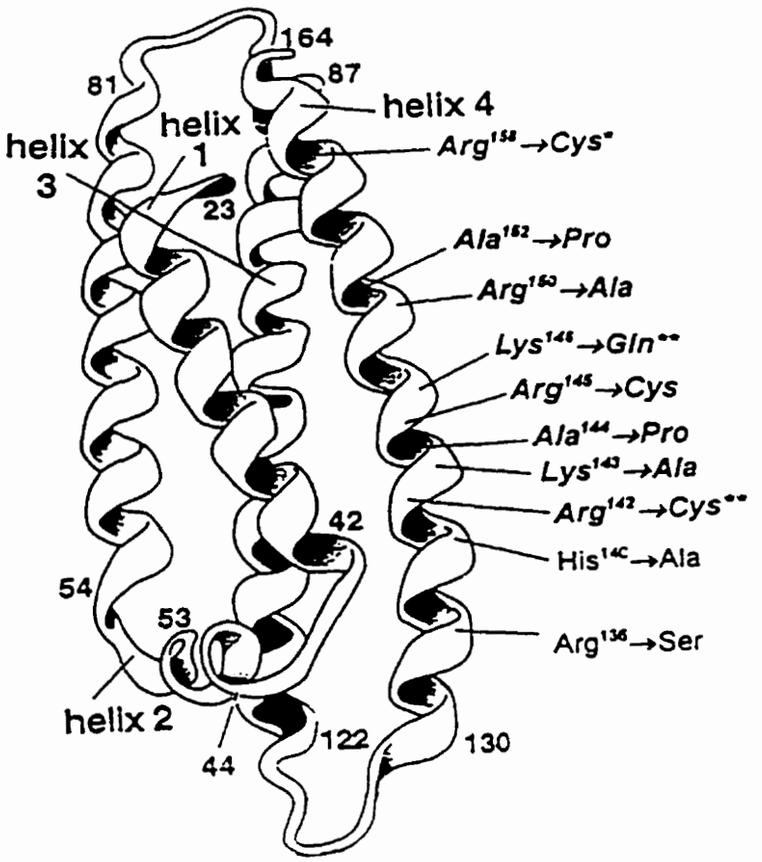

Figure II-22 Comparison of apoE variants with respect to their binding to mAbs 1D7 and 2E8 and to the LDLr. The positions of amino acid substitutions that have been shown to decrease affinity of apoE for the LDLr are indicated with respect to their position in the four helix bundle that constitutes the amino terminal 22-kDa fragment of apoE. Those variants that also have reduced reactivity with mAbs 1D7 and / or 2E8 are represented in bold italics. Of these, apoE(Arg^{158}→Cys) (*) showed reduced reactivity with 2E8 but not with 1D7. ApoE(Arg^{142}→Cys) and apoE(Lys^{146}→Gln) (**) showed reduced reactivity with 1D7 but were not tested with 2E8.

ApoE Variant		Antibody 3H1	1D7	2E8
ApoE3	k_{on}	$1.3 \times 10^5 \pm 2.6 \times 10^5$	$1.2 \times 10^5 \pm 8.2 \times 10^3$	$3.0 \times 10^5 \pm 1.7 \times 10^4$
	k_{off}	$3.1 \times 10^{-4} \pm 1.5 \times 10^{-5}$	$2.2 \times 10^{-3} \pm 1.3 \times 10^{-4}$	$9.2 \times 10^{-3} \pm 1.5 \times 10^{-5}$
	K_d	2.4 nM	19 nM	25 nM
ApoE(Arg^{136} → Ser)	k_{on}	$1.3 \times 10^5 \pm 9.3 \times 10^3$	$1.0 \times 10^5 \pm 6.8 \times 10^3$	$1.2 \times 10^5 \pm 4.7 \times 10^3$
	k_{off}	$3.6 \times 10^{-4} \pm 1.8 \times 10^{-5}$	$1.8 \times 10^{-3} \pm 7.0 \times 10^{-5}$	$8.3 \times 10^{-3} \pm 3.2 \times 10^{-4}$
	K_d	2.9 nM	18 nM	69 nM
ApoE(His^{140} → Ala)	k_{on}	$2.1 \times 10^5 \pm 9.5 \times 10^3$	$2.0 \times 10^5 \pm 4.8 \times 10^3$	$6.6 \times 10^5 \pm 6.5 \times 10^4$
	k_{off}	$1.0 \times 10^{-3} \pm 8.0 \times 10^{-5}$	$4.9 \times 10^{-3} \pm 2.1 \times 10^{-4}$	$1.2 \times 10^{-2} \pm 4.4 \times 10^{-4}$
	K_d	5.0 nM	24 nM	18 nM
ApoE(Lys^{143} → Ala)	k_{on}	$1.3 \times 10^5 \pm 7.2 \times 10^3$	$2.1 \times 10^5 \pm 1.3 \times 10^4$	< 1000
	k_{off}	$3.9 \times 10^{-4} \pm 2.2 \times 10^{-5}$	$1.5 \times 10^{-2} \pm 5.6 \times 10^{-4}$	$3.7 \times 10^{-3} \pm 2.0 \times 10^{-4}$
	K_d	2.9 nM	73 nM	N.D.
ApoE(Arg^{150} → Ala)	k_{on}	$7 \times 10^5 \pm 5.3 \times 10^3$	1.;tb2.0 $\times 10^5 \pm 1.8 \times 10^4$	N.D.
	k_{off}	$3.1 \times 10^{-4} \pm 1.1 \times 10^{-5}$	$1.2 \times 10^{-2} \pm 5.2 \times 10^{-4}$	$7.7 \times 10^{-4} \pm 6.2 \times 10^{-5}$
	K_d	1.8 nM	60 nM	N.D.
ApoE(Arg^{158} → Cys)	k_{on}	$1.7 \times 10^5 \pm 5.4 \times 10^3$	$6.9 \times 10^4 \pm 4.9 \times 10^3$	N.D.
	k_{off}	$9.5 \times 10^{-4} \pm 6.5 \times 10^{-5}$	$1.9 \times 10^{-3} \pm 1.1 \times 10^{-4}$	N.D.
	K_d	5.4 nM	28 nM	N.D.

Table II-1 Association (k_{on}) and dissociation (k_{off}) rate constants of mAbs 3H1, 1D7 and 2E8 with apoE variants as determined by surface plasmon resonance.

1D7 mAb / 2E8 mAb	Light Chain	Heavy Chain
Subgroup	V / V	IB / IIC
Family	MISC / XX	IV / IX

Table II-2 Identification of the origin of the 1D7 and 2E8 light and heavy chain variable region genes, from within the mouse imnoglobulin locus.- This Table illustrates the results of the search conducted within the Kabat database. The nucleotide sequences of the 1D7 and 2E8 light and heavy chain variable regions were submitted to the immunoglobulin "Subgrouping" service, provided by the Kabat Database Server: http://immuno.bme.nwu.edu/scripts/subgroup, accessible through the world wide web. The 1D7 light chain was found to be a possible member of family MISC. The MISC family means thay no sequence in the reference dataset matched the sequence with a maximum of 34 base differences.

	CDR1	CDR2	CDR3
1D7 Light Chain	2	1	1
1D7 Heavy Chain	1	1	Not available
2E8 Light Chain	2	1	1
2E8 Heavy Chain	1	2	Not available

Table II-3 Canonical Class assignment results for the 1D7 and 2E8 light and heavy chain variable region CDRs.- The assignment of the cannonical class of the three light chain and two first heavy chain hypervariable regions of mAbs 1D7 and 2E8, were determined by subjecting the antibody protein sequences to a search on the "Chothia SDR template" program. This service was graciously provided by the Dr. Andrew Martin, at the (http://www.biochem.ucl.ac.uk/cgi-bin/AndrewMartin/Cothi.per) world wide web site.

Chapter III

Molecular characterization of a monoclonal antibody specific for rat atrial natriuretic factor.

Summary

In this Chapter, I describe the molecular cloning of the light and heavy chains of the murine mAb 2H2, which is specific for the rat cardiac hormone; atrial natriuretic factor (ANF) (Milne et al. 1987). The analysis of this antibody at the molecular level was performed for two reasons. First, the recombinant form of this antibody was to serve as a control for the anti-apoE rFab bacterial expression experiments described in Chapters IV and V. More importantly however, we hoped to use the recombinant 2H2 as a probe to study ANF structure and function. The primary structure of the 2H2 CDRs, not surprisingly, showed little homology to either 1D7 or to 2E8. They contain a total of 8 acidic residues, 5 of which are located in heavy chain CDR3. Previous studies have shown that arginine residues in ANF form part of the 2H2 epitope. As in the case of the 2E8-apoE complex, ionic interactions between basic residues of antigen and acidic residues of the antibody may make a major contribution to the binding energy of the 2H2-ANF complex.

Objective

The goals described in this Chapter were to clone the light and heavy chains of mAb 2H2. Subsequently, the chains were to be co-expressed as recombinant Fab fragments, both in a soluble as well as in a phage-displayed form. The recombinant Fab fragments would serve as a control for the expression of the anti-apoE recombinant antibodies and would be used as probes of ANF structure and as reagents for quantification of ANF in biological samples.

Introduction

Atrial natriuretic factor (ANF) is a small peptide hormone composed of 28 amino acids, which circulates in blood (Flynn *et al.* 1983) (Figure III-1). The primary site of ANF synthesis is the right atrium of the heart, although it is also produced in many other tissues. The physiological function of ANF is to reduce blood pressure, which it performs by causing water and salt excretion into the urine and by relaxation of blood vessels (de Bold A.J. 1985). Its regulatory roles in electrolyte and vascular pressure maintenance have been documented to be in direct opposition to the actions of the renin / angiotensin II / aldosterone system (Brenner *et al.* 1990; Rosenzweig and Seidman, 1991). In fact, it is well established that the circulating levels of ANF are elevated in certain conditions such as congestive heart failure. It has been demonstrated that the physical stretch of the right atrium, which can occur during congestive heart failure, causes the cardiac muscle cells to release increased amounts of the hormone into the

blood (Bruneau *et al.* 1995). ANF is produced as a 126 amino acid polypeptide pro-hormone, which must be specifically cleaved to form the active ANF^{99-126} peptide. As only the prohormone ANF^{1-126} is found within the specific granules of atrial cardiocytes, whereas, only the mature, biologically active ANF^{99-126}, and the amino terminal ANF^{1-98} fragment are found in the circulation, it has been proposed that ANF maturation occurs as a co-secretional event. Three distinct 120 kDa transmembrane proteins have been described as physiological receptors for ANF. ANF-R1 (Chinkers *et al.* 1989) and ANF-R2 (Chang *et al.* 1989), which are both guanyl cyclases, mediate all known physiological actions of ANF. The function of the 60-70 kDa ANF-R3 receptor, is thought to be related to the clearance of ANF from plasma, by leading to its internalization and degradation, and thus providing the hormone with a plasma half life of three minutes (Espiner *et al.* 1985).

A mAb specific to rat $ANF^{101-126}$, 2H2, has been previously isolated (Milne *et al.* 1987), and has been used to determine the tissue distribution of ANF in immunoassays (Chapeau *et al.*), to quantify ANF in tissues extracts (Thibault *et al.* 1989), and to study ANF prohormone maturation (Milne and Gutkowska 1996). The 2H2 mAb can neutralize the *in vivo* diuretic activity of ANF (Milne *et al.* 1987) and block binding of ANF to both the ANF-R1, ANF-2 and ANF-R3 receptors on cultured cells (Milne and Gutkowska 1996). The 2H2 epitope on ANF includes Arg^{101}, Arg^{102} and Ile^{110}, but not residues that compose the carboxy terminus of mature ANF (Milne *et al.* 1987).

Native ANF^{99-126} is a cyclic peptide with a disulfide linkage between Cys105 and Cys121 as shown in Figure III-1. In aqueous solution it is inherently flexible and does not adopt a definable conformation (Fesik *et al.* 1985) and, as consequence , its structure has not yet been solved by nuclear magnetic resonance spectroscopy (NMR). Studies of ANF in DMSO solutions as well as in SDS micelles, indicated several regions having partially ordered structures (Koyama *et al.* 1990; Olejniczak *et al.* 1988). Recently, the structure of a variant form of ANF in which amino acid subsitutions were introduced to reduce its flexibiliy in solution has been solved using two-dimensional NMR. In spite of the modifications to its primary structure, this ANF variant could bind to ANF-R1 receptors indicating that it was capable of adopting a physiologically relevant conformation. (Fairbrother *et al.* 1994).

The technique of transferred nulear Overhauser effect (NOE) (Dyson, H.J. *et al.* 1990) has been applied to the determination of the structure of immune complexes. A prerequsite for this technique is that the dissociation of the bound antigen is fast relative to the T_1 relaxation time of the protons of the antigen and antibody, i.e. a property normally associated with low affinity antibodies (Anglister, J., and Zilber, B., 1990). This approach is also facilitated by the use of small antibody fragments, such as scFv fragments, that reduce the probability of low affinity secondary binding of antigen outside of the antibody combining site that can complicate the interpretation of the NMR spectra. In addtion, the availability of svFc fragments potentially permits alternative approaches to the determination of peptide-antibody complexes, such as isotope-edited NMR. With the long term goal of determining the structure of $ANF^{101-126}$ using NMR, I

undertook to molecularly clone and to express in *E.coli*, the Fab fragment of the 2H2 antibody. The actual NMR structural determinations will be done in collaboration with colleagues at the Institut de Recherches Cliniques de Montréal.

A further goal was to express the 2H2 Fab on the surface of filamentous phage. While 2H2 has been shown to be a useful reagent for quantifying mature (Milne *et al.* 1987) or proANF (Thibault *et al.* 1989) in atrial tissue extracts, we have been unable to optimize a 2H2-based immunoassay with a sensitivity that is sufficient for the measurement of ANF in plasma. Phage that express 2H2 monovalently on their surface could, in principal, be labeled to a very high specific activity with a minimal risk of modifying antibody function. Such a reagent may permit the direct measurement of ANF in plasma using a convenient solid phase immuoassay.

Methods

The methodologies used for the isolation and characterization of cDNA clones encoding the light and heavy chains of mAb 2H2 were essentially identical to those described in the previous chapter for the anti-apoE mAbs. With the exception of the oligonucleotide primers used in the PCR amplification of the heavy chain, all other reagents used were the same.

Results

1. **Cloning of the light and heavy chains of mAb 2H2**.-The cDNA encoding the light and heavy chains of mAb 2H2 were cloned using the polymerase chain reaction as described for the cloning of mAb 2E8. The light chain was amplified using the same primers that were used for the amplification of the 2E8 light chain. However, the heavy chain was amplified using a 5' primer specific for the leader (signal peptide) region (amino acids -20 to -13) of the immunoglobulin heavy chain mRNA, as well as by anchored PCR. A 3' primer complementary to codons 224-232 located within the hinge region, as previously mentioned for the cloning of the 2E8 heavy chain, (5'-AGG CTT **ACT AGT** ACA ATC CCT GGG CAC A-3') and which contains an SpeI site indicated in bold, was used in combination with the leader region specific 5' primer MH-ALT.1 (5'- ATG (GA)A(GC) TT(GC) (TG)GG (TC)T(AC) A(AG)C T(GT)G (GA)TT -3'). Bases in parentheses are substitutions at a given position; i.e., (AT) indicates that A and T were present in equimolar amounts during the synthesis of the oligonucleotide. Following the succesful amplification of the heavy chain, the fragment was cloned "blunt end" into pBluescript as described in Chapter II. Three positive clones were selected and their nucleotide sequence determined as described previously.

2. **Characterization of the primary structure of the light and heavy chain variable regions.-** The primary structure of the variable regions of both the light and

heavy chains were determined using the dideoxy-chain termination method. The compiled nucleotide and amino acid sequences for both the light and heavy chain, are presented in Figures II-13, II-14, II-15 and II-16 in the result section of Chapter II.

3. Identification of the variable region genes families used by mAb 2H2.- The variable region sequences of both the light and heavy chains were compared with those in the Kabatman server (http://immuno.bme.nwu.edu/scripts/subgroup.tc). As shown in Table III-1, the light chain originates from within the mouse variable region subgroup II, and is possibly a member of family VI. The nucleotides encoding codons 96 to 103 are from the MUSJK1 kappa J-minigene. The heavy chain is a member of mouse variable region subgroup V, and is possibly a member of family IV. Codons 101-117 were found to be derived from the MUSJH2 mouse heavy chain J-minigene family (Kurosawa and Tonegawa 1982). Its D-minigene could not however be identified.

4. Canonical class assignment of the light and heavy chain CDRs.- The amino acid sequences of both the light and heavy chains were entered into the "Chothia SDR Template" server (http//www.biochem.ucl.ac.uk/cgi-bin/AndrewMartin/cothi.per), where they were compared to the current databank. The results obtained following sequence comparison are summerized in Table III-2. The light chain CDR1, CDR2, and CDR3 were found to belong to class 4, class 1 and class 1, respectively. The heavy chain CDR1 and CDR2 were found to belong to class 1 and class 2, respectively.

5. Analysis of the complementary determining regions.- The mAb 2H2, which was raised against rat ANF, was composed of light and heavy chain CDRs which, not surprisingly, did not bear much primary sequence homology to anti-apoE mAbs, 1D7 and 2E8 (Figure II-15 and II-16). Compared to 1D7 and 2E8, the 2H2 light chain CDR1 is unusually long with five extra amino acids which correspond to residues 27a through 27e. This is characteristic of antibodies having a light chain CDR1 class 4 canonical structure. A further interesting feature of the 2H2 CDRs is the presence of eight acidic amino acids, five of which are located in the heavy chain CDR3, the remaining two in the light chain CDR1.

Discussion

The primary structure of an antibody specific to rat ANF was determined. As shown in Figures II.13 through Figures II.16, this antibody is very different from our two anti apoE-antibodies, in terms of CDR homologies. Given the difference in their respective specificities, this is not unexpected. Of particular interest is the unusually long CDR1 of the light chain and the presence of five acidic residues in CDR3 of the heavy chain. It is, therefore, possible that acidic residues in the CDRs of 2H2 form ionic bonds with basic residues of ANF. It has been previously shown that Arg^{101} and Arg^{102} are implicated in the 2H2 epitope (Milne et al. 1987). The affinity of 2H2 for the peptide

$ANF^{102-126}$ was only 30% of $ANF^{101-126}$ and the $ANF^{103-126}$ and shorter amino-terminally truncated ANF peptides were not recognized. In addition, as Ile^{110} has also been shown to be important for 2H2 binding, given their proximity, Arg^{109} and Arg^{112}, could also potentially participate in the 2H2 epitope.

In view of these previous observations, it is logical to assume that, notwithstanding the contribution of many other residues from the six CDRs, mAb 2H2 may make use of the acidic residues in LC CDR1 and HC CDR3 in order to form an immune complex with the polypeptide. The arguments which I proposed for the interaction between mAb 2E8 and apoE in Chapter V, may justifiably be used in a similar context, for the association between 2H2 and ANF. Indeed, a strong electrostatic component, of opposing poles, may well contribute to the initial association of the complex, which then, within a short period of time, rearranges itself to a correct fit. As ANF is flexible in solution, a non-specific electrostatic component may favour an initiation of the immune-complex, which would then evolve into a correct, stronger fit. The phenomenon of "induced fit" in some antibody / antigen interactions, has now been well described (Wilson and Stanfield, 1994). Although most of the potential antibody "molding" has been observed to result from a structural rearrangement of the heavy chain CDR3, the structure of the CDR1 of some antibody light chains within an immune complex, has also been observed to differ slightly from their ascribed canonical structure (Satow *et al.* 1986). Investigators have noted that the tip of this CDR can, in certain cases, have a certain amount of mobility and flexibility. The long light chain CDR1 of 2H2 may play an important structural role in the formation of the ANF / 2H2 immune

complex. This CDR would be predicted to have two solvent exposed acidic residues near its apex. Being slightly mobile and negatively charged, this portion of the antibody paratope may be key to the initial association with ANF. Subsequent to complex formation, the participation of the six other acidic residues would help stabilize the complex along with the many large aromatic residues found in the heavy chain CDR3. Interestingly, in the solved crystal structure between Fab 131 and the peptide hormone angiotensin II, the antibody was found to make use of residues found in its light chain CDR1 and heavy chain CDR3, which were both unusually long. In this case, the peptide hormone, which was folded into a compact structure, was found to be deeply buried within a cavity formed by the long CDRs (Garcia, K.C., et al. 1992).

One of the initial reasons for cloning the 2H2 cDNA was to have a non-apoE-specific recombinant antibody to serve as a control for the characterization of the 1D7 and 2E8 recombinant Fabs. I had hoped to evaluate the relative contributions of the respective heavy and light chains of 1D7 and 2E8 to apoE binding by expressing chimeric Fab fragments in which either the heavy or light chain component of the anti-apoE Fab is replaced by its homologue from 2H2. For several reasons, 2H2 proved to be a poor choice for such a control antibody. First, during my characterization of the recombinant mAbs, I observed very significant binding of 2H2 recombinant Fab fragments to purified apoE in solid phase immunoassays. This was also seen with the 2H2 IgG purified from the ascitic fluid of 2H2-hybridoma-bearing mice. Others in the laboratory have previously observed surprisingly high binding of 2H2 to plasma lipoproteins. This apparently non-specific binding of 2H2 to apoE may reflect ionic

interactions mediated by the highly electronegative paratope of 2H2. Secondly, the lack of similarity between 2H2 and the anti-apoE mAbs in terms of the predicted loop conformations for their respective CDRs may make the interpretation of binding results of chimeric molecules difficult to interpret.

Finally, with respect to the long term goal of preparing a probe to aid in solving the three dimensional solution structure of the ANF peptide, the characterization of the cDNA clones has provided some clues as to how the antibody might be modified to produce a variant with the appropriate binding kinetics for NMR structural analysis. I would propose that a 2H2 variant with the high dissociation rate required for transfered nuclear overhauser NMR might be obtained by replacing one or more of the acidic residues in the 2H2 CDRs with neutral residues.

Ser^{99} Leu Arg Arg Ser Ser Cys Phe Gly Gly Arg Ile Asp Arg Ile Gly Ala Gln Ser Gly Leu Gly Cys Ans Ser Phe Arg Tyr^{126}

Figure III-1 Amino acid sequence of mature rat ANF.- The amino acid sequence of mature ANF found within the circulation is composed of a 28 amino acid peptide. A disulfide bond exists between cysteines 105 and 124 that is necessary for ANF biological activity. Arginines 100 and 101, which are critical to 2H2 recognition of ANF are underlined. In addition, replacement of Ile^{110} (underlined) by Met reduces ANF affinity by an order of magnitude (Milne et al. 1987).

2H2 mAb	Light Chain	Heavy Chain
Subgroup	II	V
Family	VI	IV

Table III-1 Origin of the variable regions of both the light and heavy chains within the mouse immunoglobulin gene locus.- This table represents the results obtained following a search of the Kabatman database (http://immuno.bme.nwu.edu/scripts/subgroup.tc). The nucleotides encoding the entire variable regions of both the light and heavy chains were used to determine the variable subgroups and families for the 2H2 heavy and light chains.

2H2 mAb	CDR1	CDR2	CDR3
Light Chain	4	1	1
Heavy Chain	1	2	

Table III-2 Canonical structures for the hypervariable regions of the 2H2 light and heavy chains.- This table depicts the ascribed canonical structures of the 2H2 hypervariable regions, based on their comparison to the "Chothia SDR Template" server (http://www.biochem.ucl.ac.uk/cgi.bin/Andrewmartin/Cothi.per). The entire amino acid sequence of both the light and heavy chains were used for the search. All canonical structures are illustrated in Figure II-20.

Chapter IV

Production and purification of recombinant 2E8 and 2H2 antibody Fab fragments in *Escherichia coli*

Summary

In this Chapter, I present my experience in optimizing the methodologies for the production in *E. coli*, and for the purification of the recombinant mAbs 2E8 and 2H2, as well as for the many variant forms of mAb 2E8 which I generated and which are described in Chapter V. The recombinant antibodies were produced as Fab fragments, both displayed on the surface of M-13 filamentous bacteriophage and in a soluble form. The phage-displayed Fabs were assayed for antigen binding activity using a biological rescue methodology. The soluble recombinant antibodies were purified to homogeneity, and assayed for antigen recognition using solid phase radio-immunoassays. I will describe how I have optimized expression conditions and how I have identified and overcome a number of problems associated with the production of recombinant antibody fragments using *E.coli*.

Objective

The goal of this chapter was to succeed in producing recombinant antibody Fab fragments derived from hybridoma cell lines, using the bacterial host *E.coli*. The antibodies were to be produced in two forms; displayed on the surface of M-13 filamentous bacteriophage, and in a soluble form that could be easily purified.

Introduction

Heterologous expression of antibody fragments

For almost a decade, recombinant antibody genes have been successfully expressed in various eukaryotic as well as prokaryotic organisms (Plückthun and Skerra 1989; Better *et al.* 1988; Winter and Milstein 1994; McCafferty *et al.* 1996). In eukaryotic cells, antibodies have been expressed both as secreted, as well as intracellular resident proteins. In the latter case, recombinant antibodies have been used as probes for the *in vivo* study of intracellular protein function. Activity-neutralizing antibodies made to accumulate within a cell, and targeted to various organelles, have the potential for *in vivo* inhibition of the cellular function of the protein to which they are specific (Biocca *et al.* 1994). The most common use of recombinant antibody technology remains, however, the large scale production of useful immunoglobulin fragments. Through the many

available methods which allow their molecular remodeling, recombinant antibodies have the potential of becoming much more efficient as diagnostic and therapeutic reagents than traditional immunoglobulins. For example, the cytotoxic portion of a recombinant protein can be fused to a single chain Fv antibody fragment. If the antibody is specific for a tumour antigen, it should target the toxin to diseased cells, and decrease toxicity to healthy tissue. One such antibody has been constructed that consists of a scFv specific for a cancer antigen fused to the bacterial superantigen, staphylococcal enterotoxin A (SEA). This scFv-SEA binds to many cancer cell lines and through its SEA subunit, targets them for destruction by a powerful T cell attack (Giantonio *et al.* 1997; Hansson *et al.* 1997; Gidlof *et al.* 1997). Moreover, with the advent of murine antibody humanization (Baca *et al.* 1997; Holmes and Foote 1997), one can now fully exploit the antigen-binding capabilities of xenogeneic antibodies, altered to be minimally antigenic to the human immune system. The tissue-infiltration capability of antibodies has also been improved by the production of smaller, antigen-binding Fv antibody fragments, which are comprised of the antigen-binding region only. With the advent of this technology, the wide spread therapeutic use of recombinant antibodies now seems imminent.

The development of recombinant phage-display technology by George Smith in 1989 (Smith, 1985), opened an entirely new avenue for the generation of monoclonal antibodies. As first demonstrated by McCafferty and collaborators in 1990 and then by Barbas and collaborators in 1991, phage-display antibody libraries allow the rapid isolation of recombinant antibodies without the drawbacks associated with animal

generated hybridoma repertoires. In fact, the potential now exists for the isolation of antibodies capable of reacting to almost any molecular structure. In addition, and as it will be described in Chapter V of my thesis, extensive *in-vitro* as well as *in-vivo* mutagenic protocols can be applied for the generation of newly desired forms of a defined antibody.

Many bacterial expression vectors have been developed which allow the inducible production of recombinant antibodies. Such antibody fragments can be made both in a soluble form which can be isolated from the organism, or as a fusion protein displayed on the surface of M-13 filamentous phage (McCafferty *et al.* 1990; Barbas *et al.* 1991). These vectors allow the direct cloning of light and heavy chain fragments, which give rise to recombinant heterodimeric Fab molecules or single chain Fv antibodies, formed by the fusion of the variable regions of the light and heavy chains. Consequently, these vectors allow one to conveniently express antibody genes obtained either from a single hybridoma clone, from an entire animal repertoire, either in an immunized or naive state, or from a synthetic library (Plückthun *et al.* 1997). With the use of phage-display technology, one can generate and isolate novel antibodies having desirable binding properties through successive rounds of affinity selection procedures. Importantly, recombinant antibody fragments isolated through such methodologies, have been documented to bind antigen with similar affinities as observed with natural or hybridoma produced antibodies. With such methodologies, one can totally bypass the use of animals in the generation of antibodies and, consequently, can avoid certain drawbacks that are associated with classical mAb production.

Many methodologies that permit rapid isolation and purification of recombinant antibodies have been elaborated. Of particular interest are affinity purification techniques based on the addition of a peptide tag or "Flag" engineered on one of the expressed antibody chains. For example, the peptide epitope of the anti-Myc mAb 9E10, has been fused to the heavy chain of recombinant antibodies, and shown to efficiently serve as a detection marker for the expressed protein (McCafferty *et al.* 1996). In addition, this peptide tag is capable of serving as a ligand in a one-step affinity chromatography purification protocol, using the immobilized anti-myc mAb. A disadvantage associated with immunoaffinity chromatography, rests with the often harsh measures needed to elute the bound antigen. An alternative methodology for identification and purification of recombinant proteins, is based on metal chelate technology which exploits specific interactions between juxtaposed histidine residues that are introduced into the recombinant protein, and a nickel complex. The nickel complex can be either linked to Sepharose beads or to enzymes such as horseradish peroxidase, for purification and detection of the protein, respectively (Porath, J. 1992).

Background to methodologies used in this chapter

The expression system for recombinant Fab fragments that I have used was developed by Dr. Richard Lerner and his colleagues at the Scripps Research Institute. For additional background on the bacterial expression of recombinant antibodies, I refer

the reader to a recent comprehensive review entitled "Human Antibodies from Combinatorial Libraries" (Burton and Barbas, 1994).

1.1 The pComb3 antibody expression vector.- The pComp3 expression vector depicted in Figure IV-1, is a M-13 type phagemid vector developed by members of Dr. Richard Lerner's group in 1991 (Barbas *et al.* 1991). Phagemid vectors consist of a modified bacterial expression plasmid, which contain the origin of DNA replication for M-13 phage as well as the signal for phage assembly (McCafferty *et al.* 1996). This type of vector is carried as a double stranded plasmid in bacteria, conferring ampicillin resistance, and upon infection with M-13 helper phage, is converted into single stranded DNA which is specifically packaged into infectious progeny phage virions. Recombinant progeny phage can in turn infect male *E.coli* bacteria carrying the F' pili, and release their single stranded vector which is promptly made double stranded and carried in a stable fashion.

The pComb3 vector allows for cloned antibody light and heavy chains to be co-expressed within a single bacterium as shown in Figure IV.1. The light chains are inserted into the vector using the unique SacI and XbaI restriction sites. Heavy chains on the other hand, are inserted using the XhoI and SpeI restriction sites, which fuse the heavy chain with the carboxyl-terminal domain of the g3p phage coat protein. When cloned in this way within the plasmid, both chains are under independent, IPTG inducible LacZ expression control. Both chains are produced with the *pelB* bacterial leader sequence at their amino terminus, which directs the recombinant proteins to the

periplasm. Consequently, the pComb3 phagemid vector allows for recombinant Fab fragments to be expressed on the surface of filamentous M-13 bacteriophage, through the heavy chain-g3p fusion protein. Alternatively, the same vector may also be used to generate soluble antibodies, through the Spe1 \ Nhe1 endonuclease excision of the nucleotides encoding the heavy chain-associated g3p fusion protein, which generates compatible ends, allowing the religation of the vector.

1.2 Expression of antibody fragments in *E.coli*, both as Fab displayed on the surface of M-13 bacteriophage or as soluble Fab.- Male *E.coli* bacteria, typically of the XL1-Blue or TG1 strains (Stratagene), which produce the F' sex pili allowing for M-13 phage infection, are transformed with a phagemid construct containing both light and heavy chains, and plated on LB agar plates containing ampicillin. The presence of an ampicillin resistance gene encoded within the vector, allows for transformed bacteria to grow as independent colonies. Upon induction with the non-metabolic lactose-analog IPTG, both antibody chains are expressed individually within the cell, as depicted in Figure IV-2a. The amino-terminal *pelB* bacterial leader sequence allows for both chains to be translated and transported to the periplasm, where it is subsequently cleaved by the enzyme signal peptidase. The secretion of proteins containing a signal sequence into the periplasm, is a well known process in *E.coli* (Pugsley, A.P., 1993), which has been shown to be improved by the overexpression of the bacterial proteins secY and secE gene products (Pérez-Pérez *et al.* 1993). Within the periplasm, appropriate oxidizing conditions allow for the antibody chains to correctly fold and assemble as heterodimeric

proteins, presumably with the aid of the periplasmic disulfide-forming machinery (Better et *al.* 1988; Skerra and Plückthun 1988).

Expressed recombinant heavy chains, fused to the g3p phage protein, remain associated with the bacterial plasma membrane. G3p is an M-13 phage-coat protein of 406 amino acid composed of two structural / functional domains. The amino-terminal domain is implicated in the infection process and interacts directly with the tip of the bacterial F'pili. Presumably, infection occurs as the pili retracts within the bacteria together with the bound phage, which then associates with the outer membrane of the bacteria and is internalized within the cell. The second g3p domain, composed of residues 198-406, appears to be important in phage morphogenesis. In the virion, there are normally three to five copies of g3p. Normal phage morphogenesis leads to the incorporation of the Fab-g3p fusion as well as the helper phage produced g3p into the trailing cap of the virion, according to the vectorial polymerization model (Makowski L., 1994). Native g3p is thus necessary for infection as the infectivity domain should not be present in the Fab-g3p fusion. Therefore, the use of helper phage superinfection leads to the expression of two forms of the coat protein, which both compete for insertion into the virus coat. Phage that are both infectious and display antibody on their surface must, therefore, express both the wild type g3p protein as well as the Fab-g3p fusion protein.

Infection of phagemid transformed *E.coli* bacteria with M-13 helper phage, causes the synthesis of single stranded phagemid DNA due to the presence of an f1 origin of replication. In addition, the helper phage allows the phagemid to be processed as if it

were true viral DNA, as shown in Figure IV-2b. The viral proteins g5 encoded by the helper phage, associate in large numbers with the single stranded phagemid DNA, and allow it to be packaged as if it were true viral genome. The single stranded pComb3 DNA is then packaged as progeny phage, which mature and extrude across the cell membrane. As the progeny phage exit the cell, they acquire some of the fused recombinant g3p-Fab heavy chain fusion protein as mentioned above, embedded in the cell membrane and covalently associated with the light chain. Subsequent to their release into the culture media, phage displaying recombinant Fabs on their surface can then be concentrated through polyethylene glycol precipitation protocols, and resuspended in water. Conversely, soluble recombinant Fabs can also be obtained from within the periplasm of an IPTG induced bacterial culture, through mild osmotic shock protocols, which selectively release periplasmic proteins. Such crude antibody preparations can then be purified using affinity chromatography techniques described below.

Lastly, relating to the use of bacterial cells in the mass production of antibody molecules, it would appear that the bacterial periplasm is the only anatomical location from which functional antibodies can be directly isolated, using standard strains of *E.coli*. Indeed, since all antibody molecules need to form a number of appropriate disulfide bonds (one internal bond per domain, and one for heteromolecular assembly) in order for them to be functional and capable of antigen recognition, the chains must be moved out of the cytoplasm, where the redox conditions are known to be reducing. Thus, with the exception of only a few specialized bacterial cell strains, antibody folding within

bacteria would appear to occur only in the periplasm where oxidizing conditions prevail, presumably aided by bacterial disulfide-forming enzymes. The limitations set by their folding requirements, makes antibody molecules a class of recombinant proteins which require special care, both for their production as well as to their functional isolation (Plückthun *et al.* 1996).

1.3 **Recombinant phab rescue.** - The biological activity of recombinant antibodies displayed on the surface of M-13 phage, called "phabs" or phage antibodies, can be assayed using immuno-panning methodologies as shown in Figure IV.3. This first involves the immobilization of an appropriate antigen onto the surface of polystyrene microtiter wells. A preparation of PEG precipitated phab can then be incubated in the coated wells. Subsequent to an incubation period, non-bound phabs are washed away, and those that are retained, are eluted at pH 2.0 . Such a change in pH will cause a dissociation between the Fab-antigen complex, and will consequently cause the release of the phab. Eluted phab remain infectious and, when mixed with a culture of male *E.coli*, transfer the phagemid vector harboring the antibody genes. Once in the host bacteria, the single stranded phagemid vector is rapidly made double stranded, and subsequently carried stably as a plasmid coding in part, for antibiotic resistance. The infected culture can then be plated onto LB agar supplemented with ampicillin, and resultant bacterial colonies picked for plasmid preparation or soluble antibody expression. This revolutionary protocol reflects an excellent example of biological linkage between the function of a protein and its genetic imprint; the same principle that forms the basis of the vertebrate humoral immune system.

Methods

Much of the basic methodology relating to the experimental manipulation of nucleic acids and cloned DNA, have been described in detail in Chapter II.

2.1 Subcloning of light and heavy chains of mAbs 2E8 and 2H2 into pComb3.- The bacterial expression phagemid vector pComb3 shown in Figure IV.1, is engineered for the cloning and expression of antibody light and heavy chains as Fab fragments (Barbas *et al.* 1991). Briefly, previously characterized immunoglobulin light and heavy chain cDNAs were amplified by PCR, using the appropriate sense / antisense primers described in Chapter II, which in each case, created unique restriction endonuclease sites. The amplified fragments were then resolved on a 1% agarose gel. The gel was stained by soaking in a 0.01% ethidium bromide solution and visualized under a U.V. transilluminator. As shown in Chapter II (Figure II-17), a 700 base pair fragment, corresponding to both light and heavy chain products of amplification, was excised from the gel, extracted using the Qiagen extraction kit (Qiagene), and eluted in 30 µl of water. Eluted immunoglobulin DNA was subjected to digestion with a combination of appropriate endonucleases in a volume of 30 µl (Sac1 / Xba1 for the light chain, and Xho1 / Spe1 for the heavy chain). Following digestion, the DNA was extracted with phenol and precipitated with ethanol. The resultant DNA was dissolved in a 40 µl solution of TE pH 8.0, and its concentration determined using spectrophotometric

analysis. The phagemid vector pComp3 was similarly prepared following digestion with the appropriate set of endonucleases which allow for either light or heavy chain cloning, and for the shuffling of the genes (Figure IV-4).

2.2 Expression of recombinant Fab on the surface of M-13 bacteriophage.- A bacterial colony harboring 2E8 or 2H2 light and heavy chains cloned in pComb3, was inoculated into 2 ml of LBA growth media, grown with vigorous agitation at 37 ^{o}C to an O.D.$_{600}$ nm of 0.6. M-13 helper phage (5 µl of a stock solution containing 10^{11} pfu) (Stratagene) was added to the culture and incubated for 2 hours at 37 ^{o}C. The culture was then supplemented with the antibiotic kanamycin to a concentration of 10 µg / ml and grown overnight at 30 ^{o}C with vigorous agitation. The following day, 1 ml of the culture was transferred to a microcentrifuge tube and spun at 14 000 x g to pellet the bacteria. Phage were isolated from the supernatant by adding 250 µl of a 5 x solution of polyethylene glycol solution (20% PEG 8000 / 2.5M NaCl). The tubes were mixed and stored at 4 ^{o}C for one hour to allow for phage aggregation. The tubes were then spun at 14 000 x g for 10 minutes to collect the aggregated phage. The supernatant was removed by aspiration and the phage pellet dissolved in 200 µl of PBS and stored at 4 ^{o}C. Alternatively, the phage were frozen at -80 ^{o}C in a 20% glycerol solution for long term storage.

2.3 The titration of an M13 phage preparation.- The amount of active, infectious phage particles present following a PEG precipitation of an infected bacterial culture, was determined by titering the viral preparation on fresh *E.coli*. Essentially, the method

consisted of diluting the initial preparation within a range of 10^{-6} to 10^{-10} . Serial dilutions of the original phage preparations were prepared in 100 µl volumes of bacterial LBA growth buffer. To each dilution was added 50 µl of an *E.coli* bacterial culture in exponential phase ($O.D._{600}$ nm = 0.8) and the tubes were mixed and incubated at 37 °C for 1 hour. The infected bacteria were then plated onto fresh LBA agar plates, and grown overnight at 37 °C. The phage titre of the phage preparation reflects the number of transformed bacterial colonies and the dilution factor.

2.4 Assessment of the antigen binding capability of the recombinant 2E8 and 2H2 phabs using radio-immunoassays and phage rescue protocols.- The antigen biding ability of recombinant phab preparations were determined using both direct radioimmunometric detection of the bound phab by anti-M-13 specific mAbs, and the biological rescue procedure described in section 1.3.

2.5 Conversion of pComb3 from a phage display to a soluble expression vector.- Typically, 50 µg of a pComb3 phagemid DNA preparation was digested with the endonucleases Spe1 and Nhe1, causing the excision of the nucleotides encoding the g3p phage coat protein (Figure IV-4). The 600 bp fragment was separated from the remainder of the vector as described above. A 4.9 kb fragment corresponding to the vector which harbored both an antibody light and heavy chain (Figures IV-1 and IV-4) was purified from the gel, and self-ligated, since the two endonucleases generate compatible ends which can be rejoined, and which destroys both original restriction sites.

2.6 Expression and isolation of soluble recombinant Fab fragments.- A single colony of XL1-Blue or TG1 *E.coli.* bacteria, transformed with an appropriate pComb3 phagemid, containing antibody genes but deficient in the g3p fusion protein, was inoculated into a culture tube containing 2 ml of LBA culture media. The culture was grown at room temperature (25 °C) overnight with constant agitation and then transferred to a 2 L Erlenmeyer flask filled with 1 L of super broth (12 g tryptone, 24 g yeast extract, 4 ml glycerol per liter and supplemented with ampicilin at 100 μg / ml). The culture was grown at room temperature with agitation until an OD_{600}nm of 0.6 was reached. It was then supplemented with IPTG to a final concentration of either 0.1 or 1 mM, and left to grow for an additional day. The following day, the culture was spun in 250 ml centrifuge bottles, at 5 000 x g in a Sorval SS-40 rotor. Following the spin, the centrifuge bottles were inverted and the remaining growth buffer dried with tissue paper. The bacterial pellets were then resuspended in 200 ml of an ice-cold solution of STE buffer (20 % sucrose, 10 mM tris pH 8.0, 5 mM EDTA). Following a one hour incubation on ice, with an occasional inversion, the bottles were spun at 8 000 x g for 20 minutes. Again the supernatant was removed and this time the bacterial pellet was resuspended in 50 ml of ice-cold deionized water, and incubated for 15 minutes at 4 °C. Finally, the periplasmic extract, or shockate, was obtained by pelleting the bacteria at 15 000 x g for 15 minutes. The 50 ml periplasmic shockate was then put into a dialysis bag (Spectra/Por Spectrum Medical Industries, Ca.) and dialyzed overnight at 4 °C in a 4 L solution high in salt (500 mM NaCl, 10 mM HEPES pH 7.0). The leftover TSE solution was also kept at 4°C, and analyzed for the presence of rFab on a western blot.

2.7 Expression of soluble recombinant Fab fragments tagged with a histidine tail.- The original pComb3 phagemid vector was modified in order to permit the production of a carboxyl-terminal histidine tail fused to the antibody heavy chain. Two complementary oligonucleotides, **His-1** sense (5' CT AGT **CAT CAT CAT CAT CAT** TAA GCT AGC 3') and **His-2** anti-sense (5' C TAG GCT AGC TTA **ATG ATG ATG ATG ATG** A 3') were synthesized which encoded five in-frame histidine residues as shown in bold. In addition, both extremities were designed to provide compatible ends for directional cloning into an SpeI generated site in the pComb3 vector as shown in Figure IV-5.

Briefly, both oligonucleotides dissolved in TE buffer, were mixed in equimolar concentrations, heated to 95 ^{o}C for 10 minutes and allowed to anneal at room temperature. The hybridized product was then directly cloned into the SpeI / NheI digested pComb3 vector by standard ligation. Heat-shock transformed recombinant XL1-Blue bacteria, that contained plasmid that included the sequence encoding the five-histidine addition, were identified first through positive endonuclease digestion of isolated plasmid DNA with SpeI endonuclease to yield a single band of linearized plasmid. If the vector religated without the insert, both the SpeI and NheI sites are destroyed and it would be resistant SpeI digestion. Clones identified as positive through restriction-digest analysis, were subsequently subjected to DNA sequencing in order to confirm the integrity of the reading frame.

2.8 Identification of the presence of recombinant Fabs in the bacterial periplasmic extract.- Western blot detection was employed in order to ascertain the presence of recombinant Fabs in the isolated bacterial periplasm. Typically, 50 µl of the extract was boiled in an SDS loading buffer, and run on a 12 % SDS PAGE. The gel was then transferred onto nitrocellulose, and blocked in a solution of 1% PBS-BSA for an hour at room temperature. The detection of antibody light chain was performed by incubating the membrane in a 1% PBS-BSA solution containing ^{125}I radiolabled rabbit anti-mouse kappa antibodies. The blot was then washed in a PBS solution containing 0.01% Tween-100, and exposed overnight under X-ray film. Conversely, antibody heavy chains were visualized by incubating the same blot in a solution containing an HRP-conjugated nickel reagent; Ni-AT (Qiagene), in an appropriate buffer (0.5 M NaCl, 0.15 M Tris pH 7.5, 0.01% Tween-100). This product binds to the histidine tail present in the heavy chain, with a high affinity. The presence of the heavy chains was then revealed by incubating the rinsed blot with a chemiluminescent substrate (Amersham), which generated photons as it was converted by horseradish peroxidase, linked to the nickel reagent. The wet blot was then quickly exposed to X-ray film for a very short period of time, and developed.

2.9 Purification of the recombinant Fabs.- Recombinant soluble antibodies were purified from the periplasmic shockate using metal-chelate affinity chromatography. As mentioned above, the original pComb3 vector was modified in order to fuse a histidine tail to the carboxyl-terminal end of the heavy chain, when the latter was produced in a soluble form. Upon the dialysis of the periplasmic shockate in a high salt buffer, 300 µl

of a resuspended Ni-NTA (nitrilo-triacetic acid resin, Qiagen) resin slurry was added directly to the extract in a 50 ml conical Falcon tube. The tube was then incubated overnight at 4 ^{o}C with constant inversion. The following morning, the periplasmic extract was poured into a 3 ml syringe, previously plugged with glass wool. The resin was then washed with 3 ml of ice-cold, EDTA-free PBS pH 7.0. It was then progressively washed with 2 ml of ice-cold Ni-NTA wash solution (100 mM citrate / phosphate) of pH 7.0, 6.5, 6.2, and finally eluted with the buffer adjusted to pH 5.0. All filtrates were collected in microcentrifuge tubes containing 20 µl of 2 M Tris, pH.8.0. Samples (20 µl) of each tube were then run on a 12 % SDS-PAGE and stained with Coomasiee blue. Alternatively, the gel was transferred to nitrocellulose paper for immunodetection using radiolabeled rabbit anti-mouse kappa antibodies, or through chemiluminescence technology using the nickel reagent, Ni-AT (Qiaex) linked to the enzyme horse radish peroxidase (HRP), which detected heavy chains containing the histidine tail.

2.10 Assessment of the binding capability of the recombinant 2E8 and 2H2 Fab fragments using a solid phase radio-immunoassay.- Polystyrene microtiter wells were coated with pure recombinant human apoE, or with pure rat ANF, in a volume of 100 µl at a concentration of 1 µg / ml overnight. The following day they were blocked with a volume of 200 µl of 1 % solution of BSA-PBS for an hour, and incubated with serial dilutions of both the recombinant 2E8 and 2H2 Fab fragments as well as the eukaryotic hybridoma generated 2E8 Fab at a concentration starting at 2.5 µg / ml, for an entire day. The following morning, the wells were washed three times with PBS-Tween, shaken dry

and incubated with 100 µl of a solution containing 100,000 cpm of a radio-labeled rabbit anti-mouse kappa light chain mAb in 1% BSA-PBS (Cedarlane) overnight. The following day, the wells were again washed with PBS-Tween and counted in a gamma counter.

2.11 Concentration of the purified Fab preparations.- The recombinant Fab fragments which were purified through metal chelate chromatography, were subsequently concentrated using centrifugal ultrafiltration. The entire volume of the eluted Fab was concentrated in microsep™ (Filtron, Ma.) microconcentrators spun at 6 000 x g in a fixed angle rotor. Usually, the final volume following concentration, was 500 µl. The concentration of the antibody preparation was then determined spectrophotometrically, at an $O.D._{280}$ nm using a 1 % extinction coefficient of 13.6.

2.12 Isolation of Fab monomers using FPLC.- Recombinant Fab preparations were subjected to FPLC chromatography, in order to remove any residual impurities such as aggregated antibodies and contaminating *E.coli* proteins. A Superdex-75 FPLC column (Pharmacia) was used at a flow rate of 0.5 ml / minute, in PBS. In all cases, a 250 µl solution of concentrated recombinant Fab was injected onto the column, and the elution profile was monitored using a U.V. monitoring system set at $O.D._{280}$ nm. Appropriate fractions were pooled as a function of the elution profile.

2.13 Generation of monoclonal antibodies specific for bacteriophage M-13.- A panel of mAbs directed against the M-13 bacteriophage were produced using the cell hybridization methodology described by Milne and collaborators (Milne *et al.* 1992). Briefly, five, 8 week old BALB/c mice were immunized intraperitoneally with 5 µl of stock M-13 helper phage (10^{11} pfu / ml) (Stratagene), emulsified in 150 µl of complete Freunds adjuvant. They received two subsequent "booster" injections, which were administered at two week intervals, using equivalent amounts of antigen, emulsified in incomplete Freunds adjuvant. Two weeks following the final immunization, sera from the immunized mice and from a control non-immunized animal were evaluated for anti-M-13 phage antibodies using a solid phase radioimmunometric assay. The assay consisted of coating phage antigen onto plastic microtiter wells, adding freshly isolated mouse serum in serial dilutions, and detecting bound IgG immunoglobulins using a radiolabeled rabbit anti-mouse antibody. Thus, following a 4 hour incubation period of the plasma, the wells were washed with PBS-Tween, and filled with 100 µl of a ^{125}I-rabbit anti-mouse IgG, in 1 % BSA-PBS. After an overnight incubation, the wells were washed with PBS-Tween, and counted in a gamma counter. The animal with the highest titer of anti-serum was then used for the cell fusion experiment.

Three days before the fusion, the mouse was boosted intravenously with a small dose of M-13 phage suspended in 100 µl PBS. The day of the cell fusion experiment, the mouse, under ether anesthesia, was killed by cervical dislocation, and the spleen was removed using aseptic techniques. In a 10 cm petrie plate, containing 10 ml of Dulbecco's modified Eagles medium (DMEM), a spleen cell suspension was prepared by

gently teasing the spleen using two 18 gauge sterile needles. The released cells were then transferred into a 50 ml conical tube filled with 30 ml of warm DMEM. They were then pelleted at 300 x g, and were resuspended in 30 ml of fresh, warm DMEM. The cells were washed two subsequent times, and were finally resuspended in 2 ml of DMEM, by gentle tapping of the pellet. The SP2-0 myeloma cell line was used as the fusion cell partner. Rapidly growing SP2-0 cells (about $4x10^5$ cells / ml, viability > 95%) were harvested, and washed twice with DMEM. Both the splenocytes and the SP2-0 cells were counted separately and then mixed at a splenocyte:SP2-0 ratio of 3:1. The cells were pelleted at 300 x g for 10 minutes and the supernatant was removed. Without adding additional medium the pellet was loosened by flicking the tube and the cells were incubated for 1 minute at 37°C. Fusion was initiated by the slow (over 1 minute) addition of 1 ml of a 47 % solution of polyethylene glycol (1300-1600 Da, American Type Culture Collection (ATCC)) in DMEM with gentle stirring using the pipette tip. The cells were left for a further minute before the addition of 2 ml of DMEM over a period of 3 minutes. The cells were then slowly pipetted into 90 ml of warm DMEM supplemented with 30 % fetal bovine serum (FBS) and HAT (hypoxanthine, aminopterine, thymidine, 100x pre-prepared solution from ATCC). As the SP2-0 cells lack the enzyme hypoxanthine guanine phosphoribosyltransferase, they can not grow in HAT-supplemented medium and, as splenocytes have a limited survival in culture (about 1 week), the addition of HAT selects for splenocyte-myeloma hybrids, i.e. hybridomas. The cells were then plated in 100 µl aliquots in 96 well microculture dishes, and placed into a 37 ^{0}C incubator, with an atmosphere of 5 % CO_2. The following day, a further 100 µl of DMEM, containing both 30 % FBS and HAT were added to the wells.

When HAT-resistant colonies occupied about 10% of the surface of the wells (10-14 days after the fusion) 100 µl of the culture supernatants were removed and assayed for the presence of anti-M-13 antibodies using the solid phase radioimmunometric assay described above. Cells from wells containing positive hybridomas were plated in 96 well microculture plates at a density of 0.5 cells / well, and grown for two weeks and wells in which growth occurred were tested for anti-M-13 antibody production. Cells from wells showing the highest antibody production were expanded and subjected to two further rounds of limiting-dilution subcloning. Hybridoma clones were then slowly frozen at a concentration of 10^6 cells / ml in DMEM medium containing 10% fetal bovine serum and 10% dimethylsulfoxide and transferred to a liquid nitrogen tank for long term storage. Hybridoma cells (about 5 x 10^6 / animal) were injected into the peritoneal cavity of BALB/c mice for the production of ascitic fluid. When the accumulation of ascitic fluid could be detected macroscopically, the mice were anesthetized and exsanguinated by cardiac puncture. The peritoneal cavity was opened and the ascitic fluid was harvested and mixed with the blood. The ascites / blood was incubated for 30 minutes at 37°C and overnight at 4°C to allow clot retraction. After centrifugation the serum / ascites was removed and frozen in aliquots.

Results

1. **Subcloning of light and heavy chains of mAbs into pComb3.-** The light and heavy chains of mAbs 1D7, 2E8 and 2H2 were all successfully amplified, purified and sub-cloned into the pComb3 expression vector. As shown in Figure IV-4, the pComb3 phagemid vector, containing an antibody light and heavy chain, could be digested with the endonucleases; Sac1 / Xba1, Spe1 / Xho1 or Spe1 / Nhe1, which consequently caused it to loose a fragment, and be resolved as a 4.8 to 4.9 kb linear band on a 1% agarose gel. The corresponding pComb3 vectors, capable of shuffling light or heavy chains fragments, were then excised from the gel, purified and used both for phage display or soluble Fab expression. Following their sub-cloning, the integrity of all newly subcloned antibody variable region genes were verified through DNA sequencing.

2. **Expression of the 2E8 and 2H2 recombinant Fabs on the surface of M-13 bacteriophage.-** The presence of functional recombinant Fab on the surface of M-13 bacteriophage was demonstrated using phab rescue experiments, as shown in Figure IV-3. Initially, the presence of light and heavy chain heterodimers displayed on the surface of M-13 phage were identified, by performing a phab rescue in microtiter wells containing immobilized rabbit anti-mouse kappa light chain mAbs (CedarLane). As shown in Figure IV-6., the rescue of both 2E8 as well as 2H2 phab preparations, was specifically inhibited when kappa light chain-containing mouse mAbs were added as competitors of the phabs.

3. Titering of a recombinant phab preparation.- The infectious titre of recombinant phab preparations, expressed in colony forming units (cfu), were routinely determined. On average, a 1.5 ml culture of *E.coli* infected with M-13 helper phage, precipitated with PEG and resuspended in 200 µl of water, resulted in a titer of 10^6 to 10^7 infectious particles per ml or cfu, whereas 100 ml cultures typically gave 10^9 to 10^{12} cfu.

4. Generation of anti- M-13 bacteriophage mAbs.- A series of mAbs specific for M-13 phage were produced using the cell hybridization procedure. Initially, out of 1000 microwell cultures of hybridized cells screened for antigen-specific antibody expression, 40 were selected for further analysis. Following limiting dilution re-plating, the clones were expanded and again tested for specific antibody productuion. Of the original 40 clones, 10 were retained and once again replated, tested for mAb production and frozen in liquid nitrogen.

5. Determination of the binding capability of 2E8 recombinant phab against apoE.- The binding ability of recombinant 2E8 Fab expressed on the surface of phage was determined using phage rescue and radio-immunometric assays. Figure IV-7 shows a histogram which corresponds to the specific inhibition of 2E8 phab rescue on apoE-coated microtiter wells, by the addition of increasing amounts of the 1D7 mAb. A 2E8 phab prep (100 µl) was added to microtiter wells containing increasing amounts of the 1D7 IgG, which is known to compete with 2E8 for binding to immobilized apoE. Figure IV-8 shows the specific inhibition of 2E8 phab binding to immobilized apoE, in a radio-immunometric assay. In this experiment, the bound phage is detected by the

addition of mixture of four radiolablled mouse anti - M-13 phage mAbs, as described in section 2.4 of the methods section. In control experiments, where the same amount of phabs were incubated in BSA-coated wells, no significant binding was recorded.

6. Determination of the binding specificity of the 2H2 recombinant phab for rat ANF.- The functional binding capability of the 2H2 recombinant phab was also determined using the phage rescue protocol and the radio-immunometric assay. The histogram in Figure IV-9 depicts the results of a phage rescue experiment. Figure IV.10 represents the results of the radio-immunometric assay as described in section 2.4.

7. Conversion of pComb3 from a phage display to a soluble expression vector.- The removal of the g3p (P198-S406) fusion protein from all phage display vectors was successful. The digestion of the vectors with the enzymes Spe1 / Nhe1 caused the release of a 600 bp fragment as seen on agarose gel electrophoresis (Figure IV-4). The vector, which migrated as a 4.9 Kb band, was cut out of the gel, purified and self ligated, then transformed into *E.coli* for expression.

8. Engineering of a histidine-tail in the pComb3 soluble expression vector.- In order to facilitate the purification of my recombinant antibody fragments, I engineered the pComb3 soluble expression vector so as a five residue histidine tail would be fused to the carboxy terminus of newly synthesized recombinant heavy chains. The nucleotides encoding the 5 residue carboxy-terminal tail were inserted into the vector as a double-stranded oligonucleotide which had at either ends, an appropriate Spe1 overhang as

shown in Figure IV-5. As described in section 2.6 of the methods section, and depicted in Figure IV-4, the g3p fusion protein was removed by Spe1 / Nhe1 digestion, and the histidine construct was inserted via the appropriately designed Spe1 cohesive ends. As shown in Figure IV-11, the presence of the histidine tail in the pComb3 soluble expression vector was first identified by Spe1 restriction digestion analysis. As shown in the photographed agarose gel, lanes 4, 9 and 10 were positive for the presence of the histidine tail, as the miniprep DNA was successfully cut with Spe1. Bacterial clones which harbored plasmids that had not taken up the fragment, but had simply recircularized were resistant to Spe1 digestion, and consequently did not migrate at the appropriate size, but rather as a lower molecular weight band which represented uncut super-coiled DNA. In addition to the Spe1 digestion assay, positive clones were sequenced and determined to code for five in-frame histidine residues followed by a stop codon (data not shown). A number of positive clones were retained, and a large scale plasmid preparation of the histidine vector was produced in order to sub-clone all of the light and heavy chains of mAbs 2E8 and 2H2 as well as the altered forms of the 2E8 heavy chain, according to previously described methods.

9. Expression and purification of recombinant 2E8 and 2H2 Fab from E. coli.- Both recombinant mAbs, as well as seven heavy chain mutant forms of 2E8, were expressed in the *E. coli.* strains XL1-Blue and TG1 (Stratagene). The Fabs were isolated from the bacteria, and identified first through western blots detected with radiolablled anti-kappa mAbs. Figure IV-12 shows a recombinant Fab preparation that had been eluted from an nickel affinity column using a discontinuous pH gradient, separated on a

12 % SDS PAGE and stained with Coomassie-blue. The purified recombinant Fabs were always seen to co-migrate with hybridoma Fab fragments generated by papain digestion of 2E8 IgG, with an apparent molecular weight of 50 kDa under non-reducing conditions. In fact, Figure IV-12 demonstrates the specific disappearance of a bacterial protein, of equivalent size as a hybridoma Fab control, from the periplasm which had been run through the nickel affinity column. The left panel of Figure IV-13 shows a Western blot of an SDS-PAGE gel which had served to resolve some 2E8 rFab fragments, and which was transferred onto nitrocellulose, and revealed with radiolabeled anti-kappa mAb. In the right panel of the same Figure, is the same nitrocellulose transfer, but this time detected with the Ni-AT HRP conjugated chemiluminescent reagent. Of note in this Figure, is that the control hybridoma Fab is not detected with the Ni-At reagent, but is detected with the radiolabled anti kappa as would be anticipated. In addition, the 30 kDa protein, bovine carbonic anhydrase, which is one of the molecular weight standards, was recognized by the Ni-AT reagent, and thus served as a convenient molecular weight marker in such experiments. Most preparations of Fab purified by nickel-chelate chromatography were contaminated with a bacterial protein that had an apparent molecular weight of 25 kDa on SDS-PAGE. This contaminant was seen on Coomassie blue-stained gels, and was occasionally detected on Western blots revealed with the Ni-At reagent, but not with ^{125}I-anti-Kappa. This protein may be the bacterial periplasmic enzyme β-lactamase, as other investigators have reported the co-purification of this protein using the nickel-chelate chromatography. In order to minimize the amounts of this protein in my recombinant Fab preparations, I sequentially washed the resin with buffers adjusted to a progressively lower pH. This pH step gradient, achieved a partial

separation of the recombinant Fab and the contaminating protein (Figure IV-12) with the majority of the Fab being eluted at pH 5.0. As described below, a homogeneous preparation of monomeric Fab could be obtained by subjecting the pH 5.0 fraction to size exclusion chromatography.

To estimate the amounts of an expressed recombinant antibody, the detected bands on a western blot were compared to a known amount of hybridoma generated Fab, which was always run on the same SDS-PAGE gel. An example of such an experiment is shown in Figure IV-14, where 200 ng of pure hybridoma generated Fab is compared to serial dilutions of crude 2E8 and 2H2 rFab preparations. As shown in Table IV-1, 200 to 600 μg of purified wildtype 2E8 could be obtained from 1 L cultures of appropriately transformed XL1-Blue bacteria, grown in either LB or super broth that had been induced with 0.1 mM IPTG. Induction with a higher concentration of IPTG (1mM), did not significantly increase the yield of antibody. Supplementing the cultures with 0.4 M sucrose reduced Fab production in contrast to what has been reported for the bacterial expression of scFv fragments (Figure IV-15). Finally, as shown in Table IV.1, most of the rFab was found to be located in the periplasm. The STE solution, to which the bacteria were exposed for one hour and which caused their periplasms to become hypertonic, contained little antibody and, with the exception of certain isolated cases, very small amounts of antibody were detected in the culture medium.

When the same expression vectors were grown in the TG1 strain of *E.coli*, under identical growth conditions as described for the XL1-Blue strain, I consistently obtained 5 to 10 times more recombinant antibody (Table IV-2). With the exception of the total mass of expressed antibody Fab, this strain of *E.coli* behaved as the XL1-Blue strain with respect to the production of the antibody under various conditions. Thus, an increase in the amount of IPTG used for induction had little effect on the production rate, and the addition of 0.4 M sucrose to the growth media, dampened the expression of the antibody. Again, with this strain as with XL1-Blue, rFab was primarily present in the periplasm.

10. Isolation of rFab monomers using FPLC.- In order to purify the recombinant Fabs to homogeneity, 250 µl of a concentrated rFab preparation was injected onto a Superdex-75 FPLC column. As shown by the elution profile depicted in Figure IV-16a, a small broad peak, consisting primarily of aggregated rFab, eluted first. Following this peak was the elution of a much larger and narrower peak which corresponded to monomeric Fabs, often closely followed by a second sharp peak which corresponded to the 25 kDa bacterial protein believed to be β-lactamase. This purification methodology was crucial in order for the accurate determination of the affinity constant of the rFabs using surface plasmon resonance, as described in Chapter V. Figure IV-16b depicts the purity of the isolated rFab when resolved on a 12 % SDS PAGE, both under reducing and non-reducing conditions.

11. Loss of the histidine tail fused to the heavy chain in the bacterial periplasm.- By comparing autoradiograms of recombinant Fabs on a single western blot membrane, detected by the two previously described techniques, I observed that, on some occasions, rFab reactive to anti-kappa mAbs, was not always detected by the nickel reagent (Figure IV-13 lane D^{FT}). The periplasmic extract which had previously been run through Ni-NTA resin was collected, and analyzed for residual rFab presence. A 100 µl sample was run along side of the purified eluted rFab, on an SDS-PAGE that was transferred to nitrocellulose and blotted with the nickel reagent as well as with the ^{125}I-anti- kappa mAb. In most cases no residual rFab was observed in the flow-through periplasm, but on occasion there was immunoreactivity with the anti kappa mAbs but not with the nickel reagent. In addition, when the Coomassie blue stained gel was examined, there was a protein band which co-migrated with the anti kappa revealed rFab (data not shown). This suggested that cleavage of the histidine tail occurred on a subpopulation of molecules within the bacteria.

12. Binding capability of the recombinant 2E8 Fab using a solid phase radioimmunometric assay.- Figure IV-17 presents the anti-apoE immunoreactivity of preparations of the recombinant 2E8 Fab when assayed in solid phase radio-immunometric assay. The results demonstrate that the recombinant Fab displays the same reactivity towards apoE as does Fab prepared by papain digestion of 2E8 IgG. In addition to using purified apoE, freshly isolated human VLDL were also used in determining the reactivity of the recombinant 2E8. Figure IV-18 depicts the reactivity observed for identical serial dilutions of recombinant versus parental 2E8 Fab, incubated

in VLDL-coated microtiter wells. Again, the recombinant form of the 2E8 Fab recognized apoE with an affinity similar to that of the parental hybridoma Fab. The total counts representing Fab binding to VLDL were consistently lower than for radio-immunoassays using pure apoE. This reflects the fewer apoE epitopes available in VLDL coated wells compared to those in apoE coated wells. This difference was also seen with mAb 6C5, a high affinity mAb specific for an epitope in the amino terminus of apoE.

13. Assessment of the binding capability of the recombinant 2H2 Fab using a solid phase radioimmunometric assay.- Finally, I present in Figure IV-19 the relative immunoreactivity of the 2H2 rFab against rat ANF. As in all previously described direct radioimmunometric assays, pure rat ANF was coated onto microtiter wells at a concentration of 1 μg / ml. Following a blocking step, using 1 % BSA-PBS, appropriate amounts of the pure rFab was incubated in the well overnight. As shown in Figure IV-19, the rFab was found to be specific for ANF, as it was nonreactive towards control, BSA coated wells. Furthermore, 2E8 rFab fragments did not bind to the ANF-coated wells.

Discussion

In this chapter, I have described the subcloning of the light and heavy chains of mAbs 2E8 and 2H2 into the pComb3 phagemid expression vector. In addition, I have detailed the production and purification of both antibodies as rFab fragments, using *E.coli* as a host organism. The recombinant Fabs were generated both as soluble antibodies and displayed on the surface of filamentous bacteriophage. The antigen-binding capability of recombinant 2E8 was found to be identical to the Fab that was generated by papain digestion of 2E8 IgG. These experiments form the basis for the characterization of 2E8 variants that are presented in Chapter V. I have also described the expression of a second recombinant Fab, 2H2, that is specific for the rat cardiac hormone ANF. Again, the recombinant 2H2 fragments were shown to possess antigen-binding activity whether they were expressed in a soluble form, or on the surface of M-13 filamentous phage.

A problem that I noted early on during the subcloning of the antibody chains, was that mutations had been introduced into the cloned cDNAs in the form of single base pair transitions, transversion and deletions. Presumably, these errors corresponded to misincorporated as well as deleted nucleotides, due to the PCR amplification of the antibody genes. Owing to a lack of a 3'→5' exonuclease proof-reading activity in Taq polymerase, a nucleotide transition misincorporation frequency of one every 10^3 to 10^4 base pairs copied has been reported, with transversions occurring at a one to two orders

of magnitude lower frequency. The infidelity of Taq polymerase is known to be further exacerbated by elevated concentrations of deoxyribonucleoside triphosphate (dNTP) substrates and by the replacement of magnesium ions by manganese equivalents, in the reaction mixture (Goodman M. 1995). As a consequence, efforts were always made to respect the appropriate levels of dNTPs as well as the other salts within the reaction buffer. Nevertheless, I have observed a number of mutations attributable to nucleotide misincorporation by the Taq polymerase. In particular, is the loss of an adenosine nucleotide at position # 33 in the 1D7 light chain, which resulted in the disruption of the antibody reading frame, and subsequently to the lack of production of soluble Fab. In addition, the polymerase caused the conversion of a thymidine into a guanosine at position # 61 leading to a change of a histidine to a glutamine in the heavy chain of antibody 2H2. A second clone of the 2H2 heavy chain, which was amplified using the leader sequence primer, was observed to have a lysine converted to an asparagine residue. However this mutation was not incorporated into the 2H2 heavy chain clone which was used in expression studies. Finally, certain 2E8 light chain subclones were found to have acquired point mutations and, as a consequence, were not retained. Therefore, the predicted misincorporation rate of Taq polymerase was confirmed through the amplification of these antibody genes.

Because of its relatively low fidelity of DNA replication, I discontinued the use of Taq polymerase when thermal stable polymerases, with proofreading ability, such as Vent polymerase, became available. The increased fidelity of Vent polymerase in the replication of DNA, was however accompanied by an observable reduction in the total

yield of the amplified product, in comparison to the same PCR reactions performed with the use of Taq polymerase. This is consistent with the previously observed activity of DNA polymerases, whose exonuclease activity is known to excise some 5 to 15% of correctly inserted nucleotides (Clayton *et al.*, 1979; Fersht *et al.* 1982), a factor that is known to affect PCR cycling time as well as product yields. Although my studies did confirm the improved fidelity of Vent polymerase, I nonetheless observed several cases where nucleotides were misincorporated during PCR amplification. Indeed I have documented a variant form of the 2E8 mAb, which I engineered through site-directed mutagenesis, with an A to G transversion within codon 52a, which fortunately did not cause a change the amino acid encoded by the codon.

I consistently observed important differences in the amounts of recombinant Fab that were expressed in different *E.coli* strains, with yields being 5 to 10 times higher in the TG1 strain of *E.coli* as compared to the XL1-Blue (Tables IV-1 and IV-2). The yields of Fab fragments that I obtained using XL1-Blue and TG1 bacterial cultures were similar to values previously reported for other Fab fragments expressed in the respective strains (Kipriyanov *et al.* 1997, Roger MacKenzie personal communication). The reasons for higher levels of expression of the heterologous protein in the TG1 strain are not clear. Although the transformed TG1 bacteria always grew faster than XL1-Blue bacteria, the higher expression of Fab by the TG1 strain was not solely the result of a higher density of bacteria in the cultures, as the strain differences were also apparent when yields were expressed in terms of wet bacterial mass.

As documented by many laboratories active in the field of antibody engineering, it would seem that the limiting step of antibody production by prokaryotes is the folding of the proteins. Since the bacterial cytoplasm is a reducing environment in most strains, disulfide bond formation does not occur, and heterologous Fab fragments must either be transported to the periplasm for proper folding and assembly, or denatured protein will accumulate within the cytoplasm or in inclusion bodies. Over-expression of heterologous proteins can pose an undue strain on the organism, which can lead to the death of the host, a phenomenon which I observed early in my expression experiments, and that has been recently reported by others (Plückthun *et al* 1996). I have found that this problem could be largely circumvented by incubating the induced culture at room temperature rather than at 37 °C, a condition now recommended by many experts in the field. The reasons for the toxicity that occurs when bacteria are induced to express recombinant antibodies, is at this date still unknown. However, they are likely linked to the over-expression of recombinant antibodies in a fast growing culture, which accumulate and aggregate within the cytoplasm and periplasm. Furthermore, excessive accumulation of folded antibody within the periplasm, may cause the outer membrane to leak and perhaps even to collapse.

The properties which allow for recombinant antibodies to be isolated in an abundant and active form within bacteria, would appear to reside with the primary structure of each individual antibody. In most cases, it has been determined that recombinant antibodies, once transported to the periplasm, can fold on their own due to favorable thermodynamic forces. However, it is thought that the bacterial disulfide-

forming machinery may help at this stage. Unfortunately, it would seem that not all antibodies can fold appropriately within the periplasm of *E.coli*, and consequently cannot be isolated in an active form, even when the bacterial culture is grown at room temperature. It has recently been shown that defective folding of a particular antibody, can be corrected by the substitution of certain amino acids within its framework regions. In a recently documented case, specific residues within the framework regions of the light chain, caused the antibody to fold with much better kinetics within the periplasm leading to enhanced amounts of soluble antibody (Forsberg *et al.* 1997). Moreover, these investigators demonstrated that substitutions introduced into the heavy chain caused the expressed scFv fragments to be localized preferentially in either the periplasm or within the growth medium. Clearly, the implications of such work emphasize the inadequacies in our knowledge of the metabolism of expressed recombinant antibodies within bacteria.

The bulk of soluble antibody was found in the periplasm of both TG1 and XL1-Blue bacteria, and both strains were relatively insensitive to a 10 fold increase in the inducing agent, IPTG. Similarly, both strains behaved similarly when grown in media containing 0.4 M sucrose, in displaying a reduced amount of expressed antibody. The rational for supplementing the media with high concentrations of sucrose was based on the report that sucrose was found to promote the production of scFv fragments in *E. coli* (Kipriyanov *et al.* 1997). In this report, the addition of 0.4 M sucrose to the induced culture, resulted in a 2 to 10 fold increase in expressed antibody, both in the STE solution as well as within the media. Previously, it had been shown that the addition of 0.4 M sucrose to the culture medium of *E.coli* transformants expressing the β-lactamase gene

downstream of an IPTG inducible promoter and a bacterial leader sequence, caused an increased accumulation of the soluble product (Bowden and Georgiou, 1990). It is believed that sucrose infiltrates the periplasm causing it to swell due to an increased osmotic pressure. This enlarged periplasm would then allow more recombinant protein to accumulate. In contrast, I consistently observed lower yields of expressed soluble antibody when cultures of both *E.coli* strains were supplemented with sucrose. This apparent discrepancy in the effects of sucrose on antibody expression observed by myself and those reported by Kipriyanov *et al.*, could reflect both differences between expression of Fab and scFv fragments in bacteria and features intrinsic to individual antibodies.

The isolation of proteins through the use of metal chelate chromatography is an extremely powerful and convenient way of selectively purifying recombinant proteins tagged with a poly-histidine tail. However, this methodology does have its drawbacks, in that certain host proteins that contain histidine-rich sequences, are known to react with the resin, and co-elute with the desired protein. Many of my rFab preparations eluted from a Ni-NTA column, were contaminated with equimolar amounts of a protein with an apparent molecular weight of 25 kDa which likely represented β-lactamase. Many different methodologies were attempted in order to minimize the co-purification of this and other bacterial proteins with the rFabs. Firstly, since the ability of a protein to interact with the Ni-NTA resin is dependent on the presence of clusters of histidine residues present in a non-protonated form, I adjusted the pH of bacterial periplasms to a value close to 6.4, using dialysis. A pH of this value ensured that the histidine imidazol

groups resided close to their pKa, and thus in a physical state less likely to couple ionically to the resin. Secondly, the resin was washed with buffers of pH values which approached the pKa of histidine by only 0.2 unit values. Washing the resin with citrate / phosphate buffers adjusted to pH settings ranging from 7.0 to 6.0, permitted the removal of much of the undesired protein as depicted in Figure IV-12. While some loss of rFab occurred during the washes, the major portion of the rFab was eluted with a citrate / phosphate buffer adjusted to pH 5.0. The use of a shallow discontinuous pH gradient, improved the purity of the rFab preparations but a small amount of the contaminating 25 kDa protein persisted as did some aggregated Fab. Homogeneous monomeric rFab could, however, be obtained by subsequent size exclusion chromatography of the partially purified Fab fraction using size exclusion FPLC chromatography.

The loss of the histidine tail, which is fused to the heavy chain carboxyl- terminal when the Fab is produced in a soluble form, was observed following the purification of the recombinant Fab from bacterial periplasm. The literature reports many problems associated with bacterial proteases, which often damage recombinant proteins. In particular, a well known proteolytic event occurs during the production of recombinant antibodies expressed on the surface of M-13 phage, in association with a phage coat protein. It has been documented that the recombinant antibodies are often cleaved off the surface of the phage, if left for a prolonged period of time in the bacterial supernatant (McCafferty *et al.* 1996). This problem is only partially alleviated by polyethylene glycol precipitation of the phage, as the protease appears to co-precipitate with the phabs, and continue to cleave the recombinant proteins. For this reason preparations of phage-

displayed antibody fragments were only stable for a short while at 4 ^{0}C, and were stored at -80 ^{0}C in a glycerol solution. Soluble recombinant antibodies are also known to be susceptible to the hydrolytic activity of certain proteases found in the periplasm. An EDTA-sensitive protease has been documented to cause the digestion of a poly-glycine linker which holds recombinant single chain Fv fragments together (Roger MacKenzie, personal communication). The action of this protease varies from mild to almost complete digestion, resulting in the total dissociation of the recombinant antibody (Jelena Vukmirica, personal communication). The situation with the soluble recombinant antibodies is similar to the phage-displayed preparation. The purification of the antibodies by metal chelate chromatography does not seem to eliminate the presence of the protease which co-purifies with the antibodies. Only further purification, through the use of size exclusion FPLC chromatography, ensures the integrity of the antibody preparations. It has been recently shown that the addition of all known protease inhibitors did not prevent the degradation of the antibodies (Plückthun *et al.* 1996). Moreover, the elimination of all known loci encoding for bacterial proteases, still did not totally resolve this problem (Meerman and Georgiou, 1994). In my case, the loss of the histidine tail not only caused a decreased in the amount of isolatable antibody, but more importantly, it prevented detection of the truncated Fab fragments with the Ni-AT reagent.

The biological activity of the recombinant antibodies was assayed when they were expressed on the surface of M-13 phage and in a soluble form. The binding capability of soluble purified recombinant 2E8 was equivalent to the parental hybridoma generated

Fab, when tested against both lipid-free apoE lipoprotein-associated (Figures IV-17 and IV-18). Similarly, r2H2 Fab was shown to have good binding capability to rat ANF (Figure IV-19). The antibodies also showed specific binding to immobilized antigen when they were expressed on the surface of filamentous M-13 phage, when assayed by either phage rescue or a solid phase radio-immunometric assay. The recombinant phage could be rescued on immobilized anti-mouse kappa chain antibodies and on immobilized antigen, demonstrating the presence of antibody on the phage surface and its binding activity, respectively (Figures IV-7 – IV-10). The specificity of the interaction between the Fabs on the surface of phage was ascertained by demonstrating that antigen-specific antibody could compete with the phage displayed Fab for binding to antigen.

In conclusion, in this Chapter I have documented the functional production of recombinant Fab fragments using *E.coli*. Both mAbs 2E8 and 2H2 were shown to be expressed on the surface of filamentous phage M-13, as well as in a soluble form. The soluble Fabs were purified to homogeneity and the biological activity of antibody 2E8 was determined to be identical to the corresponding parental hybridoma generated Fab. Finally, the antigen-binding capability of the 2H2 recombinant Fab was demonstrated to be specific for ANF.

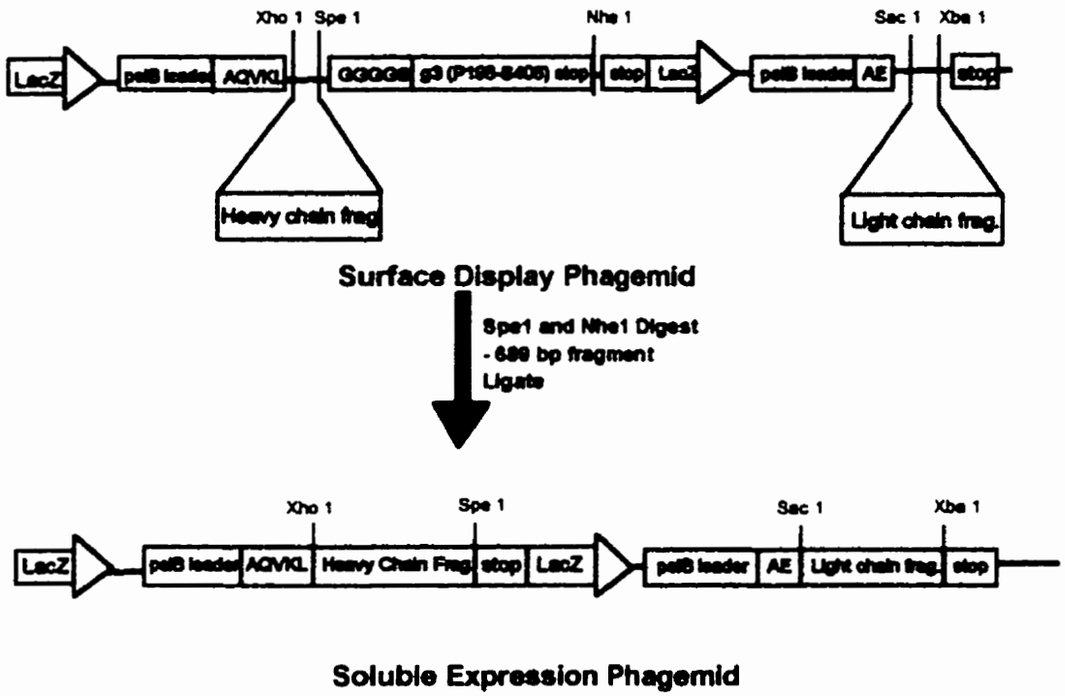

Figure IV-1 The pComb3 expression phagemid vector.- The figure depicts the organization of the pComb3 antibody expression vector, which corresponds to a 4,2 Kb bacterial phagemid. The unique restriction endonuclease sites Sac1 and Xba1 facilitate light chain insertion. The Xho1 and Spe1 sites allow for heavy chain insertion whereas the Spe1/Nhe1 sites permit the removal of the g3 gene which codes for the M-13 carboxyl-terminal fragment of g3p. Expression of the heavy chain-g3p fusion protein results in the Fab being displayed on the surface of the phage whereas, removal of the nucleotides encoding the g3p fragment results in assembled recombinant Fab being expressed in a soluble form. As both chains are produced with an amino terminal bacterial leader sequence, following translation, they are directed to the periplasm, where they assemble as heterodimers.

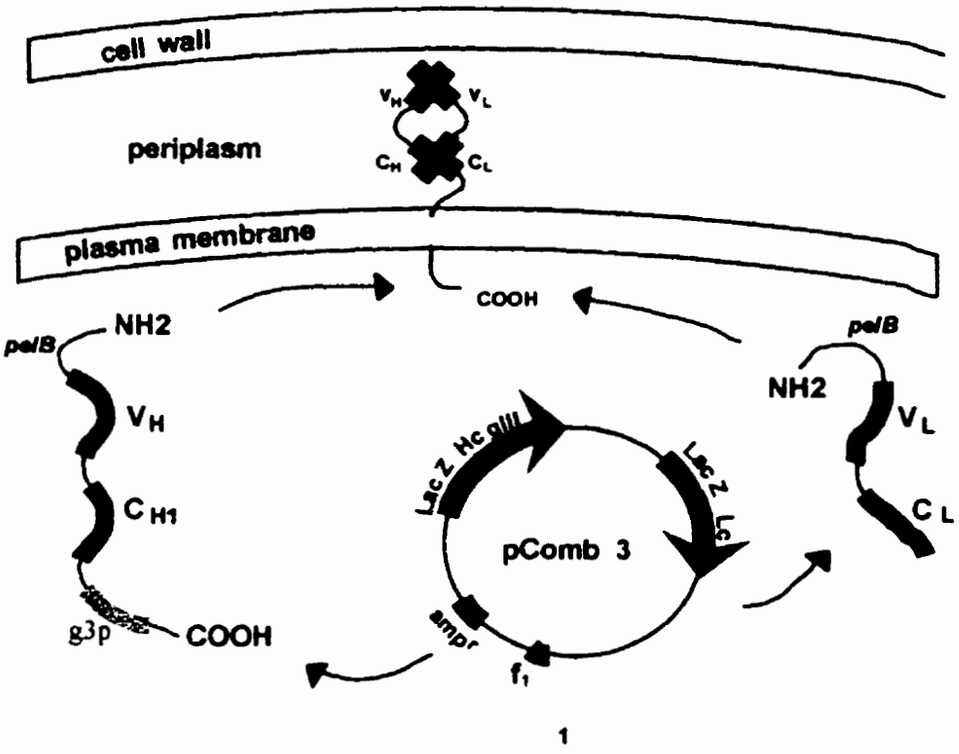

Figure IV-2a Bacterial expression of recombinant antibody fragments.- The phagemid vector pComb3 is represented within a bacterial cell. Both light chains as well as heavy chain-g3p fusion proteins are produced independently, under the IPTG-inducible control of Lac Z promoters. Both recombinant proteins are synthesized with the *pelB* amino-terminal leader sequence, which allows for them to be translated and directed to the bacterial periplasm. Once transported across the plasma membrane, the leader sequences are cleaved by the bacterial enzyme signal peptidase, and the antibodies then fold and associate as heterodimeric Fab fragments linked through a disulfide bond, and remain anchored to the inner membrane. Soluble recombinant Fab fragments, devoid of the g3p fusion protein, can be isolated as crude periplasmic preparations, or a "shockate", using a gentle osmotic shock treatment.

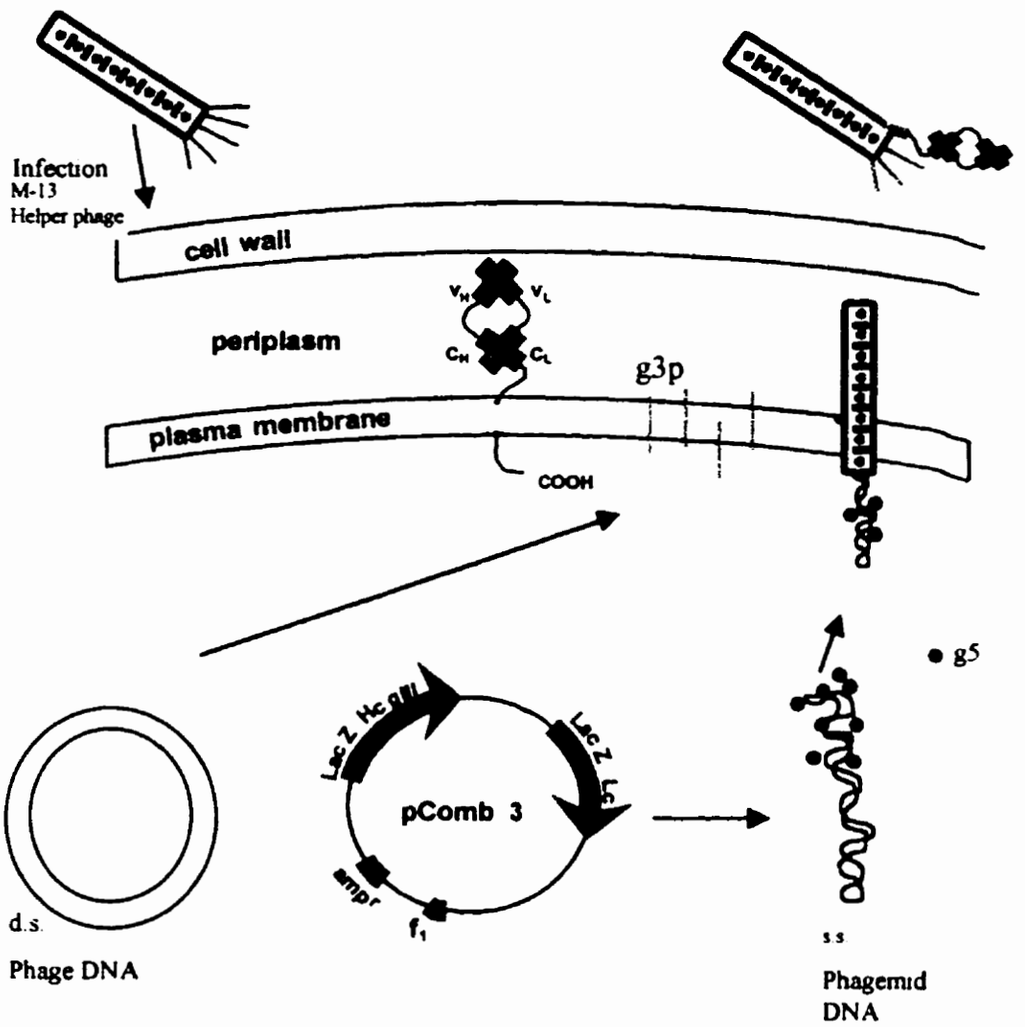

Figure IV-2b Assembly of recombinant antibodies displayed on the surface of filamentous phage.- Recombinant Fab fused to the g3p protein remain associated with the plasma membrane. Upon infection with M13 helper phage, single stranded phagemid DNA is synthesized by a viral DNA polymerase, which is promptly packaged as progeny phage, through the help of several phage encoded proteins, in particular g5. As the progeny phage mature and extrude across the plasma membrane, the recombinant Fab-g3p fusion protein become associated with, and cap the trailing extremity of the particles. As only five to six g3p proteins associate with the progeny phage extremity, there is a competition between the M-13 helper phage-encoded g3p and the Fab-g3p fusion protein for the phage. It has been estimated, than on average there is one to three Fab-g3p fusion proteins per phage particle.

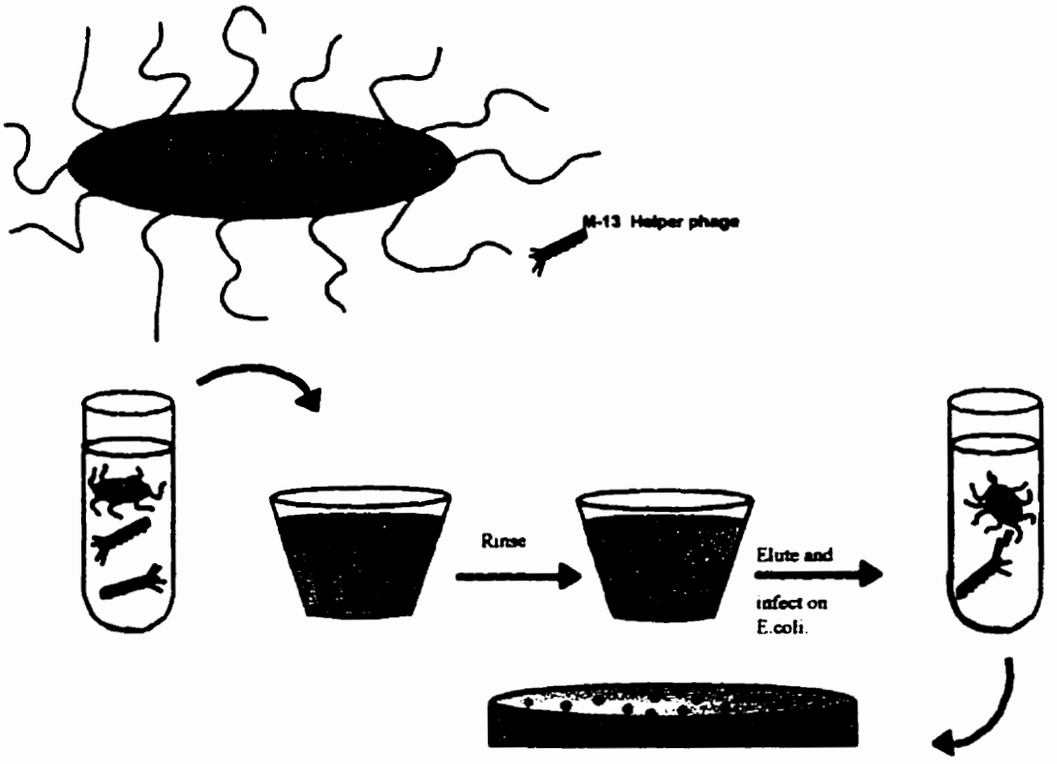

Figure IV-3 Phab rescue: Scheme depicting the biological assay of recombinant phab activity. Male *E.coli* bacteria expressing the F'pili, transformed with a pComb3 vector containing antibody light and heavy genes, are infected with M-13 helper phage. As described in the text, the infected culture is incubated overnight and resultant progeny phage are isolated and tested for antibody activity in a microtiter well coated with an appropriate antigen. Following the removal of unbound phage through several washes, the specifically-bound phage are eluted with an acidic solution. Once neutralized, the eluted phage are then added to a fresh culture of male *E.coli*, allowed to infect the cells, and finally plated onto ampicilin containing LB agar, and placed into a 37 °C incubator overnight. The resultant bacterial colonies correspond to individual "rescued" phage particles which have transferred their pComb3 plasmid coding for antigen-competent antibody genes.

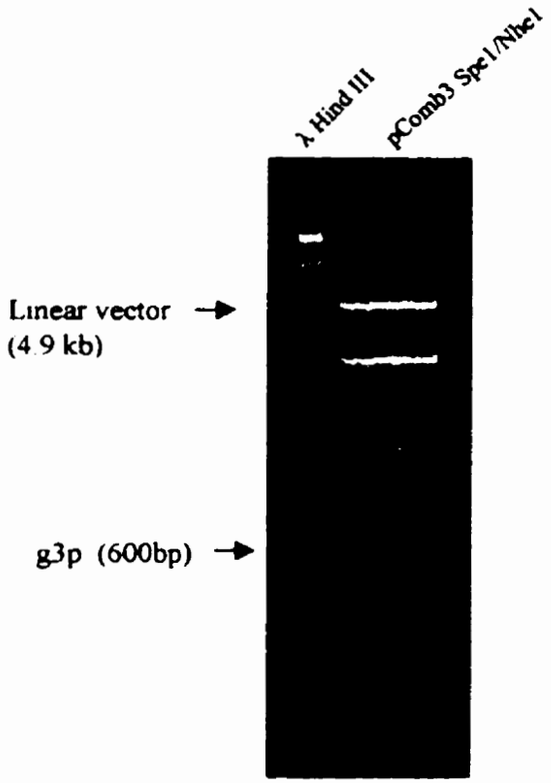

Figure IV-4 Gene shuffling in pComb3.- This figure shows the resolution of the pComb3 expression vector containing both a light and heavy chain, digested with the endonucleases Spe1 / Nhe1, and run on a 1% agarose gel. The linear band which is seen to migrate at position 4.9 kb is then cut out of the gel, and purified using the Qiaex DNA purification reagents. In fact, this resolution pattern is what is always observed when the vector is subjected to the excision of a gene fragment, be it the light, heavy or g3 fusion protein, which all migrate with a size of 600 - 700 bp.

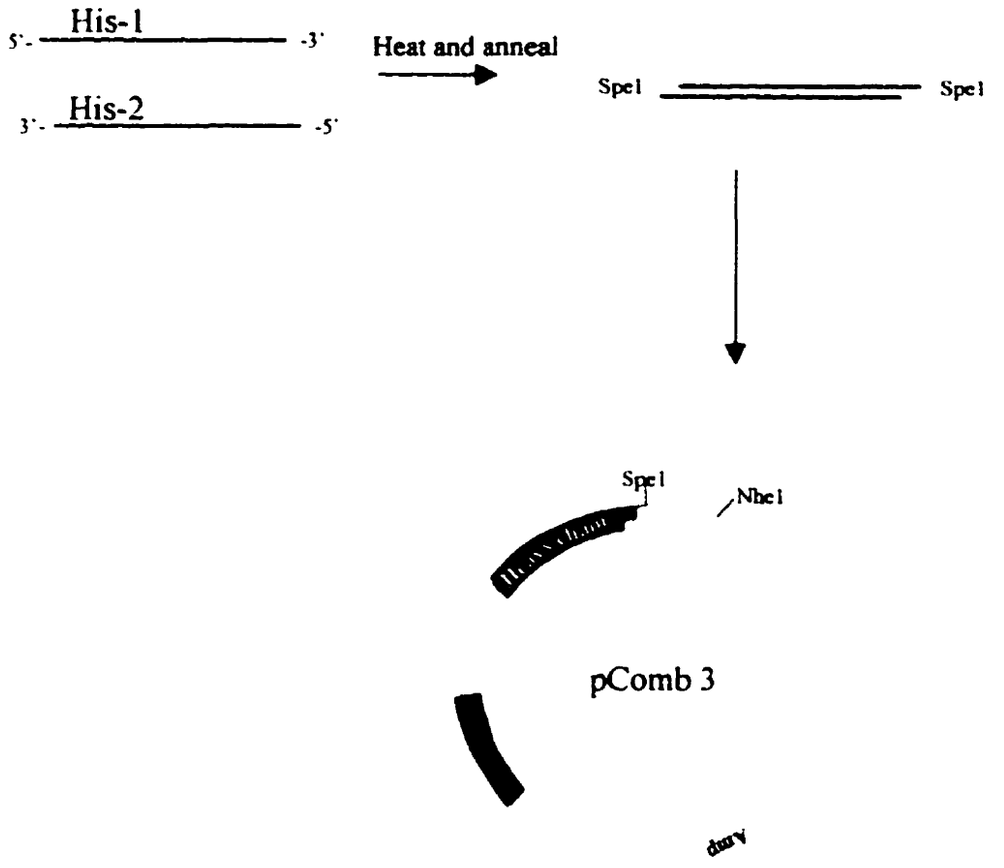

Figure IV-5 Addition of a carboxy-terminal histidine tail to the heavy chain of the pComb3 expression vector. The diagram depicts the methodology used in the addition of a five-residue histidine tail to carboxyl-terminal end of the heavy chain cloned into pComb3. First, an equimolar mixture of the complementary His-1 and His-2 oligonucleotides were denatured at 95 ^{0}C, and let to slowly anneal in a water bath set at 60 ^{0}C. A certain amount of this annealed material was then mixed with a preparation of pComb3 which had previously been relieved of its g3 fusion protein. The mixture was supplemented with the enzyme T4 ligase, and incubated overnight. Following the transformation of the ligated DNA into *E.coli*, isolate bacterial clones were individually chosen for restriction digest analysis. The enzyme SpeI was used to identify clones which had incorporated the short insert. As shown in Figure IV.13, those clones which had acquired the insert, were cut by the endonuclease, and migrated with the same molecular weight as a control soluble pComb3 vector which had been linearized.

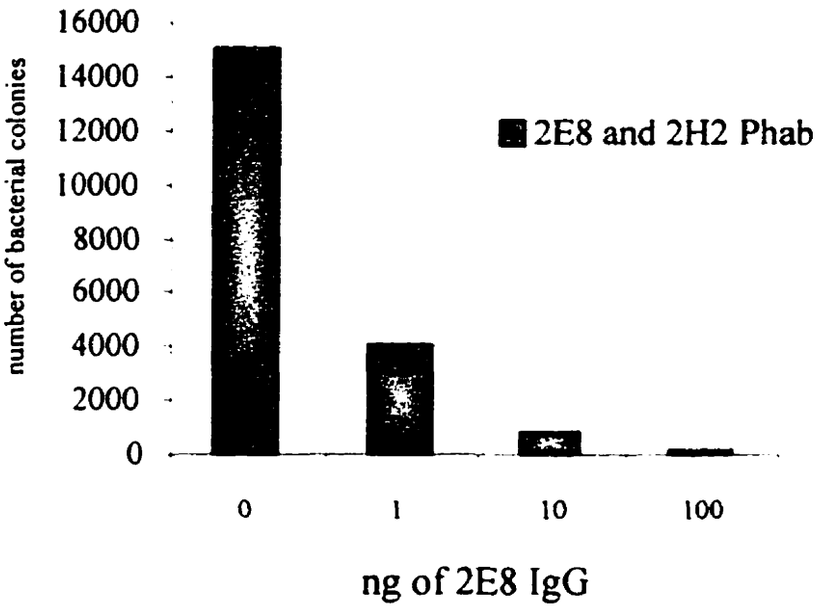

Figure IV-6 Assessment of the presence of rFab displayed on the surface of M-13 phage: Phab rescue using rabbit anti-mouse kappa antibodies.- This Figure is representative of results of many phab rescue experiments, for both 2E8 as well as 2H2 preparations, which were carried out in order to detect the presence of rFab on the surface of the phage. Microtiter wells were coated with rabbit anti-mouse kappa antibodies, which served to retain rFab-bearing phab. The first bar represents the incubation of phab with no competing antibody, and thus always gave rise to a confluent lawn of bacteria. The subsequent bars represent the effect of added amounts of the competitor, kappa-containing mouse IgG. As increasing amounts of the competitor were added, a corresponding decrease in the amount of rescued bacteria could be observed on the petrie plate, indicating that the rescue was specific for phab.

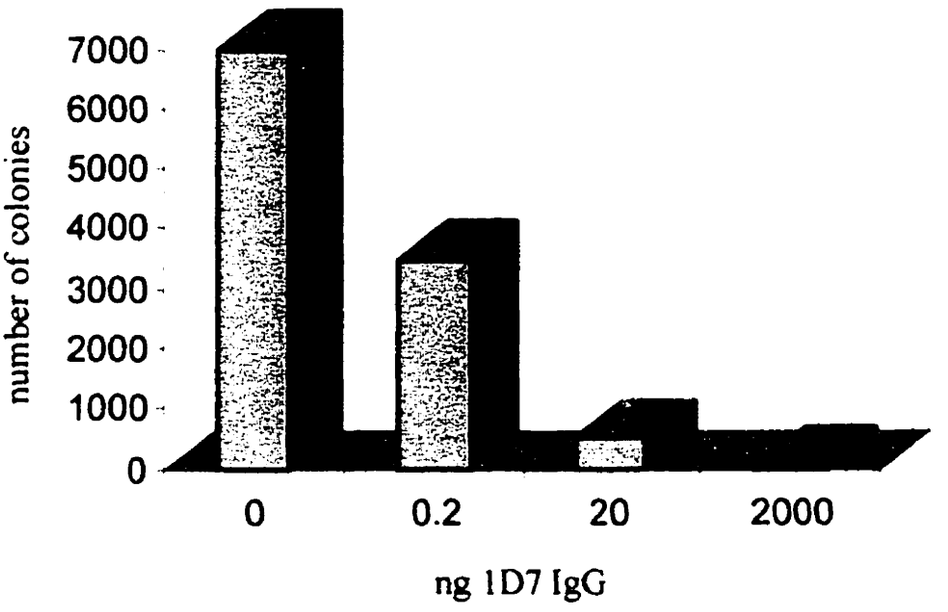

Figure IV-7 Assessment of the antigen-binding specificity of 2E8 phab preparations.- This histogram depicts the antigen-binding specificity of 2E8 phab preparations, as determined using the phage rescue procedure. ApoE coated wells were filled with equal amounts of freshly isolated 2E8 phab, diluted once in 4 % BSA-PBS, and increasing amounts of the cross-reacting, apo-E specific mAb 1D7 were added as a competitor. As shown by the first bar in the diagram, when no competitor mAb was added, many colonies were observed. However, as increasing amounts of the 1D7 mAb were added, correspondingly fewer bacteria were rescued, demonstrating the specificity of the 2E8 phab interaction. This type of competition was not observed when an irrelevant mAb, such as mAb 3H1 was added as a competitor.

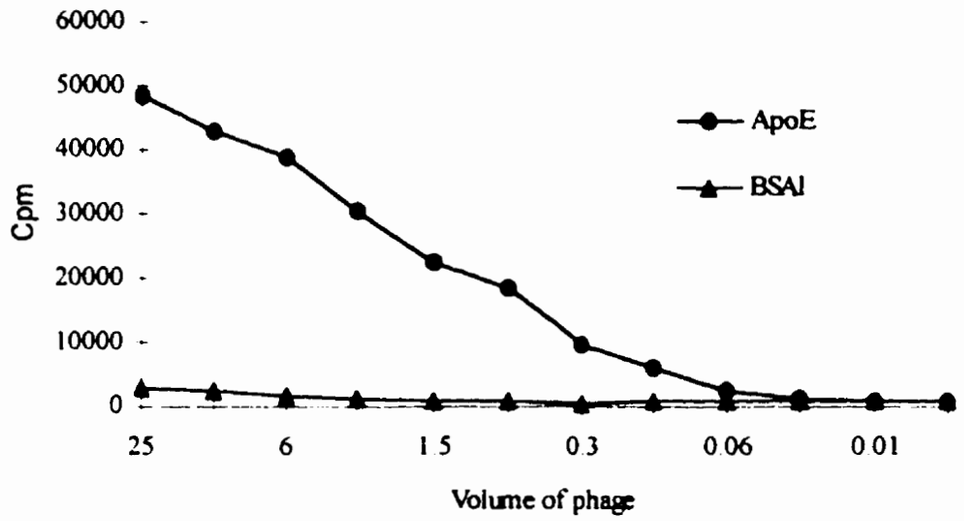

Figure IV-8 Assessment of the antigen-binding specificity of 2E8 phab preparations using a solid phase radioimmunometric assay.- In order to further confirm the antigen specificity of the 2E8 rFab expressed on the surface of M-13, freshly isolated phab were assayed for apoE specificity using a solid phase radioimmunometric assay. Isolated phabs were incubated as serial dilutions made in 3 % BSA-PBS, in microtiter wells which had previously been coated with pure apoE. Following an overnight incubation, the plates were washed with PBS-Tween, and were filled with 100 µl of a mixture of four radiolabled mAbs, specific for M-13 phage. The plates were incubated for five hours, washed and counted in a gamma counter. To ensure the validity of the binding results, an equivalent serial dilution of the phab preparation was incubated in control, BSA coated microtiter well.

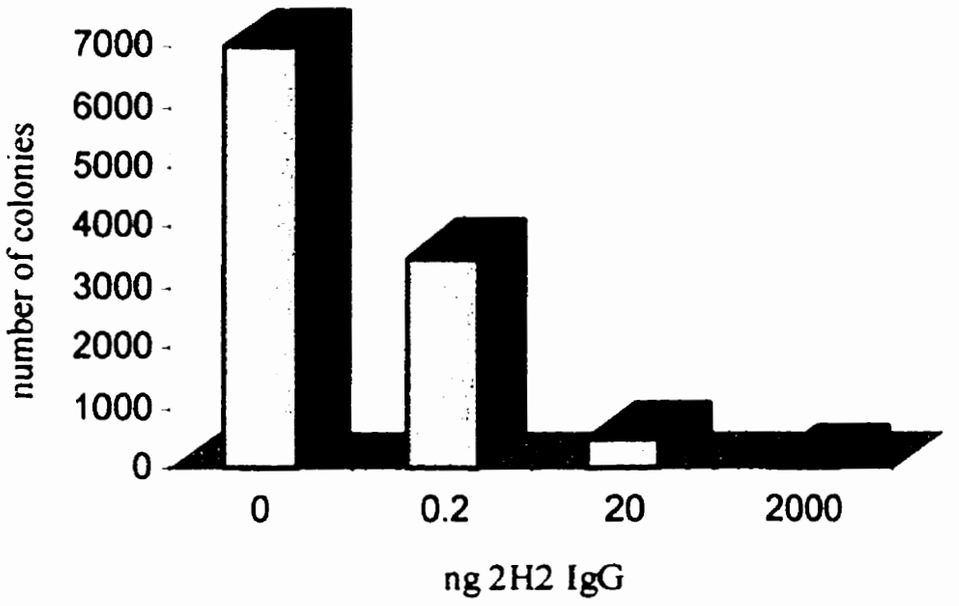

Figure IV-9 Assessment of the antigen-binding specificity of 2H2 phab preparations.- This histogram depicts the antigen-binding specificity of 2H2 phab preparations, as determined using the phage rescue procedure, and which has been described in Figure IV.9 for the 2E8 phab. ANF coated wells were filled with equal amounts of freshly isolated 2H2 phab, diluted once in 4 % BSA-PBS, and increasing amounts of the parental, ANF- specific mAb 2H2, were added as a competitor. As shown by the first bar of the diagram, when no competitor mAb was added, many bacteria were rescued. However, as increasing amounts of the 2H2 mAb were added, correspondingly fewer colonies were obtained, demonstrating the specificity of the 2H2 phab - ANF interaction. No competition was seen with an irrelevant antibody.

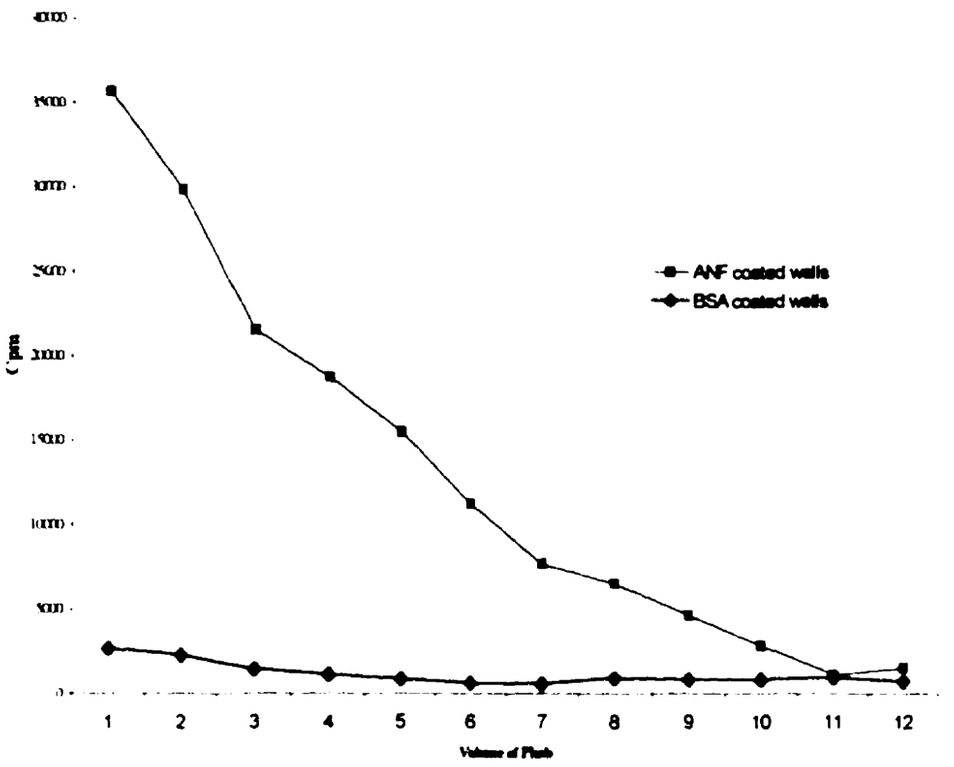

Figure IV-10 Assessment of the antigen-binding specificity of 2H2 phab preparations using a solid phase radioimmunometric assay.- In order to further confirm the antigen specificity of the 2H2 rFab expressed on the surface of M-13, freshly isolated phab were assayed for ANF binding specificity using a solid phase radio-immunoassay. Isolated phab were incubated as serial dilutions made in 3 % BSA-PBS, in microtiter wells which had previously been coated with pure rat ANF. Following an overnight incubation, the plates were washed with PBS-Tween, and were filled with 100 µl of a mixture of four radiolabled mAbs, specific for M-13 phage. The plates were incubated for five hours, washed and counted in a gamma counter. To ensure the validity of the binding results, an equivalent serial dilution of the phab preparation was incubated in control, BSA coated microtiter wells.

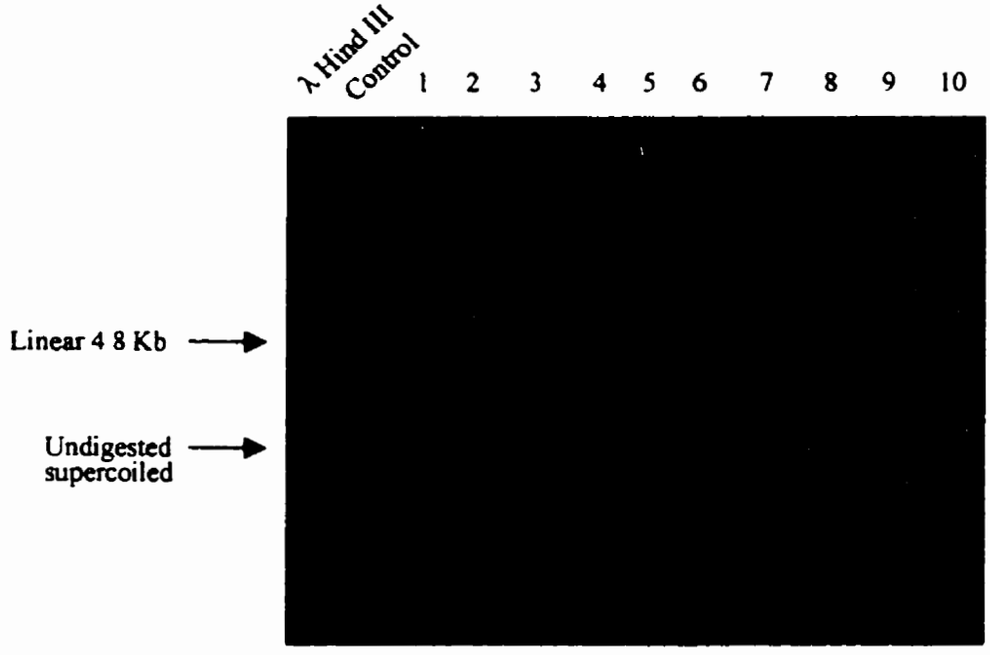

Figure IV-11 Identification of soluble expressing pComb3 clones positive for the acquisition of a histidine tail, using restriction digest analysis.- This figure represents the primary secreening of bacterial clones transformed with a soluble expressing pComb3 vector which may have acquired a histidine tail, using restriction enzyme digest analysis. Plasmid minipreps were subjected to Spe1 digestion and resolved on an 1 % agarose gel. As seen in the photographed gel, only three out of the ten clones were found positive for histidine tail acquisition. Indeed, clones 4, 9 and 10 all migrated as a linear band, with the same size as the soluble espression vector shown in lane A, which corresponded to a 4.8 Kb band.

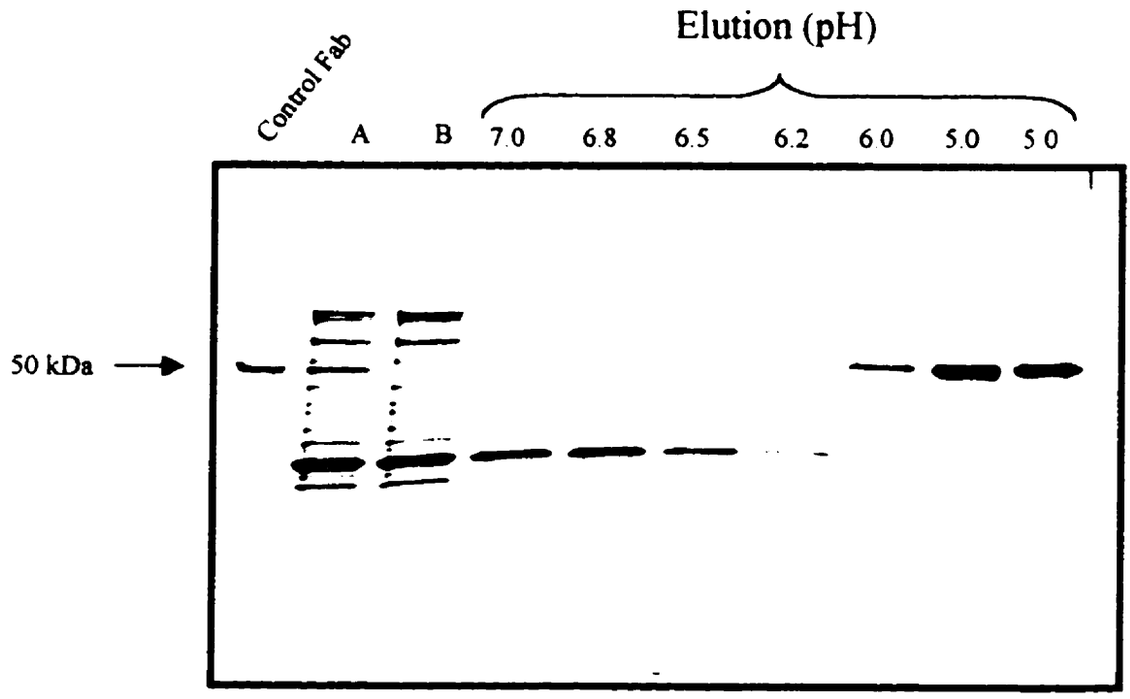

Figure IV-12 Elution profile of rFabs purified on an nickel affinity chromatography column.- This figure illustrates a typical elution profile of a soluble rFab expressed with a histidine tail purified on a nickel affinity column, resolved on a 12% SDS PAGE and stained with coomasie blue. Lane A represents 2 μg of pure Fab generated by digesting IgG with papain, which was used as a visual control. Lane B corresponds to 10 μl of a periplasmic extract, whereas lane 3 represents the same volume of the extract following a single pass over the nickel affinity chromatography column. Lanes 4 through 10 represent the washing and finally the elution of the bound rFab, using a discontinuous pH gradient of a 100 mM citrate / phosphate buffer, starting with a pH of 7.0 and ending with pH 5.0. Exact pH values are indicated.

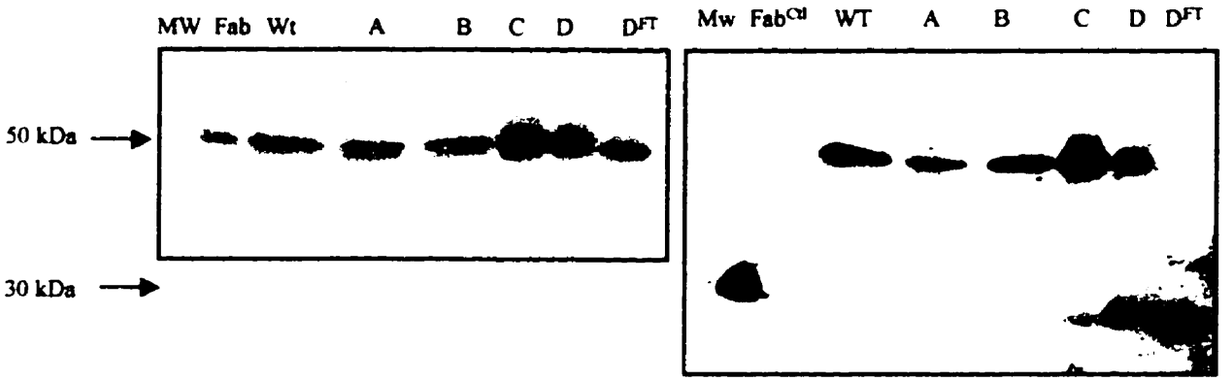

Figure IV-13 Western blot detection of purified rFab preparations.- This figure represents an identical SDS PAGE western bot, consisting of various rFab preparations which was detected in using a radiolabled anti mouse kappa mAb shown in the left panel, and in the right panel with a nickel reagent linked to the enzyme HRP. The first lane of the blot corresponds to a molecular weight marker which contained the 30 kDa protein bovine carbonic anhydrase which reacted with the nickel reagent. Lane 2 corresponded to 200 ng of pure Fab, which was only revealed with the radiolabled anti kappa mAb as expected. Lanes 3 through 7 corresponded to purified; wild type, CDR2.A, B, C and D recombinant Fabs. Lane 8 represents periplasmic extracts consisting of the CDR2.D rFab which had been passed over the nickel affinity chromatography column.

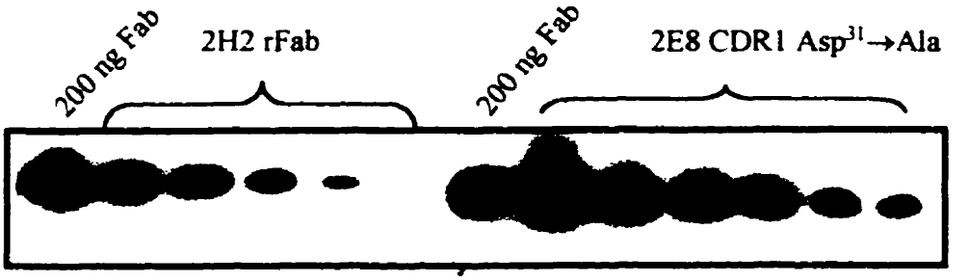

Figure IV-14 Titration of soluble rFab preparations for quantification purposes.- This figure represents an autoradiogram of two rFab preparations, 2H2 and the 2E8 CDR1 $Asp^{31}\rightarrow$Ala mutant, which were purifed using nickel affinity chromatography. Both preparations were evaluated for antibody concentration on a 12 % SDS PAGE western blot as serial dilutions, and detected with a radioablled anti-mouse light chain mAb. Visual estimation of a known amount of papain generated Fab run alongside the rFabs thus provided a rough estimate as to their concentration.

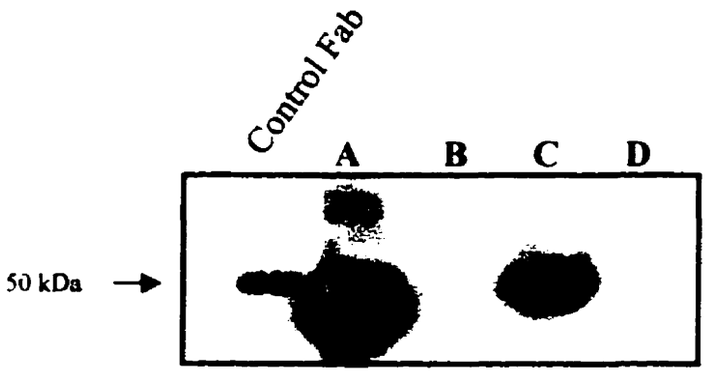

Figure IV-15 The effect of sucrose on rFab production.- This figure represents an autoradiogram of an SDS-PAGE Western blot, detected with a radiolabled anti-mouse kappa mAb. The first lane consists of 250 ng of pure hybridoma Fab. Lanes A and C correspond to 50 µl periplasmic extracts of a 2E8 wild type and a 2H2 rFab bacterial culture respectively, induced with IPTG. Lanes B and C correspond to cultures identical to A and B, but which were supplemented with 0.4 M sucrose during the induction period. The autoradiogram was overexposed to emphasize the absence of antibody protein from both cultures supplemented with sucrose.

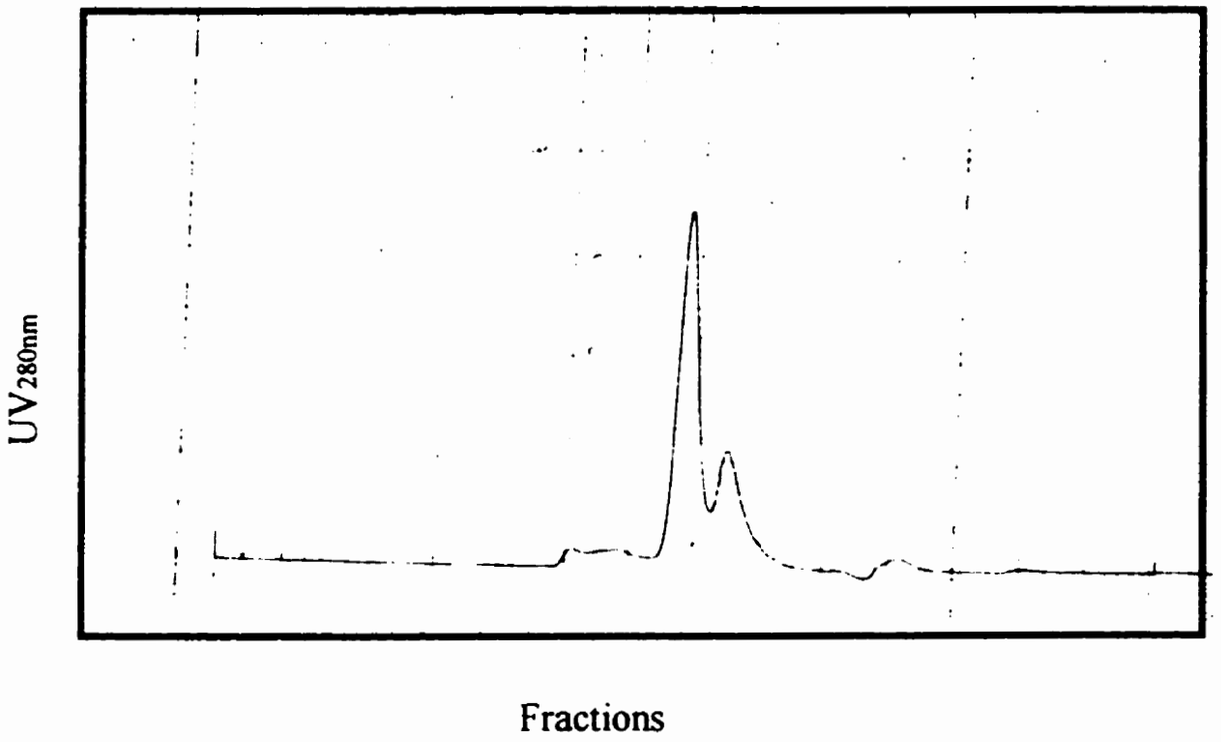

Figure IV-16a Purification profile of a rFab using FPLC gel filtration chromatography.- This figure represents the results obtained from a typical rFab purified using FPLC gel filtration chromatography. 250 µl of a rFab preparation, purified from a nickel chromatography column and concentrated using ultrafiltration, was injected onto a Superdex-75 FPLC column, which was run at a flow rate of 0.5 ml/minute in PBS buffer. The profile shows the separation of the monomeric form of the rFab, which appears as a single large and sharp peak, from aggregated material, which eluted immediately before the monomer and appeared as a broad peak. Following the elution of the monomeric rFab, was the appearance of a second sharp peak, which represented the 25 kDa bacterial protein which on occasion, co-purified with the rFab on the nickel-affinity column.

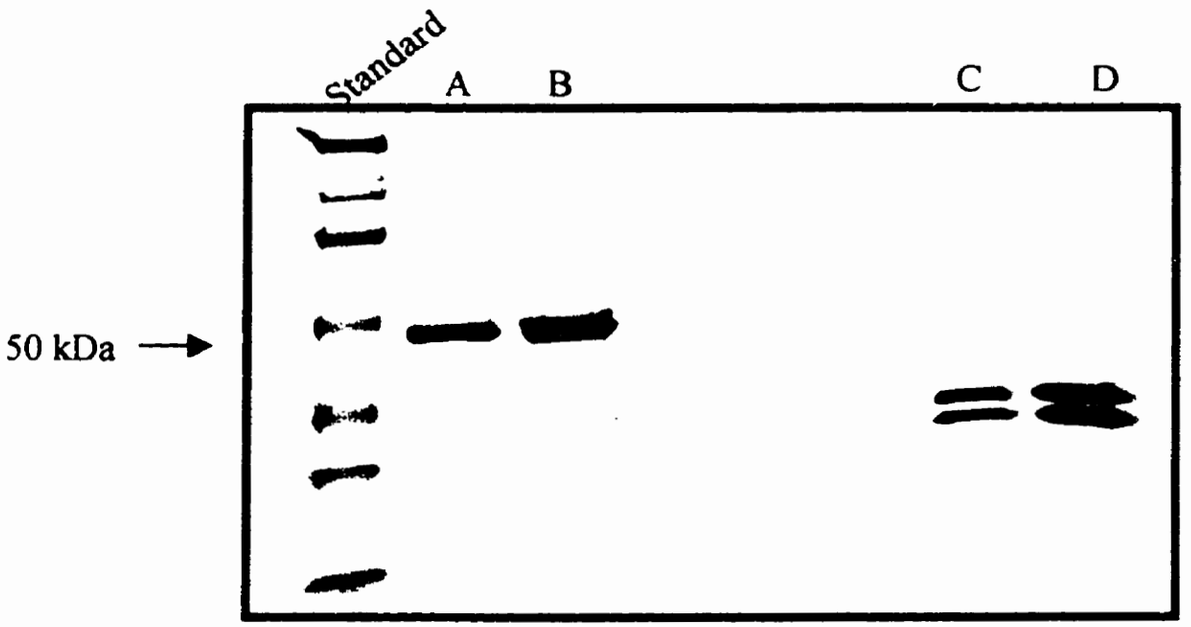

Figure 16b. FPLC purified recombinant Fab compared to hybridoma Fab.- This figure illustrates the purity and integrity of recombinant Fab preparations run through an FPLC size exclusion chromatography column, when resolved on a 12 % SDS-PAGE and stained with coomassie blue. Lanes A and B represent pure hybridoma Fab and recombinant Fab respectedly, which co-migrate with an apparent molecular weight of 50 kDa. Lane C and D represent the same material as in A and D, but run under reducing conditions, resulting in the separation of the light and heavy chains.

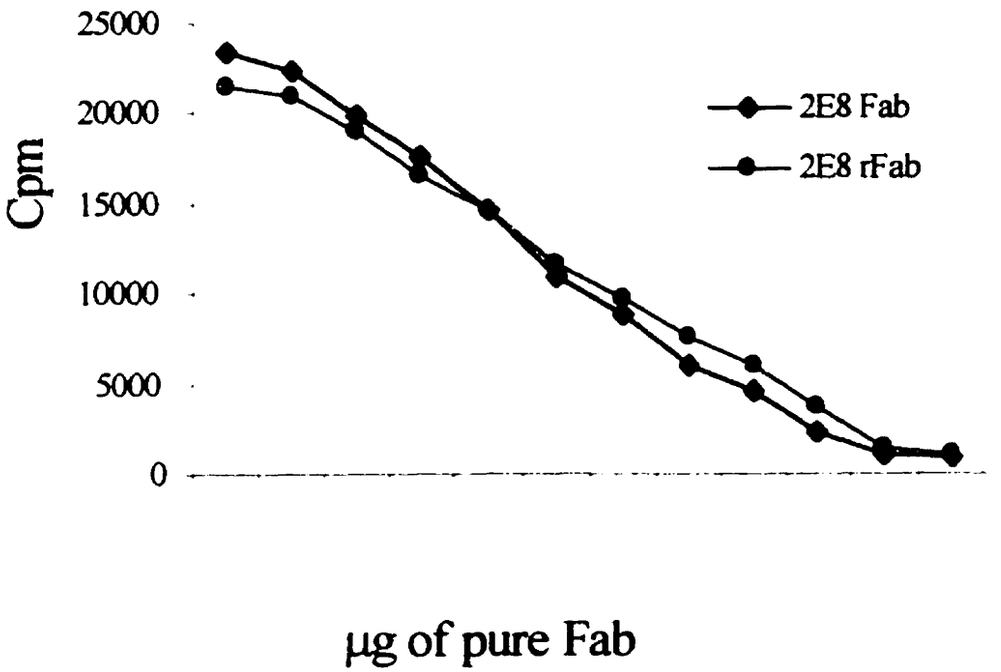

Figure IV-17 Relative immunoreactivity of pure r2E8 Fab vs hybridoma Fab against pure apoE.- This figure illustrates the binding abilities of equal amounts of the 2E8 rFab vs the parental hybridoma Fab against pure apoE. The assay consisted of a solid phase radio-immuoassay, with pure apoE coated onto microtiter wells at a concentration of 2µg/ml. Bound Fab was detected using radiolablled rabbit anti mouse kappa mAbs.

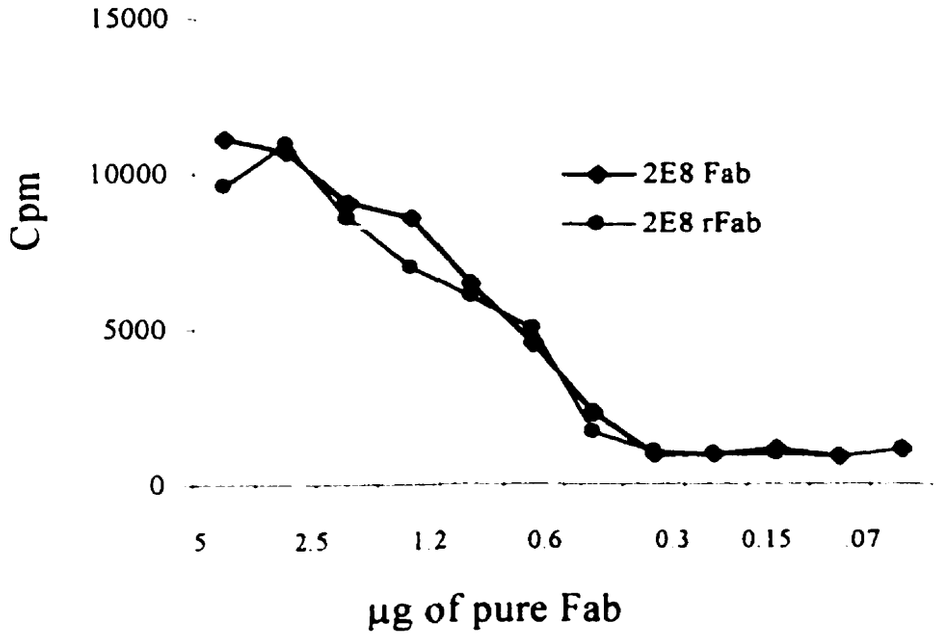

Figure IV-18 Relative immunoreactivity of pure r2E8 Fab vs hybridoma Fab against human VLDL.- This figure illustrates the binding abilities of equal amounts of the 2E8 rFab vs the parental hybridoma Fab against pure apoE. The assay consisted of a solid phase radio-immuoassay, with isolated human VLDL coated onto microtiter wells at a concentration of 30 µg/ml. Bound Fab was detected using radiolablled rabbit anti mouse kappa mAbs.

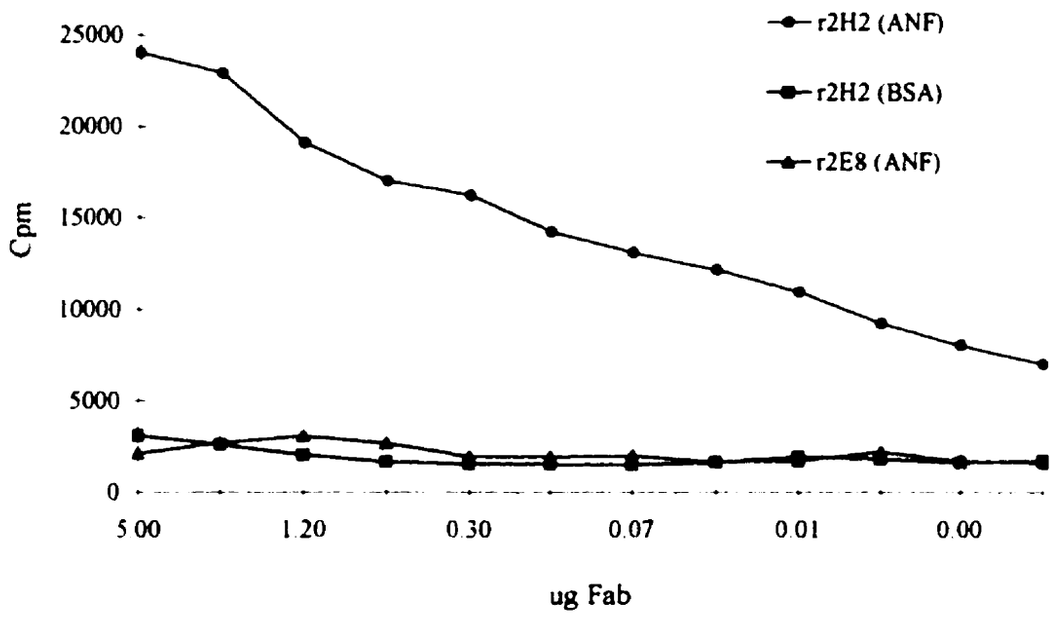

Figure IV-19 Relative immunoreactivity of recombinant 2H2 against rat ANF.- This figure depicts the antigen-binding activity of recombinant 2H2 Fab. The red curve shows binding of 2H2 against rat ANF coated at 1 ug/ml, whereas the blue curve shows its activity against control, bovine serum albumin coated well. The brown curve represents the binding of the 2E8 CDR2.A mutant Fab against rat ANF. In all cases, the amount of rFab in the first well was 5ug, and all were revealed by a radiolabled rabbit anti-mouse kappa antibodies.

Bacterial strain	IPTG	Sucrose	Yield of soluble Fab (mg/L of culture)			
	mM	0.4 M	Periplasm	STE	Medium	Total
XL1-Blue	0	no	0 - 0.1	–	–	< 0.1
	0	yes	0 - 0.1	–	–	< 0.1
	.1	no	0.2 - 0.5	< 0.1	–	0.2 - 0.6
	.1	yes	< 0.1	–	–	< 0.1
	1	no	0.4 - 0.8	< 0.1	< 0.05	< 2.0
	1	yes	0.1 - 0.4	< 0.05	< 0.05	< 1.0

Table IV.1 Production levels of soluble 2E8 recombinant Fab fragments in *E.coli* under different conditions of growth and induction.- For all experiments, induction was performed at room temperature. The results depicted in the table reflect the expression of the wild type 2E8 Fab in the pComb3 construct using the XL1-Blue *E.coli* bacterial strain. The quantitative mesurments of recombinant antibody in each preparation, was performed by comparing the signals obtained on a western blot detected with radiolabled anti-kappa mAb. In all cases, a standard amount of hybridoma generated Fab was used for comparion.

Bacterial strain	IPTG	Sucrose	Yield of soluble Fab (mg/L of culture)			
	mM	0.4 M	Periplasm	STE	Medium	Total
TG1						
	0	no	0 - 0.1	--	--	< 0.1
	0	yes	0 - 0.1	--	--	< 0.1
	.1	no	1 - 5	< 0.8	< 0.5	< 6
	.1	yes	< 1	< 0.1	< 0,5	< 1
	1	no	2 - 8	< 0.8	< 0,5	2 -10
	1	yes	0.5 -2	< 0.05	< 0,05	< 3

Table IV.2 Production levels of soluble 2E8 recombinant Fab fragments in *E.coli* under different conditions of growth and induction.- For all experiments, induction was performed at room temperature. The results depicted in the table reflect the expression of the wild type 2E8 Fab in the pComb3 construct using the TG1 *E.coli* bacterial strain. The quantitative mesurments of recombinant antibody in each preparation, was performed by comparing the signals obtained on a western blot detected with radiolabled anti-kappa mAb. In all cases, a standard amount of hybridoma generated Fab was used for comparion.

Chapter V

The mutational analysis of monoclonal antibody 2E8

Summary

This chapter is a preliminary analysis of the functional paratope of mAb 2E8. To this end, I have made use of three mutational approaches to alter residues within the heavy chain CDRs. Initially, I altered the primary structure of the heavy chain CDR2, to increase its resemblance to either cysteine-rich repeat 5, or to the consensus sequence for the seven repeats of the ligand-binding domain of the LDLr. When a single acidic residue was added to the heavy chain CDR2, thereby increasing its resemblance to repeat 5, there was a two-fold increase in its affinity for apoE compared to the wild type Fab. When the heavy chain CDR2 was made to resemble the consensus sequence of the LDLr, the rFab displayed a preference for lipid-bound apoE, and gained cross-reactivity towards apoB. The functional consequences of these alterations would be consistent with 2E8 being an antibody mimetic of the LDLr. The second mutational strategy was designed to assess the electrostatic component of the immune complex, through the use of "charged

to alanine" scanning mutagenesis. Preliminary results emerging from this analysis, support the notion of an electrostatic component for the associated complex. One variant, in which an acidic residue of CDR1 was replaced with an alanine, acquired the ability to bind to human apoE2, a property that is not possessed by the parental antibody. Thus, the side chain of the targeted residue may dictate the isoform-specificity of the 2E8 mAb. Lastly, to further identify residues that are necessary for antigen binding and to generate new variants with altered binding characteristics, the nucleotides that encode the residues of heavy chain CDR2 were randomized by PCR mutagenesis. The pool of cDNAs that encode the variant 2E8 Fabs were used to construct a phage display library. Clones that retain high binding affinity for apoE3 will be characterized and the library will be screened for 2E8 variants that have novel binding properties.

Objectives

The experiments described in this chapter were designed with two major objectives. The first was to alter the fine specificity of the anti-apoE mAb, 2E8, so that it is identical to that of the LDLr, i.e. convert 2E8 into an antibody mimetic of the LDLr. More specifically, I wished to test the hypothesis that, by modifying the primary structure of the second CDR of the 2E8 heavy chain so that it would show greater homology to the cysteine-rich repeats of the ligand-binding domain of the LDLr, the fine specificity of the antibody would also be altered to more closely mimic that of the LDL receptor. The

second objective was to identify the residues within the CDRs of the 2E8 mAb that are directly implicated in binding antigen. Specifically, I wanted to test the hypothesis that the acidic residues within the heavy chain CDRs were important for binding to apoE, possibly through electrostatic interactions with basic residues within the apoE LDL receptor-binding site.

Introduction

As was described in Chapter I, the specificity of an antibody is dictated by the amino acids that compose its CDRs as well as by certain adjacent framework residues. The repertoire of antibody specificities that is expressed by an individual is in part encoded in the germline and in part generated during the VDJ rearrangement at the immunoglobulin loci. Moreover, during an immune response, a somatic hypermutation mechanism is activated in proliferating B cells that introduces mutations into the sequences encoding the variable regions of rearranged immunoglobulin genes. The amino acid substitutions that result from this latter process are responsible for the affinity maturation that characterizes a secondary immune response and can greatly influence both the affinity and specificity of antibodies. As was also described in Chapter I, many investigators have used *in vitro* mutagenesis of CDRs to modify the binding characteristics of antibodies. In some cases the mutagenesis and selection strategies are analogous to the mechanisms that operate during an immune response.

Random or site-specific mutagenesis methodologies can be used to alter amino acids found within antibody CDRs. The choice of the mutagenic methodology will often reflect the prior understanding of the structure of the immune complex. The specific and random approaches to altering antibody specificity bear some analogy to rational and combinatorial approaches to drug discovery, respectively. When structural data is not available, a random approach is often taken. Mutations can be introduced by error-prone PCR, by passage of the plasmid in mutagenic bacteria or by oligonucleotide-directed mutagenesis using spiked oligonucleotides. Given the importance of heavy chain CDR3 in immune complexes, it is often the initial target of random oligonucleotide-directed mutagenesis, followed by the other CDRs. In the extreme case, the heavy chain CDR3 can be totally randomized to generate a random single-chain Fv CDR3 'single-pot' phage display library, from which antibody clones reactive to many different antigens can be isolated (Nissim *et al.* 1994).

When the atomic structure of an antibody-antigen complex is known or can be predicted using computer-assisted molecular modeling, one can rationally target specific residues within the antibody for substitution in order to test their role in determining the binding characteristics of the antibody (Vakser and Aflalo, 1994). In some cases, analysis of the primary structure of the CDRs may suggest the possible involvement of a particular CDR or particular residues within a CDR in antigen binding. For example, charged residues within the CDRs may mediate binding through electrostatic interactions with complementarily charged residues of the epitope. (Novotny and Sharp,1992; McCoy *et al.* 1997). In addition, specific motifs within the CDRs may be identified as

being potentially implicated in binding. An Arg-Gly-Asp (RGD) triplet is present in the respective heavy chain CDR3s of three anti-platelet fibrinogen receptor antibodies (Taub *et al.* 1989, Barbas *et al.* 1993). The RGD triplet is also present in fibrinogen and forms part of the epitope on fibrinogen that is recognized by the receptor. Thus, the antibodies were predicted to mimic fibrinogen in their mechanism of binding to the fibrinogen receptor. Mutagenesis experiments subsequently confirmed the importance of the RGD sequence in the antibody's binding to antigen.

In Chapter II, I propose that 2E8 binds to apoE through electrostatic interactions between acidic residues within the heavy chain CDRs and basic residues within the epitope. Moreover, as I have noted similarities between the heavy chain CDR2 of 2E8 and the ligand-binding domain of the LDL receptor, I have proposed that 2E8 and the LDL receptor may bind apoE in a similar fashion. In this Chapter, I describe the binding characteristics of a series of 2E8 variants whose heavy chain CDR2 has been modified in order to enhance its resemblance to either the consensus sequence repeat or repeat five of the ligand binding domain of the LDLr. In order to evaluate the electrostatic component of the apoE / 2E8 interaction, I have used a systematic "charged-to-alanine-scanning" strategy to substitute alanines for acidic residues present in the 2E8 heavy chain CDRs. Finally, in order to further examine the relevance of the heavy chain CDR2 in the immune complex beyond its electrostatic component, a CDR2 random library was generated, which can be screened for functional activity using a bacterial phage display system. The long term goal of these studies is to produce an antibody mimetic of the LDL receptor.

Methods

1. **Site-directed mutagenesis.-** The mAb 2E8 heavy chain CDRs 1, 2 and 3 were mutated using splice overlap extension (SOE) PCR (Higushi *et al.* 1988). This methodology consists of PCR amplifying the entire gene of interest using two separate overlapping PCR fragments, previously amplified with appropriate mutant oligonucleotide primers. In the procedure, two complementary "mutant" oligonucleotides, designed to create the desired alteration, are both used in conjunction with primers specific to the heavy chain cloned in the expression vector. As depicted in Figure 1, a 3' mutant primer specific for the upper coding strand, called "**lower primer**", is used with a 5' primer specific for vector DNA called "**milne 23**". The product of this PCR reaction generates a 700 bp fragment which will have an Xho1 restriction site as well as a mutated 3' end. A second mutant primer, specific for the non coding strand, or "**upper primer**", is used in conjunction with an oligonuleotide specific for a sequence of the 3' end of the heavy chain constant region called "**milne 5**" which has an Spe1 site, and which was used in the PCR cloning of all heavy chains described in Chapter II. The successful amplification of this product will generate a 600 base pair fragment, mutant at the 5' end, and which will contain the Spe1 endonuclease site.

The design of all site-directed mutagenic primers was made to minimize the number of mismatched base pairs, through the use of codon degeneracy. In all cases, twelve nucleotides corresponding to the correct antibody sequence, the sequence targetted for mutagenesis. Furthermore, the 3' end of all PCR designed oligonucleotides

were engineered to terminate with either a cytosine or guanosine, which would favor a more tightly annealed primer-template hybrid, and thus generate a better substrate for PCR extension. Typically, the primers were used at a concentration of 0.4 μM in the PCR reaction mixtures. Vent DNA Polymerase (New England Biolabs) was used for PCR to minimize misincorporation of nucleotides as well as the non-templated addition of nucleotides at the 3' end of PCR products. The PCR protocol was identical for the generation of all site-directed fragments, and has previously been described in the methods section of Chapter II. Conditions for PCR were optimized in preliminary experiments using a Stratagene Robocycler.

Following the successful amplification of both antibody fragments, the same experimental conditions were applied in a larger preparative volume, typically of 500 μl. As described in the methods section in Chapter II, the fragments were purified using agarose gel electrophoresis as shown in Figure V-2. The purified altered PCR products were in their turn used in a second round of PCR amplification. In this case, the fragments served as template, due to their homologous mutant site which upon denaturation, hybridized and formed a splice overlap extention variant or "SOE" which was extended in the first round of polymerization, as shown schematically in Figure V-1. The subsequent rounds of PCR, initiated with the 5' primer of the upstream fragment and the 3' primer of the downstream fragment, served to generate large quantities of this product, which consequently, yielded a full length heavy chain variant that included the desired mutations. The DNA was ethanol precipitated and digested with the endonucleases Spe I and Xho I. The digested material was resolved on a 1% agarose

gel, and the appropriate 700 bp fragment isolated as shown in Figure V-3. This purified mutant DNA was finally subcloned into the pComb3-histidine expression vector digested with SpeI / XhoI.

2. Random mutagenesis of the 2E8 heavy chain CDR2.- The method used to randomize the second hypervariable region of the 2E8 mAb, was similar to that of the site-specific mutagenesis described above. In this case however, two quite long mutagenic oligonucleotides were used in concert with the previously described 5'-pComb3 expression vector specific oligonucleotide "**milne 23**" and the heavy chain 3'-specific oligonucleotide "**milne 5**", complementary primers. All nucleotides encoding the heavy chain CDR2 (codons 49 to 65) were subjected to limited, random mutagenesis with the exception the codons corresponding to Pro^{52a} and Gly^{54}, which are believed to be essential in the maintainance of the class 2 murine heavy chain CDR2 canonical structure. The oligonucleotides; "**random-CDR2-lower**" and "**random-CDR2-upper**" which both consisted of 81 nucleotides, were constructed to contain five wild type codons on either end of the mutated sequence. The sequences of both primers are shown in Table V-3. Mutagenic oligonucleotides were synthesized to include 11.25% degeneracy at each position that was targeted for mutagenesis. At these positions the oligonucleotide synthesizer was programed to incorporate 85% of the wildtype base and 15% of a mixture of the four nucleotides. Theoretically, when taken in the context of the length of the altered sequence, every single oligo thus synthesized, should posses anywhere from 0 to 4 altered nucleotides, with no bias for a preferred residue. As described above, the mutagenesis was accomplished using SOE PCR. The PCR products

were sublcloned into the pComb3 expression vector for phage display format. The sole variation from the standard PCR protocol, which I found to be essential in order for the amplified products to be created, was a four fold reduction in the primer concentration.

3. Construction of the 2E8 heavy chain CDR2 Random Library.- A phage display library was constructed in order to assess the functional role of the altered CDR2 in the rFabs antigen recognition. The first step involved with the construction of the library, resided in the generation of a large amount of the mutant SOE-PCR product. Subsequently, as described in the section concerning site-directed mutagenesis, the SOE fragment was digested with the endonucleases Spe1 and Xho1. The appropriate gel purified mutant fragments were then isolated and sub-cloned into the pComb3 vector, which had previously been digested with the same endonucleases. The resultant ligations were then transformed into competent XL1-Blue *E.coli* bacteria, and in order to test the ligation efficiencies, were plated onto LB-agar plates supplemented with ampicillin. The actual phage display library consisted of an M-13 helper phage infected and transformed bacterial culture, which was cleared of bacteria and concentrated through PEG precipitation protocols.

4. Isolation of human VLDL and LDL lipoproteins.- Human VLDL and LDL lipoproteins were isolated using ultracentrifugation in defined salt densities. Fresh human plasma was spun at 10 000 x g for an hour, in order to first remove the chylomicrons which were cut away from the remainder of the tube. VLDL were isolated from the remaining plasma, which was then spun at 140 000 x g for 20 hours. The tube

was cut just below the apparent floating lipoproteins, which were thus collected and the remaining plasma was saved for density adjustment. The density of the VLDL-free plasma was then set to 1.02 g/ml, using pure potassium bromide, and was resealed into ultracentrifuge tubes and placed in an appropriate rotor for a second 20 hour spin of 140 000 x g. At the end of the run, the floating IDL's were collected by once again cutting below the apparent lipoprotein flotation line. The density of the IDL-free plasma was then finally set to 1.063 g/ml, using pure potassium bromide, and again it was resealed into ultracentrifuge tubes and placed in an appropriate rotor for a third 20 hour spin of 140 000 x g. At the end of this final spin, the LDL were collected by once again cutting below the apparent lipoprotein flotation line. Fresh human plasma lipoproteins were always immediately dialyzed at 4 ^{0}C, against PBS set at pH 7.4 which contained 0.1 % sodium azide to prevent the growth of microorganism. Following extensive dialysis, the lipoproteins were supplemented with 0.01 M EDTA to minimize oxidation caused by metal ions, and were stored at 4 ^{0}C for up to two months. Protein concentration was determined by the method of Lowry.

5. Reductive methylation of isolated human lipoproteins.- Isolated plasma lipoproteins, both VLDL as well as LDL, were reductively methylated in order to modify exposed lysine residues of the apolipoproteins. Briefly, a 1 ml suspension of plasma lipoprotein (1 to 2 mg of apolipoprotein), was dialyzed overnight against 0.1 M sodium borate, pH 8.0. The following day, 50 µl of a freshly prepared 40 mg / ml solution of $NaBH_4$ was added to the dialyzed lipoprotein suspension. The methylation reaction was started by the addition of 1µl of a 38% aqueous solution of formaldehyde. Over the next

30 minutes, an additional 1 µl of 38 % formaldehyde was added every five minutes. Following the first 30 minute incubation period, 50 µl of the $NaBH_4$ solution was again added, followed by the repeated addition of formaldehyde at the five minute intervals, for an additional 30 minutes. The reaction was ended by extensively dialyzing the lipoproteins against PBS set at pH 8.0 at 4 °C.

6. **Preparation of apoE-free LDL using affinity chromatography.-** In order to prepare apoE-free LDL lipoproteins, an affinity chromatography column was generated using cyanogen bromide (CNBr) activated sepharose (Pharmacia) coupled to a panel of four mouse mAbs specific for apoE. Briefly, 1.5 g of the dry CNBr-sepharose was hydrated in water and activated by soaking in a 30 ml volume of 0.01 M HCL for one hour. The resin was then extensively rinsed with water and incubated overnight at 4°C with a 6 mg mixture of the four mAbs; 1D7, 2E8, 3H1 and 6C5 in 0.1 M sodium bicarbonate, pH 8.0. The coupling efficiency was estimated from the absorbance of the supernatant at 280 nm. The remaining active sites of the resin were then blocked by incubating the resin by incubation with 0.5 M ethanolamine for 2 hours. The resin was then extensively washed in PBS pH 8.0, and packed into a small chromatography column. The column was subjected to three cycles of washes, each wash consisting of three column volumes of a 0.01 M HCl solution adjusted to pH 2.0, and a rinsed with five column volumes of a PBS buffer at pH 8.0, in order to remove any noncovalently-bound IgG. Typically, 3 mg of human LDL was applied to the anti-apoE affinity column and eluted in PBS by gravity. Fractions were monitored at 280 nm and the LDL peak was pooled and stored at 4°C. The column was regenerated with 0.01 M HCl and neutralized

with PBS and stored at 4°C. The effectiveness of the anti-apoE affinity column at depleting apoE-containing LDL from a total LDL preparation is shown in Figures V-7. The figure depicts an SDS PAGE western blot of 20 μg of crude LDL run along side of 20 μg of an apoE-depleted LDL preparation, detected with mAb 6C5. Finally, as shown in Figure V-8, apoE-depleated LDL preparations were subjected to a solid phase radio-immunoassay and compared to starting LDL for apoE content, using the mAb 6C5 as a detection probe.

7. Determination of the binding affinity of the altered 2E8 rFabs using a solid phase radio-immunoassay.- The antigen binding capability of the rFabs were tested against various isoforms of human apoE, as well as against isolated plasma lipoproteins. In all cases, the relative immunoreactivities of the rFabs were determined using a solid phase radio-immunoassay, with the antigen immobilized to plastic microtiter wells. The antigens consisted of the purified recombinant human apoE3, apoE2, apoE2$^{Arg154 \rightarrow Ala}$, which were coated at a concentration of 2 μg/ml. In addition, human VLDL, LDL, apoE-depleted LDL, and finally reductively methylated VLDL, were also used as antigens, and were coated at a concentration of 30 μg/ml. In all cases, antigen coating was performed overnight at 4 °C, in a 5 mM glycine solution adjusted to pH 9.0. Immediately before the assay, the wells were washed with PBS pH 8.0 and blocked with 200 μl of a 1 % PBS-BSA solution for 2 hours. The rFabs were then added in serial dilutions performed in 100μl of the 1% PBS-BSA solution, and left to incubate at 4 °C overnight. The following morning, the wells were rinsed four times with PBS pH 8.0, and then filled

with 100 µl of 1% PBS-BSA containing 100,000 cpm of a ^{125}I-affinity-purified rabbit anti-mouse kappa light chain antibody, and left to incubate at room temperature overnight. The following morning, the wells were washed three times with PBS pH 8.0, and the bound radioactive material was determined using a gamma counter. The counts were plotted directly as a function of rFab mass, and the curve taken as a indication of the relative immunoreactivity of the rFab for the coated antigen.

8. Determination of the binding affinity of the recombinant 2E8 rFab as well as the CDR2.A rFab, using surface plasmon resonance.- Surface plasmon resonance was used to determine the affinity constant of the recombinant wild type 2E8 rFab as well as the heavy chain CDR2 structural mutant CDR.A, for human apoE3. This methodology has been previously described in the methodology section of Chapter II. Briefly, pure apoE3 was chemically cross-linked to the surface of a research-grade sensor chip (Pharmacia), using the coupling solutions provided by the manufacturer. The integrity of the apoE3 surface was assessed by passing a pulse of purified 1D7, 2E8 and 3H1 mAbs, and regenerating the surface with a 100 mM HCl wash. Upon confirmation concerning the integrity of the apoE3 surface, a set of 9 different concentrations of the rFabs freshly purified using FPLC, ranging from 0.2 µM to 8 µM were subjected to the surface, and the binding data collected and plotted as sensorgrams. Following the end of data collection, a pulse of either 2E8 and 1D7 IgG were again passed over the apoE3 surface in order to assess the integrity of the antigenic surface. The binding constants of the rFabs were determined through the curve fitting equations supplied by the manufacturer.

Results

1. Alteration of the 2E8 heavy chain CDR2 with structural perspectives.- As shown in Figure V-4, the CDR2 of the heavy chain was modified in order to increase its structural resemblence to the cysteine-rich repeats that compose the ligand-binding domain of the LDLr. The alterations were based both on the sequence of repeat five, which appears to be critical for apoE-mediated binding of lipoproteins by the LDLr, and on the consensus sequence of all of the cysteine-rich repeats of the LDLr. Four 2E8 variants; 2E8 CDR2.A, B, C, and D, containing amino acid substitutions in heavy chain CDR2 were produced through splice overlap PCR (SOE PCR) using the mutagenic oligonucleotides described in Table V-1. The amplified products were subsequently confirmed through DNA sequencing as shown in Figure V-5. The CDR2.A mutant was engineered to resemble repeat five of the LDLr, by replacing Thr^{57} with glutamic acid. This modification resulted in the creation of the "Asp-Glu-Glu" sequence, a triad of acidic residues which is a distinguishing feature of LDLr repeat five. Mutant CDR2.B was engineered to further improve the structural resemblence of mutant CDR2 A to repeat five, by $Glu^{53} \rightarrow$Asp, $Ile^{54} \rightarrow$Lys, $Gly^{55} \rightarrow$Ser substitutions in addition to the $Thr^{57} \rightarrow$Glu alteration. The presence of Ser^{55} was of special interest, as all of the seven cysteine-rich repeats of the LDLr ligand-binding domain possess the "Ser-Asp-Glu" motif. As described in Chapter I, these residues have been proposed to be directly implicated in binding to the ligand or to form a Ca^{+2}-binding site. As will be discussed below, however, replacement of Gly^{55} of 2E8 could potentially disrupt the backbone

conformation of CDR2. Finally, mutants CDR2.C and CDR2.D were constructed to progressively transform the heavy chain CDR2 into one that would structurally resemble the consensus sequence of the LDLr ligand-binding domain. Mutant CDR2.C was altered to resemble mutant CDR2.B, with the exception of Glu^{58} which was converted to an alanine. This alteration eliminated the characteristic tri-acidic amino acid repeat that characterizes LDLr repeat five. Mutant CDR2.C did retain the potentially deleterious serine at postition 55 as described above for mutant CDR2.B. Mutant CDR2.D was simply a variant of mutant CDR2.C, but with a additional $Lys^{54} \rightarrow$Gly substitution. This alteration both increased the resemblance of the CDR2 and the LDLr consensus sequence and, as will be described below, introduced a residue that was compatible with the mouse heavy chain class 2 canonical structure. Thus, CDR2.D shows homology with the consensus sequence of the LDLr ligand-binding domain over five consecutive amino acids and is compatible with the CDR2 canonical structure.

2. "Charged-to-Alanine" mutational analysis of the heavy chain CDR1, CDR2 and CDR3 with functional perspectives.- In order to investigate the importance of electrostatic and possibly ionic interactions which may contribute to the energetic forces within the immune complex formed between the heavy chain of 2E8 and apoE, a second mutagenic approach was undertaken. By SOE PCR, acidic residues of the 2E8 heavy chain CDRs were converted to alanine or, in one case, to a valine residue (Figure V-6). Thus, recombinant 2E8 Fab clones were generated to code for mutants: $Asp^{31} \rightarrow$Ala, $Asp^{97} \rightarrow$Ala, $Asp^{99} \rightarrow$Ala. The mutants; $Asp^{52} \rightarrow$Ala, $Glu^{53} \rightarrow$Val, $Asp^{56} \rightarrow$Ala and

$Glu^{58}Ala$, were identified through the limited screening of the 2E8 heavy chain CDR2 random library as shown in Figure V-6, and described in Table V-4.

3. Generation of a random 2E8 heavy chain CDR2 library.- In order to investigate the relevance of all residues within CDR2 of the heavy chain in apoE recognition, and to potentially generate novel rFabs with interesting binding capabilities, CDR2 was mutagenized using SOE PCR with primers having 11.25% degeneracy at targeted positions. The two degenerate oligonucleotides which served in the radomization of CDR2 are depicted in Table V-3. As described earlier, the primers allowed for every nucleotide encoding CDR2 to be randomized, with the exception of those that encoded the residues at positions 52a and 55 that are thought to be important in maintaining the conformation of the loop. Following the successful amplification and cloning of the randomized fragment, the library was sampled on a small scale, by sequencing 48 individually transformed *E.coli* clones. Results are depicted in Tables V-4 and V-5. Of a total of 43 isolated clones, and although most had at lest one altered nucleotide, 23 % had nucleotide alterations which led to no altered codon. Furthermore, 33 % of the clones had one altered codon, 23 % resulted in two altered codons, whereas 5 and 2 % of the clones had three and four altered codons respectedly. Finally, 14 % of the clones resulted in nonfunctional antibodies, as a stop codon was generated.

4. Assessment of the antigen-binding capabilities of the altered 2E8 heavy chain CDR2 "structural mutants" through solid phase radio-immunoassay. In order to determine the functional alterations imparted to the 2E8 antibody through the

modifications made to its heavy chain CDR2, all four structural mutants described in Figure V-3 including the wild type 2E8 rFab, were expressed and purified from *E.coli*. As shown in Figures V-9 through V-16, the antigen-binding capability of the rFabs were tested against various isoforms of human apoE, as well as against isolated human plasma lipoproteins. In all cases, the relative immunoreactivities of the rFabs were determined using equivalent amounts of the Fabs in solid phase radio-immunoassays, with the antigen coated onto plastic microtiter wells, and the bound rFab detected through the use of ^{125}I- anti-mouse kappa mAb. Figure V-9 depicts the relative affinities of the mutants for human apoE3. The CDR2.A Fab was consistently found to display better reactivity compared to the wild type rFab, followed by the CDR2.D Fab. In contrast to these rFabs, the CDR2.B and CDR2.C rFabs were found not to react with apoE3. Figure V-10 shows the reactivities of the rFabs against the LDLr-defective isoform apoE2(Arg^{158} →Cys). Both the wild type r2E8 and the CDR2.A and CDR2.B reacted poorly with apoE2. In contrast the CDR.D rFab showed retactivity with apoE2 and thus partially lost the ability to distinguish between apoE isoforms. The CDR.C Fab failed to react with either apoE2 or apoE3. When the antibodies were tested against apoE2(Asp^{154} →Ala), a recombinant apoE variant that retains reactivity with the LDL receptor in spite of the presence of cysteine at position 158 (see Chapter I), the pattern of reactivities of the 2E8 variants were similar to those seen with apoE2 (Figure V-11). Neither the CDR2.A, the CDR2.B nor CDR2.C rFabs recognized apoE2(Asp^{154} →Ala) whereas the CDR2.D rFAb displayed a reactivity that was as good if not better than that with apoE2. In all cases, the non-specific binding activities of the rFabs were determined in microtiter wells coated with 1% BSA, and were found to be very low.

The rFabs were also tested for their abilities to bind to VLDL that had been isolated from human plasma by equilibrium ultracentrifugation and coated onto microtiter wells at a concentration of 30 μg/ml (Figures V-12). The presence of apoE on the surface of the VLDL was ascertained by the use of the high affinity anti-human apoE mAbs 6C5 and 3H1. The CDR2.D variant was found to possess the best immunoreactivity with VLDL, followed by the CDR2.A and wild type 2E8. While the CDR.B and CDR.C rFabs show little reactivity with VLDL in this experiment, in other experiments some immunoreactivity was observed although it was always less than that observed with wild type r2E8 and the CDR2.A and CDR2.D variants. Hence, all of the rFabs were found to react to human VLDL, with the rFab CDR2.D having the highest activity. Interestingly, none of the rFabs recognized reductively methylated VLDL (data not shown). This suggests that the binding of the recombinant Fabs is specific as neither wildtype 2E8 IgG nor the LDL receptor can bind reductively methylated VLDL. It also confirms the importance of lysine residues in the epitope recognized by 2E8 epitope and the 2E8 variants.

Since the four heavy chain CDR2 "structural variants" were designed to increase their similarity to the ligand-binding domain of the LDL receptor, I have tested each for possible cross-reactivity with the second ligand of the LDL receptor, apoB-100. LDL contain apoB-100 as their predominant apolipoprotein athough they can also contain some apoE. The r2E8 Fab variants were found to bind to freshly isolated LDL in a solid phase radio-immunometric assay (results not shown). This reactivity could be indicative of cross-reactivity with apoB-100 or, more likely, reactivity with apoE that is present in

the LDL. The presence of apoE in the LDL preparations was confrimed by both western blot analysis and by RIA experiments using anti-human apoE specific mAbs (Figures V-7 and V-8). In order to test the anti-apoE rFabs for cross-reactivity with apoB, LDL was depleted of apoE by immunoaffinity chromotography on immobilized anti-apoE mAbs 6C5, 1D7, 3H1 and 2E8 (see Figure II-1 in Chapter II for an epitope map of human apoE). As shown in Figures V-7 and V-8, the fraction that was not retained by the anti-apoE Sepharose column contained immunoreactive apoB but no immunoreactive apoE. When apoE-free LDL was used as an antigen for the rFab mutant antibodies in a solid phase radio-immunometric assay, only mutant CDR2.D showed specific binding (Figure V-13). To obtain further evidence that CDR2.D had acquired binding specificity for apoB, it was tested for reactivity with reconsitituted lipoproteins containing apoB as their sole apolipoprotein. As shown in Figure V-14, CDR2.D rFAb and several anti-apoB mAbs reacted with the reconstituted apoB-containing lipoproteins whereas anti-apoE mAb 6C5 showed no reactivity. Finally, in order to obtain direct evidence that the CDR2.D rFab was binding to the epitope on apoB that includes all or part of the apoB LDLr-receptor-binding site, I tested the rFab against LDL that contains an apoB-100 variant that is not recognized by the LDLr. In this variant, generated by Drs. Jan Borèn and Thomas Innerarity of the Gladstone Institute of Cardiovascular Disease in San Francisco using *in vitro* mutagenesis, the basic amino acids between residues 3357-3367, were replaced by alanine as shown in Figure V-15. In wildtype apoB, this sequence is characterized by an enrichment in arginine and lysine residues and shows some homology to the apoE LDLr-binding site. As shown in Figure V-16, CDR2.D did not discriminate between this LDLr-defective form of LDL and wildtype LDL.

5. Assessment of the antigen-binding capability of the 2E8 heavy chain CDR2 "structural mutants", using surface plasmon resonance.- The technique of surface plasmon resonance was used in order to determine the equilibrium affinity constants of the rFabs for apoE. Pure apoE3, apoE2 as well as apoE2($Asp^{154}\rightarrow Ala$), were immobilized on the sensor chip as described in Chapter II. The immunoreactivity of the immobilized apoE was verified using mAbs 6C5 and 3H1. Examples of the sensorgrams that were obtained using rFabs 2E8 and CDR2.A are shown in Figure V-17 and V-18. Association and dissociation rate constants as well as equilibrium dissociation constants were calculated from the sensorgram data as described in Chapter II. As shown in Figures V-19 and V-20, the equilibrium dissociation constants for apoE3 of wild type rFab and CDR2.A were determined to be 4.3 uM and 2.0 uM, respectively. Of the three other structural mutant Fabs, only CDR2.D was found to display reactivity against apoE3, however, its binding constants could not be accurately determined due to impurities in the rFab preparation. When the rFabs were tested against apoE2, no reactivity could be recorded for any of the antibodies, even at the highest Fab concentrations of 8 uM, for the CDR2.A and wild type rFabs respectively. Finally, when the rFabs were assayed on the apoE2($Asp^{154}\rightarrow Ala$) surface, only the CDR2.D Fab was found to react with the surface (data not shown).

6. Assessment of the antigen-binding capabilities of the 2E8 heavy chain "charged-to-alanine" "Functional Mutants", through solid phase radio-immunoassay.- The relative immunoreactivity of three of the eight 2E8 heavy chain functional mutants; or CDR1 $Asp^{31}\rightarrow Ala$, CDR3 $Asp^{97}\rightarrow Ala$ and $Asp^{99}\rightarrow Ala$, were determined against the

same panel of apoE and lipoprotein antigens as used in the analysis of the heavy chain CDR2 structural mutants. All three mutants were produced and purified in a soluble recombinant form, and tested for antigen recongnition using a solid phase radio-immunometric assay. As shown in Figure V-21, all three rFabs were found to be less reactive with apoE3 when compared to the wild type rFab. However, the CDR1 (Asp^{31}→Ala) mutant was found to be more reactive than either of the two CDR3 mutants, which essentially had comparable reactivities. Interestingly, the Asp^{31}→Ala subsititution resulted in a variant that acquired reactivity with apoE2 (Figure V-22). The relative immunoreactivities of the three alanine mutant and wildtype rFabs were also determined against apoE2(Asp^{154}→Ala). As observed with apoE2 as an antigen, only the CDR1 Asp^{31}→Ala mutant rFab could bind to apoE2(Asp^{154}→Ala) (Figure V-23). The immunoreactivities of these rFabs were then assayed against human lipoproteins consisting of apoE/apoB-100 containing VLDL, apoE-depleted LDL as well as reductively methylated VLDL. As shown in Figure V-24, the immunoreactivity of the CDR1 Asp^{31} →Ala mutant for human VLDL was found to be superior to that of the wild type rFab and the two CDR3 mutants. When reductively methylated VLDL were used as antigen, only the CDR1 Asp^{31} →Ala mutant was found to retain a certain amount of immunoreactivity as compared to either the wild type or the CDR3 mutants, as shown in Figure V-25. When apoE-depleted LDL was used as an antigen, once again, the CDR1 Asp^{31} →Ala rFab was found to react whereas none of the CDR3 variants or the wild-type rFab were found to react, (Figure V-26).

Additional control experiments were performed to confirm that the binding was apolipoprotein-specfic. The rFabs were tested for their ability to bind to immobilized BSA and apoA-I - dimyristoyl phosphotidyl choline (DMPC) complexes. In this experiment, none of the rFabs bound to either BSA or apoA-I-DMPC coated wells (data not shown).

Discussion

The major objectives for the experiments described in this chapter were to use oligonucleotide-directed mutagenesis to define the molecular interactions responsible for the binding of 2E8 to human apoE and to convert 2E8 into a true antibody mimetic of the LDL receptor. I have used two strategies of mutagenesis. In the first approach, I have introduced substitutions into the 2E8 heavy chain CDR2 to increase its homology with the ligand-binding domain of the LDLr. By increasing the homology in primary structure between the 2E8 mAb and the ligand-binding domain of the LDLr, I predicted that the antibody would acquire binding properties that would be identical to those of the LDLr and thus fulfill my working definition of an antibody mimetic of the LDLr. In the second approach, I have replaced specific residues in the 2E8 heavy chain CDRs and have determined the effect of the substitutions on the binding properties of the antibody. A major change in antibody affinity or specificity due to the replacement of a residue would indicate a direct or indirect participation of the residue in binding antigen.

My first experimental strategy was to redesign the heavy chain CDR2 of 2E8 based on its structural homology with cysteine-rich repeat 5 of the LDLr as was described in Chapter II. Four HC CDR2 structural variants of the antibody were thus generated, expressed and purified from *E.coli*, and finally appraised for their antigen-binding properties. In the first mutant, CDR2.A, Thr^{57} was replaced by a glutamic acid, which

generated an acidic triplet in CDR2, "Asp^{56}-Glu^{57}-Glu^{58}". This triplet would correspond to Asp^{206}, Glu^{207}, Glu^{208} of repeat five of the LDLr. The presence of these three consecutive negatively-charged amino acids distinguishes repeat five from the other cysteine-rich repeats that compose the LDLr ligand-binding domain and may be responsible for the critical role for this repeat in apoE-mediated lipoprotein binding (Russell *et al.* 1989). The functional consequence of of the Thr^{57}→Glu substitution was the generation of a rFab 2E8 variant with a two-fold higher affinity for apoE compared to wildtype 2E8 rFab. This enhanced affinity for antigen was displayed regardless of whether apoE was lipid free or present on the surface of VLDL.

The observed increase in affinity displayed by this rFab could be the result of the increased electronegative character of the antibody paratope. This could favor enhanced electrostatic interactions between the antibody and its epitope on apoE whose electropositive character has been established. However, without the solved crystal structure of this rFab, one cannot exclude the possibility that the side chain of Glu^{57} is actually buried within the paratope, and consequently not available for intermolecular association. Moreover, one cannot assume that the increased affinity of the CDR2.A variant is the result of any new direct chemical bonds that have been created in the antigen-antibody complex. In fact, it has been well documented that the creation of a hydrogen bond or a salt bridge, even if weak in character within the interface, causes the association constant to increase by two to three orders of magnitude (Padlan E., 1994). More likely, therefore, the increase in affinity seen with the CDR2.A rFab is a through a more subtle, indirect, effect of the Thr^{57} →Glu substitution. The introduction of an

acidic residue at position 57 may alter the topography of the paratope which could, in addition to providing a favorable electrostatic component, allow for an enhanced complementary fit, and consequently contribute a few supplementary van der Waals interactions to the complex. Such a mechanism could account for the small but significant increase in affinity. It will be interesting to evaluate the binding kinetics of CDR2.A to immobilized apoE using surface plasmon resonance to determine if the increased affinity reflects alterations in the association or dissociation rates.

The two subsequent structural mutants; CDR2.B and CDR2.C, resulted in rFabs which were almost completely devoid of apoE recognition capability. Initially, these results were disappointing as the heavy chain CDR2 alterations resulting in CDR2.B, represented a structural extension of CDR2.A so that its second hypervariable region would have even greater homology with cysteine-rich repeat five of the LDLr. Similarly, the CDR2.C rFab was conceived to resemble the consensus sequence for the ligand-binding domain of the LDLr. The fact that these 2E8 variants had little or no reactivity with apoE could indicate that our experimental approach of modifying the 2E8 CDR2 to resemble the primary structure of ligand-binding domain of the LDLr in order to create an antibody mimetic of the LDLr may not be feasible.

It was, therefore, very signficant that the variant CDR2.D not only retained its binding activity towards apoE but also showed a fine specificity which resembled that of the LDLr. CDR2.D differs from CDR2.C by a single $Lys^{54} \rightarrow$Gly substitution. When the heavy chain variable regions of wildtype 2E8, and the CDR2.B and CDR2.C variants

were submitted to homology modeling using the Swiss Model program and the predicted structure viewed with the RASMOL molecular visualization program, as can be seen in Figure V-27, the substitutions that characterized the variants would not be predicted to have a major influence on the main chain conformation of any of the heavy chain CDRs. Nevertheless, when the requirements in primary structure needed to satisfy the rules relating to the mouse heavy chain class 2 canonical structure are considered, a potential reason for the loss of antigen reactivity by the CDR2.B and CDR2.C mutants becomes apparent. The substitution of Gly^{55} by a serine constitutes a non-allowable replacement of a key residue involved in the maintenance of the "canonical" hydrogen-bonded heavy chain CDR2, class 2, structure (Clothia *et al.* 1989). An alteration in the CDR2 loop conformation by the Gly^{55} →Ser substitution, that may not have been predicted by homology modeling, could have had a deleterious effect on the topography of the paratope. Alterations in the main chain conformation by substitutions of residues that are key in maintaining the canonical structure of CDR2 may also explain the restored reactivity of the CDR2.D variant. As the presence of glycine at either positions 54 or 55 is compatible with the CDR2 class 2 canonical structure, the introduction of a glycine at position 54 in the CDR2.D variant, may have restored a CDR2 loop conformation that permits antigen binding.

A second possibility is that the Ile^{54} →Lys substitution (CDR2.B, CDR2.C), but not the Ile^{54} →Gly (CDR2.D) substitution, prevents antigen binding by a mechanism that is independent of the main chain conformation of the CDR2 loop. In fact, replacement of a hydrophobic isoleucine residue by a positively charged lysine residue could alter

inter-atomic interactions and side chain packing and impose greater steric constraints upon antigen binding than the Ile^{54} →Gly subsitution. Based on homology modeling, using the Swiss Model Program, Lys^{54} is predicted to be solvent-exposed in CDR2.B. As shown in Figure V-28, its side chain could potentially prevent antigen binding by steric inhibition or, given the proximity of its epsilon amino group to the free carboxyl group of Asp^{53}, could possibly participate in an intramolecular salt bridge. Finally the introduction of a positively charged residue into the antigen-binding surface of the antibody would reduce the large patch of electronegative potential that results from the acidic residues, primarily in heavy chain CDR2. This could negatively affect antigen binding if, as I propose in Chapter II, 2E8-apoE complex formation is indeed dominated by electrostatic interactions.

Whatever the mechanism, the Lys^{54} →Gly interchange that differentiates CDR2.D from CDR2.C caused a reversal of phenotype with respect to lipid-free apoE binding. More importantly, however, the sum of substitutions that characterize the CDR2.D variant also resulted in its having acquired several important binding properties that one would attribute to an antibody mimetic of the LDLr that were not a feature of the wildtype 2E8. The apparent increased reactivity of CDR2.D with lipoprotein-associated apoE is consistent with the proposed mimicry between the antibody and the LDLr. It is currently thought that apoE undergoes a structural rearrangement as it associates with lipoproteins (Weisgraber, K.H. 1994) that renders it reactive with the LDLr. I suggest that CDR2.D is specific for this receptor-active form of apoE. The lack of reactivity of CDR2.D with apoA-I - DMPC complexes and the loss of reactivity with VLDL, when

lysine residues of the apolipoprotein were chemically modified, suggests that the binding of CDR2.D to VLDL is apolipoprotein-specific. At the moment, however, I cannot exclude that the preferential binding of CDR2.D to VLDL is not due to its recognition of apoB. I will test this directly by determining the respective binding affinities of CDR2 with lipid-free apoE and with apoE-DMPC complexes.

The second, and perhaps more remarkable, property of CDR2.D is its apparent cross-reactivity with apoB, another characteristic that is shared with the LDLr. As shown in Figures V-13 and V-14, CDR2.D, but not wildtype 2E8, could react with apoE-depleted LDL and with reconstituted LDL that contain apoB as their sole apolipoprotein. While there is no extensive homology in terms of primary structure between apoE and apoB, two short sequences of apoB (residues 3147-3157 and 3359-3367) have been identified that show some similarity to the apoE LDLr-binding site and both have been proposed to participate in apoB-mediated binding to the LDLr (Knott *et al.* 1985, Milne *et al.* 1989). Both sequences are rich in basic amino acids and residues 3359-3367 do show some homology to the apoE LDLr-binding site. I therefore considered the possibility that both CDR2.D and the LDLr may recognize an epitope that is common to both apoE and apoB. In the case of apoB, the most probable candidate sequence would be residues 3359-3367. This similarity between apoB and apoE in terms of primary structure does not, however, appear to be responsible for the apoB-binding property of CDR2.D, as CDR2.D is reactive with LDL that contains an apoB variant in which all the basic residues between 3359-3367 have been replaced by alanine residues (Figure V-15).

Thus, the structural basis for this intriguing property of CDR2.D has not yet been elucidated.

Alteration of the 2E8 CDR2 also caused some notable changes in the isoform specificity of the variants. Both the wildtype rFab as well as the CDR2.A mutant were found to be unreactive with apoE2 as well with the LDLr-competent mutant, apoE2(Asp^{154} →Ala). These results were not surprising as the wildtype 2E8 hybridoma-derived Fab is also unreactive with both forms of the protein. The CDR2.D rFab, on the other hand, reacted with the apoE2(Asp^{154} →Ala) variant when assayed by both a solid phase radio-immunometric assay and by surface plasmon resonance. CDR2.D also showed some reactivity with apoE2 in the radio-immunometric assay although this was not observed when binding was monitored by surface plasmon resonance. The antibody's gain of function towards the LDLr-competent form of apoE is remarkable, in that it directly implicates the alterations in the heavy chain CDR2 for this activity, and would further support the contention that CDR2.D represents an antibody mimetic of the LDLr.

It is interesting to compare the functional consequences of modification of the 2E8 CDR2 to those that result from modification of the ligand-binding domain of the LDLr. It has been shown that substitution of conserved residues or deletion of cysteine-rich repeat five of the LDLr impairs both apoB- and apoE-mediated binding (Esser *et al.* 1988). In contrast, modification or deletion of repeats two, three, four, six or seven

affects only apoB-mediated binding. One interpretation of these results is that repeat five is responsible for apoE-mediated binding whereas repeats two to seven all contribute to apoB-mediated binding. As discussed above, repeat five is distinguished by three consecutive acidic residues located near the carboxy-terminal end of the repeat. The CDR2.A and CDR2.B variants were designed using repeat five as a template and include the acidic triad. I propose, therefore, that the (Asp-Glu-Glu) of repeat five is responsible for its essential participation in apoE-mediated lipoprotein binding and that this same acidic triplet is also responsible for the increased affinity of CDR2.A for apoE. CDR2.C and CDR2.D were modeled on the consensus sequence of the ligand-binding domain of the LDLr and the complete engineered sequence of CDR2.D is, in fact, found in the third repeat of the LDLr. I further propose that the apparent preferential binding of CDR2.D to lipid-associated apoE, its cross-reactivity with apoB and its isoform specificity reflect its similarity, in terms of primary structure, to the consensus sequence of the LDLr.

In order to examine the role of electrostatic interactions which may occur between the 2E8 heavy chain and apoE, the technique of "charged-to-alanine" scanning was applied to the heavy chain CDRs. Thus, all of the acidic residues found within the CDRs of the heavy chain were individually replaced by alanine (or, in one case, valine), either by specific mutagenesis of by identification of the appropriate variants in a random 2E8 CDR2 library. To date, only the CDR1.(Asp^{31} →Ala), CDR3.(Asp^{97} →Ala) and CDR3.(Asp^{99} →Ala) variants have been analyzed for their binding properties.

Replacement either of the two acidic residues in the heavy chain CDR3 of 2E8 reduced, but did not eliminate, the reactivity of the respective variants with apoE and both variants maintained the isoform specificity of wildtype 2E8. Thus, while the acidic side chains of Asp^{97} is solvent exposed, in the crystal structure of wildtype 2E8 Fab (See chapter VI), it would appear that, at least individually, Asp^{97} and Asp^{99} make a relatively minor contribution to antigen binding and that the functional paratope of 2E8 may reside elswhere than in CDR3.

As was the case for the replacement of acid residues in CDR3 by alanine, the Asp^{31} →Ala sustitution had little effect on the ability of the rFab to bind to apoE3. On the other hand, the CDR1.(Asp^{31} →Ala) did acquire the ability to bind to both the apoE2 isoform and the apoE2 (Asp^{154} →Ala) variant. Surprisingly, CDR1.(Asp^{31} →Ala), like CDR2.D also showed reactivity with apoE-depleted LDL. This change in fine specificity demonstrated by the CDR1.(Asp^{31} →Ala) mutant is intriguing in light of the molecular alterations which characterize these three apoE isoforms. The Asp^{31} →Ala subsitution may have removed a steric constraint presented by the glutamic side chain that prevented the wildtype 2E8 mAb from reacting with the apoE2 and apoE2(Asp^{54} →Ala) variants. There may be a very limited restructuration of the antibody paratope due to the loss of the aspartic acid side chain, which may consequently allow this antibody to tolerate certain modifications within its epitope on apoE. The small loss of reactivity towards apoE3, may result from an overall decreased electronegativity at the antigen-binding surface, rather than the loss of an important hydrogen bond or salt link. As will be

disscussed in chapter VI, Asp^{31} may be located in a strategic area of the antibody paratope, which may dictate the wildtype antibody's apoE isoform selectivity.

In conclusion, the results generated through this initial investigation of the binding characteristics of a series of 2E8 variants have provided interesting insights into the antibody's usage of CDRs in recognizing apoE. I have demonstrated that by modifying the 2E8 heavy chain CDR2 to increase its resemblance to either cysteine-rich repeat 3 or cysteine-rich repeat 5 of the ligand-binding domain of the LDLr, the variant antibodies acquire certain of the binding properties that characterize the respective repeats. Of particular interest, I have converted an apoE-specific mAb to one which reacts with both apoE and apoB. These results justify, at least in part, my strategy of attempting to generate an antibody mimetic of the LDLr by a rational modification of the 2D8 CDR based on primary structure homology with the LDLr. Secondly, I have begun to identify the roles of specific residues in the binding specificity of 2E8. I have shown that, while acidic residues in CDR1 and CDR3 make only a minor contribution to the binding of apoE3, Asp^{31} does appear to be a key residue in defining the isoform specificity of mAb 2E8.

Nevertheless, a number of experiments remain to be done to complete the characteriztion of this series of 2E8 mutants. Notably, CDR2.D should be assessed for its ability to block the binding of apoE-depleted LDL to the LDLr on cultured human fibroblasts. I also plan to map the CDR2.D epitope within apoB structure. This will be accomplished by testing the ability of a large panel of well characterized anti-apoB

mAbs, whose epitopes have been previously mapped (Milne *et al.* 1989, Pease *et al.* 1990), to compete with CDR2.D for binding to imobilized apoE-depleted LDL. The variants that I have produced and identified, in which the acidic residues of CDR2 have been replaced by neutral residues, will also be expressed in E.coli and their binding properties determined. In addition, complete binding kinetics of all of the variants will be established using surface plasmon resonance analysis. Finally, I will use the 2E8 phage library in which the CDR2 has been randomized to select for variants that retain the ability to bind to antigen. These variants will be sequenced to identify those residues in CDR2 that are essential for antigen binding.

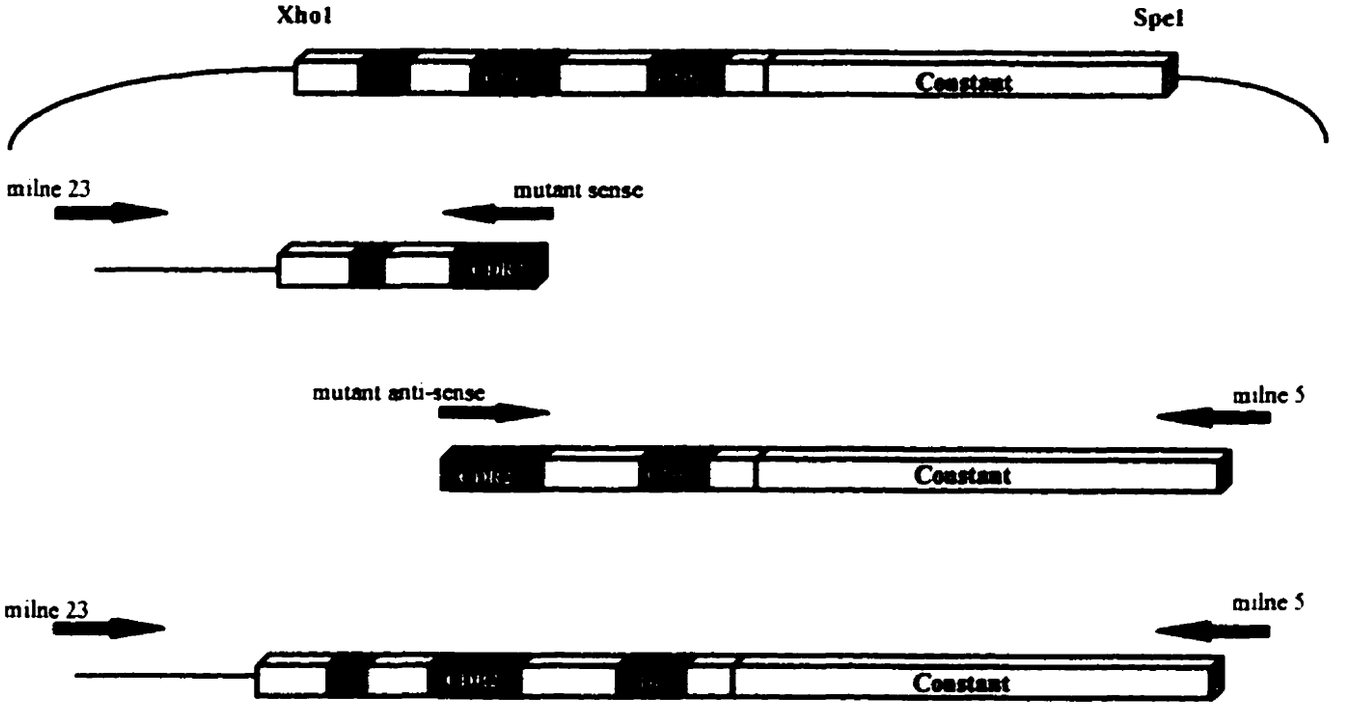

Figure V-1 Mutational analysis of the 2E8 heavy chain variable region using splice overlap extension PCR.- The diagram illustrates the site directed mutagenesis methodology of splice overlap extension PCR, or "SOE PCR", which was used to modify the primary structure of the 2E8 heavy chain variable region. As described in the text, the two red arrows represent the sense and anti-sense mutagenic oligonucleotides used in conjunction with either the milne-5 or milne-23 PCR primers, in separate amplification experiments. Subsequent to the successful amplification of both mutant products, they were purified using agarose gel electrophoresis, mixed together and served as a template in a second PCR reaction mixture, which contained both terminal primers, which resulted in the amplification of the entire heavy chain fragment with the appropriate modifications as well as with the Xho1 and Spe1 restriction sites.

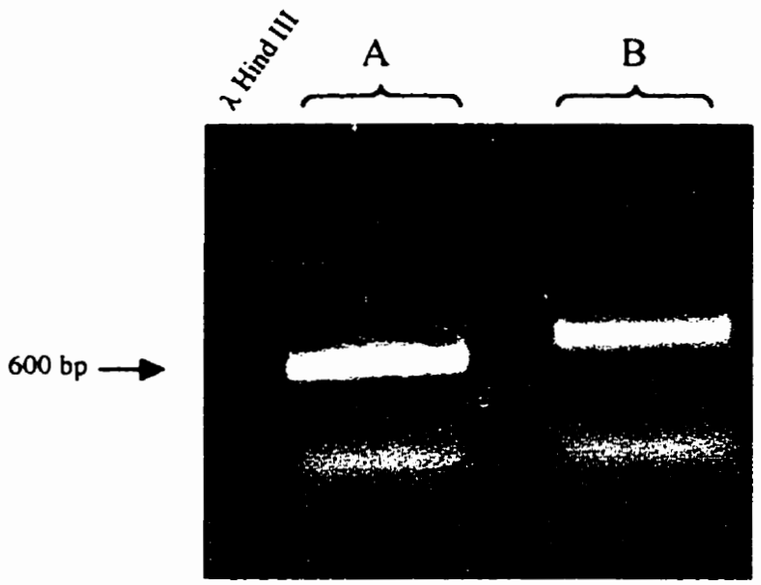

Figure V-2 First step of the SOE PCR mutagenesis methodology.- This figure illustrates the results of the first step of the SOE PCR mutagenesis methodology described in Figure V-1. A 1 % agarose gel was used to purify the two mutant PCR products. Lane A corresponds to the product of the 2E8 heavy chain amplified with the mutant primers; CDR2.D-Upper and milne-5, which as see on the gel, gave rise to a specific 600 base pair fragment. Lane B corresponds to the product of the same template DNA, amplified this time with the mutant primers; CDR2.D-Lower and milne-23, which gave rise to a specific 700 base pair fragment. In both cases, a diffuse band of DNA is observed migrating with a size corresponding to 400 base pairs. This material is likely a non-specific by-product of the PCR reaction, which is of no consequence to the specifically amplified DNA

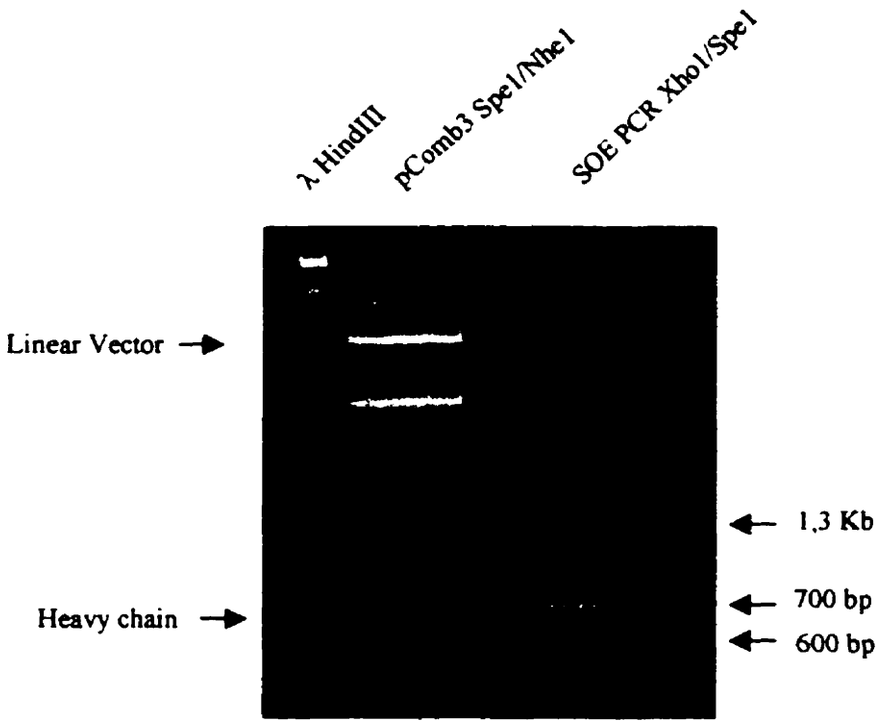

Figure V-3 Second step of the SOE PCR mutagenesis methodology.- This figure illutrates the result of the second, and final step of the SOE PCR mutagenesis methodology. This step involved the use of the two products of PCR amplification described in Figure V-2, as a template for a final amplification. The figure showes the resolution of the intact SOE-mutant product, which migrates with a size of 1300 base pairs. In addition, the figure depicts the resolution of the two fragments, when the SOE-product is cleaved with the endonucleases XhoI and SpeI. The XhoI endonuclease cleaves the product almost in half, which generates a 700 base pair fragment corresponding to the complete heavy chain Fd portion, which is then cloned into an appropriately prepared pComb 3 vector.

198	199	200	201	202	203	204	205	206	207	208	209	210	
Gly	Pro	Asp	Cys	Lys	Asp	Lys	Ser	Asp	Glu	Glu	Asn	Cys	**LDLr Repeat 5**
		Asp	Cys		Asp	Gly	Ser	Asp	Glu			Cys	**LDLr Consensus residues**

50	51	52	52b	53	54	55	56	57	58	59	60	
Trp	Ile	Asp	Pro	Glu	Ile	Gly	Asp	Thr	Glu	Tyr	Val	**2E8 w.t.**
Trp	Ile	Asp	Pro	Glu	Ile	Gly	Asp	***Glu***	Glu	Tyr	Val	**2E8 CDR2. A**
Trp	Ile	Asp	Pro	***Asp Lys Ser***			Asp	***Glu***	Glu	Tyr	Val	**2E8 CDR2. B**
Trp	Ile	Asp	Pro	***Asp Lys Ser***			Asp	***Glu Ala***		Tyr	Val	**2E8 CDR2. C**
Trp	Ile	Asp	Pro	***Asp Gly Ser***			Asp	***Glu Ala***		Tyr	Val	**2E8 CDR2. D**

Figure V-4 Mutational analysis of the 2E8 heavy chain CDR2, with structural perspectives.-The figure depicts the primary structure of the heavy chain CDR2 engineered mutants forms of mAb 2E8. The sequence of part of the 2E8 heavy chain CDR2, corresponding to residues 50-60 is compared to both the sequence of the LDLr repeat 5 as well as to the LDLr consensus sequence. The sequence of the heavy chain CDR2 is written so as to emphasize the homology in primary structure between the antibody and the LDLr repeats, in terms of acidic amino acids. The amino acids altered through site-directed mutagenesis, and which correspond to mutants CDR2.A through D, are underlined and written in italics.

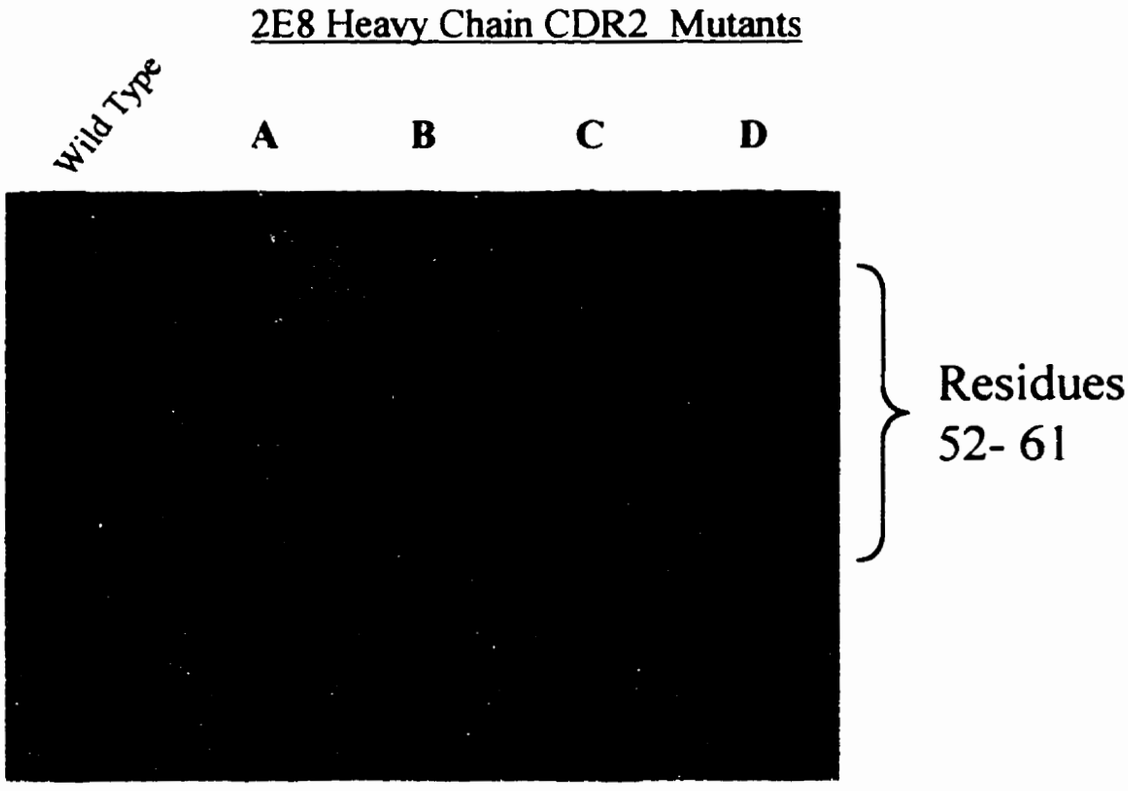

Figure V-5 Nucleotide sequence of four altered forms of the 2E8 heavy chain CDR2.- This autoradiogram corresponds to the nucleotide sequence of the wild type 2E8 heavy chain CDR2, in addition to four altered forms of the CDR, generated through SOE PCR mutagenesis. Mutants CDR2.A through D correspond to the ones presented in Figure V-4. Nucleotide encoding residues 52 through 61 are indicated.

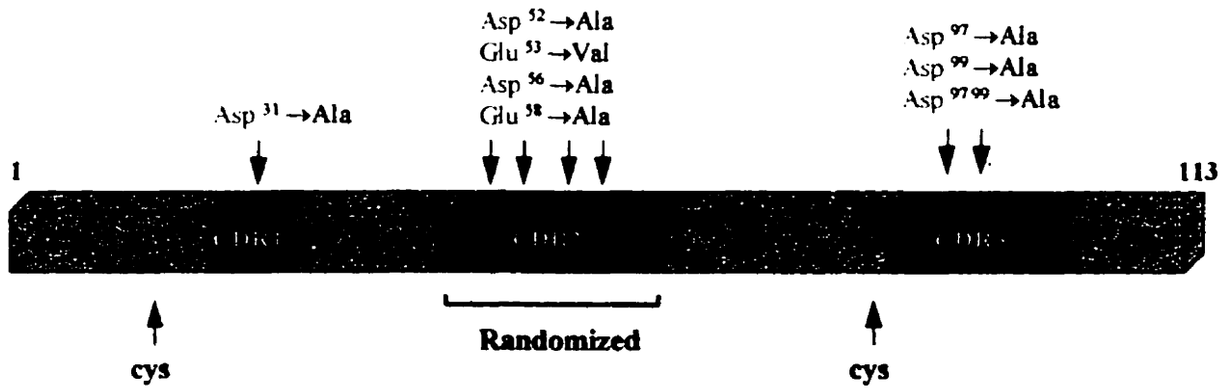

Figure V-6 "Charged-to-Alanine" mutational analysis of the heavy chain CDRs.- This figure illustrates the acidic amino acids which were all converted to an alanine residue, with the exception of Glu53 which was altered to a valine. The segments of the heavy chain appearing in green represent the residues which collectively form the three CDRs. The approximate location of the two cysteine residues involved in an intradomain disulfide bond are also indicated. Lastly, the portion of the heavy chain which was randomized is also presented. Here, all of the nucleotides, with the exception of two residues involved in the CDR2 heavy chain class 2 canonical structure, were randomly replaced.

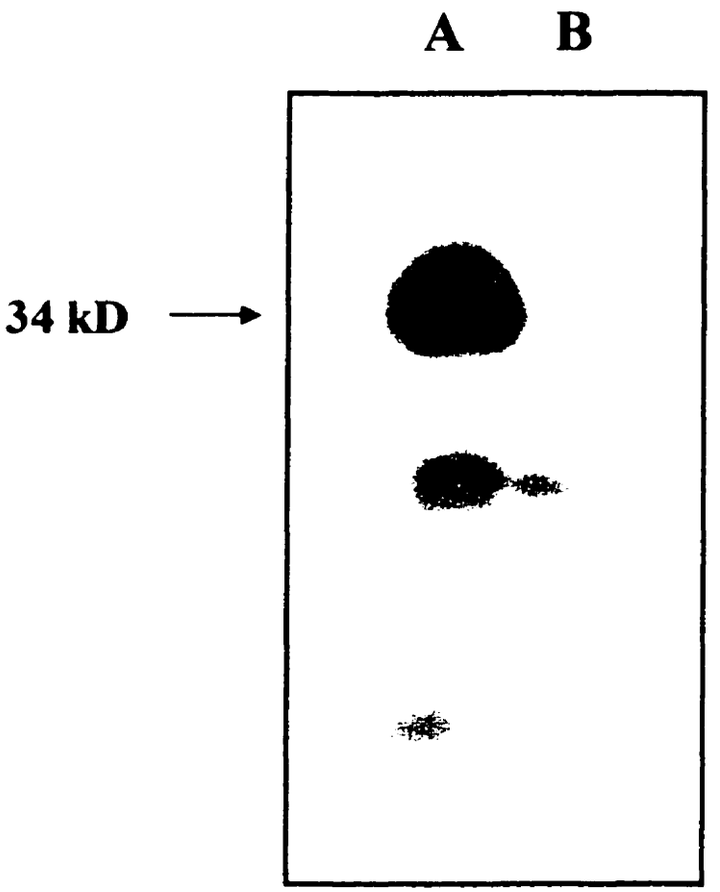

Figure V-7 Immunodepletion of apoE-containg LDL lipoproteins from crude isolates.- This autoradiogram represents an SDS PAGE western blot of 20 ug of crude LDL in lane A, run along side of 20 ug of an apoE-depleated LDL preparation shown in lane B. The blot was detected with the radiolabled mAb 6C5. A unique major band was consistantly observed at 34 kDa for the crude LDL preparations, indicating a substantial amount of apoE associated to the isolated LDLs. In contrast, no band of equivalent size was observed in the apoE immunodepleated preparation, indicating an efficient removal of the apolipoprotein from the preparation. The smaller, less abundant protein, which appears in both lanes A and B, presumably represents small quantities of the 22 kDa degradation product of apoE.

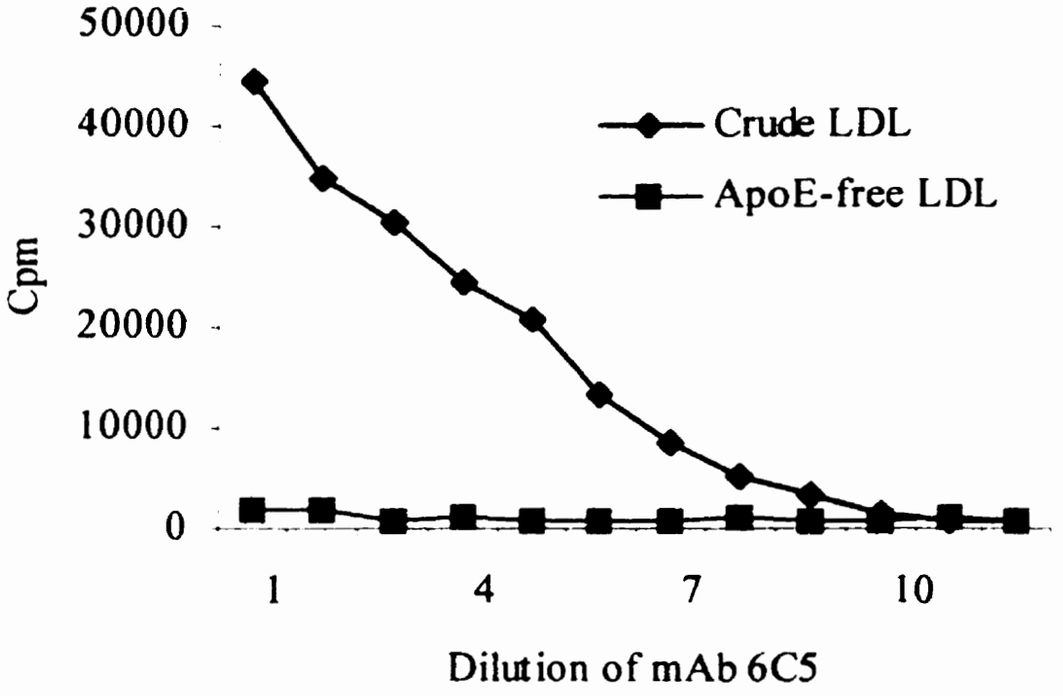

Figure V-8. Determination of apoE content in apoE immuno-depleated LDL preparations, using a radio-immunoassay.- This figure represents a radio-immunoassay of an LDL preparation which had previously been passed over an apoE immuno-affinity chromatography column, as described in Figure V-7. LDL preparations were coated onto plastic microtiter well, and detected with the radiolabled mAb 6C5. Consistent with the results obtained through the western blot experiment shown in Figure V-8, no apoE was detected in the immuno-depleated LDL preparations.

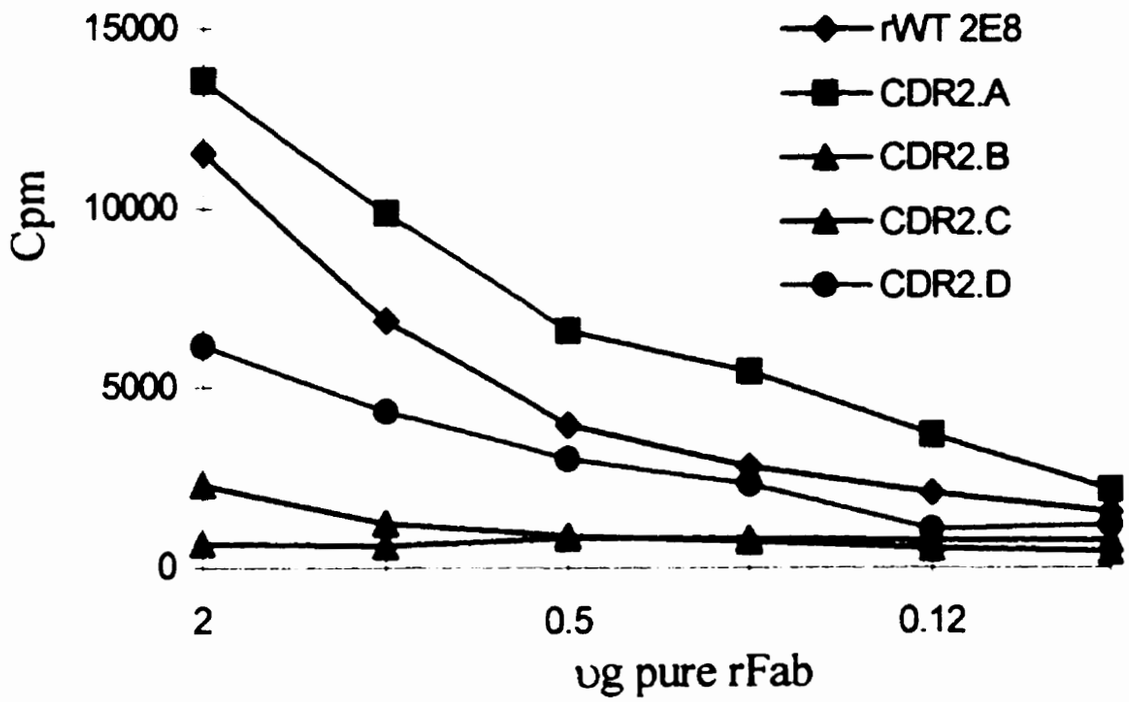

Figure V-9. Relative immunoreactivity of altered HC CDR2 structural mutants against human apoE3.- This figure depicts the binding activity of the four 2E8 CDR2 structural mutants, as well as the recombinant wild type Fab, against human apoE3 coated at 2 ug/ml in microtiter wells. The bound Fab was determined using radiolabled rabbit anti-mouse Kappa antibodies.

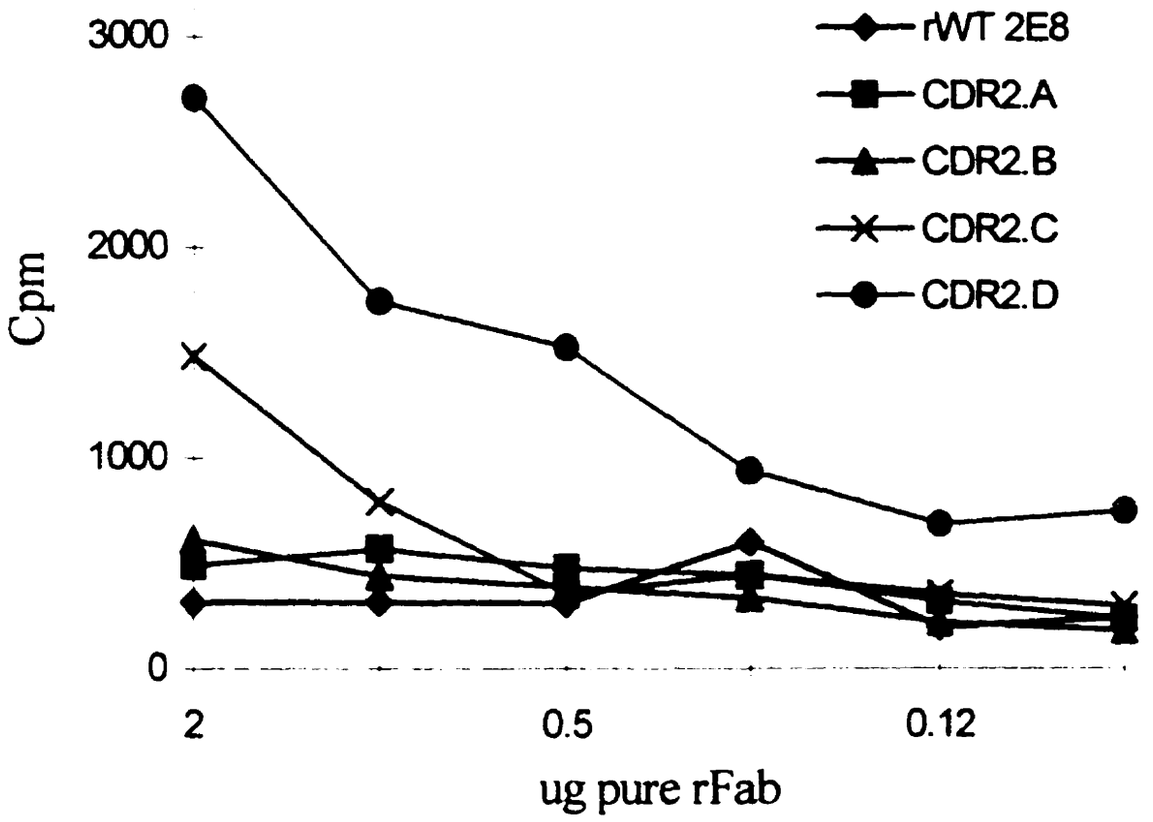

Figure V-10. Relative immunoreactivity of the 2E8 CDR2 mutants against human apoE2.- This figure depicts the binding activity of the four 2E8 CDR2 structural mutants, as well as the recombinant wild type Fab, against human apoE2 coated at 2 ug/ml in microtiter wells. The bound Fab was determined using radiolabled rabbit anti-mouse Kappa antibodies.

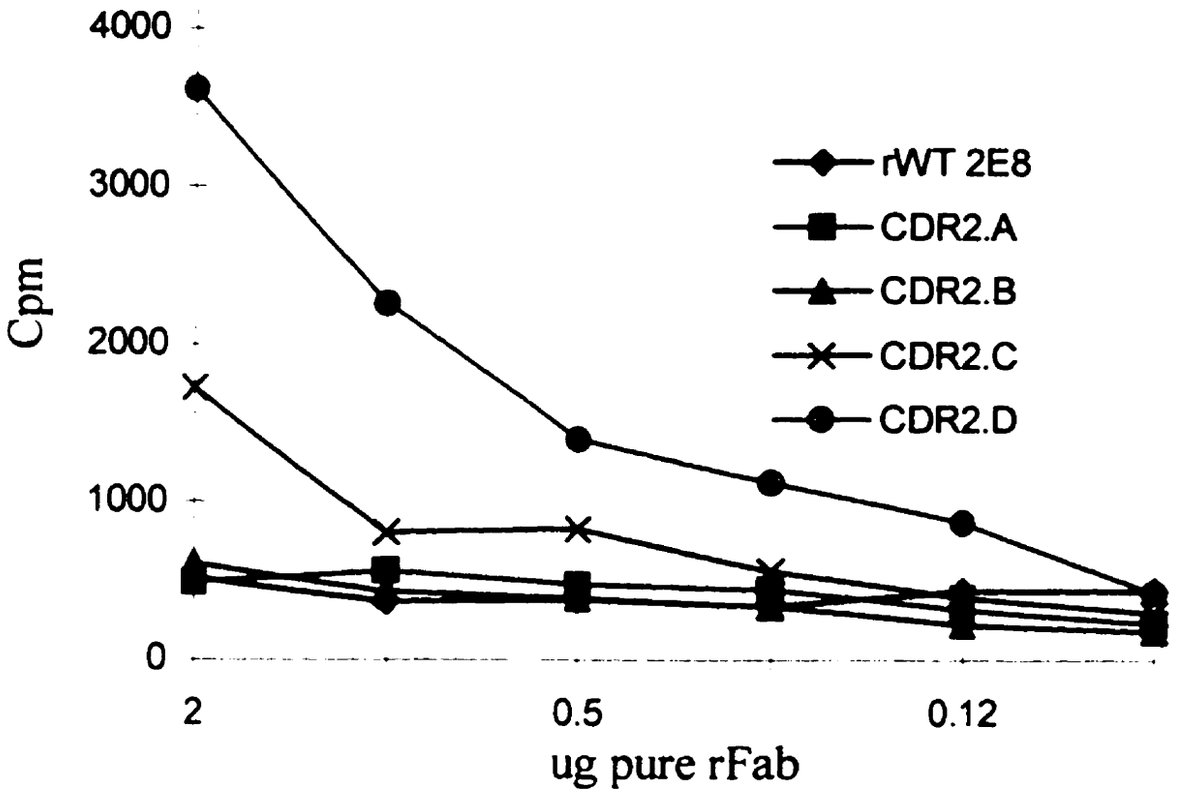

Figure V-11. Relative immunoreactivity of the 2E8 CDR2 mutants against apoE2 $Asp^{154} \rightarrow$ Ala.- This figure depicts the binding activity of the four 2E8 CDR2 structural mutants, as well as the recombinant wild type Fab, against human apoE2 $Asp^{154} \rightarrow$ Ala coated at 2 ug/ml in microtiter wells. The bound Fab was determined using radiolabled rabbit anti-mouse Kappa antibodies.

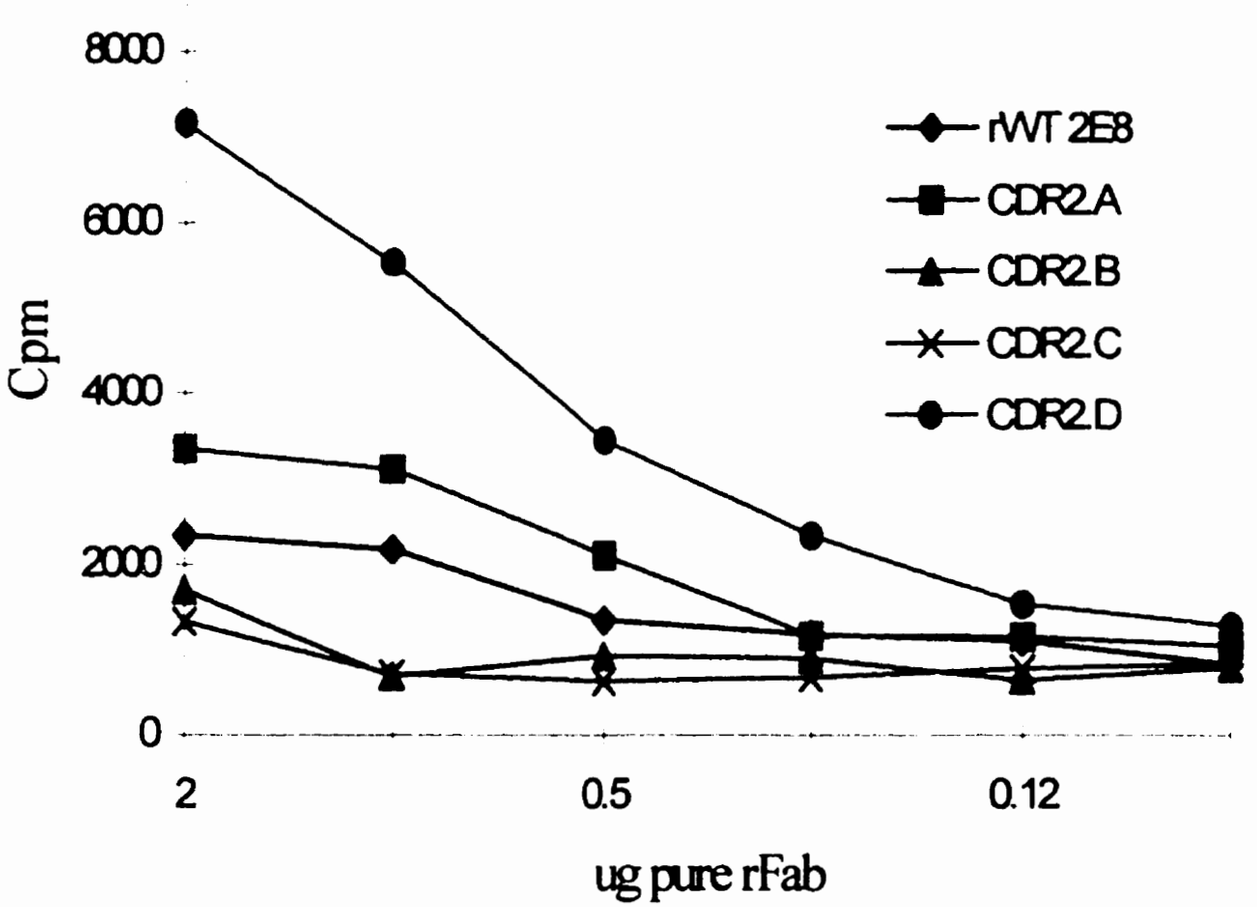

Figure V-12. Relative immunoreactivity of the CDR2 mutants against human VLDL.- This figure depicts the binding activity of the four 2E8 CDR2 structural mutants, as well as the recombinant wild type Fab, against human VLDL coated at 30 ug/ml in microtiter wells. The bound Fab was determined using radiolabled rabbit anti-mouse Kappa antibodies.

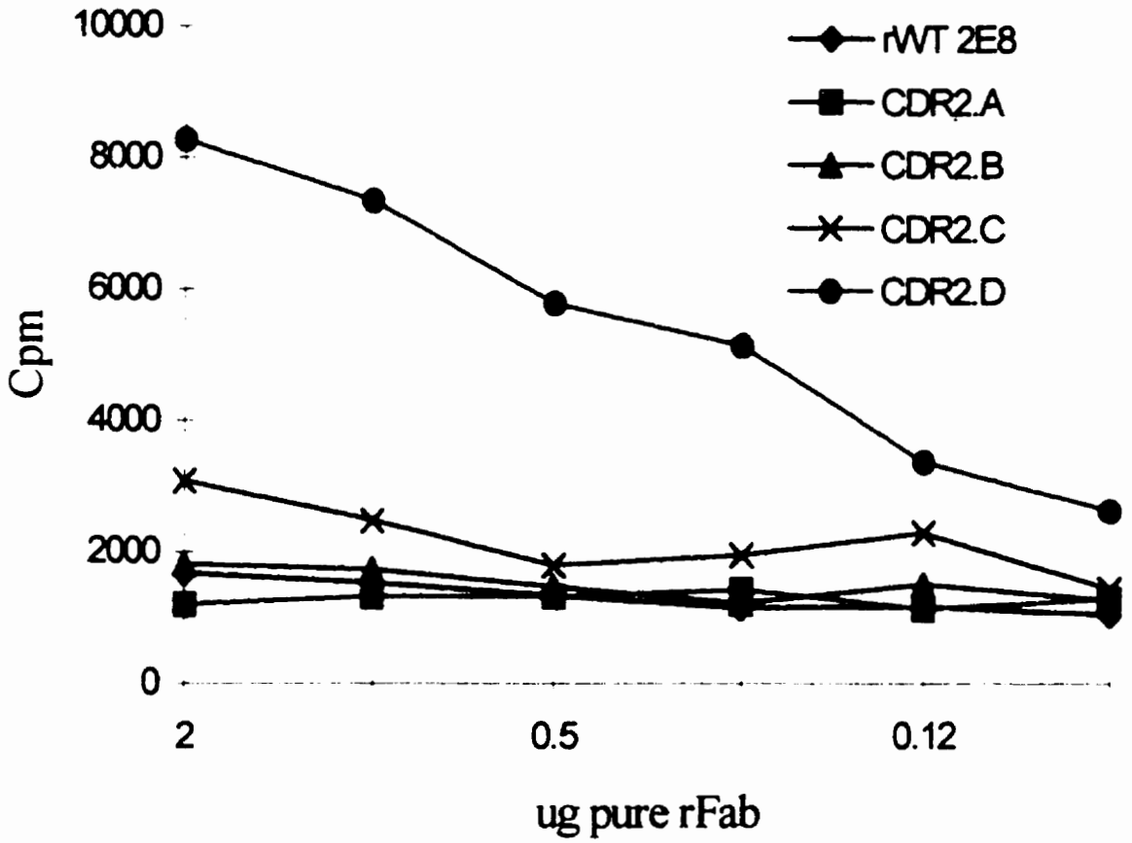

Figure V-13. Relative immunoreactivity of the 2E8 CDR2 mutants against human LDL immuno-depleated of apoE.- This figure depicts the binding activity of the four 2E8 CDR2 structural mutants, as well as the recombinant wild type Fab, against human LDL depleated of apoE, coated at 30 ug/ml in microtiter wells. The bound Fab was determined using radiolabled rabbit anti-mouse Kappa antibodies.

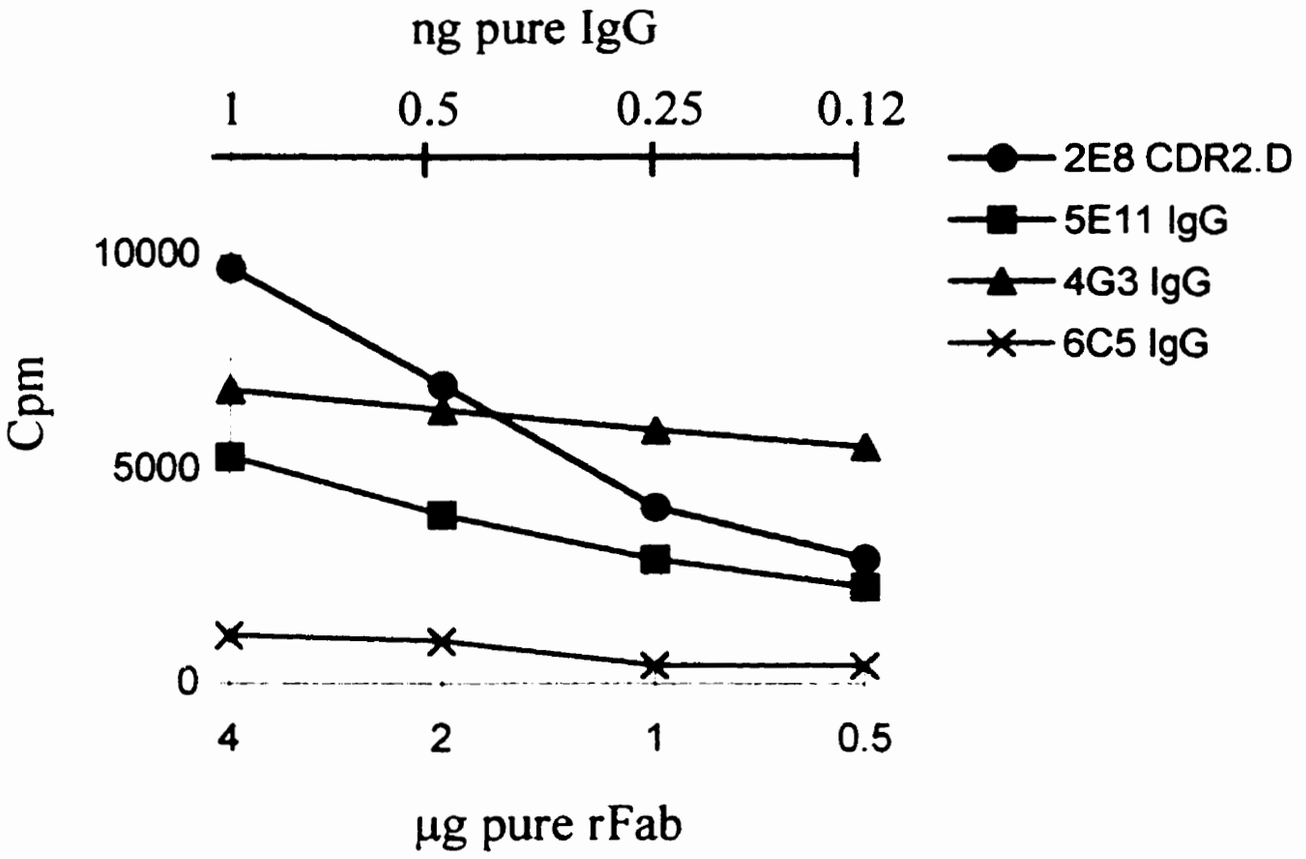

Figure V-14. Relative immunoreactivity of recombinant 2E8 CDR2.D against reconstituted human apoB-100.- The figure shows the binding capability of r2E8 CDR2.D Fab against reconstituted human apoB-100, coated at 30 ug/ml in microtitrer wells. As shown in the figure, the amount of recombinant Fab used in the first well was 4 ug. The immunoreactivity of control immunoglobulins are also shown. The two anti-apoB-100 mAbs 4G3 and 5E11 were both used as positive control antibodies. In addition, the anti-apoE mAb 6C5 was used as a negative control antibody. The amount of control antibody used in the first well is not indicated on the figure, and in all cases corresponds to 1 ng. The binding of the antibodies was revealed through the use of a radiolabled rabbit anti-mouse kappa antibody.

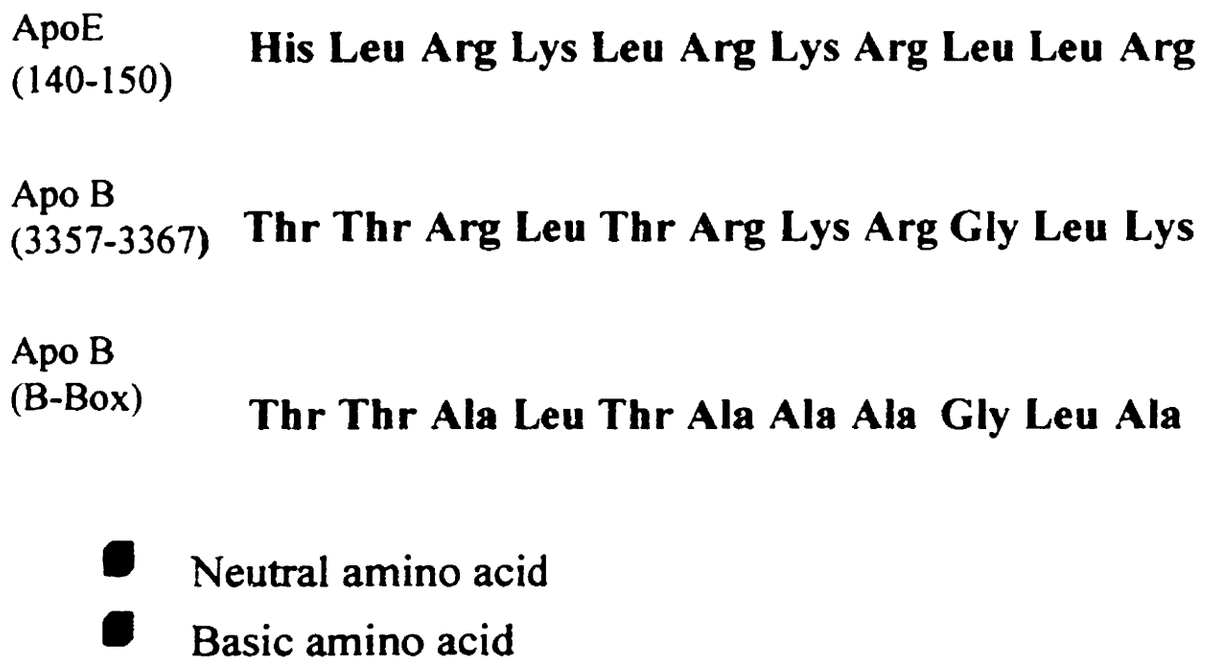

Figure V-15 ApoE / ApoB receptor binding domain homologies.- This figure illustrates the homology which exists at the amino acid level, between the LDL receptor binding site of apoE, and residues 3357-3367 in apoB. Basic amino acids are indicated in blue, whereas neutral ones are shown in green. The apoB variant "ApoB B-Box", which was engineered to result in the substitution of every basic residue found between positions 3357-3367, into a neutral one, is also shown.

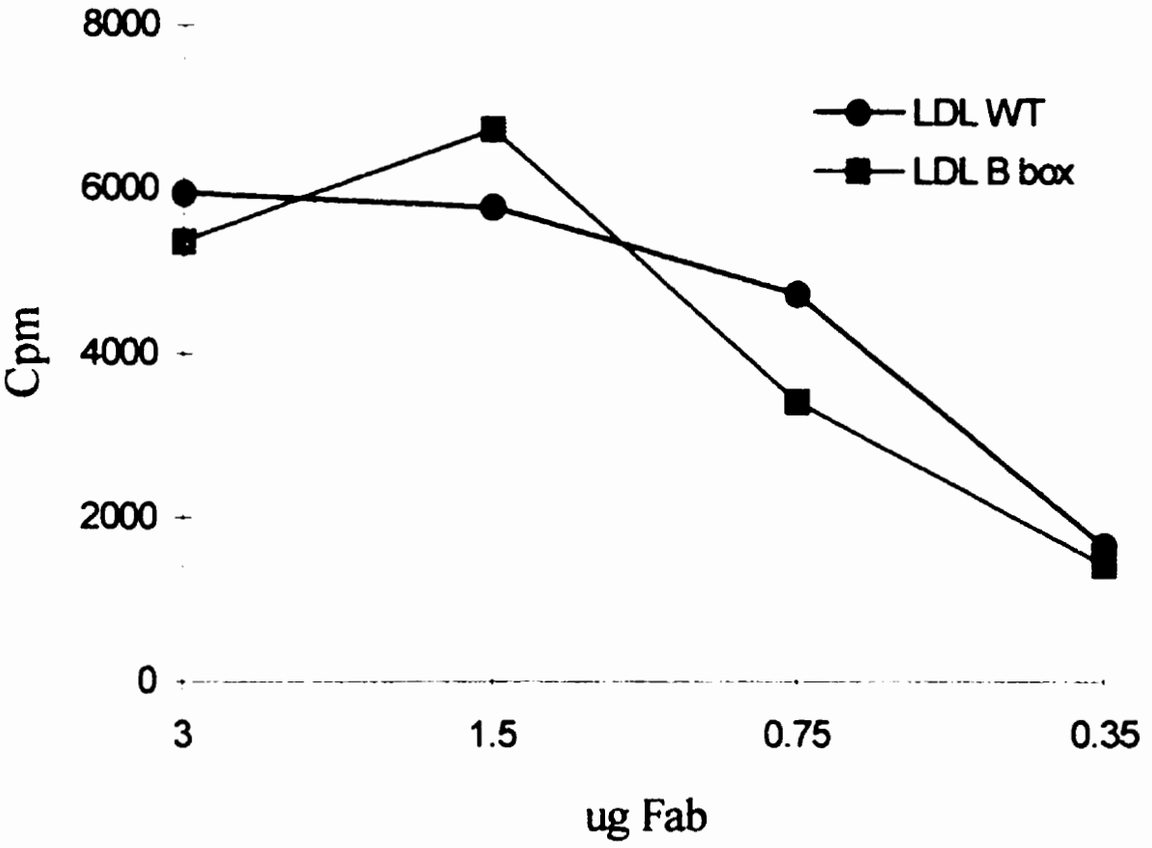

Figure V-16. Immunoreactivity of the recombinant CDR2 structural mutant 2E8 CDR2.D, against LDL receptor competent and incompetent forms of LDL.- This figure depicts the binding activity of the heavy chain CDR2 structural mutant 2E8.D, against LDL receptor competent and incompetent forms of LDL depleated of apoE, coated at 10 ug/ml In the receptor-defective form of apoB, all lysine residues between apoB-100 residues 3357-3367, termed the B-box, were replaced with alanine.

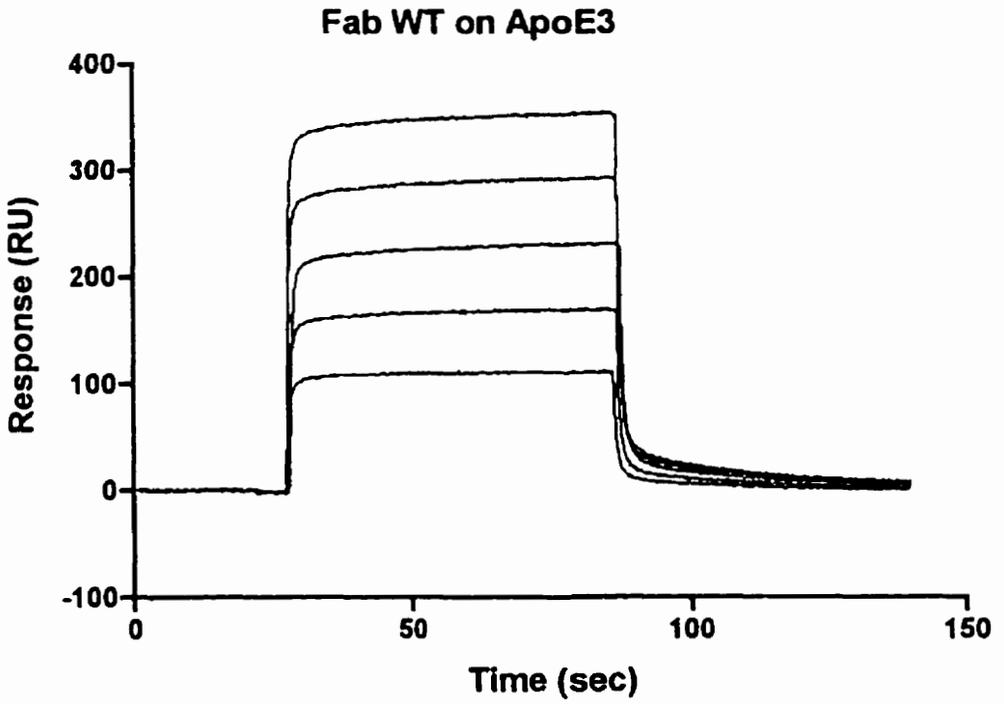

Figure V-17 Sensorgrams of pure ApoE3 with recombinant 2E8 Fab using SPR. These sensorgrams depict the kinetics of the wild type recombinant 2E8 Fab associating to ApoE3. The results that are illustrated were obtained with concentrations ranging from 0.2 μM to 8 μM of rFab.

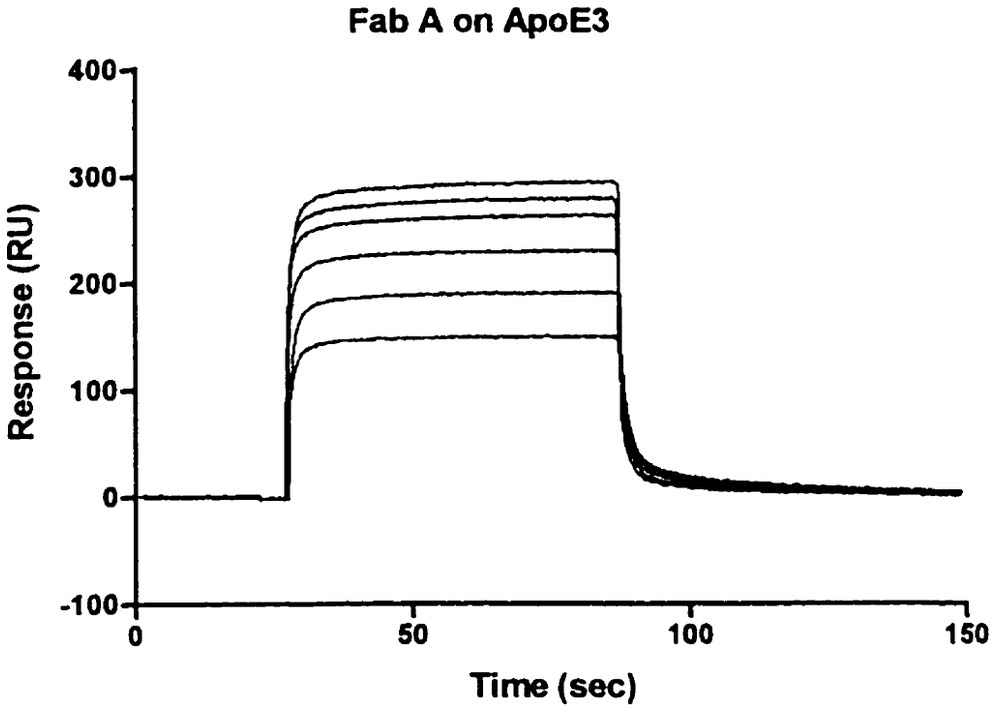

Figure V-18 Sensorgrams of pure ApoE3 with the recombinant 2E8 CDR2.A Fab, using SPR. These sensorgrams depict the kinetics of the wild type recombinant 2E8 Fab associating to ApoE3. The results that are illustrated were obtained with concentrations ranging from 0.2 μM to 8 μM of rFab.

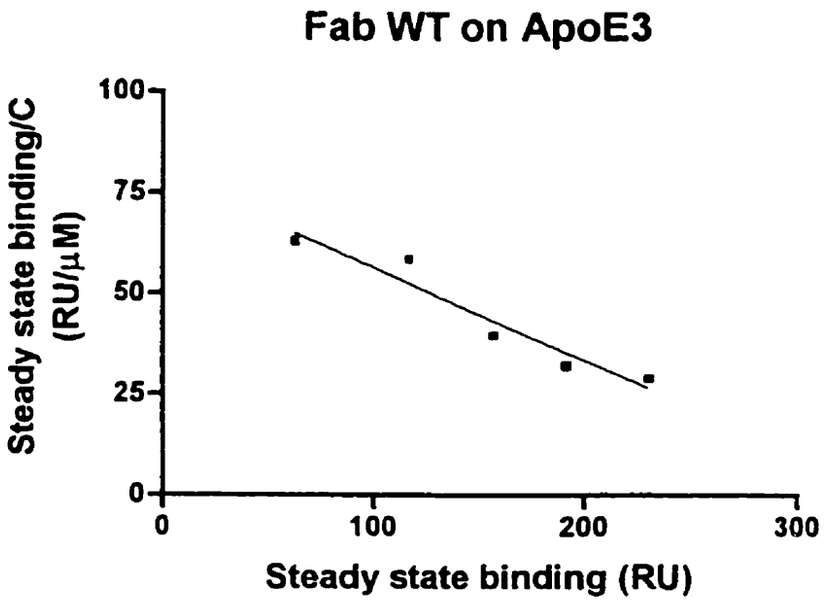

Figure V-19 Determination of the association constant of the wild type rFab against pure ApoE3.- This figure illustrates the results obtained from the sensorgrams shown in figure V-17, and plotted in order to determine the association constant. Calculations were performed according to the Biacore analytical software. As shown by the figure, all data points fall onto a straight line. The association constant was determined to be 4.3 μM.

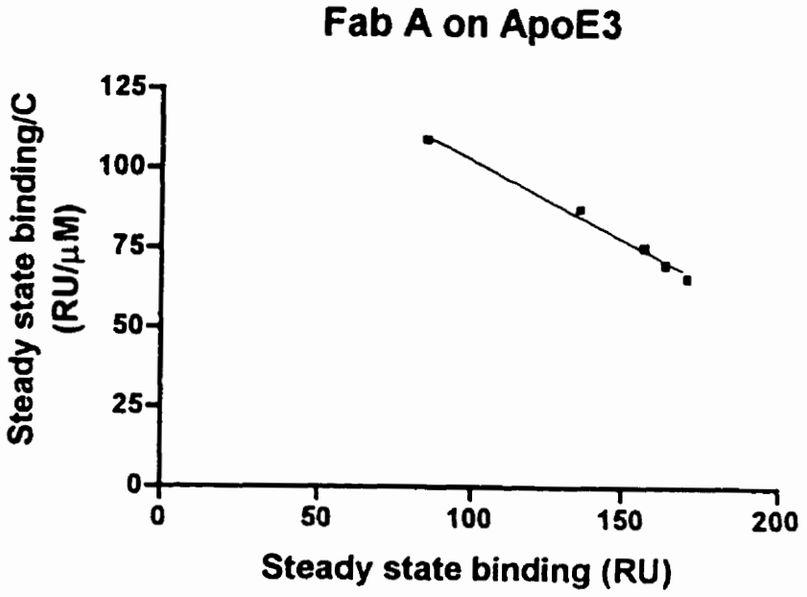

Figure V-20 Determination of the association constant of the 2E8 CDR2.A rFab against pure ApoE3.- This figure illustrates the results obtained from the sensorgrams shown in figure V-18, and plotted in order to determine the association constant. Calculations were performed according to the Biacore analytical software. As shown by the figure, all data points fall onto a straight line. The association constant was determined to be 2.0 μM.

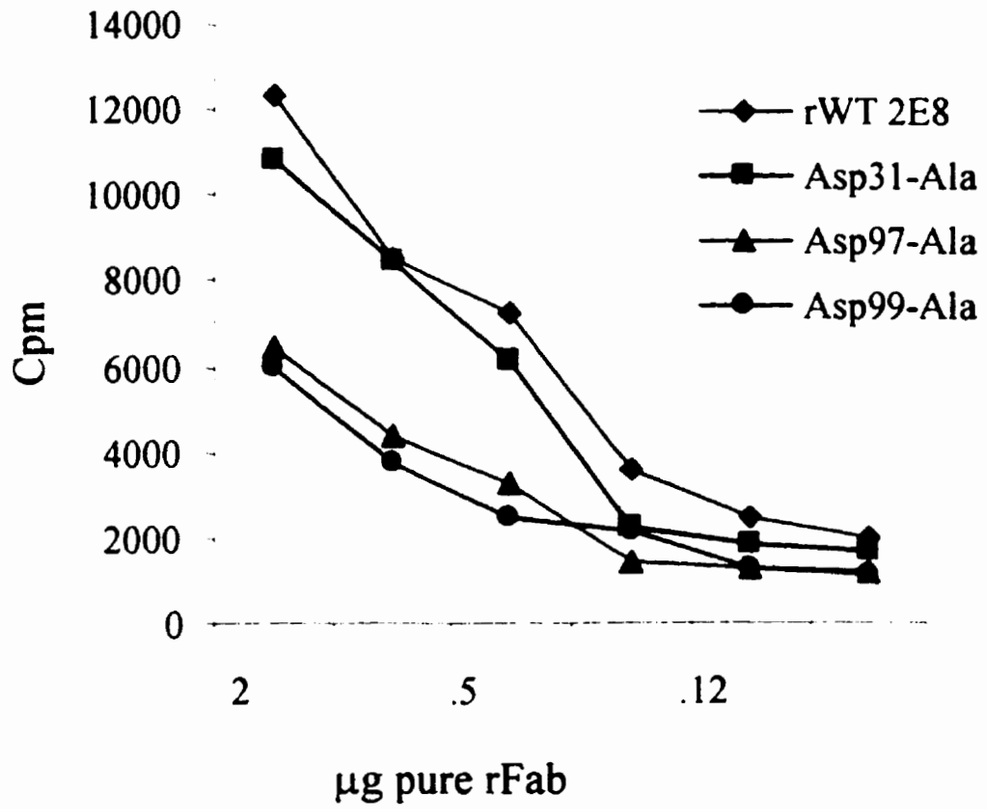

Figure V-21 Relative immunoreactivity of the 2E8 functional mutants against apoE3.- This figure depicts the binding activity of the three 2E8 functional mutants, as well as the wild type rFab against pure apoE3 coated at 2 µg/ml in microtiter wells. The bound Fab was determined using radiolabled rabbit anti-mouse kappa antibodies.

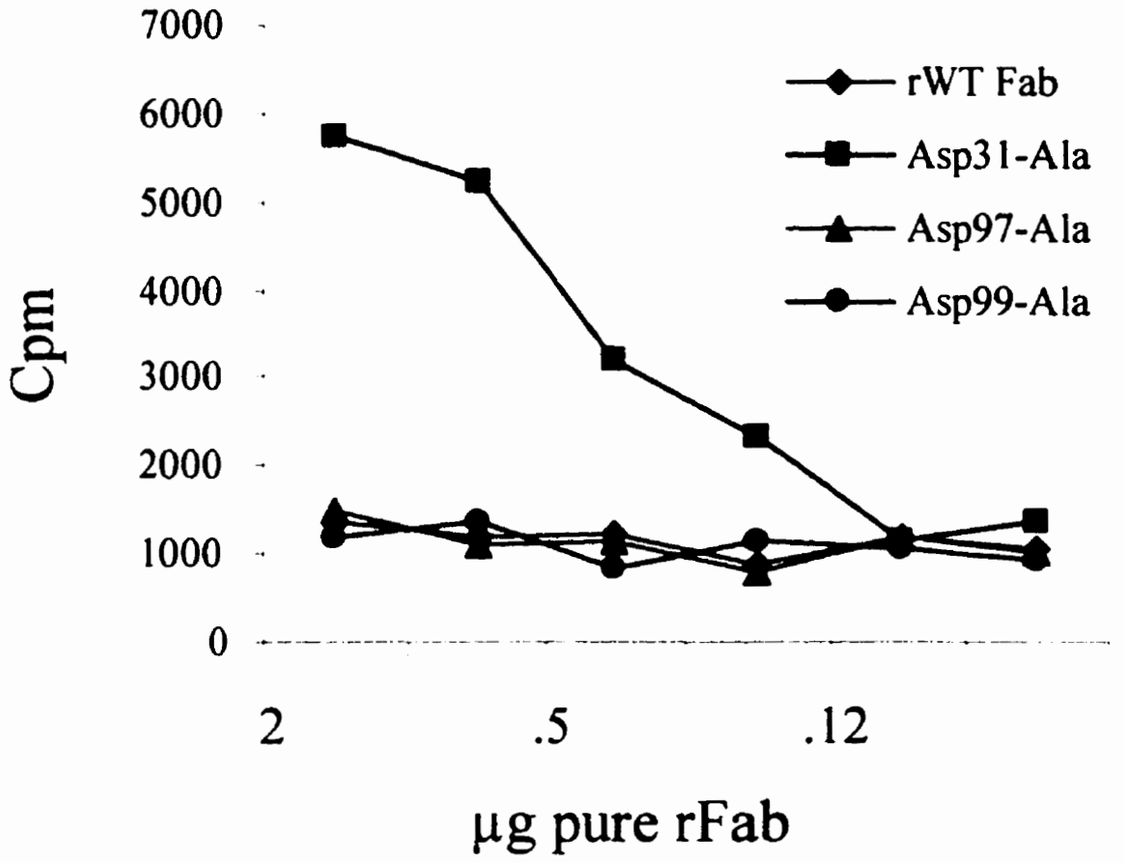

Figure V-22 Relative immunoreactivity of the 2E8 functional mutants against apoE2.- This figure depicts the binding activity of the three 2E8 functional mutants, as well as the wild type rFab against pure apoE2 coated at 2 µg/ml in microtiter wells. The bound Fab was determined using radiolabled rabbit anti-mouse kappa antibodies.

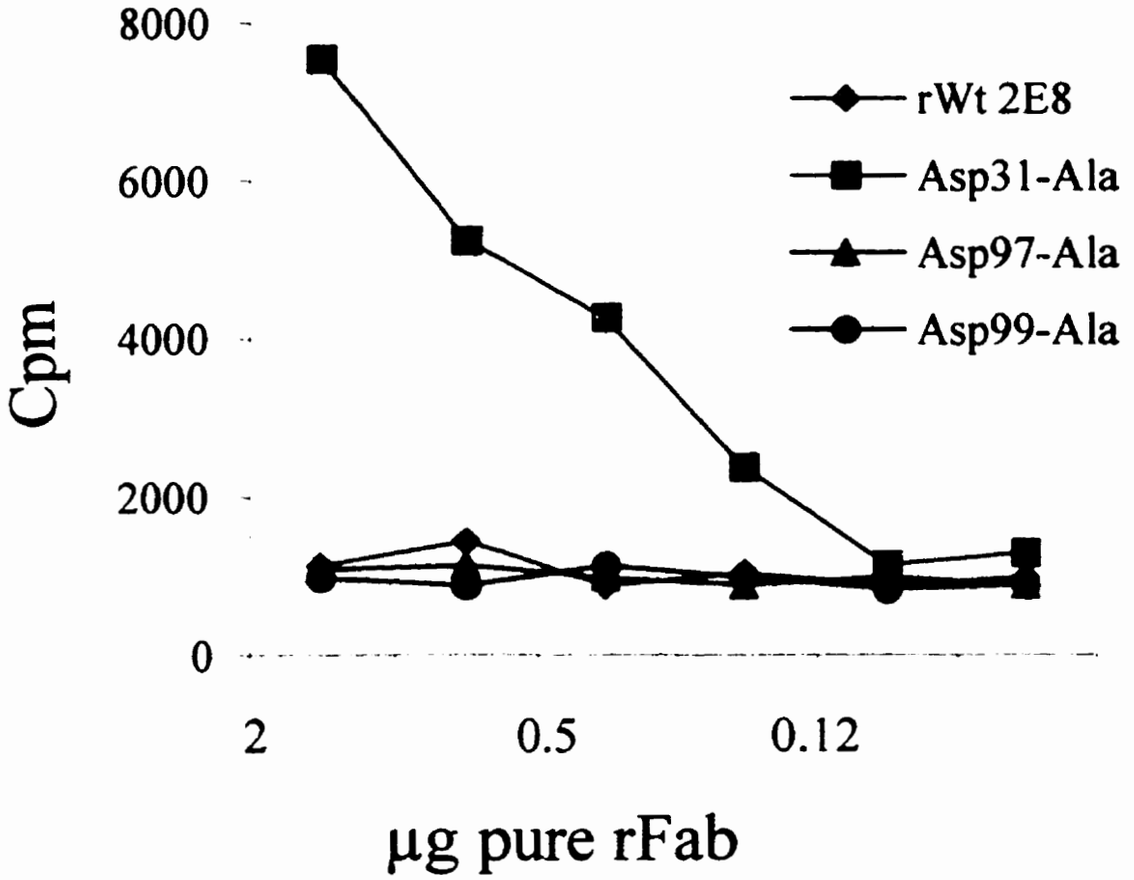

Figure V-23 Relative immunoreactivity of the 2E8 functional mutants against apoE2 Asp154→Ala.- This figure depicts the binding activity of the three 2E8 functional mutants, as well as the wild type rFab against pure apoE Asp154→Ala coated at 2 µg/ml in microtiter wells. The bound Fab was determined using radiolabelled rabbit anti-mouse kappa antibodies.

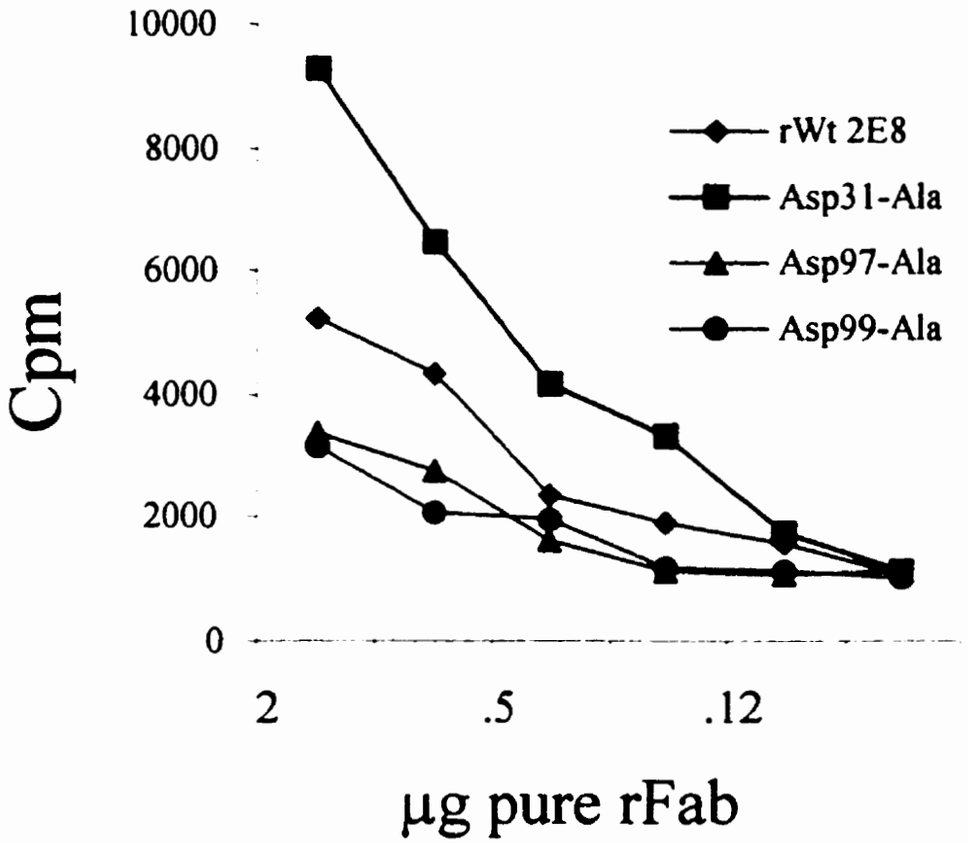

Figure V-24 Relative immunoreactivity of the 2E8 functional mutants against human VLDL. This figure depicts the binding activity of the three 2E8 functional mutants, as well as the wild type rFab against isolated human VLDL coated at 30 µg/ml in microtiter wells. The bound Fab was determined using radiolabelled rabbit anti-mouse kappa antibodies.

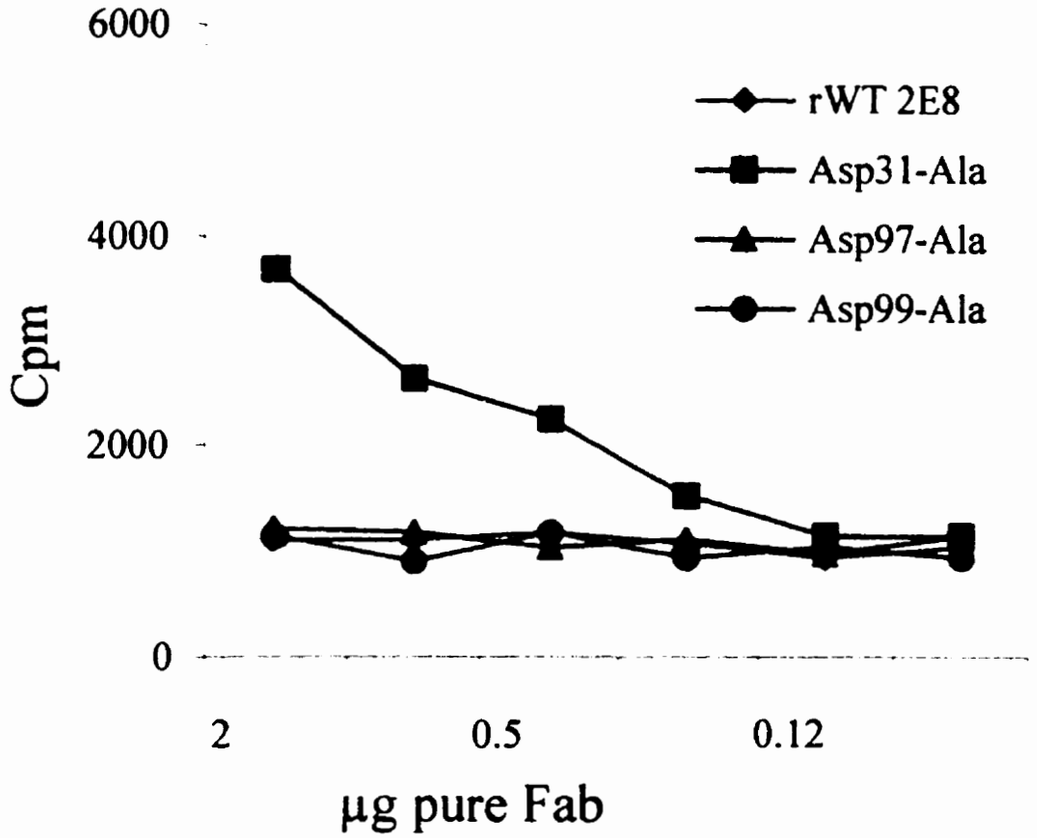

Figure V-25 Relative immunoreactivity of the 2E8 functional mutants against reductively methylated human VLDL- This figure depicts the binding activity of the three 2E8 functional mutants, as well as the wild type rFab against reductively methylated human VLDL coated at 30 µg/ml in microtiter wells. The bound Fab was determined using radiolabled rabbit anti-mouse kappa antibodies.

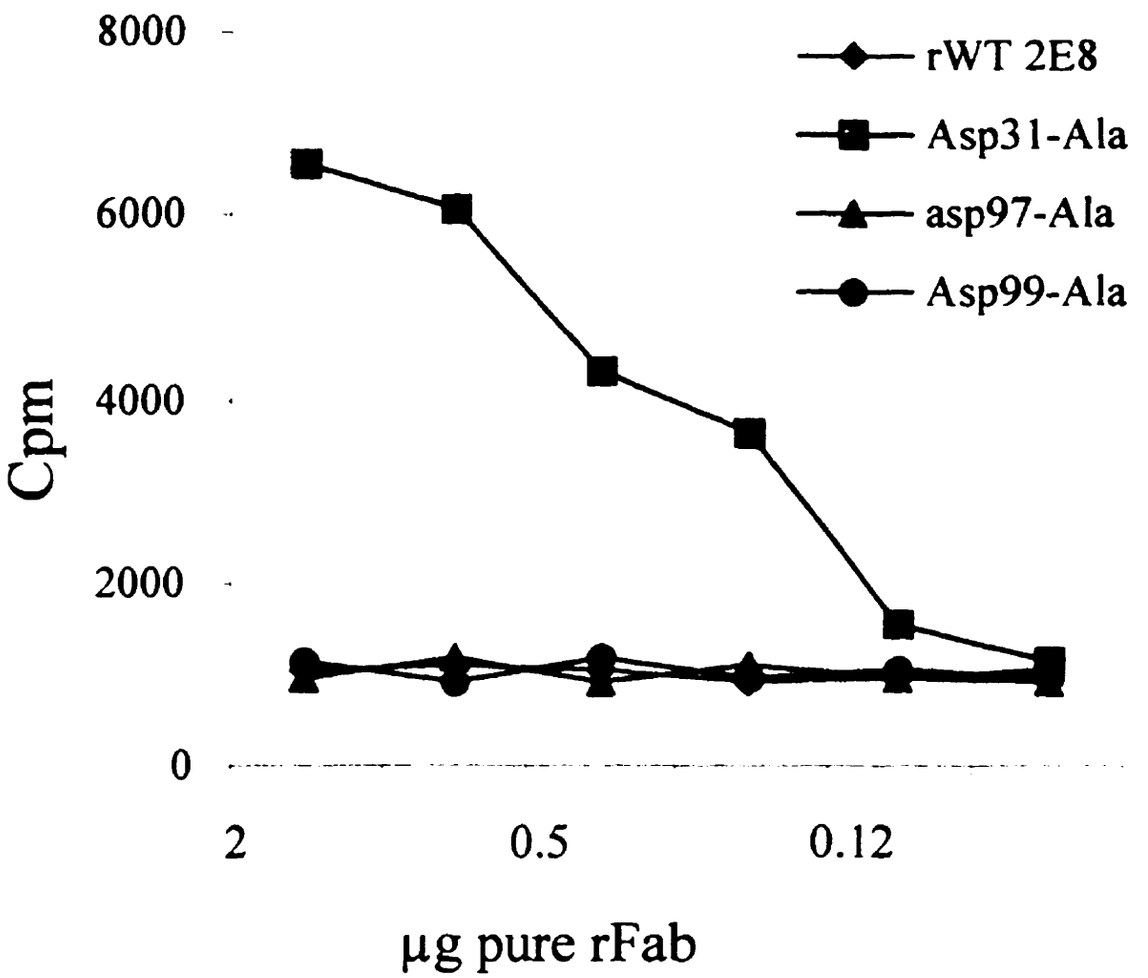

Figure V-26 Relative immunoreactivity of the 2E8 functional mutants against apoE-depleted human LDL.- This figure depicts the binding activity of the three 2E8 functional mutants, as well as the wild type rFab against apoE-depleted human LDL coated at 30 µg/ml in microtiter wells. The bound Fab was determined using radiolabled rabbit anti-mouse kappa antibodies.

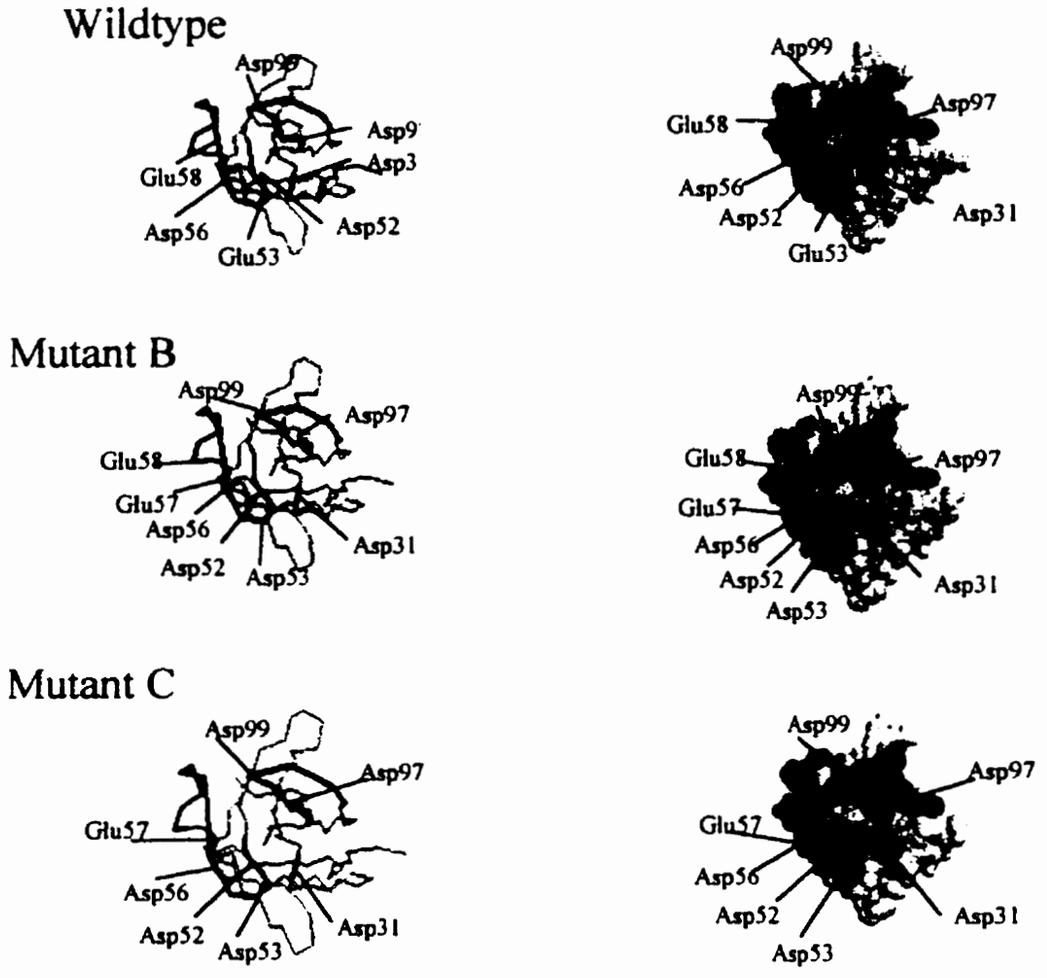

Figure V-27 Molecular model of the wild type 2E8 heavy chain compared to the structural 2E8 CDR2 variants CDR2.B and CDR2.C.- This figure illustrates the comformations adopted by the variant antibodies as compared to the wild type heavy chain, as modeled by the SWISS protein modeling program available on the world wide web (http://expasy.hcuge.ch/swissmod/SWISS-Model.html). Modeled figures on the left, show the three heavy chain CDRs colored in yellow, green and blue respectively, with negatively charged residues indicated and colored red. Figures on the right are space-fill models of the same clones, indicated in the same way.

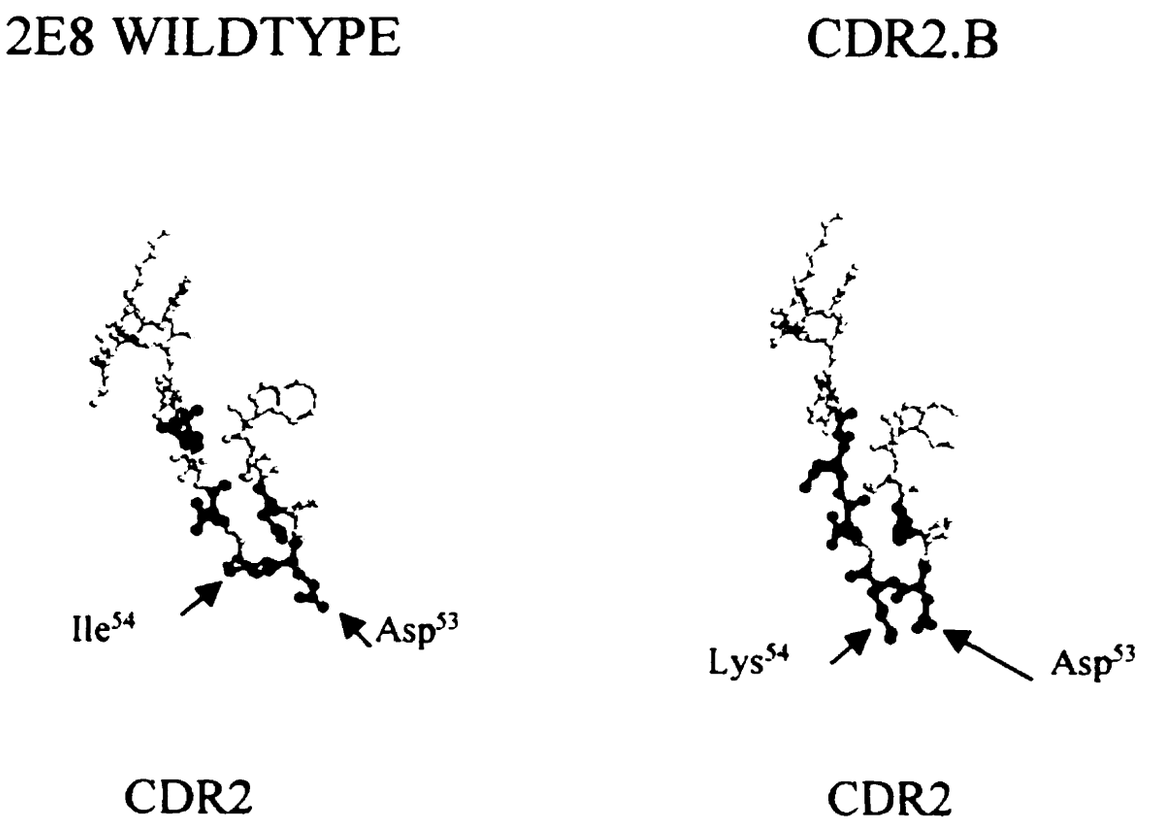

Figure V-28 Molecular model of the wild type and mutant 2E8 heavy chain CDR2.- This figure illustrates the modeled structures of the 2E8 heavy chain CDR2, as determined by the SWISS model program available through the world wide web (http://expasy.hcuge.ch/swissmod/SWISS-Model.html). Residues 53 and 54 are indicated. The side chain of Asp53 is shown protruding into the solvent in both models. In mutant CDR2.B, the replacement of Ile54 by a lysine, in the model is shown to be in close proximity to the aspartic acid, which may explain the antigen-unreactiveness of the rFab.

CDR2.A

5'- CCT GAA ATT GGT GAT GAA GAA TAT GTC CCG AAG -3'
3'- GGT CTT TAA CCA CTA CTT CTT ATA CAG GGG TTC -5'

CDR2.B

5'- GGA TGG ATT GAT CCT GAC AAA AGT GAT GAA GAA TAT GTC CCG AAG -3'
3'- CCT ACC TAA CTA GGA CTG TTT TCA CTA CTT CTT ATA CAG GGC TTC -5'

CDR2.C

5'-ATTGGATGGATTGAT CCT GAC AAA AGT GAT GAG GCA TAT GTC CCGAAGTTC-3'
3'-TAACCTACCTAACTA GGA CTG TTT TCA CTA CTC CGT ATA CAG GGCTTCAAG-5'

CDR2.D

5'-ATTGGATGGATTGAT CCT GAC GGT AGT GAT GAG GCA TAT GTC CCGAAGTTC-3'
3'-TAACCTACCTAACTA GGA CTG CCA TCA CTA CTC CGT ATA CAG GGCTTCAAG-5'

Table V-1 Nucleotide sequence of the oligonucleotide primers used in the PCR mutagenesis of the 2E8 heavy chain CDR2. The mutagenic oligonucleotide primers used in the PCR mutagenesis, are presented as a double stranded DNA molecule coding for the heavy chain CDR2. In all cases, the upper oligonucleotide is the sense primer which anneals to the non-coding strand of the antibody DNA. The lower oligonucleotide is the anti-sense primer which anneals to the coding strand of the antibody DNA. The altered codons appear in bold, whereas the altered nucleotides are underlined.

CDR1 Ala 31:

5'- TTC AAC ATT AAA GCC TAC TAT ATC CAC TGG -3'
3'- CCG AAG TTG TAA TTT CGG ATG ATA TAG GTG -5'

CDR3 Asp/Ala 97 and Asp/Ala 99:

5'- GCA GGG CAT GXT TAC GXC AGG GGA CGG -3'
3'- CGT CCC GTA CXA ATG CXG TCC CCT GCC -5'

Table V-2 Nucleotide sequence of the oligonucleotide primers used in the "Charged-to-Alanine" scanning PCR mutagenesis of the 2E8 heavy chain CDR1 and CDR3. - The mutagenic oligonucleotide primers used in the "Charged-to-Alanine" PCR mutagenesis, are presented as a double stranded DNA molecule coding for parts of the heavy chain CDR1 and CDR2. In all cases, the upper oligonucleotide is the sense primer which anneals to the non-coding strand of the antibody DNA. The lower oligonucleotide is the anti-sense primer which anneals to the coding strand of the antibody DNA. The altered codons appear in bold, whereas the altered nucleotides are underlined. In the case of the CDR1 oligonucleotides, the underlined C in codon 31 is the sole nucleotide alteration which converts the Asp into an Ala. The CDR3 oligonucleotides were synthesized so as to generate three coding sequences in a single amplification event, by inserting an equimolar mixture of an A/C in the sense primer, and a T/G in the anti-sense primer, at the two positions indicated by an underlined X, in codons 97 and 99.

CDR2 random primers:

```
                                  50
5'- CTG GAG TGG ATT GGA TGG ATT GAT CCT GAA ATT GGT GAT ACT GAA
3'- GAC CTC ACC TAA CCT ACC TAA CTA GGA CTT TAA CCA CTA TGA CTT

    TAT GTC CCG AAG TTC CAG GGC AAG GCC ACT ATG ACT GC -3'
    ATA CAG GGC TTC AAG GTC CCG TTC CGG TGA TAC TGA    -5'
```

Table V-3 Nucleotide sequence of the oligonucleotide primers used in the random SOE PCR mutagenesis of the 2E8 heavy chain CDR2. - The degenerate mutagenic oligonucleotide primers used in the random CDR2 mutagenesis, are presented as a double stranded DNA molecule coding for the heavy chain CDR2 region. The upper oligonucleotide is the sense primer which anneals to the non-coding strand of the antibody DNA. The lower oligonucleotide is the anti-sense primer which anneals to the coding strand of the antibody DNA. The altered nucleotides appear in bold and correspond to the entire CDR2 which begins at residue 50 as indicated, whereas the unaltered nucleotides within the CDR2, encoding the two class 2 canonical residues, are underlined. The nucleotides in bold represent those that will appear in 87.75 % of all cases, whereas in the other 11.25 % of cases, anyone of the three other nucleotides can be present. Of 48 transformed clones sequenced, 11 encoded the wild type heavy chain CDR2, and six had acquired a non-sense mutation.

Bacterial clone	Batch	Mutation
9	A	Asp ^{52} →Ala, Glu ^{58} →Asp
6	D	Asp ^{52} →Asn
6	A	Glu ^{53}→Val, Ile ^{54}→Ser
2	B	Glu ^{53}→Val
7	C	Glu ^{53}→Val, Ile ^{54}→Ser
11	C	Glu ^{53}→Asp, Tyr ^{59}→Asn
4	D	Glu ^{53}→Ala, Glu ^{58}→Gln
11	D	Glu ^{53}→Asn, Ile ^{54}→Phe, Gly ^{65}→Cys
3	C	Asp ^{56}→Ala
5	C	Asp ^{56}→Asn
7	A	Glu ^{58}→Ala
4	B	Thr ^{57}→Ile, Glu ^{58}→Val, Phe ^{63}→Tyr, Gln ^{64}→Pro
10	C	Glu ^{58}→Gly
4	D	Glu ^{58}→Gln, Glu ^{53}→Ala

Table V-4 List of 2E8 heavy chain CDR2 mutants restricted to one of the four acid residues.- This table groups four sets of heavy chain mutants, obtained from isolated clones of *E.coli* transformed with the CDR2 random library. The sets correspond to clones altered at residues Asp^{52}, Glu^{53}, Asp^{56} and Glu^{58}. In addition to the altered acidic residue, some clones contain multiple mutations elsewhere in CDR2. The classification of the individual clones reflects their order of initial isolation. Thus they are categorized according to the batch of A to D and according to their numerical order of selection. The clones are thus identified by the batch letter followed by the numerical value, such as for example clone 2E8 HC CDR2. A6.

Bacterial clone	Batch	Mutation
2	A	Ile $^{51}\rightarrow$ Ser
1	B	Ile $^{54}\rightarrow$ Met, Tyr $^{59}\rightarrow$ His
3	B	Lys $^{62}\rightarrow$ Phe, Phe $^{63}\rightarrow$ Ser
6	B	Ile $^{54}\rightarrow$ Asn
9	B	Ile $^{54}\rightarrow$ Ser, Gly $^{65}\rightarrow$ Val
6	C	Lys $^{62}\rightarrow$ Asn
9	C	Ile $^{54}\rightarrow$ Val
1	D	Ile $^{51}\rightarrow$ Asn, Ile $^{54}\rightarrow$ Met
3	D	Ile $^{51}\rightarrow$ Met
5	D	Trp $^{50}\rightarrow$ Leu
7	D	Ile$^{51}\rightarrow$ Asn, Pro $^{61}\rightarrow$ Arg, Gly $^{65}\rightarrow$ Leu
9	D	Pro $^{61}\rightarrow$ Lys
12	D	Lys $^{62}\rightarrow$ Ile

Table V-5 List of 2E8 heavy chain CDR2 mutants not related to the acidic residues at positions 52, 53,56 and 58.- This table presents heavy chain mutants selected from the random CDR2 library, which are not altered at one of the four acidic residues; Asp^{52}, Glu^{53}, Asp^{56} and Glu^{58} described in Table V-4. The clones are grouped as four sets, A to D, according to the batch of selected *E.coli* transformants. As described in Table V-4, the clones are named according to the batch form which they were isolated and to their numerical order. From a total of 42 isolated clones, 23 % had nucleotide alterations which led to no altered codon, while 33 % had one altered codon. 23 % resulted in two altered codons, whereas 5 and 2 % of the clones had three and four altered codons respectedly. 14 % of the clones resulted in nonfunctional antibodies, as a stop codon was generated.

Chapter VI

General Discussion

The study of a protein's specific structural features, which may form the basis of its functional activity, can be effectively dissected through the establishment of a panel of mAbs against its entire hydrated surface. Such mAb epitope maps have been instrumental in the study of protein function, as a mAb can pinpoint areas of a protein which may be involved in a functional process. Consequently, mAbs capable of inhibiting protein function in a biological setting represent invaluable tools in the biochemical study of the protein for which the antibody is specific. For example, virus-neutralizing mAbs, which bind to a viral coat protein and inhibit virus / cell interactions, have helped elaborate the basis of cellular susceptibility to viruses, as well as the mechanistic interactions which lead to viral infection (Bizebard *et al.* 1995). Other examples, related to this thesis, concern mAbs capable of competing with a cellular-receptor for its natural protein ligand. The isolation and characterization of such mAbs, allows one to have in some instances, a privileged insight into the modalities which take place between the receptor and the ligand (Amati *et al.* 1995; Smith *et al.* 1994; Taub *et al.* 1989), and to appreciate the sometimes complex structural rearrangements which may need to be adopted by the receptor, in order for it to become ligand-active (Faull *et al.* 1996). Advances in the field of molecular biology and structural chemistry have allowed

for the rapid expansion of knowledge concerning macromolecular interactions, which include the recognition processes in antibody / antigen complexes (Jones *et al.* 1996; Davies *et al* 1996; Padlan E., 1994).

Recently, it has not only been established that antibody molecules have the ability to emulate cellular protein receptors in their physical recognition of a protein ligand (Ducancel *et al.* 1996; Monfardini *et al.* 1996; Smith *et al.* 1994), but in addition some have been found to even display the selectivity which is seen to occur with a receptor and the many ligands which it may recognize with different affinities (Kunicki *et al.* 1997). In these regards, and with the availability of two mAbs known to be specific for the LDL receptor-binding site of apolipoprotein E (apoE) (Milne *et al.* 1981; Innerarity *et al.* unpublished observations), I attempted to better understand the biological interactions which occur between these antibodies and apoE.

The feature which best serves to characterize my Ph.D. graduate research training, is directly related to the development of novel recombinant mAbs. More specifically, having resorted to the application of recombinant DNA technology to the field of immunochemistry, I succeeded to further exploit the usefulness of two pre-existing mAbs. In fact, by altering the primary structure of a mAb which has as epitope the LDLr biding site of apoE, I developed a series of recombinant forms of the parental antibody, which like the LDLr, recognize apoE in a conformation-sensitive manner.

In Chapter V of this thesis, I have presented a mutational analysis of mAb 2E8. The goal of this study was to initiate a preliminary study concerning a possible molecular mimicry of the LDLr by the antibody, in apoE recognition. The impetus for this study was the existing homology in primary structure between the heavy chain CDR2 of the antibody, and repeat 5 of the LDLr. As I demonstrated in the result section of Chapter V, the heavy chain CDR2 does contribute significantly to apoE binding, and it appears to do so in a way which may be similar to the way in which the LDLr recognizes apoE. In Chapter V, I demonstrated that when the sequence of this CDR was altered so as to allow it to more closely resemble the fifth repeat of the LDLr, the antibody's behavior towards apoE changed in a way which mirrored the binding capability of the repeat in question. More importantly however, was the display of a cross-reactivenes towards the LDLr's second physiological lipoprotein ligand, apoB-100, when the antibody's CDR2 was altered to resemble the primary structure of the LDLr consensus sequence.

As detailed in section 2 of Chapter I, the ligand binding domain of the LDLr is an ordered assembly of a repeated structure. This structure, often referred to as the cysteine-rich repeat, is now known to adopt a tertiary structure based on an assembly of three specific loops. Indeed, through an ordered disulfide bond assembly which has been well defined (Figure VI-1), the sequence of this polypeptide addopts a conformation which, when in conjunction with the other members of the domain, allows the LDLr to cross-react with both apoE and apoB-100. Through an exhaustive mutational analysis of this domain, in addition to the availability of naturally occurring variants, it was concluded that each one of these repeats functions independently of each other in binding to both

ligands. The collective effect, resulting from the added individual contacts, results in the observed high affinity binding between the LDLr and its two ligands. An important conclusion resulting from the mutational analysis of the LDLr, was the finding that repeat 5 was instrumental in binding apoE-enriched lipoproteins. Hence, the structural difference present between this repeat and the six others, endows it with the most cross-reactive potential.

With the results of the 2E8 heavy chain CDR2 mutational analysis in mind, I argue in this thesis that this segment of the antibody adopts a molecular structure similar to the one which characterizes the cysteine-rich repeats of the LDLr. Moreover, I propose that the looped structure of the heavy chain CDR2, which has recently been solved through X-ray chrystalography (Trakanov *et al.* submitted) (Figure VI-2), is not unlike the one adopted by the cysteine-rich repeat, shown schematically in Figure VI-1. As the primary structure of the antibody CDR was made to resemble either the LDLr repeat most involved in apoE or apoB-100 recognition, the phenotypic result consisted of an antigen-binding mimicry of the antibody for the receptor.

As shown in Figure VI-2, the surface which characterizes the 2E8 paratope, consists of a disproportionally arranged electrostatic potential. Four negatively charged residues residing in the heavy chain CDR2, in association with one from the heavy chain CDR1 and an another from the CDR3 of the same chain, collectively serve to generate an electro-negative rim within the antibody paratope, which presumably interacts with an electropositive epitope on apoE (Figure VI-2). Presently, without the solved X-ray crystal structure of the assembled immune complex, I am unable to conclusively

implicate this acidic portion of the paratope in apoE binding. However, owing to the observed phenotypic behavior of three altered forms of the antibody, which pertained to the alanine substituted acidic residues within the heavy chain CDRs, certain intelligent assumptions regarding the importance of these residues in the recognition process can be put forth.

The reduced apoE-binding reactivities of the two CDR3 alanine mutants, imply that the two aspartic acid residues contribute favorably to antigen binding. It is interesting that although the side chain of Asp^{99} is not displayed on the paratope surface, it nonetheless is important in contributing positively to apoE recognition. The loss of apoE recognition in this case may involve a slight structural rearrangement of the paratope, due perhaps a lost internal interaction with another residue as I argued in Chapter V. The slight decrease in apoE binding due to the loss of the surface-displayed Asp^{97} is in favor of the importance of the electronegative character of the paratope for proper antigen binding. The contribution of the acidic residues within the heavy chain CDR2 in apoE binding will be shortly assessed. The results relating to their contribution in the immune complex will most certainly be informative concerning the importance of the electrostatic component of the associated complex.

Of marked interest for apoE is the need for its lipid association in order for it to interact with high affinity with the LDLr (Innerarity *et al.* 1979). When incorporated into lipid emulsion particles, both of artificial or physiological origin, apoE is known to undergo conformational changes in its tertiary structure which, presumably serve to

render it competent for recognition by the LDLr (Weisgraber *et al.* 1992). This lipid driven alteration of apoE's tertiary structure is in some way specific, as LDLr-competent / incompetent forms of the protein are known to exist on the surface of circulating lipoproteins. The current mechanism thought to lead to the unfolding of the molecule when present in lipid emulsions, involves the opening of the four helix amino-terminal bundle, as shown in Figure VI-3. Observations relating to LDLr-incompetent forms of lipoprotein associated apoE, testify to the fact that not all lipoprotein associated apoE resides in an unfolded state. Alternatively, incompletely unfolded, or conversely, over unfolded forms of apoE may exist as subpopulations of the total lipoprotein-bound apoE. The state in which an apoE molecule finds itself in, when associated to lipid, is likely to be subject to the influence of its specific lipid environment. Thus, the hydrophobic character of the lipid emulsion surely modulates apoE's tertiary structure, in way in which it can be sensed by the LDLr. Interestingly, one of the recombinant forms of the 2E8 mAb which I generated by altering its heavy chain CDR2, and which I have shown to cross-react to apoB-100, also displays preference for lipid bound apoE. Through the repeated demonstration of the preference of this rFab for lipid-bound apoE, I have argued in Chapter V, in favor of the LDLr-mimesism of this antibody, in apoE recognition. Moreover, this argument was strengthened with the demonstration that the rFab also showed a preference for a receptor-competent form of apoE2, an observation also recorded by the LDLr.

The exact modalities which characterize apoE's lipid driven restructuration, and the resulting molecular structures which are generated by this occurrence, are key to this

protein's role in lipoprotein metabolism. Having generated a panel of recombinant mAbs which, unlike the parental hybridoma Fab, recognize physiologically relevant states of the protein, will certainly help study the biological basis of this protein's function.

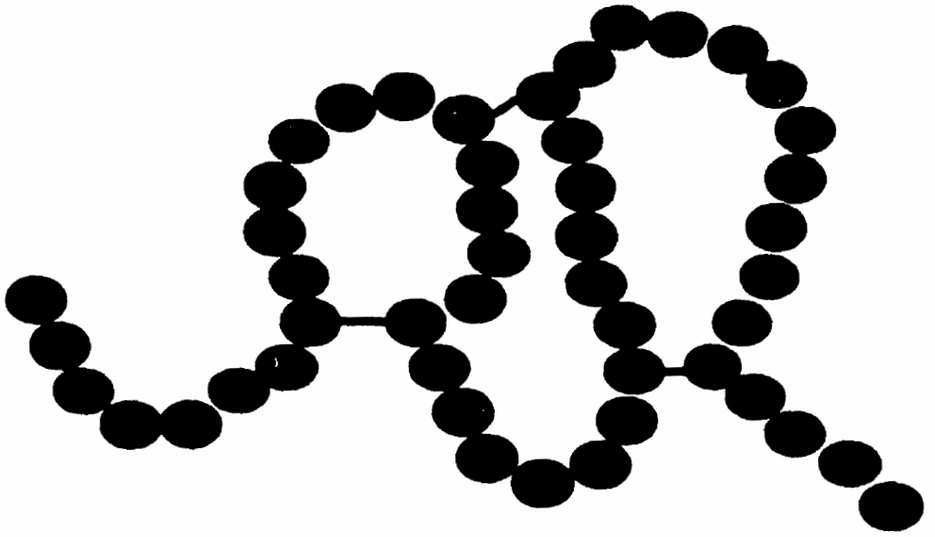

Figure VI-1 Disulfide bridges of cysteine-rich repeat number 2 of the LDL receptor ligand-binding domain.- This figure illustrates the disulfide bonding pattern which was determined to exists within one of the cysteine-rich repeats of the LDL receptor (Bieri et al. 1995). As shown in the figure, this segment of the protein is folded into three loops, owing to the covalent linkages between cysteines 1 and 3, 2 and 5, and finally 4 and 6 shown in black. Acidic residues, believed to be important in lipoprotein binding are shown in red.

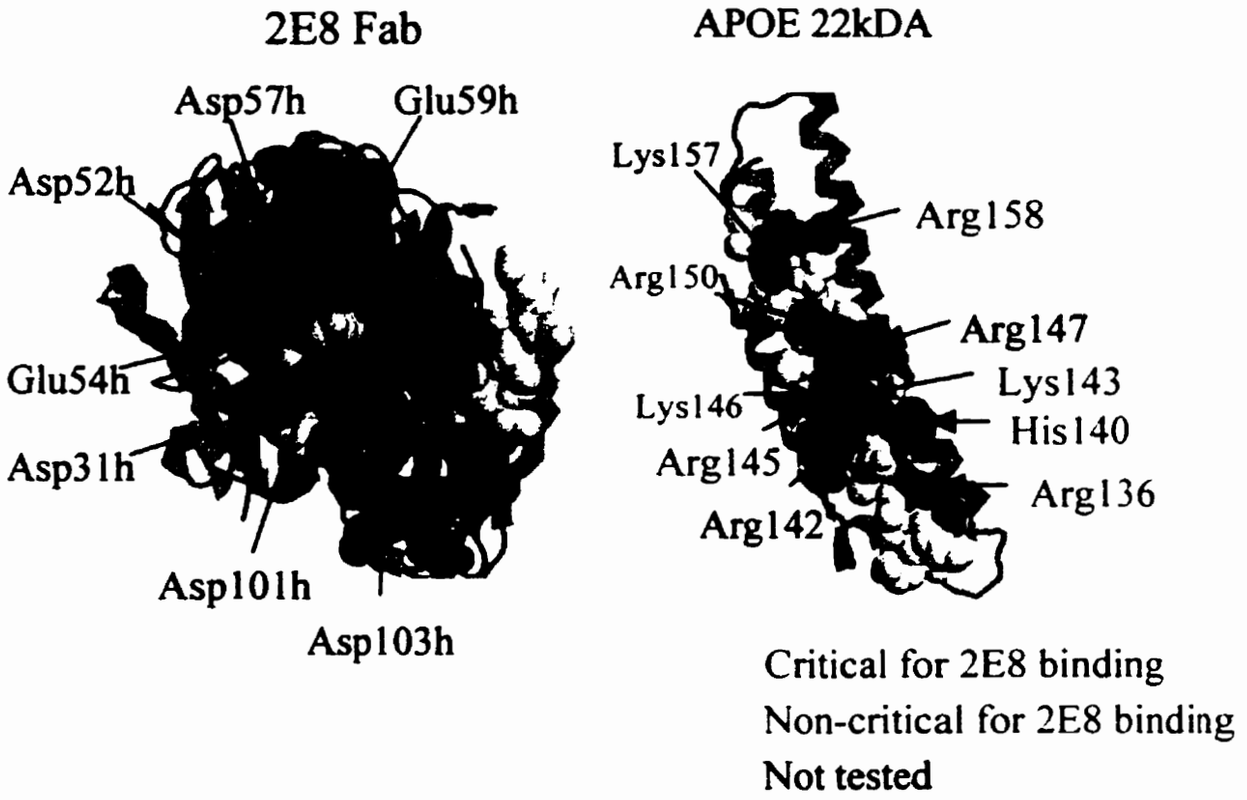

Figure VI-2 Charge complementarity between mAb 2E8 and ApoE.- This figure illustrates the charge complementarity which exists between the mAb 2E8 and apoE. The structure of the antibody paratope is shown as seen if looking down the parallel axis of the molecule. Residues belonging to the three heavy and light chain CDRs are shown as a space filled model, whereas the remainder of the antibody is shown as a ribbon model. Light and heavy chain CDRs 1, 2 and 3, are colored yellow, green and blue, respectively. Residues colored in red represent acidic amino acids, which are appropriately labled (Trakhanov *et al.* 1998). The 22 kDa fragment of apoE is shown as a ribbon model. Basic residues are shown in blue, and those involved in 2E8 binding are indicated.

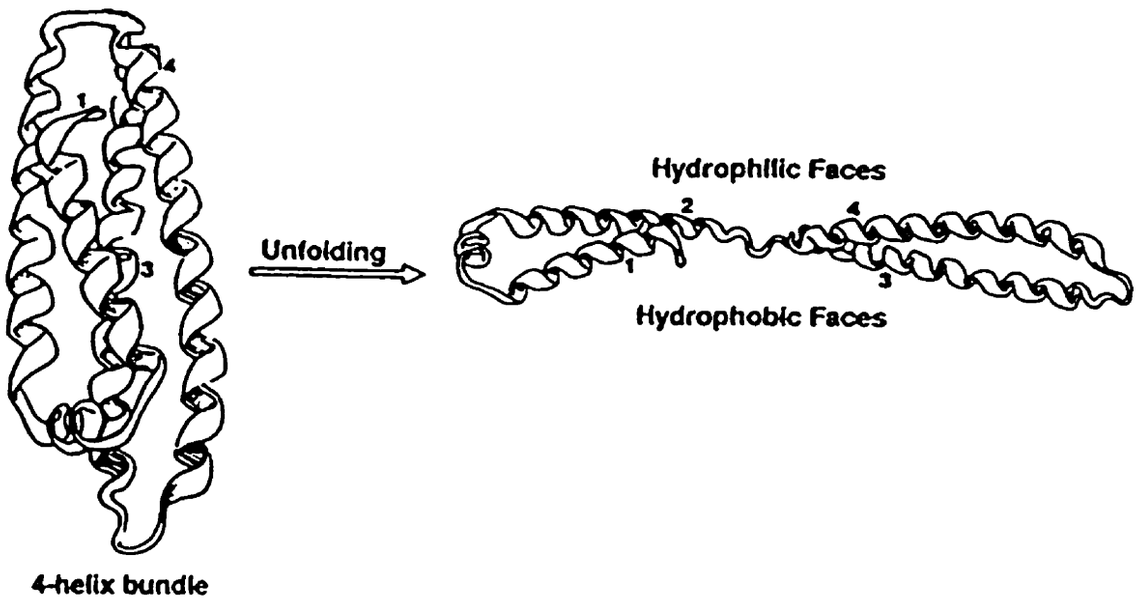

Figure VI-3 Lipid-driven molecular unfolding of apoE.- This figure depicts the postulated mode of molecular rearrangement which accounts for the lipid-driven unfolding of the 22 kDa fragment of apoE. As the protein is moved into a hydrophobic environment, it is known to unfold and occupy a larger surface area (Weisgraber, K.H., 1994). One way which would explain the protein's behavior in a hydrophobic environment, is shown by the figure, and would consist of the unfolding of the four-helix bundle.

References

Alt, F.W., and Baltimore, D. (1982). Joining of immunoglobulin heavy chain gene segments: implications from a chromosome with evidence of three D-J_H fusions. *Proc. Natl. Acad. Sci. USA* **79:** 4118-4122.

Aggerbeck, L.P., J.R. Wetterau, K.H. Weisgraber, C.-S.C. Wu, and F.T.Lindgren. 1988. Human apolipoprotein E3 in aqueous solution. II. Properties of the amino- and carboxyl-terminal domains. *J. Biol. Chem.* **263:** 6249-6258.

Amati, V., Werge, T.M., Cattaneo, A., and Tramontano, A. (1995). Identifying a putative common binding site shared by substance P receptor an anti-substance P monoclonal antibody. *Protein Engineering* 8: 403-408.

Amit, A.G., Mariuzza, R.A., Philips, S.E.V., Poljak, R.J. (1986). Three-dimensional structure of an antigen-antibody complex at 2.8 Å resolution. *Science*, **233:** 747-753.

Anderson, R.G.W., Brown, M.S., Goldstein, J.L. (1977). Role of the coated endocytic vesicle in the uptake of receptor-bound low density lipoprotein in human fibroblasts. *Cell* **10:** 351-364.

Anderson, R.G.W., Goldstein, J.L., Brown, M.S. (1976). Localization of low density lipoprotein receptors on plasma membrane of normal human fibroblasts and their absence in cells from a familial hypercholesterolemia homozygote. *Proc. Natl. Acad. Sci. USA* **73:** 2434-2438.

Anglister, J., and Zilber, B. (1990). Antibodies against a peptide of cholera toxin differing in cross-reactivity with the toxin differ in their specific interactions with the peptide as observed by 1H NMR spectroscopy. *Biochemistry* **29:** 921-928.

Arrhenius, S. (1907). Immunochemistry: The application of the principals of physical chemistry to the study of antibodies. *The Macmillan Company*: New York.

Avrameas. S., Ternynck, T. (1995). Natural autoantibodies: the other side of the immune system. *Research in Immunology*, **146:** 235-48.

Bacca M., Presta, L. G., O'Connor, S. J., and Wells, J. Antibody Humanization Using Monovalent Phage Display. *The Journal of Biological Chemistry*, 1997, **272**: 10679-10684.

Barbas, C.F., Languino, L.R., and Smith, J.W. (1993) *Proc. Natl. Acad. Sci. U.S.A.* **90:** 10003-10007

Bath, T.N., Bently, G.A., Boulot, G., Green, M.I., Tello, D., Dall'Acqua, W., Souchon, H., Schwarz, F.P., Mariuzza, R.A., Poljak, R.J. (1994). Bound watter molecules and conformational stabilization help mediate an antigen-antibody association, *Proc. Natl. Acad. Sci. USA* **91:** 1089-1093.

Basu, S.K., Brown, M.S., Ho, Y.K., Havel, R.J., Goldstein, J.L. (1981). Mouse macrophage synthesize and secrete a protein resembling apolipoprotein E. *Proc. Natl. Acad. Sci* **78:** 7545-7548.

Basu, S.K., Ho, Y.K., Brown, M.S., Bilheimer, D.W., Anderson, R.G.W., Goldstein, J.L. (1982) Biochemical and genetic studies of the apoprotein E secreted by mouse macrophages and human monocytes. *J. Biol. Chem.* **257:** 9788-9791.

Behring, E.A. and Kitasato, S. (1890) ‹ber das Zustandekommen der Diphtherie-Immunitat und der Tetanus-Immunitat bei Thieren. *Dtsh. med. Wochenschr.* **49,** 1113.

Behring, E.A. (1894) *Das neue Diphtherieheilmittel*, p.40. O. Hering, Berlin.

Beisigel, U., Kita, T., Anderson, R.G.W., Schneider, W.J., Brown, M.S., Goldstein, J.L. (1981). Immunologic cross-reactivity of the low density lipoprotein receptor from bovine adrenal cortex, human fibroblast, canine liver and adrenal gland, and rat liver. *J. Biol. Chem.* **256:** 4071-4078.

Beisigel, U., Weber, W., Bengtsson-Olivercona, G. (1991). Lipoprotein lipase enhances the binding of chylomicrons to low density lipoprotein receptor-related protein. *Proc. Natl. Acad. Sci. USA* **88:** 8342-8346.

Better, M., Chang, C.P., Robinson, R.R., Horwitz, A.H. (1988). Escherichia coli secretion of an active chimeric antibody fragment. *Science* **240:** 1041-1043.

Bereck, C., and Milstein, C. (1987). Mutation drift and repertoire shift in the maturation of the immune response. *Immunol. Rev.* 96: 23-41.

Bieri, S., Djordjevic, J.T., Daly, N.L., Smith, R., and Kroon, P.A. (1995). Disulfide bridges of a cysteine-rich repeat of the LDL receptor ligand-binding domain. *Biochemistry*, **34:**13059-13065.

Biocca, S., Pierandrei-Amaldi, P., Campioni, N., and Cattaneo, A. Intracellular Immunization with cytosolic recombinant antibodies. *Bio/Technology*, 1994, **12**: 396-399.

Bizebard, T., Gigant, B.,. Rigolet, P., Rasmussen, B., Diat, O., Bosecke, P., Wharton, S.A., Skehel, J.J., Knossow, M. (1995). Structure of influenza virus haemagglutinin complexed with a neutralizing antibody. *Nature* **376:** 92-94.

Blacklow, S.C., Kim, P.S. (1996). Protein folding and calcium binding defects arising from familial hypercholesterolemia mutations of the LDL receptor. *Nature Structural Biology*, **3:** 758-762.

Borensztajn, J., Getz, G.S., Kotlar, T., (1988). Uptake of chylomicron remnats by the liver: Further evidence for the modulating role of phospholipids. *J Lipid Res.* **29:** 1087-1092.

Bowden, G.A. and Georgiou, G. (1990) Folding and aggregation of β-lactamase in the periplasmic space of Escherichia coli. *The Journal of Biological Chemistry* **265:** 16760-16765.

Bradley , W.A., S-L. C. Hwang, J.B. Karlin, A.H.Y. Lin, S.C. Prasad, A.M. Gotto, and S.H. Gianturco. 1984. Low-density lipoprotein receptor binding determinants switch from apolipoprotein E to apolipoprotein B during cnversion of hypertriglyceridemic very-low-density lipoprotein to low-density lipoproteins. *J. Biol. Chem.* **259:** 14728-14735.

Bradley, W.A., and Gianturco, S.H. (1994). Triglyceride-rich lipoproteins and atherosclerosis: pathophysiological considerations. *J. of Internal Medicine suppl.* **736:** 33-39.

Brasaemle, D.L., Cornely-Moss, K., and Bensadouin A. (1993) Hepatic lipase treatment of chylomicron remnants increases exposure of apolipoprotein E. *Journal of Lipid Research*, **34:** 455-465.

Brenninkmeijer, B.J., Stuyt, P.M.J., Demacker, P.M.N., Stalenhoef, A.F.H., and A. van't Laar. (1987). Catabolism of chylomicron remnants in normolipidemic subjects in relation to the apoprotein E phenotype. *J. Lipid Res.* **28:** 361-370.

Bretscher, M.S., Pearse, B.M.F. (1984). Coated pits in action. *Cell* **38:** 3-4.

Braden, B.C., and Poljak, R.J. (1995) Structural features of the reactions between antibodies and protein antigens. *FASEB J.*, **9:** 9-16.

Brenner, B.M., Ballermann, B.J., Gunning. M.E., Zeidel, M.L., Diverse biological actions of atrial natriuretic peptide. (1990) *Physiological Reviews* **70:** 665-699.

Breslow, JL. (1996) Mouse models of atherosclerosis. *Science* **272:** 685-688.

Bruck, C., M.S. Co, M. Slaoui, G.N. Gaulton, T. Smith, B.N. Fields, J.I. Mullins, and M.I. Greene.1986. Nucleic acid sequence of an internal image-bearing monoclonal anti-idiotype and its comparison to the sequence of the external antigen. *Proc. Natl. Acad. Sci. USA.* **83:** 6578-6582.

Bruneau, B.G., and de Bold, A.J. (1994). Selective changes in natriuretic peptide and early response gene expression in isolated rat atria following stimulation by stretch or endothelin-1. *Cardiovascular Research*, **28:** 1519-1525.

Brown, M.S., Deuel, T.F., Basu, S.K., and Goldstein, J.L. 1978. Inhibition of the binding of low-density lipoprotein to its cell surface receptor in human fibroblasts by positively charged proteins. *J. Supramol. Struc.* **8:** 223-234.

Brown, M.S., and Goldstein, J.L. (1986). A receptor mediated pathway for cholesterol homeostasis. *Science* **232:** 34-42.

Burton, D.R., and Barbas, C.F. III. (1994). Human antibodies from combinatorial libraries. *Adv. in Immunol.* **57:** 191-280.

de Bold, A.J., Borenstein, H.B., Veress, A.T., and Sonnenberg, H. (1981) A rapid and potent natriuretic response to intravenous injection of atrial myocardial extract in rats. Life Sciences **28:** 89-94.

de Bold, A.J. (1985). Atrial natriuretic factor: A hormone produced by the heart. *Science*, **230:** 767-770.

Brown, A.J., and D.C.K. Roberts. (1991). The effect of fasting triacylglyceride concentration and apolipoprotein E polymorphism on postprandial lipemia. *Arterioscler. Thromb.* **11:** 1737-1744.

Brunzell, J.D., Familial lipoprotein lipase deficiency and other causes of the chylomycronemia syndrome, in Scriver C.R., Beaudet, A.L., Sly, W.S., Valle, D. (eds): The Metabolic Basis of Inherited Disease, 7th ed. New York, McGraw-Hill, 1995, vol. II 1985-2012.

Chang, M.S., Lowe, D.G., Lewis, M., Hellmiss, R., Chen, E., Goeddel, D.V. (1989). Differential activation by atrial and brain natriuretic peptides of two different receptor guanylate cyclases. *Nature* **341:** 68-72.

Chapeau, C., Gutkowska, J., Schiller, P.W., Milne, R.W., Thibeault, G., Garcia, R., Genest, J. and Cantin, M. (1985). Localization of immunoreactive synthetic atrial natriuretic factor (ANF) in the heart of various animal species. *J. Histochem. Cytochem.* **33:** 541-550.

Chinkers, M., Garbers, D.L., Chang, M.S., Lowe, D.G., Chin, H.M., Goeddel, D.V., Schulz, S. (1989). A membrane form of guanylate cyclase is an atrial natriuretic peptide receptor. *Nature* **338:** 78-83.

Chomczmski, P., and N. Sacchi. 1987. Single-step method of RNA isolation by acid guanidium thiocyanate-phenol-chloroform extraction. *Anal. Biochemistry.* **162:** 156-159.

Chothia, C., Lesk, A.M., Tramontano, A., Levitt, M., Smith-Gill, S.J., Air, G., Sheriff, S., Padlan, E.A., Davies, D., Tulip, W.R., Colman, P.M., Spinelli, S., Alzari, P.M., and Poljak, R.J. (1989). Conformation of immunoglobulin hypervariable regions. *Nature* **342:** 877-883.

Chuck, S.L., and Lingappa, V.R. (1993) Analysis of a pause transfer sequence from apolipoprotein B. *Journal of Biological Chemistry* **268:** 22794-22801

Clackson, T., and Wells, J.A. (1995). A hot spot of binding energy in a hormone-receptor interface. *Science* **267:** 383-386.

Clayton, L.K., Goodman, E.W., Brascomb, E.W., and Galas, D.J. (1979). Error induction and correction by mutant and wild type T4 DNA polymerases: Kinetic error discrimination mechanisms. *The Journal of Biological Chemistry*. 254:1902-1912.

Cushing, S.D., Berliner, J.A., Valente, A.J., Territo, M.C., Navab, M., Parhami, F., Gerrity, R., Schwartz, C.J., Fogelman, A.M. (1990). Minimally modified low density lipoprotein induces monocyte chemotactic protein 1 in human endothelial cells and smooth muscle cells. *Proc. Natl. Acad. Sci. USA* **87:** 5134-5138.

Cybulsky, M.I., Gimborne, M.A.,Jr., (1991) Endothelial expression of a mononuclear leukocyte adhesion molecule during atherogenesis. *Science*. **251:** 788-791.

Cygler, M., Rose, D.R., Bundle, D.R. (1991). Recognition of a cell-surface oligosaccharide of pathogenic Salmonella by an antibody Fab fragment. *Science* **253:** 442-445.

Czekay, R.P., Orlando, R.A., Woodward, L., Lundstrom, M., and Farquhar, G. (1997). Endocytic trafficking of megalin/rap complexes: Dissociation of the complexes in late endosomes. *Molecular biology of the Cell* **8:** 517-532.

Daly, N.L., Djordjevic, J.T., Kroon, P.A., Smith, R. (1995). Three-dimensional structure of the second cysteine-rich repeat from the human low-density lipoprotein receptor *Biochemistry* **34:** 14474-14481.

Daly, N.L., Scanlon, M.J., Djordjevic, J.T., Kroon, P.A., Smith, R. (1995). Three-dimensional structure of a cysteine-rich repeat from the low-density lipoprotein receptor. *Proc. Natl. Acad. Sci. USA* **92:** 6334-6338.

Das, H.K., McPherson, J., Bruins, G.A.P., Karathanasis, S.K., Breslow, J.L. (1985). Isolation, characterization, and mapping to chromosome 19 of the human apolipoprotein E gene. *J. Biol. Chem.* **260:** 6240-6244.

Davignon, J., R.E. Gregg, and C.F. Sing. 1988. Apolipoprotein E polymorphism and atherosclerosis. *Arteriosclerosis*. **8:** 1-21.

Davies, D.R., Sheriff, S., and Padlan, E. (1990). Antibody-antigen complexes. *Annul. Rev. of Biochem.*

Davies, D.R., and Cohen, G,H. (1996). Interactions of protein antigens with antibodies. *Proc. Natl. Acad. Sci.* **93:** 7-12.

Davis, G.C., J.L. Goldstein, T.C. S¸dhof, R.G.W. Anderson, D.W. Russell, and M.S. Brown. 1987. Acid-dependent ligand dissociation and recycling of LDL receptor mediated by growth factor homology region. *Nature* **326:** 760-765.

Davis, R.A., and Vance, J.E., (1996). Structure, assembly and secretion of lipoproteins. In "Biochemistry of lipids, lipoproteins and membranes". Vance, D.E., and Vance, J.E., (eds) Elsivier Science pp. 473-492.

Demant, T., Bedford, D., Packard, C.J., and Shepard, J. (1991). Influence of apolipoprotein E polymorphism on apolipoprotein B-100 metabolism in normolipemic subjects. *J. Clin. Invest.* **88:** 1490-1501

Doolittle, M.H., Wong, H., Davis, R.C., Schotz, M.C. (1987). Synthesis of hepatic lipase in liver and extrahepatic tissues. *J. lipid Res.* **28:** 1326-1331.

Dong, L.M., Wilson, C., Wardell, M.R., Simmons, T., Mahley, R.W., Weisgraber, K.H., Agard., D.A. (1994) Human apolipoprotein E. Role of arginine 61 in mediating the lipoprotein preferences of the E3 and E4 isoforms. *J. Biol. Chem.* **269:** 22358-22365.

Dong, L.M., and Weisgraber, K.H. (1996) Human apolipoprotein E4 domain interaction. Arginine 61 and glutamic acid 255 interact to direct the preference for very low density lipoproteins. *J. Biol. Chem.* **271:**19053-19057.

Dong, L.M., Parkin, S., Trakhanov, S.D., Rupp, B., Simmons, T., Arnold, K.S., Newhouse, Y.M., Innerarity, T.L., Weisgraber, K.H. (1996). Novel mechanism for defective receptor binding of apolipoprotein E2 in type III hyperlipoproteinemia. *Nature Structural Biology*, **3:** 718-722.

Downing, A.K., Knott, V., Werner, J.M., Cardy, C.M., Campbell, I.D., Handford, P.A. (1996). Solution structure of a pair of calcium-binding epidermal growth factor-like domains: implications for the Marfan syndrome and other genetic disorders. *Cell,* **85:** 597-605.

Ducancel, F., Merienne, K., Fromen-Romano, C., Tremeau, O., Pillet, L., Drevet, P., Zinn-Justin, S., Boulain, J.-C., and MÈnez, A. (1996). Mimicry between receptors and antibodies. *The Journal of Biological Chemistry* **271:** 31345-31353

Duncan, E.A., Brown M.S., Goldstein J.L., and Sakai J. (1997). Cleavage site for sterol-regulated protease localized to a leu-Ser bond in the lumenal loop of sterol regulatory element-binding protein-2. *Journal of Biological Chemistry*, 1997 **272:** 12778-12785.

Dyer, C.A., and L.K. Curtiss. (1991). A synthetic peptide mimic of plasma ApoE that binds the LDL receptor. *J. Biol. Chem.* **266:** 22803-22806.

Dyson, H.J., Lerner, R.A., Riechmann, L., and Tsang, P. (1990). Antigen-Antibody interactions: an NMR approach. *Biochem. Pharmacol.* **40:** 83-88.

Espiner, E.A., Crozier, I.G., Nicholls, M.G., Cuneo, R., Yandle, T.G., and Ikram, H. (1985). Cardiac secretion of atrial natriuretic peptide *Lancet* **2:** 398-399.

Esser, V., L.E. Limbird, M.S. Brown, J.L. Goldstein, and D.W. Russell. 1988. Mutational analysis of the ligand binding domain of the low density lipoprotein receptor. *J Biol Chem.* **263:** 13282-13290.

Ey, P.L., S.T. Prowse, and C.R. Jenkin. 1978. Isolation of pure IgG1, IgG2a and IgG2b immunoglobulin from mouse serum using protein-A Sepharose. *Immunochemistry* **15:** 429-436.

Fairbrother, W.J., McDowell, R.S., and Cunningham, B.C. (1994). Solution conformation of an atrial natriuretic peptide variant selective for the type A receptor. *Biochemistry* **33:** 8897-8804.

Feldman D.L., Hoff, H.F., Gerrity, R.G. (1984). Immunohistochemical localization of apolipoprotein B in aortas from hyperlipedimic swine. Preferential accumulation in lesion-prone areas. *Archives of Pathology and laboratory Medicine*, **108:** 817-822.

Fersht, A.R., Knill-Jones, J.W., and Tsui, W.C. 1982. Kinetic basis of spontaneous mutations. Misincorporation frequencies, proofreading specificities and cost of proofreading by DNA polymerases of *Escherichia coli*. *The Journal of Molecular Biology* **156:**37-51.

Fesik, S.W., Holleman, W.H., Perun, T.J. (1985). Two-dimensional 1H NMR studies of rat atrial natriuretic factor (1-23). Biochemical and Biophysical Research Communications **131:** 517-523.

Fielding, C.J., Fielding, P.E(1995). Molecular physiology of reverse cholesterol transport. *J. Lipid Res.* **36:** 211-228.

Fields, B.A., Goldbaum, F.A., Ysern, X., Poljak, R.J., Mariuzza, R.A.(1995) Molecular basis of antigen mimicry by an anti-idiotope. *Nature* **374:** 739-42.

Fields, B.A., Goldbaum, F.A., Dall'Acqua, W., Malchiodi, E.L., Cauerhff, a., Schwarz, F.P., Ysern, X., Poljak, R.J., Mariuzza, R.A. (1996). Hydrogen bonding and solvent structure in an antigen-antibody interface. Crystal structure and thermodynamic characterization of three of three Fv mutants complexed with lysozyme. *Biochemistry.* **35:** 15494-15503.

Flynn, G.T., de Bold, M.L., and de Bold A.J. (1983) The amino acid sequence of an atrial peptide with potent diuretic and natriuretic properties. *Biochem. Biophys. Res. Commun.* **117:** 859-865.

Garcia, K.C., Ronco, P.M., Verroust, P.J., Brünger, A.T., Amzel, L.M. (1992). Three-dimensional structure of an angiotensin II-Fab complex at 3 Å: hormone recognition by an anti-idiotypic antibody. *Science* **257:** 502-507.

Gerrity, R.G., Naito, H.K., Richardson, M., Schwartz, C.J. (1979) Dietary induced atherogenesis in swine. Morphology of the intima in prelesion stages. *American Journal of Pathology*, **95:** 775-92.

Giantonio, B.J., Alpaugh, R.K., Schultz, J., McAleer, C., Newton, D.W., Shannon, B. Guedez, Y., Kotb, M., Vitek, L., and Persson, R. (1997) Superantigen-based immunotherapy: a phase I trial of PNU-214565, a monoclonal antibody-staphylococcal enterotoxin A recombinant fusion protein, in advanced pancreatic and colorectal cancer. *J. of Clin. Oncology*, **15:**1994-2007.

Gidlof, C., Dohlsten, M., Lando, P., Kalland, T., Sundstrom, C., Totterman, T.H. (1997). A superantigen-antibody fusion protein for T-cell immunotherapy of human B-lineage malignancies. *Blood* **89:** 2089-97.

Gimbrone, M.A. Jr., Kume, N., and Cybulsky, M.I. (1993). Vascular endothelial dysfunction and the pathogenesis of atherosclerosis. In "Atherosclerosis : Cellular Interactions, growth factors, and lipids".

Glomset, J.A., (1968) The plasma lecithin:cholesterol acyltransferase reaction. *J. Lipid Res.* **9:** 155-158.

Gofman, J.W., Lindgren, F.T., and Elliott, H. (1949). Ultracentrifugal studies of lipoproteins of human serum. ***J. Biol. Chem.*** 179: **973-975.**

Goldbaum FA; Schwarz FP; Eisenstein E; Cauerhff A; Mariuzza RA; Poljak RJ. (1996) The effect of water activity on the association constant and the enthalpy of reaction between lysozyme and the specific antibodies D1.3 and D44.1. *Journal of Molecular Recognition* **9:** 6-12.

Goldstein, J.L., Brown, M.S., (1974) Binding and degradation of low density lipoproteins by cultured human fibroblasts: Comparison of cells from a normal subject and from a patient with familial hypercholesterolemia. *J. Biol. Chem.* **259:** 5153-5162.

Goldstein, J.L., Brown, M.S., Anderson, R.G.W., Russell, D.W., and Schneider, W. J. (1985). Receptor-mediated endocytosis: Concepts emrging from the LDL receptor system. *Annu. Rev. Cell Biol.* **1:** 1-39

Gordon, D.A., Jamil, H., Sharp, D., Mullaney, D., Yao, Z., Gregg, R.E., Wetterau, J. (1995). Secretion of apolipoprotein B-containing lipoproteins from HeLa cells is dependent on expression of the microsomal triglyceride transfer protein and is regulated by lipid availability. *Proc. Natl. Acad. Sci. USA* **91:** 7628-7632.

Gould et al. 1953 . Cholesterol metabolism *Journal of Biological Chemistry* **201:**519-523.

Goodman, M. F. (1995). DNA polymerase fidelity: Misincorporation and mismatched extensions. In *PCR Strategies*, 17-31. Acdemic Press. Ed. Innis, M.A., Gelfand, D.H. and Sninsky, J.J.

Gregg, R.E., Zech, L.A., Schaefer, E.J., Stark, D., Wilson, D., and Brewer Jr, H.B.,. (1986). Abnormal in vivo metabolism of apolipoprotein E_4 in humans. *J. Clin. Invest.* **78:** 815-821.

Gronski, P., Seiler, F.R., and Schwick, H.G. (1991). Discovery of antitoxins and development of antibody preparations for clinical uses from 1890 to 1990. *Molecular Immunology*. **28:** 1321-1332.

Guyton, J.R., (1995). The role of lipoproteins in atherogenesis. *Adv. in Exp. Med. and Biol.*, **369:** 29-38.

Hamilton, R.L., Wong, J.S., Guo, L.S.S., Krisans, S., Havel, R.J. (1990). Apolipoprotein E localization in rat hepatocytes by immunogold labeling of cryothin sections. *J. Lipid Res. 31:* 1589-1594.

Hansson, J., Ohlsson, L., Persson, R., Andersson, G., Ilback, N.G., Litton, M.J., Kalland, T., Dohlsten, M. (1997) Genetically engineered superantigens as tolerable antitumor agents. . *Proc. Natl. Acad. Sci.* USA **94:** 2489-94.

Havel, R.J., Chylomicron remnants: hepatic receptors and metabolism. (1995). Current Opinion in Lipidology. **6:** 312-316.

Hawkins, R.E., Russell, S.J., Baier, M., and Winter, G. (1993). The contribution of contact and non-contact residues of antibody in the affinity of binding with antigen. The interaction of mutant D1.3 antibodies with lysozyme. *The Journal of Molecular Biology*, **234:** 958-964.

Haynes, M.R., Stura, E.A., Hilvert, D., and Wilson, I. A. (1994) *Science*, **263:** 646-652.

Helenius, A., Mellman, I., Wall, D., Hubbard, A., (1983). Endosomes. *Trends biochem. Sci.* **8:** 254-250.

Herz, J., Hamann, U, Rogne, S., Myklebost, O., Gausepohl, H., Stanley, K.K. (1988). Surface location and high affinity for calcium of a 550-kDa liver membrane protein closely related to the LDL-receptor suggest a physiological role as lipoprotein receptor. *EMBO J.* **7:** 4119-4122.

Higushi, R., Krummel, B., and Saiki, R.K. (1988) *Nucleic acids Research.* **16:** 7351-7367.

Higgins, G.A., Large, C.H., Rupniak, H.T., and Barnes, J.C. (1997). Apolipoprotein E and Alzheimer's disease: A review of recent studies. *Pharm. Biochem. and behavior* **56:** 675-685.

Hixson, J.E., Vernier, D.T. (1990). Restriction isotyping of human apolipoprotein E by gene amplification and cleavage with Hpa. *J. Lipid Res.* **31:** 545-549.

Holmes M. A. and Foote, J. (1997) Structural Comsequences of Humanizating an Antibody. *The Journal of Immunology*, **158**: 2192-2201.

Honjo, T., M. Obata, Y.Yamawaki, T. Kataoka, T. Kawakami, N. Takahashi, and Y. Mano. 1979. Cloning and complete nucleotide sequence of the mouse immunoglobulin gamma 1 chain gene. *Cell.* **18:** 559-568.

Horie, Y., Fazio, S., Westerlund, J.R., Weisgraber, K.H., and Rall, S.C.,. (1992). The functional characteristics of a human apolipoprotein E variant (cysteine at residue 142) may explain its association with dominant expression of type-III hyperlipoproteinemia. *J. Biol. Chem.* **267:** 1962-1968

Hui, D.Y., T.L. Innerarity, R.W. Milne, Y.L. Marcel,, and R.W. Mahley. (1984). Binding of chylomicron remnants and β-very low density lipoproteins to hepatic and extrahepatic lipoprotein receptors. A process independent of apolipoprotein B48. *J. Biol. Chem.* **259:** 15060-15068.

Hui, D.Y., Innerarity, T.L., Mahley, R.W. (1984). Defective hepatic lipoprotein receptor binding of β-very low density lipoproteins from type III hyperlypoproteinemic patients. Importance of apolipoprotein E. *J. Biol. Chem.* **259:** 860-866.

Huettinger, M., Retzek, H., Herman, M., Goldenberg, H. (1992). Lactoferrin specifically inhibits endocytosis of chylomicron remnants but not α-macroglobulin *J. Biol. Chem.* **267:** 18551-18554.

Huse, W.D., L. Sastry, S.A. Iverson, A.S. Kang, M. Alting-Mees, D.R. Burton, S.T. Benkovic, and R.A. Lerner. (1989). Generation of a large combinatorial library of the immunoglobulin repertoire in phage lambda. *Science.* **246:** 1275-1281.

Hussain, M.M., Kancha, R.K., Zhou, Z., Luchoomun, J., Zu, H., Bakillah, A. (1996) Chylomicron assembly and catabolism: role of apolipoproteins and receptors. *Biochim Biophys Acta*, **1300:**151-70.

Hussain, M.M., Innerarity, T.L., Brecht, W.J., Mahley, R.W. (1995) Chylomicron metabolism in normal, cholesterol-fed, and Watanabe heritable hyperlipidemic rabbits. Saturation of the sequestration step of the remnant clearance pathway. *J. Biol. Chem.* **270:** 8578-8587.

Ingrahm, J.L., Maaløe, O., and Neidhardt, F.C. (1983). In Growth of the bacterial cell, Sinauer Associates, Inc. Publishers. Sundeilan, Massachusettes, 1983.

Innerarity, T.L., Mahley, R.W. (1978). Enhanced binding by cultured human fibroblasts of human apoE-containing lipoproteins as compared with low density lipoproteins. *Biochemistry* **17:** 1440-1446.

Innerarity, T.L., R.E. Pitas, and R.W. Mahley. 1979. Binding of arginine-rich (E) apoprotein after recombination with phospholipid vesicles to the low density lipoprotein receptors of fibroblasts. *J. Biol. Chem.* **254:** 4186-4190.

Innerarity, T.L., K.H. Weisgraber, K.S. Arnold, S.C. Rall Jr., and R.W. Mahley. (1984). Normalization of receptor binding of apolipoprotein E2. Evidence for modulation of the binding site conformation. *J. Biol. Chem.* **259:** 7261-7267.

Innerarity, T.L., Hui, D.Y., Bersot, T.P., Mahley, R.W. Type III hyperlipoproteinemia: A focus on lipoprotein receptor-apoE2 interactions, in Angel, A., Frolich, J., (eds): Lipoprotein Deficiency Syndromes, New York, Plenum, (1986), p. 273-286.

Jeffrey, P.D., Strong, R.K., Sieker, L.C., Chang, C.Y.Y., Campbell, R.L., Petsko, G.A., Haber, E., Margolies, M.N., Sheriff, S. (1993) 26-10 Fab-digoxin complex: Affinity and specificity due to surface complementarity. *Proc. Natl. Acad. Sci.* USA **90:** 10310-10314.

Jelesarov, I., Leder, L., and Rudolf Bosshard, H. (1996). Probing the energetics of antigen-antibody recognition by titration microcalorimetry. Methods: A Companion in Methods in Enzymology, **9:** 533-541.

Ji, Z.S., Brecht, W.J., Mirada, R.D., Hussain, M.M., Innerarity, T.I., Mahley, R.W. (1993). Role of heparan sulfate proteoglycans in the binding and uptake of apolipoprotein E-enriched remnant lipoproteins by cultured cells. *J. Biol. Chem* **268:** 10160-10165.

Ji. Z.S., Fasio, S., Lee, Y.L., Mahley, R.W. (1994). Secretion-capture role for apolipoprotein E in remnant lipoprotein metabolism involving cell surface haparan sulfate proteoglycans. *J. Biol. Chem.* **269:** 2764-2769.

Jonasson, L., Holm, J., Skalli, O., Bondjers, G., Hansson, G.K., (1986) Regional accumulations of T cells, macrophages, and smooth muscle cells in the human atherosclerotic plaque. *Arteriosclerosis* **6:** 131-138.

Josson, U., L. Fagerstam, B. Ivarsson, B. Johnsson, R. Karlsson, K, Lundh, S. Lofas, B. Persson, H. Roos, I. Ronnberg, S. Sjelander, E. Stenberg, R. Stahlberg, C. Urbaniczky, H. Astlin, and M. Malmqvist. 1991. Real-time biospecific interaction analysis using surface plasmon resonance and a sensor chip technology. *Bio Techniques* **11:** 620-627.

Kabat, E.A. (1968). Structural concepts in immunology and immunochemistry; Holt, Rinehart and Winston, Inc.: New York, 53-62.

Kabat, E.A., T.T. Wu, M. Reid-Miller, H.M. Perry, and K.S. Gottesman. 1991. In Sequences of Immunological Interest. US Public Health Service, National Institutes of Health, Bethesda, MD.

Kane, J.P. and Havel, R.L. (1995). Disorders of the biogenesis and secretion of lipoproteins containing the B apolipoproteins. in Scriver C.R., Beaudet, A.L., Sly, W.S., Valle, D. (eds): The Metabolic Basis of Inherited Disease, 7th ed. New York, McGraw-Hill, 1995, vol. II 1853-1885..

Kelsoe, G. (1996). The germinal center: a crucible for lymphocyte selection. *Seminars in Immunology* **8:** 179-184.

Kipriyanov, S.M., Moldenhauer, G., and Little, M. (1997). High level production of soluble single chain antibodies in small-scale *Escherichia coli* cultures. *Journal of Immunological Methods*, **200:** 69-77.

Kirstensen, T., Moestrup, S.K., Gliemann, J., Bendtsen, L., Sand, O., Sottrup-jensen, L. (1990). Evidence that the newly cloned low-density-lipoprotein receptor related protein (LRP) is the α_2-macroglobulin receptor. *FEBS lett.* **276:** 151-155.

Knott, T.J., S.C. Rall, T.L. Innerarity, S.F. Jacobson, M.S. Urdea, B. Levy-Wilson, L.M. Powell, R.J. Pease, R. Eddy, H. Nakai, M. Byers, L.M. Priestly, E. Robertson, L.B. Rall, C. Betsholtz, T.B. Shows, R.W. Mahley, and J. Scott. (1985). Human apolipoprotein B: structure of carboxyl-terminal domains, sites of gene expression and chromosomal localization. *Science* **230:** 37-43.

Koeler, G., and Milstein, C. (1975). Continuous cultures of fused cells secreting antibodies of pre-defined specificity. Nature, **256:** 495-497.

Koyama, S., Kobayashi, Y., Ohkubo, T., Kyogoku, Y., Sato, A., Kobayashi, M., Go, N. (1990). The differences in conformation between alpha-human atrial natriuretic polypeptide, alpha-hANP, and its derivative, Met(O)-alpha-hANP, in solution. *Protein Engineering* **3:** 393-402.

Kowal, R.C., Herz, J., Goldstein, J.L., Esser, V., Brown, M.S. (1989). Low density lipoprotein receptor-related protein mediates uptake of cholesteryl esters from apoprotein E-enriched lipoproteins. *Proc. Natl. Acad. Sci.* USA **86:** 5810-5814.

Krieger, M., and Herz, J. (1994). Structures and functions of multiligand lipoprotein receptors: macrophage scavenger receptors and LDL receptor-related protein (LRP). *Annu. Rev. of Biochem.* **63:** 601-637.

Kurosawa, Y., and S. Tonegawa. 1982. Organization, structure, and assembly of immunoglobulin heavy chain diversity DNA segments. *J. Exp. Med.* **155:** 201-218

Lalazar, A., K.H. Weisgraber, S.C. Rall, H. Giladi, T.I. Innerarity, A.Z. Levanon, J.K. Boyles, B. Amit, M. Gorecki, R.W. Mahley, and T. Vogel. 1988. Site-specific mutagenesis of human apolipoprotein E. Receptor binding activity of variants with single amino acid substitutions. *J. Biol. Chem.* **263:** 3542-3545.

Landsteiner, K. (1945). The specificity of serological reactions; Harvard University Press: Cambridge, Massachusetts, 1945, p 156.

LaRosa, J.C., Levy, R.I., Herbert, P., Lux, S.E., and Fredrickson, D.S. (1970) A specific apoprotein activator for lipoprotein lipase. *Biochem. Biophys. Res. Commun.* **41:** 57-62.

Laycock, M.V., Hirama, T., Hasnain, S., Watson, W., and Storer, A.C. (1989). Purification and characterization of a digestive cystein proteinase from the American lobster (Homarus americus). *Biochem. J.* **263:** 439-444.

Lawrence, M.C., and Colman, P.M. (1993) Shape complementarity at protein/protein interfaces. *The Journal of Molecular Biology*, **234:** 946-50.

Levi, M., Sallberg, M., Ruden, U., Herlyn, D., Maruyama, H., Wigzell, H., Marks, J., and Wahren, B. (1993). A complementary-determining region synthetic peptide acts as a miniantibody and neutralizes human immunodeficiency virus type 1 in vitro. *Proc. Natl. Acad. Sci.* USA **90:** 4374-4378.

Litton, M.J., Dohlsten, M., Hansson, J., Rosendahl, A., Ohlsson, L., Kalland, T., Andersson, J., Andersson, U. (1997). Tumor therapy with an antibody-targeted superantigen generates a dichotomy between local and systemic immune responses. *American Journal of Pathology.* **150:** 1607-1618.

Loh, E.Y., J.F. Elliot, S. Cwirla, L.L. Lanier, and M.M. Davis. (1989). Polymerase chain reaction with single-sided specificity: analysis of T cell receptor d chain. *Science* **243:** 217-220.

Macafferty, J., Griffith, A.D., Winter, G., Chiswell, D.J. (1990) Phage antibodies: filamentous phage displaying antibody variable domains. *Nature*, **348:** 552-554.

Malby, R.L., Tulip, W.R., Harley, V.R., Mckimm-Breschkin, J.L., Laver, W.G., Webster, R.G., and Colman, P.M. (1994). The structure of a complex between the NC10 antibody and influenza virus neuraminidase and comparison with the overlapping binding site of the NC41 antibody. *Current Biology* **2:** 733-746.

Mahley, R.W., Innerarity, T.L., Pitas, R.E., Weisgraber, K.H., Brown, J.H., and Gross, E. (1977). Inhibition of lipoprotein binding to cell surface receptors of fibroblasts following selective modification of arginyl residues in arginine-rich and B apoproteins. *J. Biol. Chem.* **252:** 7279-7287.

Mahley, R.W. (1988) Apoliproprotein E: Cholesterol transport protein with expanding role in cell biology. *Science*, **240:** 622-629.

Mahley et al (1979). Interaction of plasma lipoproteins containing apolipoprotein B and E with heparin and cell surface receptors. *Biochim. Biophys. Acta.* **575:** 81-85.

Mahley, R.W, and Rall, S.C. Jr., Type III hyperlipoproteinemia (Dysbetalipoproteinemia): The role of apolipoprotein E in normal and abnormal lipoprotein metabolism. In , in Scriver C.R., Beaudet, A.L., Sly, W.S., Valle, D. (eds): The Metabolic Basis of Inherited Disease, 7th ed. New York, McGraw-Hill, 1995, vol. II 1953-1980.

Makowski, L. Phage display: structure, assembly and engineering of filamentous bacteriophage M13. *Current Opinion in Structural Biology*1994, **4:** 225-230.

Manzato, E., Zambon, S., Marin, R., Baggio, G., Crepaldi, G. (1986). Modifications of plasma lipoproteins after lipase activation in patients with chylomicronemia. *J. Lipid Res.* **27:** 1248-1258.

Marcel, Y.L., M. Hogue, P.K. Weech, J. Davignon, and R. W. Milne. (1988). Expression of apolipoprotein B epitopes in lipoproteins. Relationship of conformation and function. *Arteriosclerosis* **8:** 832-844.

Max, E.E., J.V. Maizel, and P. Leder. (1981). The nucleotide sequence of a 5,5-kilobaseDNA segment containing the *k* immunoglobulin J and C region genes. *J. Biol. Chem.* **256:** 5116-5120.

McCoy, A.J., Epa, C.V., and Colman, P.M. (1997). Electrostatic complementarity at protein/protein interfaces. *J. Mol. Biol.* **266:** 570-584.

Meerman, H.J., and Georgiou G. Construction and characterization of a set of E.coli stains deficient in all known loci affecting the proteolytic stability of secreted recombinant proteins. *Bio/Technology* (1994) **12:** 1107-1110.

Menzel, H.J., Uttermann, G., (1986). Apolipoproetein E phenotyping from serum by western blotting. *Electrophoresis* **7:** 492-495.

McCafferty J, H.R. Hoogenboom, and D.J. Chiswell. *Antibody Engineering a Practical Approach*,Series Editor: B.D. Hames, Oxford University Press, (1996).Padlan, E.A. in *Antibody-Antigen Complexes*. (1994), Landes Ed. Austin, TX.

McEver, R. P. (1993). Receptor-mediated interactions of leukocytes with platelets and endothelium. In "Atherosclerosis : Cellular Interactions, growth factors, and lipids".

Mian, I.S., A.R. Bradwell, and A.J. Olson. (1991). Structure, function and properties of antibody binding sites. *J. Mol. Biol.* **217:** 133-151.

Milne, R.W., P. Douste-Blazy, Y.L. Marcel, and L. Retegui. (1981). Characterization of monoclonal antibodies against human apolipoprotein E. *J. Clin. Invest.* **68:** 111-117.

Milne, R.W., R. Theolis Jr., R.B. Verdery, and Y.L. Marcel. (1983). Characterization of monoclonal antibodies against human low density lipoprotein. *Arteriosclerosis* **3:** 23-30.

Milne, R.W., Gutkowska, J., Thibault, G., Schiller, P., Charbonneau, C., Genest, J., and Cantin, M. (1987). A murine monoclonal antibody against rat atrial natriuretic factor (ANF) which cross-reacts with mouse ANF. *Molecular Immunology*, **24:** 127-132

Milne, R.W, AND Gutkowska, J. (1996) Atrial natriuretic factor (ANF) prohormone accumulates in the IgG fraction of anti-ANF hybridoma-bearing mice. *Biochem. Biophys. Res. Commun.* **218**: 665-669.

Milstein, C. (1990). The Crooninan Lecture, Antibodies : a paradigm for the biology of molecular recognition. *Proc. R. Soc. Lond.* **239:** 1-16.

Montalto, M.B., and Bensadoun, A. (1993). Lipoprotein Lipase synthesis and secretion: effects of concentration and type of fatty acids in adipocyte cell culture. *J. Lipid Res.* **34:** 397-407.

Mullis, K.B., and F.A. Faloona. 1987. Specific synthesis of DNA in vitro via a polymerase-catalyzed chain reaction. *Methods Enzymol.* **155:** 335-350.

Myszka, D.G. (1996). Kinetic analysis of macromolecular interactions using surface plasmon resonance biosensors. *Current Opinion in Biotechnology*. **8:** 50-57.

Neri, D., Petrul, H., Roncucci, G. (1995). Engineering recombinant antibodies for immunotherapy. *Cell Biophysics*, **27:** 47-61.

Neri D; Montigiani S; Kirkham PM. (1996). Biophysical methods for the determination of antibody-antigen affinities. *Trends Biotechnol.* **14:** 465-470.

Novotny, J., Sharp, K. (1992). Electrostatic fields in antibodies and antibody/antigen complexes. *Prog. Biophys. molec. Biol.*, **58:** 203-224.

Nykjaer, A., Kjoller, L., Cohen, R.L., Lawrence, D.A., Garni-Wagner, B.A., Todd, R.F.3rd , van Zonneveld, A.J., Gliemann, J., Andreasen, P.A. (1994). Regions involved in binding of urokinase-type-1 inhibitor complex and pro-urokinase to the endocytic alpha 2-macroglobulin receptor/low density lipoprotein receptor-related protein. Evidence that the urokinase receptor protects pro-urokinase against binding to the endocytic receptor. *J. Biol. Chem.* **269:** 25668-25676.

Olejniczak ET; Gampe RT Jr; Rockway TW; Fesik SW. (1988). NMR study of the solution conformation of rat atrial natriuretic factor 7-23 in sodium dodecyl sulfate micelles.*Biochemistry*, **27:** 7124-7131.

O'Shannesy, D. J., M. Brigham-Burke, K.K. Soneson, P. Hensley, and I. Brooks. 1993. Determination of rate and equilibrium binding constants for macromolecular interactions using surface plasmon resonance: Use of nonlinear least squares analysis methods. *Anal. Biochem.* **212:** 457-468.

Padlan, E.A., Cohen, G.H., Davies, D.R. On the specificity of antibody/antigen interactions: Phosphocoline binding to McPC603 and the correlation of three-dimensional structure and sequence data. (1985) *Ann. Inst. Pasteur/Immunol.* **136C:** 271-276.

Padlan, E.A., (1994) Anatomy of the antibody molecule. *Mol. Immunol.* **31:** 169-217.

Paik, Y.K., Chang, D.J., Reardon, C.A., Davies, G.E., Mahley, R.W., Taylor, J.M. (1985). Nucleotide sequence and structure of the human apolipoprotein E gene. *Proc. Natl. Acad. Sci.* USA **82:** 3445-3449.

Pastan, I. H., Willingham, M.C. (1983). Receptor-mediated endocytosis: Coated pits, receptosomes and the Golgi. *Trends Biochem. Sci.* **8:** 250-254.

Peitsch, M., (1995). Protein modeling by e-mail. From amino acid sequence to protein structure: a free one-hour service. *Biotechnology* **13:** 658-672. (http://expasy.hcuge.ch/swissmod/SWISS-Model.html)

Perez-Perez, J., Marquez, G., Barbero, JL., and Gutierrez, J. (1993) Increasing The Efficiency of Protein Export in *Escherichia coli*. *Bio/Technology* **12:** 178-180.

Pedersen, M.E., Cohen, E.M., and Schotz, M.C. Immunocytochemical localization of the functional fraction of lipoprotein in perfused heart. *Journal of Lipid Research* (1983) **24:** 512-517.

Pitas, R.E., Innerarity, T.L., Arnold, K.S., Mahley, R.W. (1979) Rate and equilibrium constants for binding of apo-E HDLc (a cholesterol-induced lipoprotein) and low density lipoproteins to human fibroblasts: evidence for multiple receptor binding of apo-E HDLc. *Proc. Natl. Acad. Sci.* USA **76:** 2311-2315.

Pitas, R.E., Boyles, J.K., Lee, S.H., Foss, D., Mahley, R.W. Astrocytes synthesize apolipoprotein E and metabolism apolipoprotein E-containing lipoproteins. *Biochim. Biophys. Acta.* **917:** 148-152.

Plump, A.S., Smith, J.D., Hayek, T., Aalto-Setala, K, Walsh, A., Verstuyft, J.G., Rubin, E.M., Breslow, J.L. (1992). Severe hypercholesterolemia and atherosclerosis in apolipoproteins in apolipoprotein E-deficient mice created by homologous recombination in ES cells. *Cell* **71:** 343-448.

Pluckthun, A. Kerbber, A., Krebber, C., Horn, U., Kn,pfer, U., Wenderoth, R., Nieba, L., Proba, K., and Riesenberg, D. Producing antibodies in Escherichia coli: from PCR to fermentation. In *Antibody Engineering a Practical Approach*,Series Editor: B.D. Hames, Oxford University Press, 1996.

Prasad, L., S. Sharma, M. Vandonselaar, J. Wilson-Quail, J.S. Lee, E.B. Waygood, K.S. Wilson, Z.Dauter, and L. T.J. Delbaere. 1993. Evaluation of mutagenesis for epitope mapping. Structure of an antibody-protein antigen complex. *J. Biol. Chem.* **268:** 10705-10708.

Porath, J., Immobilized metal ion affinity chromatography. (1992). *Protein Expr. Purif.*, **3:** 263-281.

Pugsley, A.P. (1993) The complete general secretory pathway in gram-negative bacteria. Microbiol. Rev., **57:** 50-108.

Raffaï, R., Maurice, R., Weisgraber, K., Innerarity. T., Wang, X., MacKenzie, R., Hirama, T., Watson, D., Rassart, E., and Milne, R. (1995). Molecular characterization of two monoclonal antibodies specific for the LDL receptor-binding site of human apolipoprotein E. *J. Lipid Res.*, **36:** 1905-1918.

Rall, S.C., Jr., K.H. Weisgraber, and R.W. Mahley. 1982. Human apolipoprotein E. The complete amino acid sequence. *J. Biol. Chem.* **257:** 4171-4178.

Rall, S.C., Jr.,Weisgraber, K.H., Innerarity, T.L., and Mahley, R.W., (1982). Structural basis for receptor binding heterogeneity of apolipoprotein E from type III hyperlipoproteinemic subjects. *Proc. Natl. Acad. Sci. USA.* **79:** 4696-4700.

Redgrave, T.G., Small, D.M. (1979) Quantitation of the transfer of surface phospholipid of chylomicrons to the high density lipoprotein fraction during the catabolism of chylomicrons in the rat. *Journal of Clinical Investigation.* **64:**162-171.

Ramprasad, M.P., Li, R., bradley, W.A., Gianturco, J.H. (1995). Human THP-1 monocyte-macrophage membrane binding proteins: distinct receptor (s) for triglyceride-rich lipoproteins. *Biochemistry* **34:** 9126-9135.

Riddell, D.R., Graham, A., and Owen, J.S. (1997). Apolipoprotein E inhibits platelet aggregation through the L-arginine:nitric oxide pathway. Implications for vascular disease. *J. Biol. Chem.* **272:** 89-95.

Rini, J.M., Schulze-Gahmen, U., and Wilson, I. A. (1992) Structural evidence for induced fit as a mechanism for antibody-antigen recognition. *Science*, **255:** 959-965.

Rosenfeld, L. (1989) Atherosclerosis and the cholesterol connection: evolution of a clinical application. *Clinical Chemistry* **35:** 521-531.

Rosenzweig, A., and Seidman, C.E. (1991). *Annu. Rev. Biochem.* **60:** 229-225.

Ross, R., (1986). The pathogenesis of atherosclerosis-An update. *N. Engl. J. Med.* **413:** 488-491.

Russell, D.W., Lehrman, M.A., Sudhof, T.C., Yamamoto, T., Davis, C.G., Hobbs, H.H., Brown, M.S., Goldstein, J.L. (1986). The LDL receptor in familial hypercholesterolemia: use of human mutations to dissect a membrane protein. *Cold Spring Harbor Symposia on Quantitative Biology*, 5-13.

Russell, D.W., Brown, M.S., Goldstein, J.L. (1989). Different combinations of cysteine-rich repeats mediate binding of low density lipoprotein receptor to two different proteins. *J. Biol. Chem.* **264:** 21682-21688.

Sacks, F.M. and G.P. Krukonis. 1987. Subtypes of normolipidemic VLDL, which has the receptor binding region of apolipoprotein E exposed, causes most of the uptake of VLDL by U937 human macrophages. *Arteriosclerosis.* **7:** 544a.

Sambrook, J., E.F. Fritch, and T. Maniatis. 1989. Molecular Cloning: A Laboratory Manual. Second edition. Cold Spring Harbor Laboratory Press, Cold Spring Harbor, N.Y..

Sanan, D.A., Fan, J., Bensadoun, A., Taylor, J.M. (1997) Hepatic lipase is abundant on both hepatocyte and endothelial cell surfaces in the liver *J. Lipid Res.* **38:**1002-1013.

Sanger, F., S. Nicklen, and A.R. Coulson. 1977. DNA sequencing with chain-terminating inhibitors. *Proc. Natl. Acad. Sci. USA.* **74:** 5463-5467.

Satow, Y., Cohen, G.H., Padlan, E.A., Davies, D.R. (1986). The phosphorylcholine binding immunoglobulin Fab McPC603: an X-ray diffraction study at 2.7 Å. *J. Mol. Biol.* **190:** 593-604.

Schreiber, G., and Fresht, A.R. (1996). Rapid, electrostatically assisted association of proteins. *Nature Struc. Biol.* 3: 427-432.

Scow, R.O., Desnuelle, P., and Verger, R. (1979). Lipolysis and lipid movement in a membrane model: Action of lipoprotein lipase. *J. Biol. Chem.* **254:** 6456-6459.

Segrest, J.P., Garber, D.W., Brouillette, C.G., Harvey, S.C., Anantharamaiah, G.M. (1994) The amphipathic alpha helix: a multifunctional structural motif in plasma apolipoproteins. Advances in Protein Chemistry, **45:** 303-369.

Sehayek, E., Lewin-Velvert, U., Chajek-Shaul, T., and Eisenberg, S. (1991). Lipolysis exposes unreactive endogenous apolipoprotein E-3 in human and rat plasma very low density lipoprotein E-3. *J. Clin. Invest.* **88:** 553-560.

deSilva, H.V., Lower, S.J., Wang, J., Simonet, W.S., Weisgraber, K.H., Mahley, R.W., and Taylor, J.M. (1996). Overexpression of human apo CIII in transgenic mice results in accumulation of apoB-48 remnant lipoproteins, that is corrected by excess apoE. *J. Biol. Chem.* **269:** 2324-2335.

Steinmetz, A., Jakobs, C., Motzny, S., and H. Kaffarnik. (1989). Differential distribution of apolipoprotein E isoforms in human plasma lipoproteins. *Arteriosclerosis* **9:** 405-411.

Powell, L.M., Wallis, S.C., Pease, R.J., Edwards, Y.H., Knott, T.J., Scott, J. (1987). A novel form of tissue-specific RNA processing produces apolipoprotein-B48 in intestine. *Cell* **50:** 831-835.

Shafi, S., Brady, S.E., Bensadoun., A., Havel, R.J. (1994) Role of hepatic lipase in the uptake and processing of chylomicron remnants in rat liver. *J. Lipid Res.* **35:** 709-720.

Shelburne, F., Hanks, J., Meyers, W., Quafordt, S. (1980). Effect of apoproteins on hpatic uptake uptake of triglyceride emulsions in the rat. *J. Clin. Invest.* **65:** 652-659.

Schumaker, V.N., Phillips, M.L., Chatterton, J.E. (1994). Apolipoprotein B and low-density lipoprotein structure: implications for biosynthesis of triglyceride-rich lipoproteins. *Adv. in Prot. Chem.* **45:** 205-248.

Simonet, W.S., Bucay, N., Lauer, S.J., Taylor, J.M. (1993) A far-downstreem hepathocyte-specific control region directs expression of the linked human apolipoprotein E and C-1 genes intransgenic mice. *J. Biol. Chem.* **268:** 8221-8224.

Skerra, A., and Pluckthun, A., (1988). Assembly of a functional immunoglobulin Fv fragment in *E.coli. Science* **240:** 1038-1040.

Smith, J.W., D. Hu, A. Satterthwait, S. Pinz-Sweeney, and C.F. Barbas III. 1994. Building synthetic antibodies as adhesive ligands for integrins. *J. Biol. Chem.* **269:** 32788-32795.

Stary, H.C., (1987) Macrophages, macrophage foam cells, and eccentric intimal thickening in the coronary arteries of young children. *Atherosclerosis* **64:** 91-108.

Steinberg, D. (1997). Lewis A. Conner Memorial Lecture. Oxidative modification of LDL and atherogenesis. Circulation, **95:**1062-1071

Steinberg, D.A (1996) Docking receptor for HDL cholesterol esters. *Science.* **271:** 460-461.

Stow, J.L., Sawada, H., Farquhar, M.G. (1985). Heparan sulfate proteoglycans are concentrated on the sinusoidal plasmalemmal domain and in intracellular organelles of hepatocytes. *J. Cell. Biol.* **100:** 975-978, 1985.

Strittmatter, W.J., A.M .Saunders, D. Schmechel, M. Pericak-Vance, J. Enghild, G.S. Salvesen, and A.D. Roses. 1993. Apolipoprotein E: high-avidity binding to b-amyloid and increased frequency of type 4 allele in late-onset familial Alzheimer disease. *Proc. Natl. Acad. Sci. USA.* **90:** 1977-1981.

Sultan, F., Lagrage, D., Jansen, H., Griglio, S. (1990). Inhibition of hepatic lipase activity impairs chylomicron remnant-removal in rats. *Biochim. Biophys. Acta.* **1042:** 150-153.

Sudhof, T.C., Russell, D.W., Brown, M.S., and Goldstein, J.L. (1987). A 42 bp element from LDL receptor gene confers end-product repression by sterols when inserted into viral TK promoter. *Cell* **48:** 1061-1069.

Tall, A., Sharp, D., Zhong, S., Hayek, T., Masucci-Magoulash, L., Rubin, E.M., Breslow, J.L. (1997). Cholesteryl ester transfer protein and atherogenesis. *Ann. of the N.Y. Acad. of Sci*ences **811:** 178-182.

Tall, A.R., Small, D.M. (1978) Plasma high-density lipoproteins. *New England Journal of Medicine* **299:**1232-1236.

Taub, R., Gould, R., Garsky, V., Ciccarone, T.M., Hoxie, J., Friedman, P., and Shattil, S.J. (1989). A monoclonal antibody against the platelet fibrinogen receptor contains a sequence that mimics a receptor recognition domain in fibrinogen. *The Journal of Biological Chemistry* **264:** 259-269

Thibault, G., Milne, R., and Cantin, M. (1988). A two-site immunoradiometric assay of proatrial natriuretic factor. Application to tissue extracts. Peptides, **9:** 1059-1065.

Thomas P.S. 1980. Hybridization of denatured RNA and small DNA fragments transferred to nitrocellulose. *Proc. Natl. Acad. Sci. USA.* **77:** 5201-5205.

Trakhanov, S.D., Parkin, S., Raffai, R., Milne, R., Newhouse, Y.M., Rupp, B., and Weisgraber, K.H. (1997). Crystal structure of a monoclonal Fab fragment that blocks binding of apolipoprotein E to low density lipoprotein receptors: A model for ligand:receptor interaction. *Sumitted to Protein Science July 1997*

Tramontano, A., Chothia, C., and Lesk, A.M. (1990). Framework residue 71 is a major determinant of the position and conformation of the second hypervariable region in the V_H domains of immunoglobulins. *J. Mol. Biol.* **215:** 175-182.

Tonegawa, S., (1993) Somatic generation of antibody diversity. *Nature.* **302:** 575-581

Uttermann, G., Hees, M., Steinmetz, A. (1977) Polymorphism of apolipoprotein E and occurance of dysbetalipoproteinaemia in man. *Nature* **269:** 604.

Uttermann, G., Vogelberg, K.H., Steinmetz, A., Schoenborn, W., Pruin, N., Jaeschke, M., Hees, M., Canzeler, H. (1979). Polymorphism of apolipoprotein E II. Genetics of hyperlipoproteinemia type III. *Clin. Genet.* **15:** 37-41.

Van Regenmortel, M.H.V. (1992), Molecular dissection of protein antigens. In *Structure of Antigens.* Van Regenmortel, M.H.V., Ed. CRC Press, 1992.

Vakser, I.A., and Aflalo, C. (1994). Hydrophobic docking: A proposed enhancement to molecular recognition tecniques. *PROTEINS: Structure, Function, and Genetics* **20:** 320-329.

Verdaguer, N., Mateu, M.G., Bravo, J., Domingo, E., and Fita, I. (1996). Induced pocket to accomodate the cell attahment Arg-Gly-Asp motif in a neutralizing antibody against Foot-and-Mouth disease virus. *The Journal of Molecular Biology* **256:** 364-376.

Vogel, T., K.H. Weisgraber, M.L. Zeevi, H. Ben-Artzi, A.Z. Lavanon, S.C.Rall Jr., T.L. Innerarity, D.Y. Hui, J.M. Taylor, D. Kanner, Z. Yavin, B. Amit, H. Aviv, M. Gorecki, and R.W. Mahley. (1985). Human apolipoprotein E expression in *Escherichia coli*: structural and functional identity of the bacterially produced protein with plasma apolipoprotein E. *Proc. Natl. Acad. Sci. USA.* **82:** 8696-8700

Walfield, A., E. Selsing, B. Arp, and U. Storb. 1981. Misalignment of V and J gene segments resulting in a nonfunctional immunoglobulin gene. *Nucleic Acids Res.* **9:** 1101-1108.

Wang, S., McLeod, R.S., Gordon, D.A., and Yao, Z., (1996). The microsomal triglyceride transfer protein facilitates assembly and secretion of apolipoprotein B-containing lipoproteins and decreases co-translational degradation of apolipoprotein B in transfected COS-7 cells. *J. Biol. Chem.* **271:** 14124-14133.

Wang, Y., McLeod, R.S., and Yao, Z. (1997). Normal activity of microsomal triglyceride transfer protein is required for the oleate-induced secretion of very low density lipoproteins containing apolipoprotein B from McA-RH7777 cells. *J. Biol. Chem* **272:** 12272-12278.

Weintraub, M.S., Eisenberg, S., and Breslow, J.,L. (1987). Dietary fat clearance in normal subjects is regulated by genetic variation in apolipoprotein E. *J. Clin. Invest.* **80:** 1571-1577

Weisgraber, K.H., Innerarity, T.L., and Mahley, R.W. (1978). Role of the lysine residues of plasma lipoproteins in high affinity binding to cell surface receptors on human fibroblasts. *J. Biol. Chem.* **253:** 9053-9062.

Weisgraber, K.H., S.C. Rall Jr., and R.W. Mahley. (1981). Human E apoprotein heterogeneity. Cysteine-arginine interchanges in the amino acid sequence of the apo-E isoforms. *J. Biol. Chem.* **256:** 9077-9083.

Weisgraber, K.H., T.L. Innerarity, K.J. Harder, R.W. Mahley, R.W. Milne, Y.L. Marcel and J.T. Sparrow. (1983). The receptor-binding domain of human apolipoprotein E. monoclonal antibody inhibition of binding. *J. Biol. Chem.* **258:** 12348-12354.

Weisgraber, K.H., S.C. Rall Jr., R.W. Mahley, R.W. Milne, Y.L. Marcel, and J.T. Sparrow.1986. Human apolipoprotein E: determination of the heparin binding sites of apolipoprotein E3. *J. Biol. Chem.* **261:** 2068-2076.

Weisgraber, K.H. 1990. Apolipoprotein E distribution among human plasma lipoproteins: role of the cysteine-arginine interchange at residue 112. *J. Lipid Res.* **31:** 1503-1511.

Weisgraber, K.H., Lund-Katz, S., and Phillips, M.C. (1992). In "High Density Lipoproteins and Atherosclerosis III" (N.E. Miller and A.R. Tall, eds.), pp. 175-181. Elsivier, Amsterdam.

Weisgraber, K.H., 1994. Apolipoprotein E: structure-function relationships. *Adv. in Prot.Chem.* **45:** 249-302.

Weisgraber, K.H., Mahley, R.W., (1996). Human apolipoprotein E: the Alzheimer's disease connection. *Faseb J.* **10:** 1485-1494.

Webster, M.D., Henry, A.H., and Ress, A.R. (1994). Antibody-antigen interactions. *Current Opinion in Structural Biology*, **4:** 123-129.

Wetterau, J.R., Lin, M.C., Jamil, H. (1997) Microsomal triglyceride transfer protein. *Biochim Biophys Acta*, **1345:** 136-50.

Williams, W.V., Moss, D.A., Kieber-Emmons, T., Cohen, J.A., Myers, J.N., Weiner, D.B., and Green, M. (1989). Development of biologically active peptides based on antibody structure. *Proc. Natl. Acad. Sci.* USA. **86:** 5537-5541.

Wilson, C., M.R. Wardell, K.H. Weisgraber, R.W. Mahley, and D.A. Agard. 1991. Three-dimensional structure of the LDL receptor-binding domain of human apolipoprotein E. *Science.* **252:** 1817-1822.

Wilson, C., T. Mau, K.H. Weisgraber, M.R. Wardell, R.W. Mahley, and D.A. Agard. (1994). Salt bridge relay triggers defective LDL receptor binding by a mutant apolipoprotein. *Structure* **2:** 713-718.

Wilson, I.A., Stanfield, R.L. (1994). Antibody-antigen interactions: new structures and new conformational changes. *Current Biology* 4: 857-867.

Windler, E., Chao, Y.S., Havel, R.J. (1980) Determinants of hepatic uptake of triglyceride-rich lipoproteins and their remnants in the rat. *J. Biol. Chem.* **255:** 5475-5479

Winter, G., and Milstein, C. (1991). Man-made antibodies. *Nature*. **349:** 293-299.

Winter, G., Griffiths, A.D., Hawkins, R.E., Hoogenboom, H.R. (1994) Making antibodies by phage display technology. *Annual Review of Immunology*, **12:** 433-455.

Yao, Z.M., and Vance, D.E. (1989). Head group specificity in the requirement of phosphatidylcholine biosynthesis for very low density lipoprotein secretion from cultured hepatocytes. *Journal of Biological Chemistry* **264:**11373-11380.

Ysern, X., Fields, B.A., Bath, T.N., Goldbaum, F.A., Dall'Acqua, W., Schwarz F.P., Poliak, R.J., Mariuzza, R.A. (1994). Solvent rearrangement in an antigen-antibody interface introduced by site-directed mutagenesis of the antibody combining site. *J Mol Biol* **238:** 496-500.

Zambon, A., Schmidt,I., Biesiegel, U., and Brunzell, J.D. (1996). Dimeric lipoprotein lipase is bound to triglyceride-rich plasma lipoproteins. *Journal of Lipid Research*, **37:** 2394-2404.

Zannis, V.I., and Breslow, J.L. (1981). Human very low density lipoprotein apolipoprotein E isoprotein polymorphism is explained by genetic variation and posttranslational modification. *Biochemistry* **20:** 1033

Zdanov, A., Li, Y., Bundle, D.R., Deng, S.J., MacKenzie, C.R., Narang, S.A., Young, N.M., Cygler, M. (1994). Structure of a single-chain antibody variable domain (Fv) fragment complexed with a carbohydrate antigen at 1.7-A resolution. **91:** 6423-6427.

Zhang, S.H., Reddick, R.L., Piedrahita, J.A., Maeda, N. (1992). Spontaneous hypercholesterolemia and arterial lesions in mice lacking apolipoprotein E. *Science* **258:** 468-470.

Books

Atherosclerosis X (International Congress Series) 1994, ed. Davignon,J. Montréal.

Atherosclerosis : Cellular Interactions, growth factors, and lipids, volume 25 (1993) Raven Press, editors, Peter C., Weber, Alexander Leaf.

Biochemistry of lipids, lipoproteins and membranes. (1996) Vance, D.E., and Vance, J.E., (eds) Elsevier Science

Fundamental immunolgy, Second Edition, (ed) William Paul, Raven Press LTD., New York 1989.

Growth of the bacterial cell (1983) eds. Ingrahm, J.L., Maaløe, O., and Neidhardt, F.C., Sinauer Associates, Inc. Publishers. Sundeilan, Massachusettes, 1983.,

Human physiology, second edition (19920. Rhodes and Pflanzer, Saundes College Publishing.

Immunoglobulin genes, second edition (1995) Academic press, editors, Honjo, T., Alt, F.W.

Methods in Enzymology, 128/129. (1986). (eds.) Colowick, S.P., and Kaplan, O.

The Metabolic Basis of Inherited Disease, 7th (eds.) Scriver C.R., Beaudet, A.L., Sly, W.S., Valle, D. (eds): New York, McGraw-Hill, 1995, vol. II.

IMAGE EVALUATION
TEST TARGET (QA-3)

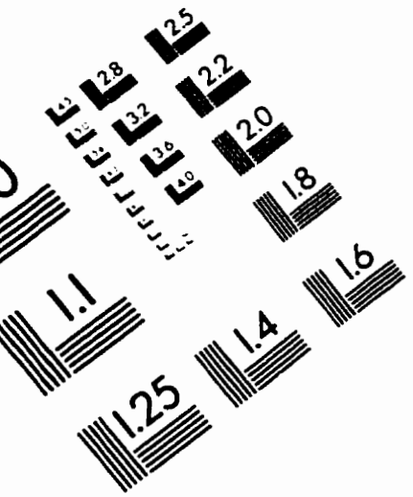

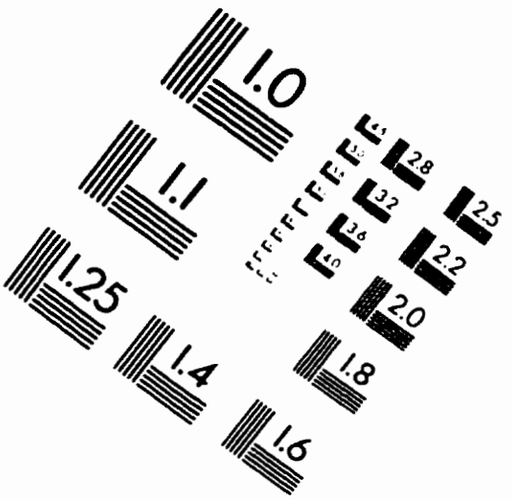

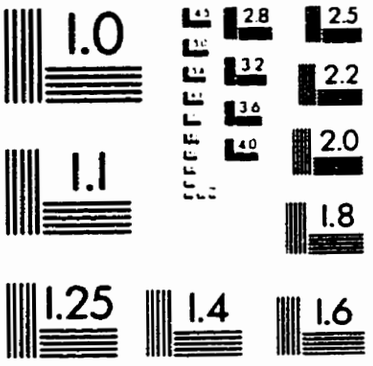

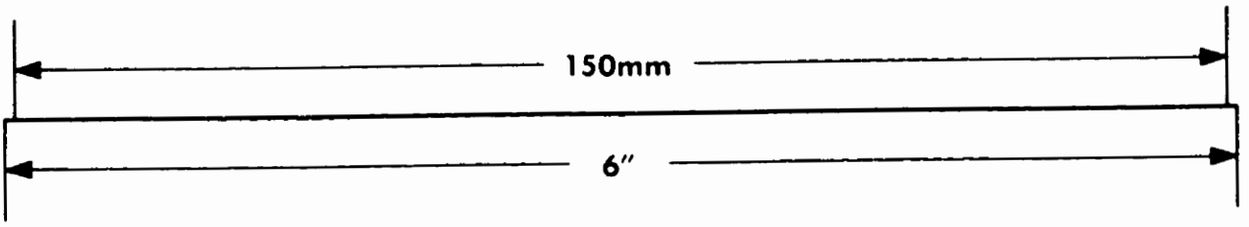

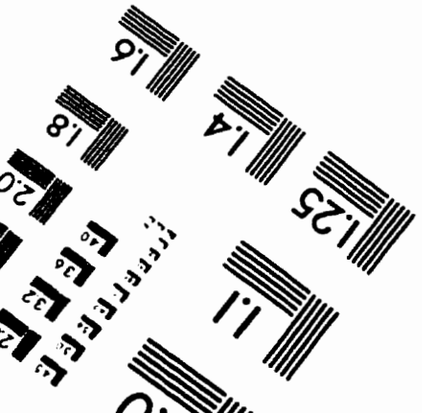

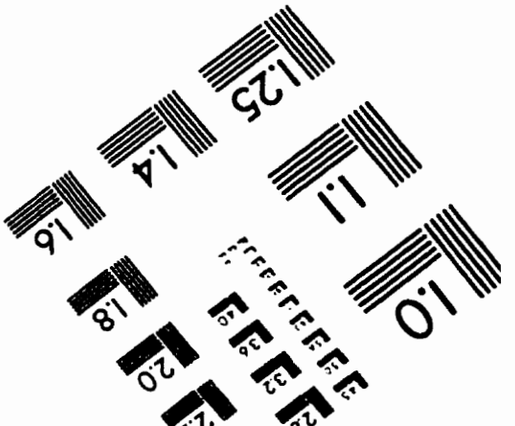

APPLIED IMAGE, Inc
1653 East Main Street
Rochester, NY 14609 USA
Phone: 716/482-0300
Fax: 716/288-5989